

TECHNICAL REPORT
NO. 9843-37

THE EFFECT OF NONUNIFORM AXIAL HEAT FLUX DISTRIBUTION
ON THE CRITICAL HEAT FLUX

by

Neil E. Todreas

Warren M. Rohsenow

Support extended by the
National Association for the Advancement of Science
under Contract NsG-496 with the
Center for Space Research
DSR Project No. 9843

September 20, 1965

Department of Mechanical Engineering
Massachusetts Institute of Technology
Cambridge 39, Massachusetts

Abstract

A systematic experimental and analytic investigation of the effect of nonuniform axial heat flux distribution on critical heat flux was performed with water in the quality condition. Utilizing a model which ascribes the critical condition, to either a nucleation-induced disruption of the annular liquid film or annular film dryout, the experimental results taken at low pressures (50-200 psia) were confirmed. Application of this model to higher pressure conditions (500-2000 psia) indicated qualitative agreement with available data of other investigators.

Experimental data was obtained for flux distributions representing cosine, linear increasing and decreasing, inlet and exit peaked, spike and uniform shapes. These flux distributions were achieved by electrical resistance heating of test sections whose outside diameter had been machined to the required dimensions. In each case the critical location as well as the total critical power was obtained by testing the tubes in vertical upflow to failure.

The analytic prediction of the results for all flux shapes has been achieved by development of a model which considers the effect of nucleation within the annular film. It is shown that the occurrence of the critical condition is related to the local degree of nucleation (the ratio of the local flux to the flux required to cause nucleation at the local conditions) and the local film flow rate. Both the experimental total critical power and the critical location are confirmed by this model. The results indicate that the total critical power for the outlet peaked flux distributions tested (ratios of maximum to minimum flux of 2, 4, and 5.75 to 1) can be 15 to 30% lower than for uniform flux distributions at comparable hydrodynamic operating conditions. In addition, from this model for given operating conditions, a locus of critical conditions can be constructed from uniform flux distribution data which will enable prediction of the performance of nonuniform flux distributions at similar conditions of mass velocity, pressure and diameter.

ACKNOWLEDGEMENT

Support for this study was extended to the Massachusetts Institute of Technology by the National Aeronautics and Space Administration under contract with the Center for Space Research. In addition support to facilitate initiation of the study was provided by the Shell Companies Foundation. This study was done in part at the Computation Center at the Massachusetts Institute of Technology.

The permission granted by the Babcock and Wilcox Company and the Atomic Energy Commission to include results from a Babcock and Wilcox Company preliminary report is gratefully acknowledged.

Professors P. Griffith, A. Bergles, H. Fenech and M. Suo gave their time generously to discuss the program during the course of the investigation.

Mr. F. Johnson and Mr. E. Hartell of the Heat Transfer Laboratory were of great assistance in constructing the experimental arrangement and keeping the facility operational.

Mr. A. Werthen of the Whitman Tool and Die Company and Mr. P. Wassmouth were responsible for developing the techniques for fabricating the required test sections to specified tolerances. The machining of all test sections was performed by the Whitman Tool and Die Company.

TABLE OF CONTENTS

	PAGE
Title Page	1
Abstract	11
Acknowledgement	111
List of Figures	vi
Nomenclature	
Conversion of Units	
CHAPTER I: INTRODUCTION	1
1.1 Background of Problem	1
1.2 Scope of the Research	2
1.3 Literature Survey	3
CHAPTER II: TWO PHASE FLOW WITH HEAT ADDITION	18
2.1 Flow Regimes	18
2.2 Critical Heat Flux	22
CHAPTER III: EXPERIMENTAL PROGRAM	28
3.1 Description of Apparatus	28
3.1.1 Hydraulic System	28
3.1.2 Power Supply	30
3.1.3 Instrumentation	31
3.1.4 Test Section	33
3.2 Experimental Procedures and Experience	34
3.2.1 General Loop Operation	34
3.2.2 Loop Operation for Critical Heat Flux Data	36
3.2.3 Two Phase Heat Transfer Coefficient Measurements	38
3.2.4 Correction of Oscillatory Instabilities	39
3.2.5 Critical Flow Considerations	41

	PAGE
CHAPTER IV: PRESENTATION AND DISCUSSION OF RESULTS	43
4.1 Experimental Results	43
4.1.1 Total Critical Power	44
4.1.2 Critical Location	46
4.1.3 Reproducibility of the Data	48
4.2 Formulation of the Method of Analysis	50
4.3 Calculation Procedure for the Method of Analysis	54
4.4 Application of the Method of Analysis to Experimental Data	57
4.4.1 Discussion of Results	60
4.4.1.1 Total Critical Power	61
4.4.1.2 Critical Location	61
4.4.2 Discussion of Results - Flux Spikes	66
4.5 Application to Higher Pressures	70
CHAPTER V: SUMMARY AND CONCLUSIONS	74
5.1 Summary	74
5.2 Conclusions	75
5.3 Design Procedure (50-200 psia)	76
APPENDIX A Error Analysis	78
APPENDIX B Test Section Analysis	82
APPENDIX C Test Section Design	110
APPENDIX D Data Reduction and Analysis	115
APPENDIX E Program for Data Reduction and Analysis	122
APPENDIX F Tabulation of Data	170
BIBLIOGRAPHY	177
FIGURES	181

LIST OF FIGURES

FIGURE

- 1 Effect of Local Heat Flux Spike on Burnout
- 2 Prediction of Critical Condition by Local Condition Method of Janssen and Kervinen (Ref. 6)
- 3 Prediction of Critical Condition by Equivalent Length Method of Lee and Obertelli (Ref. 9)
- 4 Regimes of Two-Phase Flow
- 5 Flow Regime Map for Test Conditions
- 6 Comparison of Uniform Flux Data with Existing Correlations, $G = 0.5 \times 10^6$ BTU/HR-FT²
- 7 Comparison of Uniform Flux Data with Existing Correlations, $G = 1.0 \times 10^6$ BTU/HR-FT²
- 8 Comparison of Uniform Flux Data with Existing Correlations, $G = 2.0 \times 10^6$ BTU/HR-FT²
- 9 Schematic Layout of Experimental Facility and Test Section Arrangement
- 10 Axial Flux Distributions Tested
- 11 Confirmation for Test Section 112 That the Overall Slope Goes to Zero at the Flow Rate ($G = 2.0 \times 10^6$ LBM/HR-FT²) where Oscillation Occurred
- 12 Total Critical Power for Uniform and Cosine Flux Distributions at $G = 0.5 \times 10^6$ LBM/HR-FT²
- 13 Total Critical Power for Linear and Peaked Flux Distributions at $G = 0.5 \times 10^6$ LBM/HR-FT²
- 14 Critical Locations (Inches from Inlet) for the Nonuniform Axial Distributions Investigated at $G = 0.5 \times 10^6$ LBM/HR-FT²
- 15 Total Critical Power for Uniform and Cosine Flux Distributions at $G = 1.0 \times 10^6$ LBM/HR-FT²
- 16 Total Critical Power for Linear and Peaked Flux Distributions at $G = 1.0 \times 10^6$ LBM/HR-FT²

FIGURE

- 17 Critical Locations (Inches from Inlet) for the Nonuniform Axial Flux Distributions Investigated at $G = 1.0 \times 10^6$ LBM/HR-FT²
- 18 Total Critical Power for Uniform and Cosine Flux Distributions at $G = 2.0 \times 10^6$ LBM/HR-FT²
- 19 Total Critical Power for Linear and Peaked Flux Distributions at $G = 2.0 \times 10^6$ LBM/HR-FT²
- 20 Critical Locations (Inches from Inlet) for the Nonuniform Axial Flux Distributions Investigated at $G = 2.0 \times 10^6$ LBM/HR-FT²
- 21 Summary of Effect of Linear Increasing and Decreasing Flux Distributions on Total Critical Power
- 22 Summary of Effect of Peak Inlet and Exit Flux Distributions on Total Critical Power
- 23 Total Critical Power for Data of Bertoletti et al (Ref. 11)
- 24 Total Critical Power for Data of Swenson (Ref. 5)
- 25 Total Critical Power for Data of Babcock and Wilcox (Ref. 15)
- 26 Schematic Presentation of Method of Analysis
- 27 Bergles-Rohsenow Criteria (Ref. 35) for Incipient Boiling $(q/A)_1 = 15.60 P^{1.156} (T_{WALL} - T_{SAT})^{2.30} / P^{0.0234}$
- 28 Variation of Two Phase Heat Transfer Coefficient (h) with Mass Flow Rate (G) and Quality (X) h_{TP} per Dengler-Addoms Correlation (Ref. 38)
- 29 Typical Determination of Heat Flux Required for Incipient Boiling, $(q/A)_1$, at the Critical Location
- 30 Heat Flux Conditions Along Test Section Length
- 31 Operating Lines for Test Section 1271 for Q_{TOT} Equal to and Less Than Q_{CRIT}
- 32 Critical Flux Results at $G = 0.5 \times 10^6$ LBM/HR-FT²
- 33 Critical Flux Results at $G = 1.0 \times 10^6$ LBM/HR-FT²

FIGURE

- 34 Critical Flux Results at $G = 2.0 \times 10^6$ LBM/HR-FT²
- 35 Dimensionless Representation of Bergles-Rohsenow Nucleation Theory. The Effect of Limited Maximum Cavity Sizes is Shown for $P = 100$ psia ($\tau_w \sim .1$) Only
- 36 Uniform Flux Distribution Data of Hewitt et al (Ref. 41)
- 37 Operating Histories for Total Input Power up to the Critical Power (Uniform and Linear Flux Distributions)
- 38 Operating Histories for Total Input Power up to the Critical Power (Cosine and Peaked Flux Distributions)
- 39 Effect of Axial Flux Distribution on the Critical Location
- 40 The Effect of M Value (Ratio of Maximum to Minimum Flux) on the Critical Location
- 41 The Effect of Inlet Subcooling on the Critical Location (Peak Exit and Inlet Flux Distributions)
- 43 Comparison of Critical Flux Results for the Range of Mass Velocities Investigated
- 44 Effect of Length on the Critical Condition
- 45 Effect of Inlet Subcooling on the Critical Condition
- 46 Effect of Flux Shape Length on the Critical Condition for $G = 1.0 \times 10^6$ LBM/HR-FT²
- 47 Effect of Flux Spike Length and M Value (Ratio of Maximum to Minimum Flux) on the Critical Condition for $G = 1.0 \times 10^6$ LBM/HR-FT² and $\Delta H_{IN} = -100$ BTU/LBM
- 48 Critical Flux Results at 1000 Psia from Babcock and Wilcox Data (Ref. 15)
- 49 Estimation of the Critical Region Width (in % Total Input Power) of Figure 48 for 1000 psia Data (Ref. 15)

FIGURE

- 50 Critical Flux Results at 2000 psia from Babcock and Wilcox Data (Ref. 5)
- 51 Estimation of the Critical Region Width (in % Total Input Power) of Figure 50 for 2000 psia Data (Ref. 5)
- 52 Effect of Inlet Subcooling on Critical Flux Results for Cosine Flux Distribution with Flux Spike (Ref. 5)

NOMENCLATURE

<u>Symbol</u>	<u>Variable</u>	<u>Units</u>
A_F	Flow cross sectional area	ft^2
A_S	Inside surface area	ft^2
A_X	Wall cross sectional area	ft^2
D_i	Inside diameter	inches
C_p	Specific heat at constant pressure	$\text{btu/lbm}^\circ\text{F}$
C_1	Constant associated with peaked inlet and outlet flux distributions defined by Eq. B-53	inches
C_7	Constant associated with spike (Cosine Shaped) flux distribution defined by Eq. B-85	inches
D_o	Outside diameter	inches
E	Test section voltage drop	volts
g	Acceleration due to gravity	ft/sec^2
g_o	Gravitational constant, 32.2	$\frac{\text{lbm}}{\text{lbf}} \frac{\text{ft}}{\text{sec}^2}$
G	Mass velocity	$\text{lbm}/\text{hr}\text{-ft}^2$
h	Heat transfer coefficient	$\text{btu}/\text{hr ft}^{2\circ}\text{F}$
H	Enthalpy	btu/lbm
I	Test section current	amperes
k	Thermal conductivity	$\text{btu}/\text{hr ft}^\circ\text{F}$
ℓ	Test section heated length	inches
ℓ'	Length of cosine portion of test section length or spike length (see Fig. 10)	inches
L	Half-wavelength of cosine test section which is truncated to length ℓ (see Fig. 10)	inches
L'	Half-wavelength of cosine portion of test section which is truncated to length ℓ' (see Fig. 10)	inches

Nomenclature (Continued)

<u>Symbol</u>	<u>Variable</u>	<u>Units</u>
\mathcal{L}	Length of test section for peaked and spiked flux distributions defined in Fig. 10.	inches
$L_{X=0}$	Location at which saturation condition is reached	inches
L_S	Length over which quality condition exists	inches
M	Ratio of maximum to minimum flux	dimensionless
P	Pressure	psia
P_r	Prandlt number	dimensionless
$q/A, \phi$	Heat flux	btu/hr-ft ²
Q	Integrated power input	btu/hr
r	Maximum cavity size required for nucleation	ft
R	Overall tube resistance	OHM
Re	Reynolds number	dimensionless
T	Temperature	°F
X	Quality	$\frac{\text{lbm steam}}{\text{total lbm}}$
X_{tt}	Martinelli-Nelson Parameter	dimensionless
u, x, y, z	Axial position indices (see Fig. 10)	inches
v	Specific volume	ft ³ /lbm
V	Velocity	ft/sec
W	Mass flow rate	lbm/hr

Subscripts

ANN	Tube length in annular flow condition
C	Critical location
CRIT	Critical condition
EXIT	Exit
f	Saturated liquid
fg	Liquid to vapor
film	Film
G	Gas
i	Required to initiate nucleation
IN	Inside, inlet
INLET	Inlet
L	Liquid
MAX	Maximum
MIN	Minimum
OUT	Outlet
p	Pump
S	Saturation location
SAT	Saturation condition
SUB	Subcooled
TOT	Total
TP	Two Phase
V	Vapor
WALL	Wall
u,x,y,z	Axial position indices

Greek Letters

ρ	Specific resistivity	ohm/ft
ξ	Constant associated with peaked flux distributions defined by Eqs. B-51 and B-73	dimensionless
σ	Surface tension	lb _f /ft
τ	Shear stress	lb _f /ft ²
μ	Viscosity	lbm/hr ft
γ	Kinematic viscosity	ft ² /hr
ϕ or q/A	Heat flux	btu/hr ft ²

CONVERSION OF UNITS

ENGLISH TO METRIC (MKS, CGS)

PRESSURE (P)	$\text{kg/cm}^2 = 0.0702 \times \text{psia}$
UNIT MASS FLOW RATE (G)	$\text{kg/m}^2 \text{sec} = 1.361 \times 10^{-3} \times \text{lb/hr ft}^2$ $\text{g/cm}^2 \text{sec} = 1.361 \times 10^{-4} \times \text{lb/hr ft}^2$
HEAT FLUX (ϕ)	$\text{watts/cm}^2 = 3.15 \times 10^{-4} \times \text{BTU/hr ft}^2$ $\text{kJ/m}^2 \text{sec} = 3.105 \times 10^{-3} \times \text{BTU/hr ft}^2$
DENSITY (ρ)	$\text{gm/cm}^3 = 62.4 \times \text{lb/ft}^3$
KINEMATIC VISCOSITY (γ)	$\text{cm}^2/\text{sec} = 3.88 \times \text{ft}^2/\text{hr}$
VISCOSITY (μ)	$\text{gm/cm sec} = 243 \times \text{lb(m)/hr ft}$
LENGTH (l)	$\text{mm} = 25.4 \times \text{in}$

METRIC TO ENGLISH

PRESSURE (P)	$\text{psia} = 14.25 \times \text{kg/cm}^2$
UNIT MASS FLOW RATE (G)	$\text{lb/hr ft}^2 = 735 \times \text{kg/m}^2 \text{sec}$ $\text{lb/hr ft}^2 = 7350 \times \text{g/cm}^2 \text{sec}$
HEAT FLUX (ϕ)	$\text{BTU/hr ft}^2 = 3170 \times \text{watts/cm}^2$ $= 322 \times \text{kJ/m}^2 \text{sec}$
DENSITY (ρ)	$\text{lb/ft}^3 = 0.016 \times \text{gm/cm}^3$
KINEMATIC VISCOSITY (γ)	$\text{ft}^2/\text{hr} = 0.258 \times \text{cm}^2/\text{sec}$
VISCOSITY (μ)	$\text{lb(m)/hr ft} = 0.00412 \times \text{gm/cm sec}$
LENGTH (l)	$\text{in} = 0.0394 \times \text{mm}$

CHAPTER I

INTRODUCTION

1.1 Background of the Problem

Forced convection boiling of water in axial flow is being utilized in pressurized and boiling water reactors and has been investigated as a means for cooling the nozzles of electro-thermal engines, electric-arc wind tunnels and nuclear rockets. One of the most important limits in the thermal performance of such systems is the so-called critical or burnout condition. This condition is characterized by a sharp reduction in ability to transfer heat from the heated surface. Much test data are available for uniform heat flux distributions along the test section and numerous correlations of these data have been proposed. However, in reactor systems as well as high temperature flow nozzles mentioned above, the heat flux distributions are inherently nonuniform and possess such large gradients that the existing uniform flux burnout correlations are not applicable. In addition, although interpretation of the limited data available on nonuniform heat flux distributions varies as discussed in the literature survey of section 1.3, the overall conclusion is that certain non-uniform heat flux distributions can significantly lower the critical heat flux compared to a uniform heat flux distribution under similar hydrodynamic operating conditions. Therefore, it is highly desirable for design purposes to have a satisfactory method for predicting the effect on the critical condition of nonuniform heat flux distributions which exist in practice.

In general three basic axial flux shapes exist:

- (a) A reasonably symmetrical flux distribution with central peak, approximated by a "chopped" cosine. This corresponds to an end-of-core-life condition where the flux is not significantly perturbed by control rods or nonuniform burnup, or to a core with chemical control
- (b) A flux distribution markedly peaked near the inlet of the channel, corresponding to a new, clean core with control rods in the upper part of the core (upflow); and
- (c) A flux distribution markedly peaked near the exit of the channel, corresponding to a maximum xenon override condition where the control rods are withdrawn but the upper part of the core has had less burnup.

In addition to these macroscopic flux distributions, there may be superimposed microscopic flux peaks which may occur at any point along the channel. These flux peaks may be due to nuclear effects (fuel peaks or water holes) or manufacturing dimensional tolerances (fuel thickness or eccentricity) and are of some short but undefined axial extent. It is the purpose of this investigation to determine the effect of these types of axial flux distributions on the critical heat flux in the quality region by a systematic experimental and analytic investigation. The two quantities of interest are (1) the location of the critical condition and (2) the power input to the reactor channel required to cause the critical condition.

1.2 Scope of the Research

A comprehensive experimental program was undertaken to

investigate nonuniform axial flux distributions under bulk boiling conditions. In addition to the flux shapes of direct reactor interest, additional nonuniform as well as uniform shapes were tested to permit more thorough analysis of the fundamental nature of the critical condition. Also the flux gradient was varied for several of the distributions tested as tabulated below to bracket and extend data available in the literature.

<u>Flux Distribution</u>	<u>Approximate Ratio Maximum Flux Minimum Flux</u>
Uniform	1.0
Cosine	2.27, 4.03, 5.75
Linear Increasing	2.27, 5.75
Linear Decreasing	2.27, 5.75
Peak Inlet	5.75
Peak Outlet	5.75
Flux Spike (Step)	4.1 to 5.1
Flux Spike (Cosine)	2.27, 5.75, 7.00

The experimental program was run on the flow loop available in the Heat Transfer Laboratory of the Mechanical Engineering Department. Therefore the operating pressure was limited to approximately 200 psia but the analytic results obtained from this data were successfully applied qualitatively to the higher pressure regions of practical interest. The ranges of other operating and test section conditions are listed below.

TEST SECTION

Material - Aluminum Tubes

Inside Diameter - .214 Inches (.544 cm)

Heated Length - 30 and 48 Inches (76.2 and 122 cm)

Inlet Calming Length - 3.7 Inches (9.4 cm)

OPERATING CONDITIONS

Pressure - 60 to 200 psia (4.2 to 14 kg/cm² abs)

Mass Flow Rate - .5, 1.5 and $2.0 \times 10^6 \frac{\text{lbm}}{\text{hr ft}^2}$ (680, 2040,
and 2720 $\text{kg/m}^2\text{sec}$)

Inlet Temperature - 60 to 290°F

Power - Direct Current Resistance Heating

Burnout Detection - Tubes Tested to Failure

It should be noted that several definitions of the critical condition are used throughout the literature. Generally the definition selected by an experimenter is related to the burnout detection mechanism used. In this work since each tube was tested to failure, the critical condition is taken as the physical destruction of the aluminum test section. Correspondingly the critical location is defined as the location of the test section failure.

1.3 Literature Survey

Review of the literature on the subject of axial heat flux distribution reflects the developing interest in this area manifested by expanding experimental programs and more sophisticated analytic procedures. However, as this literature is reviewed it should be noted that for all efforts except that of Becker⁽¹⁶⁾ and Tong⁽¹⁷⁾, which are the most recent, workers have attempted to characterise the results by intuitive judgments based on uniform flux results. Since uniform flux data indicates that the critical condition occurs at the exit where enthalpy is a maximum but heat flux is equivalent to that all along the tube, it is not possible to distinguish whether the critical heat flux is governed by local or integrated conditions. Hence, in the case of nonuniform flux distributions, we find some test results are interpreted to suggest that the critical heat flux is a function of local conditions along the nonuniformly heated test section, while other results

are interpreted to suggest that the total integrated heat transfer or exit enthalpy determines the critical condition which is therefore independent of the local conditions at the critical location.

The seemingly perplexing part of this disagreement is that reliable data supporting each interpretation has been presented. In anticipation of the conclusions of this work it can be stated that both the above interpretations can be shown to be correct, if each is viewed within the framework of a broader interpretation of the critical phenomenon. That is, the critical condition is a phenomenon which, when represented by the analytic model developed in this work, is dependent on both local and integral conditions, the relative importance of each, depending upon the existing thermal and hydrodynamic conditions.

Among the earliest results were those of the Bettis Plant reported in the summary report by DeBertoli et al^{(1)*} which includes results of DeBortoli, Roarty and Weiss⁽²⁾ and Weiss⁽³⁾. These results consisted of the two basic kinds of nonuniform heat flux experiments (1) gradual variation of axial heat flux in cosine or other shape distributions where $(d(q/A)/dx$ is small) and (2) axial step changes in heat flux commonly called hot-patch or spike tests.

The cosine tests reported by DeBertoli were for a rectangular test section (0.055 in. x 2.116 in. x 27 in. or 0.14 cm x 5.36 cm x 68.5 cm) with 2000 psia (136 atm) water

*Numbers in parentheses refer to references listed in the Bibliography.

for a center-peak-to-minimum heat flux of 4.0 and maximum-to-average of 1.38. The critical condition always occurred between the peak flux location and the channel exit. A plot of local heat flux vs. local enthalpy at the critical condition resulted in a downward sloping curve which was approximately 70% of the critical heat flux calculated for a uniform flux distribution at the same mass flow velocity and exit enthalpy by the Bell⁽⁴⁾ correlation. A surprising result was the observation that with the central peak in the cosine distribution, the magnitude of average heat flux vs exit enthalpy when a critical condition exists somewhere along the tube length would lie close (+15% to -25%) to a plot of critical heat flux vs exit enthalpy for the uniform flux distribution data.

The hot-patch tests performed at Bettis utilized a rectangular channel (0.097 in. x 1.0 in. x 27 in. or 0.25 cm x 68.5 cm) with water at 2000 psia (136 atm). The first 26 5/8 in. (67.5 cm) of the channel were at a uniform heat flux ϕ_1 and the last 3/8 in. (0.95 cm) was operated at heat flux ϕ_2 where ϕ_2/ϕ_1 was maintained at 1.98 throughout the tests. The results are shown in Fig. 1 where the upper curve is ϕ_2 at the critical condition and the lower curve is the corresponding magnitude of $\phi_1 = \phi_2/1.98$. Superimposed on this plot is the curve for ϕ_3 , the critical heat flux obtained for the same exit enthalpy and flow rate when the channel is uniformly heated along the entire 27 in. (68.5 cm) length. At around 60 °F (33 °C) exit subcooling, $\phi_2 = \phi_3$, and at exit quality of around 50%, $\phi_3 = \phi_1$. It is seen that the ratio

$$E_p = \left(\frac{\phi_3 - \phi_1}{\phi_2 - \phi_1} \right)$$

decreases from around unity well in the subcooled region to near zero as quality increases. These results show that for the subcooled exit region, where $E_p=1$, the equivalent hot-patch heat flux must be achieved in the uniformly heated case to obtain burnout, hence suggesting the importance of local conditions in the burnout phenomena. On the other hand, in the 50% quality region, where $E_p=0$, burnout is achieved at the same exit enthalpy even though the hot-patch heat flux is greater than the uniformly heated tube flux. This suggests that the integrated conditions are of prime importance in this region.

These initial results illustrated the existence of non-uniform flux effects and indicated the need to allow for these effects in design, particularly since these distributions could lower the critical heat flux from that expected by extrapolation of uniform flux distributions data. The next investigation in this area was an extensive program performed by Swenson et al⁽⁵⁾, with 2000 psia (136 atm) water for cosine distributions with central peak, central peak with spike, peak near inlet and peak near outlet in 0.411 to .446" dia. (1.04 to 1.17 cm) and 72 in. (183 cm) long tubes. The flux spike tests were very limited but did indicate a decrease in effectiveness, E_p , as the exit quality increased in agreement with the Bettis results. However, in this case the quality range was limited to approximately 30% to 24%. For the central-peak flux distribution, the data at the critical location was about one-half of the magnitude of $(q/A)_{crit}$ at the same enthalpy in a tube with uniform flux distribution.

The data for both skewed cosine distributions were still lower. The average heat flux vs exit quality (critical condition existing between the location of the peak flux and the exit) agreed reasonably well with $(q/A)_{crit}$ vs. exit enthalpy for uniform flux distribution for the central peak and the peak-near-outlet data but the data for peak-near-inlet fell much below this. These results indicate that when additional flux distributions are considered, the apparent success obtained with cosine and central peak distributions in comparing the average critical heat flux to the critical heat flux for uniform distributions cannot be generalized. This fact should be borne in mind in the following discussion of other programs which have achieved success in applying such techniques or their variations to cosine shape distributions only. From a practical point of view, these techniques of simple comparison with, or extrapolation of, uniform heat flux data give reasonable answers when applied to cosine distributions and can be used in these cases. However, for the important cases of peaked inlet and outlet distributions, these techniques fail dramatically and thus indicate that these methods are not based on a correct fundamental interpretation of the critical phenomena.

Reported programs in this group which deal exclusively with the cosine flux distribution include that of Janssen and Kervinen⁽⁶⁾, Casterline and Matzner⁽⁷⁾, Shaefer and Jack⁽⁸⁾, Lee and Obertelli⁽⁹⁾ and Lee⁽¹⁰⁾. Janssen and Kervinen carried out experiments for cosine, and truncated-cosine heat flux distributions for an annulus (0.54 in. x 0.875 in. x 100 in. or 1.37 cm x 2.22 cm x 254 cm) with only

the inner rod heating 1000 psia (68 atm) water. The ratios of maximum flux to minimum flux, M , were 1.86, 3.25 and 3.5. In all cases the inlet was subcooled and the operation was reported to be stable without noticeable flow oscillations. The data from these experiments was analysed by plotting local heat flux versus local quality for all points on the cosine test section at the critical power on the same curve with similar data for uniform flux distributions as represented by a General Electric correlation for such data (see Fig. 2). Assuming that the critical condition depends only on local conditions, the point of tangency between these curves will allow prediction of (1) the burnout location and (2) the power level at burnout. Based on this type of analysis, the cosine data was about 9 to 20% lower than predicted. Considering that (1) the actual burnout location was uncertain to at least ± 1 inches due to placement of thermocouples whose temperature rise was monitored and (2) that the uniform rod data upon which the correlation was based had a deviation of the same order as above (9 to 20%), the method predicts the cosine distribution behavior well. However, it should be noted that using the same uniform correlation and the integrated burnout concept, the cosine average heat is also within 20% of the uniform critical heat flux. Thus for cosine data of reasonable steepness, predictions of comparable accuracy can be obtained with the two basically divergent views of the burnout phenomenon.

Similar results were obtained in the high mass flow range ($G \geq 3.0 \times 10^6$ lbm/hr ft²) by Casterline and Matzner⁽⁷⁾ who carried out cosine distribution experiments in a 192 in. long (487 cm)

.400 inch diameter (1.02 cm) tube with water at 1000 psia ($70.2 \frac{\text{kg}}{\text{cm}^2}$). However for lower mass flow rates, the cosine tube supported higher heat fluxes for the same local conditions than the uniform tubes. Thus for lower mass flow rates, analyses based on both local and average conditions fail for this distribution with the rather extreme ratio of MAXIMUM FLUX/MINIMUM FLUX = 34.8. However this discrepancy may be due to the presence of reported severe pressure oscillations which were probably due to the inherent compressibility existing in the void fraction in the long tube since the inlet conditions were in all cases subcooled.

Limited but interesting data applicable to nozzle cooling applications was obtained by Schaefer and Jack⁽⁸⁾ for central peak shapes at very high heat fluxes. These experiments were performed with tubes having heated lengths of 1.5 and 5.5 in. (3.81 and 14.0 cm), .120 in. (.304 cm) diameters in 200 psia ($14.0 \frac{\text{kg}}{\text{cm}^2}$) water. The flux gradient was large since the heated length was short and M large (5.88). The experiments were run at high mass velocity ($G = 4.0 \times 10^7 \frac{\text{lbm}}{\text{hr ft}^2}$) and yielded high local critical heat fluxes ($q/A = 4.0 \times 10^7 \frac{\text{BTU}}{\text{hr ft}^2}$). Hence this data which is outside the normal range of variables is available for comparison with new methods of analysis.

Extensive additional tests with cosine flux distributions have been reported by Lee and Obertelli⁽⁹⁾ and Lee⁽¹⁰⁾. These experiments were performed with 60 to 144 in. (152 to 366 cm) tubes of diameters .373 or .383 in. (.95 or .975 cm) in water at pressures of 550 to 1600 psia (38.6 to $112 \frac{\text{kg}}{\text{cm}^2}$). The first report surveys the entire range of variables listed, while the

second report contains data from the 144 in. long tubes at 1000 psia only. These reports show that the average heat flux condition for estimating burnout is satisfactory. This condition can be expressed as the equivalence of the average cosine heat flux with the critical uniform heat flux under the same thermal and hydrodynamic test conditions or simply as equivalence of total input power to the test sections in each case. The reports also introduce another prediction method based on the integrated condition concept. In this case prediction of burnout power and location is obtained as the point of intersection between cosine and uniform data on a local heat flux versus length plot. However, the length used on this plot for the uniform case is an equivalent length which is defined as

$$L_E \times \phi(Z) = \int_0^Z \phi_{MAX} \cos\left(\frac{\pi Z}{L_T}\right) dz$$

where $\phi(Z)$ = heat flux on the cosine tube at a point distant (Z) from the inlet. In this manner, for each location on the cosine tube, an equivalent length of a uniform tube is defined such that the local heat fluxes and integrated power inputs are the same at that point (Z) for uniform and cosine heat flux distributions (see Fig. 3). Using this refined method good results for the critical power and location are achieved for the range of cosine shapes tested ($M=5.0$).

Only three additional investigations have been completed utilizing flux distributions other than the cosine shape. Bertoletti et al⁽¹¹⁾ tested rods 25.4 in. long (64.5 cm) of .318 in. diameter (.807 cm) in water at 1020 psia (71.5 kg/cm²). These sections represented linear increasing and linear decreas-

ing flux distributions in addition to cosine and uniform distributions. In all nonuniform distribution cases the maximum flux to minimum flux ratio, M , was about 2.3. The data was presented to show the equivalence of total power input for test sections of all flux distributions for the same thermal and hydrodynamic test conditions. Review of the data confirms this equivalence for the cases of inlet quality above saturation. However for subcooled inlet conditions, which are of direct interest to many practical applications, divergence of total power input of up to 10 to 20% between the various flux distributions is apparent, with the exit peaked distribution exhibiting the lowest allowable total power. Additional CISE data reported by Silvestri⁽¹²⁾ further indicates that the total power input is not independent of flux shape for subcooled inlet conditions. In these experiments, heat was added uniformly over only the first and last quarter of the tube with the middle half being unheated. The data showed that for subcooled inlet conditions, the total power for the nonuniform flux distribution was also up to 10 to 15% below that for the uniform flux. Such deviations, which were also previously pointed out for exit peaked shapes in Swenson's data of reference (5), are of direct consequence to reactor design for the control-rods-withdraw configuration. In addition this deviation illustrates that the total power input equivalence concept is not valid over the complete range of nonuniform flux distributions of interest.

The experiments of Styrikovich et al⁽¹³⁾ were performed in 6.3 in. (16.0 cm) long tubes of diameter .236 in. (.6 cm) in water at 1470 and 2000 psia (103 and 140 $\frac{\text{kg}}{\text{cm}^2}$). The outside

diameter of the test sections varied linearly (increasing and decreasing) with length, hence the flux distribution varied as the square of the external diameter. Results with subcooled inlet conditions, which did not exhibit flow pulsations, indicated that the local critical heat flux for both increasing and decreasing flux shape was greater than the uniform critical heat flux at the same inlet conditions. In addition for the linearly decreasing flux, the onset of the critical condition occurred near the inlet as contrasted to the CISE tests where it was detected by wall thermocouples to set at the tube exit in all cases. To explain these results, the proposal is advanced by Styrikovich that the deviation of the upstream heat flux distribution from uniform causes an attendant deviation in vapor content in the boundary layer. Postulating that the vapor content in the boundary layer is effective in aiding or retarding the vapor film formation which causes the critical condition, higher upstream heat flux is predicted to promote achieving the critical condition while the reverse holds for lower upstream heat flux levels. This qualitative explanation has been modified and adopted in part in the analysis of the data of the present investigation.

Duke⁽¹⁴⁾ performed a series of critical heat flux and film heat transfer coefficient measurements with an exponential decreasing flux distribution ($M=27.0$) in 36 in. (91.5 cm) long tubes of .187 in. (.476 cm) diameter in water at 535 to 1915 psia (37.5 to 134.5 $\frac{\text{kg}}{\text{cm}^2}$). The range of mass flow rates investigated was limited to the rather low values of .01 to $.24 \times 10^6$ lb/hr ft² (13.6 to 325.0 $\frac{\text{kg}}{\text{m}^2 \text{sec}}$). The results for both critical

heat flux and heat transfer coefficient were correlated by statistical techniques and hence application of these correlations outside the limited range of variables investigated is very questionable.

Additional investigations with varied nonuniform flux distributions are presently being carried out in the USA and Sweden. The U.S. work is being performed at Babcock and Wilcox Co. on 72 in. (183 cm) long tubes of .446 in. (1.13 cm) diameter in water at pressures of 1000, 1500, and 2000 psia (70.2, 105 and $140.4 \frac{kg}{cm^2}$). The flux distributions include those of the previous Babcock and Wilcox work⁽⁵⁾ as well as several of the same distributions tested in annular configurations. The most recent progress report⁽¹⁵⁾ indicated that the data agreed well with that of their previous program. Preliminary Babcock and Wilcox review of this latest data indicated that analysis based on local condition hypothesis was not valid whereas analysis based on the integrated average critical heat flux or the input power to the critical location looked promising. Such an analysis is a variation of the total input power equivalence but realistically considers only the power input to the critical location.

The Swedish work⁽¹⁶⁾ is being performed for linear increasing and decreasing flux distributions in .236 in. and .394 in. (.6 cm and 1.0 cm) long tubes. The local burnout heat flux data is apparently predicted by the correlation of Becker⁽¹⁷⁾ when the nonuniform heat flux is accounted for in the related heat balance equation. The basic correlation is a

simplification of the results of Isbin⁽¹⁸⁾ which assumes the critical condition to occur at the axial position where the annular liquid film disappears. Becker achieves simplification of Isbin's model by assuming based on his own data for uniform tubes that the critical condition is a function of local conditions only. The success of this local condition hypothesis in predicting the critical heat flux for linearly increasing flux distributions is not surprising, since in this case the local flux and local enthalpy are both a maximum at the critical location. However, this is not the case for linearly decreasing flux where upstream burnout may occur and here the accurate predictions obtained may be significant. However a significant drawback of the entire procedure is that the critical location is not predicted and in fact the calculation of critical heat flux requires knowledge, presumably to be supplied from experimental data, of the critical location. However since the completed report is not yet available, comprehensive critical review of this method of analysis is not yet possible.

The most recently published work is that of Tong et al⁽¹⁹⁾ in which the hypothesis is forwarded that the critical condition occurs when the enthalpy of a superheated liquid layer adjacent to the heated surface reaches a limiting value. The superheated layer is presumably formed and maintained by a bubble layer which isolates it from the core. The limiting enthalpy value of nonuniform flux cases was taken equal to that for a uniform flux. Using this approach a correction factor, F , was defined to enable prediction of nonuniform behavior from existing uniform data.

$$F = \frac{q_{DNB}' \text{ equivalent to uniform flux}}{q_{DNB}' \text{ local in nonuniform flux}}$$

The analytic expression for F is a function of (1) local critical heat flux, (2) a constant C which was determined to be a function of local conditions and (3) an integral of local heat flux weighted by the factor $e^{-C(l_{DNB}^{-z})}$. Thus we see F combines local (1 and 2) and integrated (3) effects in a manner determined by the model chosen. This method is applied to experimental data of many varied flux distributions yielding predicted F values within $\pm 25\%$ of experimentally determined values. While this agreement does not significantly improve the accuracies available from other schemes, the method does yield the following significant result. In the subcooled and low quality region, the factor C is large and thus the product $C(l_{DNB}^{-z})$ is small. This reduces the weighting factor and results in local conditions primarily determining the critical condition. Conversely for high qualities, C is small and integrated conditions primarily determine the critical condition. Using a basically different model for the critical condition, this same dependence of the critical condition on local versus integrated conditions is obtained in the present work.

From the foregoing review of the literature, we see that most attempts to deal with nonuniform flux effects have been based a priori on a concept that the critical condition is a phenomenon related to either local or integrated conditions. Significantly these attempts have satisfactorily predicted behavior over only narrow parameter ranges. In addition their apparent

successful interpretations of similar data from diametrically opposite viewpoints has lead to much confusion. The efforts of Becker⁽¹⁶⁾ and Tong⁽¹⁹⁾, while not yet pointing the way to a general satisfactory solution of the problem, have been based on postulated models of the heat transfer and critical phenomenon. In the case of Tong in particular, the application of the model itself to the various nonuniform flux distributions determines the relative importance of local versus integrated conditions. Such an approach seems to be the most reasonable method of analysis and it is along these lines that the subject investigation has been directed. However, to fully comprehend the formulation of the model which has been applied, it is necessary to review what is known regarding the flow of water and steam in heated tubes. In the next chapter, therefore, the subject of two phase flow in tubes with heat addition will be discussed as it relates to the subject experiment.

CHAPTER II

TWO PHASE FLOW WITH HEAT ADDITION

To provide a sound basis for the developments presented in Chapter IV, the present understanding of two phase flow in tubes with heat addition will be reviewed.

2.1 Flow Regimes

Consider a cylindrical tube with vertical upflow of water under forced convection being electrically resistance heated. Adapting the discussion of Milloti⁽²⁰⁾ let us review with reference to Fig. 4 the dominant flow regimes and associated heat transfer mechanisms which will ideally exist along the tube.

Coolant water entering the bottom of the tube is below the saturation temperature corresponding to its pressure. In Section 1, where subcooled water exists forced-convection governs the heating process.

As the water temperature approaches the saturation value, the surface temperature reaches the saturation temperature. As soon as the surface temperature exceeds the saturation temperature by a few degrees, the liquid immediately adjacent to the heated surface becomes superheated. In this condition, if the degree of superheat is sufficient, bubbles can form along the surface at suitable nucleation sites. Under certain conditions bubbles have been found to slide along the wall surface in the direction of flow. As the bubbles grow larger, they detach from the wall and enter the fluid stream where they collapse because of the cooler bulk stream temperature. This Section, 2, is the subcooled nucleate boiling region.

When the bulk stream temperature reaches saturation, the bubbles can now be sustained in the turbulent flow of water. This Section, 3, is the saturated nucleate boiling region characterized by very high heat transfer rates. It is in this region that the quality of the two-phase flow begins to increase. The bubbles cause a very high turbulence in the superheated liquid, as they grow and detach themselves from the wall. This intense turbulence of the liquid upon the surface accounts for the high heat transfer rates in this bubble flow region. As more and more bubbles form at the wall and join the bulk stream, they start to coalesce and form larger bubbles. This tendency is expected, because a large bubble has less surface area than the equivalent volume of small bubbles and thus there is a tendency for bubbles to agglomerate. The flow is now unstable under all conditions, and eventually slugs of intermittent water and steam give the hydrodynamic pattern called slug flow as shown in Section 4.

Downstream from Section 4, the steam slugs begin to predominate and the steam increases in proportion to the water to the point where it can now be considered the continuous phase. A thin film of slow moving superheated liquid forms on the wall, while the steam flows in the central core. The liquid film thickness is of the order of thousandths of an inch and has a wave-like surface. The steam moves with a much higher velocity than the liquid film, resulting in high heat transfer coefficients and an annular slip-type flow shown in Section 5. There is usually also a spray of small droplets in the steam core, hence, the name spray-annular flow region. Through Section 5,

the liquid film flow rate on the wall decreases due to net entrainment of liquid from the film and evaporation of the film. Depending on the local heat flux and quality, nucleation can also occur within the thin liquid film. Heat transfer can be thought of primarily as conduction through the liquid film with evaporation at the liquid-vapor surface.

When Section 6 is reached, the liquid film has disappeared, the wall is dry, and one finds tiny droplets of water in the steam. As soon as the liquid film is destroyed and the wall dry, the evaporative cooling of the wall breaks down, causing a very large decrease in the heat transfer coefficient with a correspondingly large increase in wall temperature. In Section 7, single-phase dry saturated or superheated steam is present. Because only single-phase steam is present in this region, it can be considered a film boiling region. However, the heat fluxes which can be carried under this condition are considerably lower than those which can be carried with non-film boiling.

From this discussion, it is seen that the critical condition can be caused by at least two different mechanisms, (1) in the subcooled or low quality region by a vapor blanketing of the tube wall, or (2) in the high quality region by dryout of the liquid film. In fact, the occurrence of the critical condition can also be postulated to be caused by a nucleation induced disruption of the liquid film or by the instability characteristics of the slug region. Hence it is desirable

to quantitatively identify the existence of the various flow regimes possible and the transitions between these flow regimes. Flow maps exist for predicting this information for adiabatic systems but since the effects of heating tend to distort the regime boundaries, such maps are not an accurate representation of conditions with heat addition. Generally speaking, heating may be expected to promote the transitions between the regimes shown in Fig. 4 so that for given pressure and mass flow rates these transitions occur at lower qualities than in the adiabatic case. In particular the bubbly flow region may be suppressed and the flow may go directly from single phase to slug flow. Similarly the slug-annular transition may occur at lower quality. From limited results reported at high pressures by Suo⁽²¹⁾ and at low pressures by Lopina⁽²²⁾, such expectations seem to be borne out.

With regard to the low pressure conditions of the subject tests, the corrections to an adiabatic flow map due to heating are small since the flow regime transitions occur at relatively low qualities. Considering the test conditions and the dimensions of the test sections, the relevant flow regime map for these experiments is presented in Fig. 5. The transitions pictured are limited to the transitions to annular from both bubble and slug.

At high mass velocities the annular transition is taken from the correlation of Baker.⁽²⁴⁾ For these conditions, the slug regime is suppressed and the transition occurs directly from bubbly to annular flow over the quality range of approxi-

maetly 6 to 10%. It should be recognized that at a given mass flow rate this transition to annular flow is gradual and intermediate flow regimes are probably encountered before true annular flow is achieved. As Fig. 5 shows, this transition describes conditions in the region of the test conditions investigated. Due to non-adiabatic conditions, additional uncertainties in the actual location of the flow regime transition are introduced. Hence a mean value of 8% was chosen to characterise the annular transition for all three flow rates of the subject data.

For completeness, the annular transition at lower flow rates is also illustrated on Fig. 5. At these low flow rates, the transition is from slug to annular flow and was calculated from the correlation of Haberstroh and Griffith.⁽²³⁾

2.2 Critical Heat Flux

Prediction of the critical heat flux for uniform flux distribution is necessary in this study for two reasons:

(a) a uniform flux distribution correlation is required to evaluate published correlation methods for nonuniform flux distributions such as that of Janssen et al⁽⁶⁾ and Lee⁽¹⁰⁾.

(b) test runs with uniform distribution should be checked against available correlations to insure that operating procedures and the experimental rig are performing satisfactorily.

Unfortunately there is no existing low pressure (14.7 to 200 psia) quality range correlation which is applicable over a wide range of test conditions and geometries. In fact data in this region is limited to that of Lowdermilk and Weiland⁽²⁵⁾, Jens and Lottes⁽²⁶⁾, Lowdermilk, Lanzo and Siegel⁽²⁷⁾, Becker⁽²⁸⁾, Becker and Persson⁽¹⁷⁾ and Lopina⁽²²⁾. From this data, four correlations are available which use certain of this data as indicated below:

<u>CORRELATION</u>	<u>DATA SOURCE</u>
Lowdermilk, Lanzo and Siegel ⁽²⁷⁾	Lowdermilk, Lanzo and Siegel ⁽²⁷⁾
Von Glahn ⁽²⁹⁾	Lowdermilk, Lanzo and Siegel ⁽²⁷⁾
MacBeth ⁽³⁰⁾	Lowdermilk and Weiland ⁽²⁵⁾ } Jens and Lottes ⁽²⁶⁾ } 15 Becker ⁽²⁸⁾ } psia 250 psia
Becker and Persson ⁽¹⁷⁾	Becker ⁽²⁸⁾ , Becker and Persson ⁽¹⁷⁾

The correlation of Lowdermilk, Lanzo and Siegel⁽²⁷⁾ is based on their data obtained at inlet temperature of 75°F, atmospheric exit pressure, and diameters from 0.051 inches to .188 in. The correlation establishes two burnout regimes: a high velocity, low-exit quality regime for $G/(L/D)^2 < 150$ correlated by $(q/A)_{CR} D^{0.2} (L/D)^{0.15} = 1400 G^{0.5}$

and a low velocity, high exit quality regime for $G/(L/D)^2 > 150$ correlated by

$$(q/A)_{CR} D^{0.2} (L/D)^{0.85} = 270G^{0.85}$$

The correlation of Von Glahn⁽²⁹⁾ is intended to cover cryogenic fluids as well as water over the pressure range 14.7 to 2000 psia. The correlation is based on a relationship developed between X_c , a critical vaporization parameter, and a function consisting of several dimensionless groups. Specifically

$$X_c = f \left[\underbrace{\frac{GD}{(L/D)^{1.3}}}_{\text{Flow Parameter}} \underbrace{\frac{P_{r_v}^{0.4}}{\mu_v} \left(\frac{\rho_e - \rho_v}{\rho_v} \right)^{0.4} \left(\frac{\mu_v}{\mu_L} \right)^{1.7} N_B}_{\text{Fluid Property Parameter}} \right]$$

where $X_c = \frac{Q_c}{w\Delta H}$

$$N_B = \frac{\sqrt{g} \mu_v^2 \sqrt{\rho_e - \rho_v}}{\rho_v (g_c \sigma_e)^{1.5}}$$

the functional relation f being graphically described in the NASA report.

The MacBeth correlation⁽³⁰⁾ also represents data as either a high-velocity or a low velocity regime with the boundary between regimes defined graphically. For a system pressure $p < 200$ psia, and a $L/D < 200$, the maximum mass velocity for existence of a low velocity regime is $.25 \times 10^6$ lb/hr ft². Thus the data for this report lies within the high velocity regime which is given as

$$q/Ax10^{-6} = \frac{A + \frac{1}{4}CD(Gx10^{-6})\Delta H_1}{1+CL}$$

where $A = y_0 D^{y_1} (Gx10^{-6})^{y_2}$

$$C = y_3 D^{y_4} (Gx10^{-6})^{y_5}$$

D ≡ inches

The "y" coefficients obtained by MacBeth by computer optimization of data at various pressures are

	<u>15 psia</u>	<u>250 psia</u>
y ₀	1.12	1.77
y ₁	-0.211	-0.553
y ₂	0.324	-0.260
y ₃	0.001	0.0166
y ₄	-1.4	-1.4
y ₅	-1.05	-0.937

Finally the correlation of Becker⁽¹⁷⁾ as discussed in Chapter I covers the pressure range 142.5 to 195.0 psia. The correlation, which is based on extension of the flow model of Isbin⁽¹⁸⁾ is presented as curves of

$$\frac{1}{q/A \left(\frac{\dot{m}}{F}\right)^{1/2}} \text{ versus } X_{\text{CRIT}}$$

where $X_{\text{CRIT}} \equiv$ the steam quality at the critical location

$$q/A \equiv \text{surface heat flux, } \frac{\text{kJ}}{\text{m}^2 \text{S}}$$

$$\frac{\dot{m}}{F} \equiv \text{mass velocity, } \frac{\text{kg}}{\text{m}^2 \text{S}}$$

Each of these correlations together with the uniform flux distribution data of this report are plotted in Figs. 6, 7, and 8. The wide variation in predicted critical heat flux values

is obvious. In addition the dependence of critical heat flux on pressure for the MacBeth correlation is opposite to that for the Becker and Von Glahn correlations. In appraising these figures the following conclusions can be drawn (the deviation between stable and unstable points will be discussed in Chapter III).

(1) The MacBeth correlation contains only the early and limited data of Lowdermilk and Weiland⁽²⁵⁾, which is suspect to flow instabilities as described in the later report by Lowdermilk⁽²⁷⁾, and the data of Jens and Lottes⁽²⁶⁾ which was taken at low flow rates ($.01$ to $.04 \times 10^{-6}$ lb/hr ft²) in large diameter (.94 in) tubes. Hence this correlation would not be expected to yield reasonable results for the subject test conditions.

(2) The Von Glahn and Lowdermilk correlations are based on Lowdermilk⁽²⁷⁾ data which had limited diameters (up to .188 inches) and a single subcooling. Thus as discussed by Lopina⁽²²⁾ for the test diameters of the subject test data, these correlations are not applicable.

(3) The Becker correlation yields good agreement with results at low flow rates ($G = 0.5 \times 10^6$ lb/hr ft²). As flow rate increases, the agreement becomes poorer.

(4) The 250 psia prediction of MacBeth's correlation agrees well with the data. However the data is at generally lower pressures than the pressure for which the correlating line was established.

These results indicate that the available low pressure correlations do not appear to be based on the correct fundamental variables. Hence although each is satisfactory over the range of data from

which it was derived, none can be safely extrapolated to the desired region of the subject test conditions. Therefore, the best empirical procedure for representing the present data appears to be use of a simple equation of the form, $(q/A)_{CR} = C_1 + C_2 \Delta H_{INLET}$ where the constants can be determined from the data of Figures 6, 7 and 8.

CHAPTER III

EXPERIMENTAL PROGRAM

3.1 Description of Apparatus

The following section contains a description of the experimental facility and test sections which was used in this investigation. This was divided into four categories: the hydraulic system, the power supply, the associated instrumentation and the test sections. Although detailed descriptions of the apparatus are available in other reports,⁽³¹⁾ they are repeated here for the convenience of the reader. The basic apparatus had been designed and constructed in a previous study by Bergles.⁽³²⁾

3.1.1 Hydraulic System

A schematic of the flow loop is shown in Fig. 9. The pipings and fittings, all of brass and stainless steel for corrosion resistance, are erected around a test bench constructed of Dexion slotted angles and plywood. Rayon reinforced rubber hose was used where flexible connections were required. Flow circulation is provided by a Fairbanks Morse two-stage regenerative pump (260 psi at 3.6 gal/min) driven through a flexible coupling by a 3 HP Allis Chalmers induction motor. To avoid contamination of the system water, the pump was fitted with special seals of teflon-impregnated asbestos. A relief valve set for 300 psi protected the pump casing from overpressure.

The main flow loop contains a Jamesbury ball valve to control the overall pressure drop. The test section line, installed in parallel with the main loop can be isolated by means of two more Jamesbury ball valves. To limit coolant

loss upon test section failure, upstream and downstream check valves were built into the test section connector pieces. The upstream valve contains a spring sized to hold the valve open during normal operation with system pressure on either side of the valve but closed at test section failure with system pressure upstream and ambient pressure downstream. The downstream valve is simply held open by system pressure during normal operation but closed at test section failure by the pressure difference between the back system pressure and the ambient test section pressure. The test section flow rate is controlled by means of Jenkins needle valves set just upstream and downstream of the test section itself. The valve downstream is particularly useful in adjusting test section pressure. The test section line also contains two basic Fischer-Porter flowmeters with the appropriate isolating valves. Four Chromalox heaters of approximately 6 kw. each are also provided to control the test section inlet temperature. Three of these are controlled simply with "off-on" switches while the fourth can provide a continuous range from 0 to 6 kw. by means of a bank of two variacs mounted on the test bench. Pressure fluctuations at the outlet of the pump are damped out by means of a 2.5 gallon Greer accumulator charged with nitrogen to an initial pressure of 40 psi. This accumulator contains a flexible bladder-type separator which prevents the nitrogen from being absorbed by the system water. A Jamesbury ball valve isolates the accumulator from the loop at shut-down.

Since the system is closed loop, the heat added to the system water is rejected to a shell-and-tube heat exchanger

connected to a city water line. Due to seasonal temperature variations, the minimum operating temperature varies from approximately 50°F in the winter to 75°F for summer operation. Continuous deionization and deoxygenation is provided in a parallel loop containing four resin beds, two of which provide deionization and the other two, deoxygenation. The conductivity of the loop water may be maintained at 1.5×10^6 ohm-cm as read on a Barnstead meter. In order to insure a minimum of dissolved air in the system, a 5 gallon degassing tank was provided with five electrical heaters (3-220 VAC and 2-110 VAC). This tank was also used to provide makeup water to the system. A storage tank for filling the system and degassing tank was mounted above the degassing tank and could be filled with distilled water from standard 5 gallon bottles with a small Hypro pump. Both the storage tank and the degassing tank were equipped with glass sight gages so that the proper levels could be maintained.

3.1.2 Power Supply

Power was supplied to the test section by means of two 36 kw. Chandrysson externally excited generators, each capable of delivering 3000 amperes at 12 volts. The generators are driven by 440 volt-3 phase-600 rpm synchronous motors.

The power could be regulated from zero to maximum power as desired through a portable control console. The generator outputs were connected in series and the output from one was added to or subtracted from the output of the other. Water-cooled shunts, installed in parallel with the test section, eliminated the shock of a sudden open circuit caused by a test section

burnout.

An existing buss-bar system was used, with the addition of air cooled copper braided cables just at the test section. The use of these flexible cables permitted flexibility in the size of the test section which could be accommodated. At the upstream end of the test section, the cable assembly is clamped to an aluminum plate to which a rigid aluminum test section holder is attached. At the downstream side, the connection to the test section holder is accomplished by a flexible braided conductor. This entire connection to the test section was put in tension by a spring arrangement to assure adequate allowance for thermal expansion of the test section. The test section holders were made of aluminum plate in two segments which, when bolted together, clamped to a bushing surrounding the test section. The downstream end of the test section was connected to the piping with rubber hose to provide electrical insulation and increased flexibility.

3.1.3 Instrumentation

Instrumentation was provided to monitor the steady-state and transient conditions throughout the system. Pressure gages on the main loop, as indicated in Fig. 9, aid in adjusting the pressure level in the test section and in determining system stability. A thermocouple was installed in the degassing tank to monitor the water temperature during degassing operations. Another at the discharge of the pump insured that the water temperatures in the deionizing beds never exceeded 140°F. A variety of metering tubes and floats which could be installed interchangeably in the basic Fischer-Porter flowmeter housing

provided measurement of the test section flows from 1.5 to 4000 lbm/hr. The results were calibrated at installation and checked periodically against the initial calibration.

The test section itself was instrumented with thermocouples to record inlet and outlet water temperatures. In both cases, the thermocouples were located at positions where the flow was well-mixed. At the downstream end, the thermocouple was located far enough from the exit of the heated section so that it could be safely assumed that the vapor fraction is completely condensed.

Thermocouples were constructed from Leeds and Northrup 24-gage duplex copper-constantan wire. Calibrations were performed and deviations from N.B.S. standard tables were found to be slight so that no corrections were necessary. All of the thermocouples were connected to a common ice junction through a twelve position Leeds and Northrup thermocouple switch. The output could be read on either a potentiometer or a recorder. The recorder is a pen-type, single channel instrument manufactured by Minneapolis-Honeywell Brown. There are five manually selected ranges for 0-6, 5-11, 10-16, 15-21, and 20-26 millivolts. Occasional calibration against the potentiometer insured the accuracy of the recorder to within .01 millivolts.

Test section pressures, both upstream and downstream were monitored on 4 1/2 inch U.S. gage supergages with 0-200 psi range. Each gage was checked on a dead weight tester and calibrated to an accuracy of approximately .5 psi over the entire range. They were checked against one another periodically at various static pressure levels under zero flow conditions.

Porous-plug snubbers were provided to protect the gages from severe pressure fluctuations.

The heat input to the test section was computed from measurements of the voltage drop across the heated length and the current to the section. The voltage drop was read on a Weston, multirange d.c. voltmeter with a specified accuracy of $\pm 1/2\%$ of full scale. The current was inferred from the voltage drop across an air-cooled N.B.S. shunt with a calibrated conductance of 60.17 amps/m.v.

3.1.4 Test Section

The required flux shapes were obtained by machining the tube outside diameter to obtain the desired variation in wall cross-sectional area since electrical power generation is directly proportional to resistance. The design was made within the limits imposed by (a) available power and hydraulic supply (b) test conditions and geometries desired for investigation and (c) materials having adequate resistivity and machinability. A discussion of the interplay between these variables and the final test section designs is presented in Appendix C. Confirmation of the shape of the experimental flux distribution was obtained on a sampling basis by room temperature incremental resistance measurements and by 100% inspection of resultant outside diameter dimensions. Details of the results of these procedures and discussion of other factors affecting the shape of the experimental flux distribution are included in Appendix A. See Figure 10 for schematic presentation of the various test sections used in the investigation.

3.2 Experimental Procedures and Experience

3.2.1 General Loop Operation

Many aspects of the experimental procedure, particularly the installation of test sections and final preparation of the loop for operation, were common to all types of runs. Distilled water was pumped into the storage tank from the standard five gallon bottles. The system and degassing tank were filled by gravity. Vents on the flowmeter, preheaters, test section, exit plenum, and the deionization tank were opened to allow the displaced air to escape. The degassing tank vent was open at all times. The other vents were closed when no further bubbles were seen. The pump was then turned on and all valves opened and closed several times to dislodge any remaining air pockets. The vents were then opened and closed again in turn until air-free water was obtained at each vent. Visual observation of the flow through the glass flowmeter tube aided in determining when the system was free of air.

At this point, all the degassing tank heaters were turned on, and water was circulated through the system. The temperature of the degassing tank water was monitored on the recorder, and all but one of the heaters turned off as the boiling point was approached. If this was not done, the degassing tank was found to boil too vigorously with the result that considerable overpressure built up in the tank and a large amount of water was forced out through the vent. When boiling occurred, water from the loop was bypassed into the degassing tank. The amount of flow was regulated so that a small but continuous

flow of steam issued from the vent hose. The system water was effectively degassed by being dumped into the boiling water at the top of the degassing tank. This was continued until the temperature in the loop rose to approximately 180°F. Care was taken to shut off flow to the deionization tank before the loop temperature exceeded 140°F. The entire procedure took about 30 minutes. A standard Winkler analysis, described in Reference (32), indicated that this method of degassing reduced the air content to less than .1 cc air/liter. Upon completion of the process, the remaining tank heaters were shut off, and the heat exchanger turned on. The flow of system water to the degassing tank was turned off as soon as steam stopped coming out the vent. The system was then ready for operation. This process was repeated at the beginning of each day of operation, where the degassing tank was refilled, or when air bubbles were visible in the flowmeter. The daily degassing was necessary since the degassing tank is vented to the atmosphere, and the water in the tank would eventually become saturated with air (18 cc/liter).

The system was then operated for at least 15 minutes at zero power before taking measurements. At the end of this time the system water was completely cool and had been thoroughly circulated through the deionizers. This time was also used to allow the generators to warm up. If the generators were used immediately after starting, fluctuations in the power level were much larger and harder to control. If a particularly low resistance test section was in place, it was necessary to disconnect one of the power leads until the generators had come up to speed. If this was not done, high

voltage drops could result from the fact that the two generators did not speed up in unison and on occasion could lead to unwanted burnouts.

At shutdown, it was necessary to isolate the accumulator from the loop. Otherwise, the water would be forced out of the accumulator, into the loop, and eventually out through the degassing tank vent. The pump and generator were connected together electrically so that the generators would be shut off if the pump should be turned off accidentally or due to a power failure. However, the generators could be shut off independently by means of a switch on the control console. Turning off the generators or the pump also interrupted the power to the preheaters. This was a safety precaution to prevent burning out the heater elements should they be left on with no flow.

3.2.2 Loop Operation for Critical Heat Flux Data

At the beginning of each test run, the bypass flow was reduced to maximize the pressure drop taken across the needle valve upstream of test section. A large upstream restriction pressure drop was desired to minimize the occurrence of flow oscillations. These oscillations did occur early in the test program and steps taken to analyse and eliminate them will be discussed in Section 3.2.4. For low mass flow rates ($G=0.5 \times 10^6$) a 3/8" exit line was used and desired exit pressure maintained throughout the entire test run by adjusting the needle valve in the line. For higher mass flow rates ($G=1.0$ and 2.0×10^6) a 1" exit line was used but in this case since valve manipulation

did not allow adequate adjustment of exit pressure, the exit pressure was not directly set but allowed to vary within the desired range with the power level and inlet subcooling.

With the mass flow rate and test pressures established, the generators were turned on and power applied to the test section. After a heat balance was taken, power level was gradually increased simultaneously with adjustment of inlet temperature by operation of the loop preheaters. This adjustment was complete before the test section power achieved approximately 50% of the anticipated burnout power. In the final approach to burnout, mass flow rate and inlet temperature were maintained constant as power was increased in small steps. Test section inlet and exit pressures were maintained approximately constant at low flow rates but increased at high flow rates as power increased. At each step in power level, values of all these variables were recorded manually. Since only inlet temperature was automatically recorded, only values of inlet temperature and test section voltage (meter was continually viewed) were noted at burnout. The values of all other parameters at burnout were obtained by extrapolating data recorded at previous power steps.

When burnout did occur, the generators, preheaters and pump were turned off and the test section line isolated from the main loop. When a new test section was inserted, a small volume of undegassed water was necessarily allowed into the system from the fill tank because the test section line was above the level of the degassing tank. Care was taken to bleed the system under such circumstances to minimize the

amount of air entrapped in the system. When the pump was restarted, the flow meter was observed to ensure that air bubbles were not present. This departure from the initial thoroughly degassed conditions for certain test runs was considered acceptable since critical test results should not be effected by slight differences in the degassed condition of the loop water.

3.2.3 Two Phase Heat Transfer Coefficient Measurements

In addition to burnout measurements, an attempt was made to measure two phase heat transfer coefficients. As discussed in Chapter IV, such data is necessary for the critical heat flux model presented. For these measurements, a test section with two independent power supplies attached was used. The inlet portion was heated with the generators described in Section 3.1.2, while a 1.5 inch portion at the exit was heated by a motor generator set capable of delivering about 17 volts at 700 amperes. The power to the inlet section was adjusted to yield a desired quality condition in the exit portion. The exit section or nucleation section was designed to minimize the heat input to the fluid (and hence the quality change) but maximize the available heat flux which could be achieved. By measuring temperature differences, $T_{WALL} - T_{SATURATION}$ at pre-established values of pressure, mass flow and quality, determination of heat transfer coefficients for these conditions was attempted.

The experimental difficulties encountered for the test conditions explored i.e. steam-water mixtures at $X=.10$ to $.60$, $P=100$ psia, $G=0.5$ to 2.0×10^6 lbm/hr ft² and $D=.214$ inches, were

- a) The mechanical strength of the nucleation portion of the test section was poor due to the thin wall

required to achieve high heat fluxes by resistance heating with the available power supply. The wall thickness could be increased by decreasing D, or by heating the test section indirectly by conduction from a resistance coil wound around the test section.

- b) The exit pressure could not be maintained constant for flows in the quality region thus causing $T_{\text{SATURATION}}$ to vary. This may be able to be corrected by installation of a pressure regulating valve, although it appears that the configuration and hydraulic characteristics of the existing loop prevent adequate correction of this problem.
- c) Accurate measurement of low temperature differences, .5 to 3^oF, was not possible due to (b) above as well as inherent difficulties in accurately measuring the wall temperature, even with a guard heater arrangement.

Although some data was obtained it was generally not internally consistent, particularly in the low temperature difference regions of interest. Hence, the heat transfer coefficients obtained were not considered accurate and therefore not used further in this work.

3.2.4 Correction of Oscillatory Instabilities

Certain of the data obtained during the loop checkout with uniform heat flux distribution exhibited critical heat flux values (see Figs. 8 and 9) significantly lower than the bulk of other data. In addition during certain of these experimental runs, the flow rate was observed to oscillate as the

critical condition was approached.

Although no compressibility was deliberately inserted in the system between the control valve and the heated section, it was felt that enough compressibility was present upstream of the control valve in the form of preheaters and accumulators to initiate an instability if other conditions were also present. These conditions reduce per the theory of Maulbetsch⁽³¹⁾ to the requirement that the slope of the overall pressure drop vs flow rate curve goes to zero. Overall pressure drop here includes both the control valve and the heated section. Check of the suspect points by this method confirmed that the instabilities resulted from this cause. A sample graphical comparison is given on Fig. 11 of the heated section versus control valve pressure drop which shows that the overall slope does go to zero at the flow rate where oscillation and the critical condition occurred. Similar calculations along with some experimental measurements were made on the points which were believed to be valid and the overall slope was established as positive.

To eliminate this oscillatory instability based on this theory, an increase in the slope of the control valve characteristic or a decrease in the slope of the test section characteristic is necessary. Since the test section characteristic is determined by the desired test conditions, only modification of the control valve characteristic is possible. For the loop available, the pump delivery pressure and the heat exchanger condensing pressure (15 psia) limit the overall pressure drop available which is distributed between the control valve, test section, and other line losses. Hence, to increase the control

valve pressure drop, extraneous line losses were reduced by increasing the exit line diameter from 3/8" to 1". With this modification, stable data at the higher flow rates was obtained. However for conditions of low inlet subcooling, instabilities were encountered for certain test sections exhibiting rapid axial variation in heat flux and data under these conditions could not be obtained. Apparently, in these cases the test section pressure drop vs flow rate characteristic became equal to the control valve characteristic thus causing the slope of the overall pressure drop characteristic to go to zero. It should be noted that this problem could probably have been corrected and data for these cases obtained by installation of a higher head pump which would permit increased pressure drop to be taken across the control valve.

3.2.5 Critical Flow Considerations

Since the sonic velocity can be quite low in a two phase flow, it is desirable to check whether or not a choked flow condition existed. Such a condition could lead to erroneous results regarding critical heat flux levels for various operating conditions. Using the slip equilibrium model of Fauske⁽³³⁾, from Fauske's Fig. 4, we see that the minimum critical velocity is achieved at minimum pressure and maximum quality. Calculating this minimum critical velocity for composite worst case test conditions, we obtain the results shown below. Basing the calculation on a hypothetical composite case which would yield a higher predicted critical velocity than any real case assures that the results obtained are conservative estimates. Since the actual

Actual Mass Velocity	Composite Worst Case				Predicted Critical Velocity	Actual is % of Predicted Critical Velocity
	Tube Num.	Minimum Observed Pressure	Tube Num.	Maximum Observed Quality		
556 $\frac{\text{lb}}{\text{sec ft}^2}$	2554	72	1256	.35	620 $\frac{\text{lb}}{\text{sec ft}^2}$	90%
278	1502	57	508	.52	320	87%
139	514	85	1552	.80	300	45%

velocities are in all cases less than the predicted critical velocities, it is reasonable to conclude that the critical velocities were not achieved during the experimental program. Direct confirmation of this conclusion by varying the test section exit pressure to achieve a critical velocity was not possible due to the operating limitations of the test loop.

CHAPTER IV

PRESENTATION AND DISCUSSION OF RESULTS

4.1 Experimental Results

The complete range of variables investigated was presented in Chapter I. Basically for each axial flux distribution, critical heat flux tests were conducted at three mass velocities, $G = 0.5, 1.0$ and 2.0×10^6 lbm/hr ft² and a range of inlet subcooling conditions. The total number of tests, each carried to physical failure of the test section was approximately 144. A complete listing of the experimental data is presented in Appendix I

The basic experimental results are presented as:

- 1) the total power applied to a channel to attain a critical condition (defined in this investigation as physical destruction of the aluminum test section). This parameter is of particular interest since maximization of Q_{crit} is a prime objective in engineering design.
- 2) the physical location of the critical condition (defined in this investigation as the failure location in the aluminum test section).

The test results for each of the three mass velocities are presented in terms of Q_{crit} and critical location in Figures 12 through 22. It should be noted that in all cases the inlet condition was subcooled and the total critical power, Q_{crit} , in these figures is presented as a function of the independent variable, inlet subcooling ΔH_{in} .

4.1.1 Total Critical Power

Considering the uniform flux results as a basis for reference, the following observations of Q_{crit} are apparent from

Figures 12, 15, and 17 which present cosine flux distribution behavior and Figures 21 and 22 which summarize behavior of the remaining flux shapes.

Q_{crit} - Cosine and Other Flux Distributions with Maximum Flux
Near or at the Test Section Inlet

The value of Q_{crit} for these distributions is general 10% larger than Q_{crit} for uniform flux data. However, for the inlet flux peak distribution, the value of Q_{crit} did drop to 10% less than Q_{crit} for uniform flux data as the mass flow velocity increased to $G = 2.0 \times 10^6$ lbm/hr ft². As the inlet condition approaches saturation, Q_{crit} for these nonuniform flux distributions decreases in the same manner as the uniform flux data. There is no apparent dependence of Q_{crit} between distributions of the same shape with different M values (ratio of maximum to minimum flux). For cosine flux distributions in particular, no apparent stratification exists between the results for M = 2.27, 4.0 and 5.75. These results indicate that the total critical power, Q_{crit} cannot be significantly increased by tailoring of the flux distribution to an optimum shape.

Q_{crit} - Flux Distributions with Maximum Flux Near or at the
Test Section Exit

The value of Q_{crit} for these distributions can be significantly less than Q_{crit} for uniform flux distributions at the same operating conditions. The deviation depends on the degree of inlet subcooling, ΔH_{in} , the mass velocity, G, the flux shape, and its associated M ratio. For the maximum inlet subcooling investigated, about -300 btu/lbm, Table IV-A below summarizes the maximum decreases observed in total critical power.

Flux Distribution	MASS VELOCITY, G, LBM/HR-FT ²		
	0.5 x 10 ⁶	1.0 x 10 ⁶	2.0 x 10 ⁶
Linear increasing (M=2.27)	-20%	-5%	-5%
Linear increasing (M=5.75)	-35%	-15%	-30%
Peak exit (M=5.75)	-15%	-15%	-30%

Table IV-A

MAXIMUM DECREASE IN Q_{CRIT} COMPARED TO UNIFORM FLUX
DISTRIBUTION RESULTS

As the inlet condition approaches saturation, the deviations of Table IV-A decrease, resulting in approximately equal values of Q_{crit} for uniform and nonuniform flux distributions at low inlet subcooling levels.

The increased deviations with increased M for a given flux shape are clearly apparent in the table above. This dependence is observed for results in the annular regime and several results which were obtained in the subcooled region. In fact the test data show (Fig. 21 and 22) that if the flux distribution is severely peaked, the flux level can be high enough to cause a critical condition at a location where subcooled conditions prevail. Thus the actual flux distribution can cause both (1) decreased Q_{crit} compared to uniform flux data when both data are in the annular regime and (2) severely decreased Q_{crit} due to a subcooled critical condition which occurs at a high flux location of the nonuniform distribution.

Similar results have also been obtained by other experimenters at higher pressures. Portions of the data of Bertolotti (11), Swenson (5) and the most recent Babcock and Wilcox inves-

tigation (15), are presented in Figures 23, 24 and 25 which confirm the principal observations of this study, namely

- 1) For cosine and other distributions with the maximum flux near or at the test section inlet, Q_{crit} is within $\pm 10\%$ of uniform flux data and decreases as ΔH_{in} approaches the saturated inlet condition.
- 2) For distributions with the maximum flux near or at the test section exit, Q_{crit} can be up to 30% less than the uniform flux data at large inlet subcoolings. This deviation approaches zero as ΔH_{in} approaches the saturated inlet condition.

4.1.2 Critical Location

The location of the critical phenomenon for each test section was also determined experimentally and is presented in Figures 14, 17, and 20. The tabulation of Appendix F in some cases indicated two critical locations. In these cases, before effective corrective action was taken, the test sections were somewhat bowed during testing and upon attaining the critical condition, both a thermal failure and mechanical failure occurred. The thermal failure was characterized by melting of approximately an 1/8" wide by 1" long (axial) rectangular portion of the test section. In Appendix F, the actual critical location is reported as the midpoint of the thermal failure with its axial extent listed as the \pm value. The mechanical failure was a complete circumferential shearing of the test section characterized by a jagged unfused cleavage. In certain cases, which are noted, a double thermal failure did occur. In all other cases, the first

listed location, is the thermal failure location and this is used in subsequent analysis. These results can be summarized as follows.

CRITICAL LOCATION - UNIFORM FLUX

The critical location occurred within 1% of the test section exit, the slight deviation probably being attributable to axial conduction effects.

CRITICAL LOCATION - MONOTONICALLY INCREASING FLUX (i.e. LINEAR INCREASING)

The critical location occurred within 1% of the test section outlet except for one case. In this case, test section 1204 which was tested at $G = 1.0 \times 10^6$ and $\Delta H_{in} = -160$ BTU/LEM, the critical location was slightly upstream from the exit ($.7 \pm .5$ inches from exit of the 30 inch test section).

CRITICAL LOCATION - FLUX PEAK ALONG TEST SECTION AT ANY LOCATION EXCLUDING EXIT (i.e. COSINE, PEAK NEAR INLET, PEAK NEAR EXIT, LINEAR DECREASING)

The critical location for these flux distributions always occurred between the flux peak and the test section exit or at the test section exit. The critical location is dependent on inlet subcooling, ΔH_{in} , and moves upstream from the tube exit with increased subcooling. In addition, for a given flux shape, the critical location appears also dependent on M. For example for cosine distributions the critical location is further upstream for M values of 2.27 and 5.75 versus 4.03. For linear decreasing flux shape, increased M value (5.75 versus 2.27) results in upstream movement of the critical location.

The data of other investigators generally confirm these results particularly the upstream movement of the critical location for the peak inlet flux distribution with increased inlet subcooling. However precise determination of the critical location was not generally obtained due to the burnout detection systems used. The CISE investigators (11) on the other hand, indicated that in all cases the onset of the critical condition occurred at the test section exit.

The possibility that the onset of the critical condition occurred at the exit but moved, causing a physical failure upstream, was considered and investigated in this work. Differential thermocouples were used with the point of interest and an unheated exit portion of the test section as the two opposing inputs. A series of thermocouples were simultaneously used to monitor several locations between the tube exit and the expected burnout location. The output from these thermocouples was recorded on a multichannel recording oscillograph by galvanometers with natural frequencies ranging from 50 to 300 cycles per second. However, these traces did not show movement of a wall temperature excursion from the tube exit to the critical location. Thus it appeared that the critical condition occurred initially and only at the location of tube failure.

4.1.3 Reproducibility of the Data

Several runs were made at almost identical inlet and mass velocity conditions to establish the reproducibility of the data. These results, tabulated below in Table IV-B, indicate that differences exist in total critical power, Q_{crit} , up to $\pm 10\%$ and in critical location up to 4.0 inches. Note that

Test Section	Date	Flux Shape	M	$\frac{G}{\text{HR FT}^2}$	ΔH_{inlet} $\frac{\text{BTU}}{\text{LBM}}$	Q_{crit} $\times 10^{-5} \frac{\text{BTU}}{\text{hr}}$	% Diff.	Critical Location Inches (From Inlet)	Inches Diff.
142	10/21	UNIFORM	1.0	2.0×10^6	-271.2	2.029	10%	29.8±0	
135	9/25			1.99×10^6	-270.8	2.232		29.6±0	
310	9/3	COSINE	4.03	1.0×10^6	-246.5	1.435	7.2%	24.0±0	3.2 to 4.0
333	9/23				-246.9	1.538		27.6±.4	
511	10/14	COSINE	5.75	0.5×10^6	-159.2	7.404	8.3%	24.3±.2	1.3 to 2.1
512	10/14				-154.4	6.837		22.6±.2	
1271	11/12	LINEAR	2.27	1.0×10^6	-249.9	7.572	5.5%	26.4±1.4	0 to 3.3
1252	11/19	DECREASING			-247.5	7.988		25.5±1.0	

TABLE IV-B REPRODUCIBILITY OF RESULTS

the error analysis of reference A indicates a probable variation of $\pm 3.4\%$ in total critical power. Thus Q_{crit} has been determined in this work to at least within $\pm 10\%$. The observed variation in the critical location is quite large. However, from the analysis to be presented, such variations are shown to be probable and still consistent with the more accurate determination of Q_{crit} .

4.2 Formulation of the Method of Analysis

With the experimental results presented, a method of analysis is desired which predicts the salient features of these results and permits interpolation and some extrapolation of these data to other conditions of interest. The most convenient approach initially appeared to be extension of the models of Becker (16) and Isbin (18) to the nonuniform distribution case. This model, applicable to the annular regime, identifies processes which increase and deplete the film flow rate and establishes dryout of the annular film as the mechanism causing the critical condition. Dryout in this model and throughout this discussion refers to the decrease of the annular film flow rate to a low value sufficient to cause the annular film to break up and expose dry patches of the heating surface. However, since the annular film flow rate calculated in this manner is generally always a minimum at the tube exit, such a model apparently cannot predict the observed occurrence of the critical condition upstream of the test section exit for certain nonuniform flux distributions. Consequently, while the decrease of film flow rate to some low value has been demonstrated by Harwell researchers (34) to be responsible for the critical phenomenon

in some cases, an additional mechanism probably is responsible for the occurrence of upstream critical conditions. This mechanism must cause a severe local decrease in the heat transfer coefficient sufficient to initiate the critical phenomenon at an axial location where the nominal film flow rate may not necessarily go to zero. Mechanisms for promoting local disruption of an annular film have been proposed by other investigators. In particular, the occurrence of bubble nucleation on the tube wall within the annular film has often been cited as a possible mechanism. Since the initiation of nucleation is principally dependent on local heat flux, the occurrence of nucleation is particularly dependent on the flux shape and its M (ratio of maximum to minimum flux) value. Hence results from a variety of axial heat flux distributions offer a particularly appropriate means to evaluate the nucleation effect as a second mechanism responsible for the occurrence of the critical phenomenon in addition to the dryout effect.

The definitions used in formulation of a model which includes this nucleation-induced disruption of the annular film are presented in Figure 26. At every point along the test section, in the quality region, the ratio of flux required to initiate nucleation to the actual flux can be obtained as indicated in Figures 26a, b, c, and d. If this ratio is at or above one, nucleation is presumed to occur, the intensity of nucleation being directly proportional to the value of the ratio. Approximation of the local film flow rate is also required since intuition leads one to conclude that the magnitude of film flow rate affects the intensity of nucleation required

to locally disrupt the annular film sufficiently to cause the critical condition.

The principal factors governing the magnitude of the film flow rate are (a) evaporation from the film surface (b) entrainment from the film and (c) re-entrainment of water droplets from the vapor core into the film. Two major simplifying assumptions were made (1) for each test section the annular film is formed at the slug-annular transition with the same initial film flow rate, and (2) the effect of (b) and (c) was assumed approximately equal for all tubes. Since the test sections investigated were all 30 inches long (except for three test sections of 48 inches length) and the quality change per unit length did not vary greatly with flux distribution, the decrease film flow rate was assumed proportional to the evaporation effect only. Consequently the local film flow rate was taken inversely proportional to the enthalpy addition from the slug-annular transition point to the point of interest, $\Delta H_{\text{ann-x}}$.

In this manner the necessary parameters are established to confirm the hypothesis that the critical condition is caused by either

(a) a nucleation-induced disruption of the annular film or if (a) does not occur, then ultimately by

(b) dryout resulting from decrease of the nominal film flow rate to zero.

The parameters are evaluated at the critical location and displayed as illustrated on Figure 26e as $(q/A)_c / (q/A)_1$ versus $\Delta H_{\text{ann-c}}$. Figure 26e also indicates the expected behavior of the experimental data. For critical conditions occurring

where the flux ratio is above one, nucleation is occurring and mechanism (a) should be operative. In this region, the nucleation intensity necessary to disrupt the annular film should decrease with decreasing film flow rate. Hence the locus of critical conditions should exhibit a negative slope as indicated.

Where the flux ratio is below one, nucleation is suppressed and hence mechanism (b) should be operative. Since the only mechanism for depletion of the initial film flow rate is assumed to be evaporation, the amount of evaporation required by mechanism (b) to produce dryout should be equal for all axial flux distributions. Hence below a flux ratio of one, the locus of critical conditions should be a vertical line representing constant $\Delta H_{\text{ann-c}}$. Since all critical conditions in this region are presumably due to dryout, the critical location of the data falling in this region should be only at the test section exit.

Figure 26e according to this model, should be valid for all axial flux distributions operated at given mass velocity and pressure. While small variations in pressure are accounted for in the calculation of the basic parameters, large variations (>100 psia for example) result in variation in nucleation bubble size and thus may fundamentally affect the basic assumed mechanism. The success of this postulated model can in part be measured by the degree of scatter of test results about a mean critical condition locus. While some distribution about a mean locus is inevitable due to the simplifying assumptions made concerning the film flow rate and experimental scatter, a

reasonable coalescence of data from all nonuniform axial flux distributions on such a plot should be achieved if the postulated model is valid.

Before presenting the experimental results, the exact method of calculating parameters required by the assumed model will be presented.

4.3 Calculation Procedure for the Method of Analysis

The presentation of data on an $\Delta H_{\text{ann-c}}$ versus $(q/A)_c / (q/A)_1$ requires determination of the following parameters.

1) QUALITY AT SLUG-ANNULAR TRANSITION - For the low pressure data of this investigation, this quality is taken as 8% as discussed in Chapter II.

2) $\Delta H_{\text{ann-c}}$, CHANGE IN ENTHALPY FROM THE SLUG-ANNULAR TRANSITION LOCATION TO THE CRITICAL LOCATION - Establishing the transition location at the location where quality equals 8% and the critical location from experimental results, $\Delta H_{\text{ann-c}}$ can be readily calculated by a heat balance as described in Appendix D.

3) $(q/A)_c$, CRITICAL HEAT FLUX - The critical heat flux can be obtained directly from experimental results as described in Appendix D.

4) $(q/A)_1$, HEAT FLUX REQUIRED FOR INCIPIENT BOILING - This heat flux must be calculated at the same conditions of pressure, quality, and mass velocity as $(q/A)_c$. The Bergles-Rohsenow result (35) is used to calculate the heat flux required for incipient boiling. Although this result was derived for single phase flow, it should also be applicable to nucleation in a liquid film in contact with the heated surface. The

implicit assumption is that the temperature distribution within the liquid film can be expressed by the Fourier conduction relation with the conductivity evaluated at the wall surface temperature. The details of the analysis are summarized in the insert on Figure 27. The result, presented below, yields $(q/A)_1$ as a function of pressure and temperature difference, $T_{WALL} - T_{SAT}$.

$$(q/A)_1 = 15.60P^{1.156}(T_{WALL} - T_{SAT})^{2.30}/P^{0.0234}$$

From Figure 27 it is seen that this result requires that a minimum cavity size in the heated surface be present to serve as a nucleation site. Hence for applicability of this result, it is essential that the existence of cavities of the required minimum cavity size be confirmed. The dependence of $(q/A)_1$ with pressure and temperature difference and the minimum cavity size required are also shown in Figure 27. For comparison the limiting condition for incipient boiling, the approximate fully developed boiling curve, for 100 psia is also shown in Figure 27. This curve was obtained by modifying the results of Jens and Lottes (36) to reflect the results of Bernath and Begell (37) which indicate that slightly larger superheats are required for an aluminum surface compared to a nickel or stainless steel surface.

To use the Bergles-Rohsenow result for predicting performance of a test system, the two phase heat transfer coefficient at the critical location conditions must be established. For the range of pressures and qualities investigated, the Dengler-Addoms Correlation (38) is directly applicable

$$h_{TP} = h_L (1/x_{tt})^{0.5}$$

A more general correlation which is also applicable to steam water mixtures at higher pressures and other fluids has been proposed by Chen (39), and is fully presented in Appendix D. This result gives heat transfer coefficients about 15% lower than the Dengler-Addoms correlation for the conditions of interest. Since the Dengler-Addoms result is based on data at similar conditions to those of this investigation, it is used unless otherwise noted to calculate heat transfer coefficients. The dependence of $h_{\text{Dengler-Addoms}}$ with mass velocity and quality at a given pressure is shown in Figure 28. Combining the results of Bergles and Rohsenow

$$(q/A)_1 = f(p) (T_{\text{WALL}} - T_{\text{SAT}})^{f(p)}$$

and Dengler-Addoms

$$q/A = h_{\text{Dengler-Addoms}} (T_{\text{WALL}} - T_{\text{SAT}})$$

at the critical conditions, (P_c , X_c , and G), the heat flux required for inception of nucleation is obtained as the intersection of the two equations as illustrated in Figure 29.

With the required parameters determined, the critical condition can be presented on a $\Delta H_{\text{ann-c}}$ versus $(q/A)_c / (q/A)_1$ plot. Similarly for every point along the test section at the total critical power condition, the pressure, quality and mass velocity can be calculated and $(q/A)_1$ established.

Figure 30 illustrates the results for test section 1271. In general, as Figure 30 shows, at low qualities $(q/A)_1$ is low and hence the flux ratio $(q/A)_x / (q/A)_1$ is large.

In this manner conditions along the entire test section at the total critical power can be represented as shown on Figure 31. For total input power levels less than the critical level, operating conditions can be calculated for all points along the test section by the methods described above. Figure 31 also presents curves for power levels less than the critical level.

It should be noted that Figure 31 presents the behavior of only the linearly decreasing flux shape. Representation of other flux shapes on a plot of the same coordinates exhibit different shapes since values of $\Delta H_{\text{ann-x}}$, $(q/A)_i$ and particularly $(q/A)_x$ are dependent on the axial flux distribution. The analysis of the experimental data using the methods just described will be presented next.

4.4 Application of the Method of Analysis to Experimental Data

The parameters $\Delta H_{\text{ann-c}}$ and $(q/A)_c / (q/A)_i$ were calculated for all experimental data. Figures 32, 33 and 34 present the experimental results at each of the three mass velocities investigated. In each case the data can be bracketed to define a critical condition region. This region should ideally reduce to a single line which represents the locus of critical conditions. However, in view of the assumptions made in representing the film flow rate, as well as experimental scatter of the results themselves, the width of the data band is to be expected.

The results of Figures 32, 33, and 34 depend on the existence in the aluminum surface of cavities of the size required by the Bergles-Rohsenow nucleation theory. For the experimental conditions of this investigation, the maximum radius size

required is about 8×10^{-5} ft. Confirmation of the existence of such cavity sizes was attempted by visual observation of the boiling surface at high magnification (1000x). However, the depth of field resolution was not sufficient to permit identification of any surface features of depth less than about 3×10^{-6} ft. Thus while no hemispherical cavities of the required dimension 8×10^{-5} ft could be observed, suitable elliptical or other irregular shaped nucleating cavities of minor radius less than 3×10^{-6} ft could not be detected by the Zeiss microscope used. However, as discussed by Brown in reference (40), the surfaces were investigated by another method which confirmed the existence of nucleation sites by their active nucleation behavior in a superheated pool. This method indicated that cavities of about $2.0 \pm 2.0 \times 10^{-5}$ ft equivalent radius were present in the test surface. Since these cavity sizes were slightly less than those required by the theory, in principle a modification should be made to the theory as shown in the insert of Figure 35 to account for this deviation. The remainder of Figure 35 presents a dimensionless representation from Brown (40) of the Bergles-Rohsenow nucleation theory modified to account for surfaces having limited cavity sizes. However, as Figure 35 shows, for the experimental conditions of this test, only slightly higher heat fluxes are required because of the actual cavity sizes present. In view of the small correction involved and the uncertainty in actually assessing the cavity sizes present in the test aluminum surfaces, this small correction was not made in analysing the data in this investigation.

As anticipated, the critical limits of Figures 32, 33, and 34 are negatively sloping lines representing the decreased nucleation intensity necessary to disrupt the annular film as the film flow rate decreases. In addition, where the flux ratio decreases below one, i.e., where nucleation ceases, the critical limits become vertical suggesting that in this region, dryout is the mechanism for causing the critical condition. As previously mentioned, data falling in this dryout region should exhibit a critical condition at the test section exit only. Table IV-C below tabulates data in this dryout region from Figure 33 (nonuniform heat flux data was obtained in the dryout region for $G = 1.0 \times 10^6 \frac{\text{LBM}}{\text{HR FT}^2}$ only). In all but one case the critical location occurred within 3% of the tube exit. In this one case (No. 1555) and other cases having the critical location between 1 and 3% from the exit, the flux profile had a severe negative gradient with length near the exit. Thus axial conduction effects probably account for the slight deviations from predicted behavior of these test sections.

Clearer delineation of this dryout region was not possible since 48 inches was the maximum length of test sections that could be fabricated and installed in the apparatus. However, Figure 36 presents additional low pressure data taken at Harwell (41) on uniform tubes from 9 to 96 inches long. In Figure 36 the dryout region is clearly apparent. In addition, however, the dotted lines in this figure identify an additional stratification within the critical region with tube length. This stratification is probably due to entrainment and re-entrainment contributions to the film flow rate which must be

expected to vary significantly with varying test section length.

Test Section	Flux Shape	M	Critical Location	ΔH_{ann-c}	$(q/A)_c / (q/A)_1$
210	COSINE	2.27	29.6 \pm 1 inches	331.2	1.2
211	COSINE	2.27	29.5 \pm 0	326.5	1.09
332	COSINE	4.03	28.9 \pm .2	313.7	1.01
336	COSINE	4.03	29.5 \pm .3	312.2	.74
508	COSINE	5.75	29.0 \pm .3	350.6	.69
1254	LINEAR DECREASING	2.27	29.8 \pm 0	333.1	1.10
1255	LINEAR DECREASING	2.27	29.8 \pm 0	343.3	1.13
1554	LINEAR DECREASING	5.75	29.2 \pm .4	339.4	.74
1555	LINEAR DECREASING	5.75	28.2 \pm .1	326.7	.86
1556	LINEAR DECREASING	5.75	28.6 \pm .5	324.9	.69
2506	LINEAR PEAK INLET	5.75	29.3 \pm .3	334.4	.71

TABLE IV-C CRITICAL LOCATIONS FOR TEST SECTIONS HAVING RATIO $(q/A)_c / (q/A)_1$ APPROXIMATELY EQUAL TO OR LESS THAN ONE. ($G=1.0 \times 10^6$ LBM/HR-FT²)

4.4.1 Discussion of Results

From Figures 32, 33 and 34, it is seen that a critical region can be established which represents both postulated mechanisms for the critical condition. This critical region is shown below to provide a reasonable criteria for predicting both Q_{crit} and critical location for all axial flux distributions.

4.4.1.1 Total Critical Power

Figure 31 previously showed the variation in test section operating lines with total input power. Since the critical condition can occur whenever any portion of the test section operating line projects into the critical region, the power change necessary for any point of an operating line to pass through the critical region represents the maximum uncertainty in predicting total critical power. As Figures 37 and 38 which represent various flux distributions show, it requires about 20% variation in total power for any given test section location to pass through the width of the critical region. Taking the critical locus through the midpoint of the critical region, prediction of Q_{crit} within $\pm 10\%$ can be made for any flux distribution investigated once the critical region for given mass velocity and pressure is experimentally established. This region can be established by a combination of tests of uniform and nonuniform flux distributions as in this study or with uniform data only as the Harwell data of Figure 36 indicates.

4.4.1.2 Critical Location

The critical location results presented in Figures 14, 17 and 20 exhibited some significant variations with flux distribution and inlet subcooling. These variations can be qualitatively explained in terms of the critical regions established for each mass velocity on the $(q/A)_c / (q/A)_1$ versus ΔH_{ann-c} plots. The basis of these qualitative arguments is that the critical condition will occur at that test section location of the operating line which first intersects the critical region.

EFFECT OF FLUX DISTRIBUTION

The most striking experimental result is that for uniform and linearly increasing flux distributions as opposed to the others tested, the critical condition always occurs at the tube exit. A clear explanation lies in the shape of the test section operating lines for these flux distributions. As shown in Figure 39, the operating lines are convex when viewed from the origin. Thus the tube exit always intersects the critical region first, causing the critical condition to occur at the tube exit.

On the other hand for the flux distributions with a flux peak along or at the exit of the test section, the operating lines are concave when viewed from the origin as illustrated in Figures 40, 41 and 42. This concave portion is always bounded by the location of maximum flux and the tube exit. Hence some location downstream of the maximum flux always will intersect the critical region before the maximum flux location. This characteristic appears to explain the observation that the critical condition always occurs between the maximum flux location and the tube exit for such flux distributions.

EFFECT OF M VALUE

The second experimental observation is that for test sections of the same flux shape at the same inlet subcooling, an increase in M will cause the critical location to move upstream from the tube exit. This is shown in Figure 40 for the linearly decreasing flux shape and for the cosine flux shape. The increased concavity resulting from increased M value causes upstream portions of the operating line to inter-

sect the critical region before the tube exit portions. However, for the cosine shape $M = 2.27$ this result does not follow as shown in Figure 40 because the M factor is so low that the operating line is a straight line almost parallel to the critical region. Hence in this case, failure at any point past the maximum flux location is generally equally probable.

EFFECT OF INLET SUBCOOLING

The significant effect on critical location due to inlet subcooling can also be qualitatively explained. First, it should be observed that the effect of decreased subcooling on the test section operating line is to extend it to larger values of ΔH_{ann-x} . This results from a net gain in total heat input over the annular region owing to a larger decrease in heat input from the inlet to the annular transition compared to the decrease in total critical power. The effect of this change in operating line length is to permit the exit portion of the operating line to approach the dryout portion of the critical region where the critical condition will occur if local conditions do not cause its prior occurrence upstream from the tube exit. For this reason, the critical location should move to the tube exit as the inlet subcooling is decreased. This effect is shown in Figure 41 for the inlet and the exit flux peak distributions, and Figure 42 for the linearly decreasing flux distribution. It should be recognized that due to the shapes of the operating lines and critical regions, in some cases several locations are equally probable as the critical location. Thus the locations of the critical conditions have a fairly large experimental spread (see Table IV-B) and consequently can be only qualitatively

confirmed by the model developed in this work.

The effect of experimental variables on the critical condition can be summarized as follows:

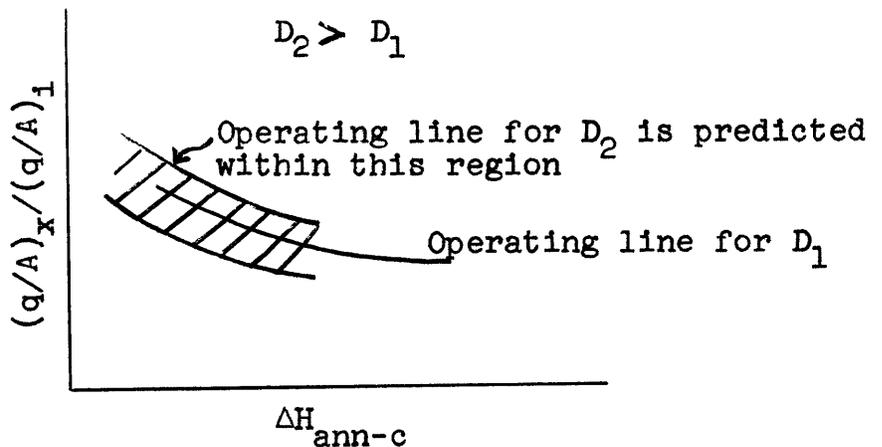
Mass velocity - The mass velocity has been the key variable in the presentation of Figures 32, 33 and 34. Figure 43 summarizes the results for the three mass velocity values selected. This data exhibits the behavior predicted by Bell (4) that for a given quality ($\Delta H_{\text{ann-x}}$ in this case) the critical heat flux is inversely proportional to the mass velocity.

Length - The test data of Figures 32, 33, 34 and Figure 36 which presents the Harwell (41) data, illustrates that the location of the critical condition approaches the dryout region as the test length increases. Figure 44 shows that for the longer tube lengths, the test section operating lines for uniform flux are S shaped instead of simply convex as are the shorter lengths. If a similar S shape can be shown to exist for long uniform tubes at high pressures, it is possible that an upstream portion of the test section operating line would first intersect the critical region. This could offer a plausible explanation for the upstream critical conditions which have been observed by Waters et al (42).

Inlet Subcooling - As previously discussed, decreased inlet subcooling tends to extend the test section operating line to larger exit quality regions (larger $\Delta H_{\text{ann-x}}$). Thus inlet subcooling variations can cause the critical phenomenon mechanism to change from nucleation-induced film disruption to dryout. Figure 45 indicates the effect of the inlet subcooling on the

Harwell data. It should be noted that in Figure 45 for the 12" long section, the inlet subcooling does not cause the $\Delta H_{\text{ann-c}}$ to increase at low values. On the Harwell presentations this effect shows as an unexplained decrease in critical heat flux with low inlet subcoolings. Unfortunately, analysis of the Harwell data by the method proposed in this report does not explain this discrepancy.

Diameter - The effect of diameter has not been investigated in this study. Prediction of the effect is difficult since a diameter change results in conflicting increases and decrease of the relevant parameters. For example at fixed G , as the diameter increases, the local flux q/A tends to be decreased but since the local quality would also decrease, $(q/A)_1$ would also tend to decrease. The net result on the flux ratio cannot easily be predicted although $\Delta H_{\text{ann-c}}$ would be expected to be decreased. Thus as diameter increased, with G , P , ℓ and ΔH_{INLET} constant, the operating curve may be elevated or lowered on the flux ratio (vertical) axis, but would be displaced toward the origin of the $\Delta H_{\text{ann-c}}$ axis.



This prediction assumes that the basic mechanism is not fundamentally altered by a diameter change. This assumption may not be valid since a diameter change will affect the ratio of surface radius of curvature to bubble diameter, a parameter which could be of importance in defining the critical condition mechanism.

4.4.2 Discussion of Results - Flux Spikes

In addition to the experimental results already presented, eleven additional tests were performed with test sections having a localized flux peak, i.e. a flux spike. These flux spikes were superimposed on available test sections already having uniform and cosine flux distributions by additional local reduction in the tube outside diameters. The flux profiles investigated are illustrated in Fig. 10 and the test geometry and results are tabulated in Appendix F.

The investigation of flux spike shapes is important for the following two reasons which are discussed in detail below.

1) The flux peak offers a unique opportunity to investigate the validity of the model already developed to describe the occurrence of the critical condition.

2) The effect of such flux peaks on the critical condition and the resultant total critical power is pertinent since flux peaks are present in reactor systems.

APPLICATION OF MODEL TO FLUX PEAK DATA

Figures 46 and 47 present the test results on the appropriate coordinates for comparison with the predictions of the model which has been developed. Note that Fig. 46 represents cosine flux distributions with stepped spikes of length varying from .085 to 1.5 inches. Figure 47 represents uniform flux

distributions with cosine spikes of length varying from 1.0 to 9.0 inches. Axial conduction effects have been investigated and determined to be negligible since in the worst case (shortest spike length), the applicable L/D ratio is about 15. From the results of Figures 46 and 47, the following conclusions can be drawn:

1) For short spike lengths, a larger value of the flux ratio, $(q/A)_c / (q/A)_1$, is necessary to cause a critical condition than predicted by the model. However, for spike lengths greater than about 1.5 inches, or as the flux peak distributions approaches the shape of the other flux distributions investigated, the critical condition can be predicted by the model. This observation indicates that conditions prior to the flux peak location play some additional role not included in the model in defining the occurrence of the critical condition. However, sufficient additional data for flux spikes was not obtained to generalize the model to accurately predict behavior of flux spikes of short length. Nevertheless, the model developed can still be applied in practice to flux peaks of short length since conservative predictions result.

2) The existence of two critical regions, one caused by nucleation induced film disruption and the other by film dryout is further confirmed. This confirmation is particularly apparent from Fig. 47 where the flux peak M values (maximum flux/minimum flux) were systematically altered. For the lowest M values, the nucleation-induced film disruption mechanism is operative since the flux peak reaches a critical condition before the test section exit reaches the dryout region.

TOTAL CRITICAL POWER

Table IV-D below presents the results of the total critical power for test sections with flux peaks. These results indicate that the total critical power for flux peak distributions up to an M value of 5.75 is slightly greater (0-15%) than that for uniform flux distributions at the same inlet conditions. The increase is inversely proportional to the M value, the test sections with lower M values exhibiting the largest increases in total critical power. For flux spikes of M = 7.0, the total critical power becomes slightly less (0 to -4%) than that for uniform flux distributions at the same inlet conditions. As mentioned above, these results can be confirmed for spike lengths 1.5 inches or greater by application of the model developed. However, for flux peaks of shorter lengths, the model yields conservative predictions and hence total critical power values less than those for uniform flux distributions would probably be predicted for these cases.

TABLE IV-D

TOTAL CRITICAL POWER RESULTS FOR TEST SECTIONS WITH FLUX PEAKS

Test Section	Spike Length inches	Ratio of Maximum to Minimum Flux	Inlet Subcooling BTU/lbm	Critical Power BTU/hr	% increase in total critical power above that for uniform flux distribution
0326	.085	4.17	-67.4	1.09×10^5	+5.0%
0345	.50	4.17	-119.3	1.255×10^5	+9.2%
0343	.50	4.52	-116.6	1.205×10^5	+5.8%
0344	1.5	5.14 to 4.54	-113.8	1.198×10^5	+5.7%
7210	1.0	2.27	-114.1	1.247×10^5	+9.4%
7510	1.0	5.75	-115.3	1.138×10^5	+0.7%
7710	1.0	7.0	-110.1	1.125×10^5	+0.5%
7250	5.0	2.27	-116.5	1.300×10^5	+14.6%
7550	5.0	5.75	-105.6	1.109×10^5	+0.0%
7750	5.0	7.0	-103.0	1.061×10^5	-4.0
7290	9.0	2.27	-116.8	1.263×10^5	+10.2%

4.5 Application to Higher Pressures

The success of the model in explaining behavior of low pressure results suggests its application to higher pressure data. In applying the model to existing high pressure data, two difficulties are encountered.

1) Measurements or a correlation of the heat transfer coefficient for annular flow at pressures above 550 psia are not available. Consequently the Chen correlation (39) was extrapolated from 550 psia to 2000 psia to yield required two phase heat transfer coefficients.

2) The critical condition locations for available non-uniform results at high pressures have a large uncertainty. This results from the burnout detection systems used to detect the location of the critical condition.

However, estimating heat transfer coefficients from the Chen correlation and carrying the uncertainty in critical location, the model has been applied to a limited amount of high pressure data with the results illustrated in Figs. 48 and 50. In these cases, the quality at the annular transition location has been approximated as 6% and 14% respectively from the preliminary results of Suo (21).

The shape of the critical locus in these figures is similar to that for low pressure data in that the flux ratio required to produce the critical condition decreases as the film flow decreases. However, the magnitude of the flux ratio required to produce the critical condition is an order of magnitude higher than for low pressure conditions. This could result from the uncertainty in the two phase heat transfer

coefficient value. A dryout region is not indicated in these figures. Additional data at the test conditions represented in these figures is necessary to fill in the regions of higher $\Delta H_{\text{ann-c}}$ to establish the existence of a dryout region. Even if the heat transfer coefficient is an error, such a region should still be indicated although it may occur at a flux ratio higher than 1.

Figure 48 represents Babcock and Wilcox data at 1000 psia from reference 15. The limit bands indicated reflect the large uncertainty in critical condition location which result in very broad limits for the critical region. As illustrated in Fig. 49, the width of the critical region including the maximum uncertainty limits is about $\pm 40\%$. However even considering the most probably critical locations, the width of the critical region is still $\pm 20\%$.

Figure 50 presents earlier Babcock and Wilcox data from reference (5) taken at 2000 psia. The width of the critical limits can be considerably reduced if the diameter difference between test sections in this experiment is recognized. As illustrated in Fig. 51, the minimum critical region in this case is approximately $\pm 15\%$. This latter Babcock and Wilcox data also contains four results for test sections with flux spikes superimposed on cosine flux distributions. These data indicates a distinct movement of the critical condition from the flux spike to the test section exit as the inlet subcooling decreased.

In terms of the model, this effect can be qualitatively explained. Recall that the effect of decreased inlet subcooling

as discussed in Section 4.4.1.2 is to extend the test section operating line to larger exit quality regions (larger $\Delta H_{\text{ann-c}}$). Thus decreased inlet subcooling should cause the critical phenomenon to shift from a nucleation-induced film disruption at the flux peak location to film dryout at the test section exit. The critical location will thus shift with decreased inlet subcooling from the flux peak to the tube exit.

Figure 52 illustrates the operating lines of the flux spike test sections. The critical location is seen to shift to the test section exit which extends to larger values of $\Delta H_{\text{ann-x}}$ with decreased subcooling. If a dryout region is assumed to exist at high values of $\Delta H_{\text{ann-x}}$ as was shown for the lower pressure results, these Babcock and Wilcox as well as the Bettis flux spike results of reference (1) can be explained. In particular the behavior of the spike effectiveness value, E_p , as introduced by Bettis (reference 1) and illustrated in Fig. 1 is readily predictable. When the critical condition is caused by nucleation-induced film disruption, ϕ_3 will equal ϕ_2 (see Chapter 1 for definitions) and E_p will equal 1. For a dryout caused critical condition, ϕ_3 will equal ϕ_1 and E_p will equal 0. Hence the model predicts the observed Bettis result that with decreased inlet subcooling E_p goes from 1 to 0 and the critical condition moves from the flux peak location to the tube exit.

However, due to the uncertainties in heat transfer coefficient and critical location determination and limited data at fixed conditions of flow, pressure and diameter, application of the model to high pressure data as yet does not indicate the existence of the dryout region and results in a broad predicted

critical region due to the film disruption mechanism. Nevertheless the model does yield the correct shape of the critical locus in the nucleation-induced film disruption region as well as a reasonable possible explanation for flux spike results. These qualitative predictions indicate that successful extrapolation of the model to the high pressure region may be accomplished when the heat transfer coefficient and critical location are determined more accurately for test runs in this region.

CHAPTER V

SUMMARY AND CONCLUSIONS

5.1 Summary

An experimental and analytic investigation of the effect of axial heat flux distribution on the critical flux has been performed. Experimental determination of the total critical power and critical location was accomplished for a wide variety of flux distributions. An analytic model describing the occurrence of the critical condition was developed which explains the behavior of the low pressure experimental results.

This model assumes that the critical condition is caused by either

- (a) a nucleation-induced disruption of the annular film or if (a) does not occur, then ultimately by
- (b) dryout resulting from decrease of the nominal film flow rate to zero.

The basic assumptions in analytically formulating this model are

- (1) an annular film is established at the annular transition location predicted by Baker (24)
- (2) the effects of entrainment and re-entrainment on the local annular film flowrate are approximately equal for tubes of similar length. Hence the local film flow rate decrease with test section length was assumed proportional to the evaporation effect only
- (3) the heat flux required to initiate nucleation can be predicted from the Bergles-Rohsenow correlation (35) using heat transfer coefficients calculated from the Dengler-Addoms correlation (38).

The resulting procedure does not allow prediction of critical conditions from simply the specification of the relevant independent variables but does provide a method by which limited experimental data can be used to establish a locus of critical conditions which is applicable to test sections with nonuniform axial flux distributions. Specifically uniform test data taken at fixed pressure, mass flow rate, and diameter can be used to predict critical conditions for various flux distributions at the same pressure, mass flow rate and diameter but with varying inlet subcooling and test section length.

5.2 Conclusions

The conclusions of this investigation can be summarized as follows.

1) Total input power to achieve a critical condition:

(a) For the cosine and other flux distributions with the maximum flux near or at the test section inlet, the total critical power is within -10% (peak inlet) to +10% (others) of that for uniform flux distribution.

(b) For flux distributions with the maximum flux near or at the test section exit, the total critical power can be up to 30% less than that for uniform flux distributions. This deviation, however, approaches zero as the inlet condition approaches the saturated condition.

(c) For flux spikes of various lengths with the ratio of maximum to minimum flux up to about six, the total critical power is about 0 to 10% greater than that for uniform flux distributions. For more severe flux spikes, the total critical power becomes less than that for uniform flux distributions.

2) The Critical Location:

(a) For uniform and monotonically increasing flux distributions, the critical location occurs very near to or at the test section exit.

(b) For flux distributions with the flux peak at any location except the test section exit, the critical condition can occur upstream depending on the inlet subcooling and the M value (ratio of maximum to minimum flux). The critical condition tends to move upstream as either the subcooling and M value increases.

3) The analytical model proposed to describe the occurrence of the critical condition successfully explains the test data for all axial flux distributions except flux spikes of short (≤ 1.5 inch) extent. For these short flux spikes, the model predicts lower local critical heat flux and total power values than were determined by experiment.

4) Application of the model to high pressure data gives qualitative agreement with test results. More precise experimental determination of the critical location and data yielding two phase heat transfer coefficients are needed at these higher pressures to effectively test the validity of the model under higher pressure conditions.

5.3 Design Procedure (50-200 psia)

Based on the conclusions of this investigation, the following design procedure can be used to establish safe operating limits for vertical up flow in tubes with nonuniform axial flux distributions.

1) Establish locus of critical conditions - For the mass velocity, pressure and tube diameter of interest, use existing

critical data to plot the critical conditions on coordinates of $(q/A)_c/(q/A)_i$ versus $\Delta H_{\text{ann-c}}$. Section 4.3 explains in detail the method of calculating these parameters from experimental data. This data may include uniform flux data or a combination of uniform and nonuniform flux data from tubes of all lengths.

2) Establish design conditions - Pick the axial flux distribution and values of inlet subcooling and test section length of interest. These values along with the previously established values of mass velocity, pressure, and diameter fully establish the design conditions.

3) Calculate the test section operating line for an arbitrary value of total input power, Q_{TOT} - Select a value of Q_{TOT} and calculate the test section operating line as described in Section 4.3. Plot this operating line with the locus of critical conditions determined per (2) above.

4) Establish Q_{crit} - For varying values of Q_{TOT} , plot operating lines until the locus of critical conditions is intercepted. The value of Q_{TOT} for this intersection is Q_{crit} and the test section axial location at the intersection is the location of the critical condition.

5) Optimize - Vary inlet subcooling, test section length and axial flux distribution as allowed by design requirements to maximize the parameters of design interest; generally the total critical power (Q_{crit}).

APPENDIX A

ERROR ANALYSIS

It is important to estimate the probable errors in the two basic parameters of interest, the critical heat input to the test section and the local heat flux.

The heat input is computed from measurements of the voltage drop across the heated length and the current to the section. Since the critical condition was generally reached while the input power was being increased to a slightly higher level, the error in the total critical power includes both an uncertainty from this operational procedure and a measuring instrument uncertainty.

For the voltage drop, this operational variation was about .15 volts over the range 12 to 27 volts and the voltmeter accuracy was $\pm 1/2\%$ of full scale. Hence in the worst case (lowest power level) the uncertainty in the voltage at the critical condition was

$$r = 12 \pm .3 \text{ volts or } \pm 2.5\%$$

The current was inferred from the voltage drop across an air-cooled N.B.S. shunt with a calibrated conductance of 60.17 amps/mv. The uncertainty from the operational procedure was .3 mv over the range 23 to 52 mv, and the voltmeter accuracy was $\pm 1/2\%$ of full scale. Hence in the worst case (lowest power level) the uncertainty in the current at the critical condition was

$$I = 60.17(23 \pm .6) \text{ amps or } \pm 2.6\%$$

Hence the most probably error in power for the lowest power cases was

$$\sqrt{(2.5)^2 + (2.6)^2} \cong 3.4\%$$

Note that the experimental reproducibility of total critical power results as summarized in Table IV-B was 5 to 10%.

The local flux for electrically heated test sections is obtained as

$$\phi(z) = \frac{dA_s}{dQ} = \frac{dA_s}{I^2 dR} = \frac{dA_s}{I^2 \frac{\rho(T) d}{A_x(\ell)}}$$

From these equations we see that perturbations in the local flux are principally caused by variations in $A_x(\ell)$, $\rho(T)$, and dQ (axial conduction effects). The variations in these parameters will be separately estimated to arrive at the overall experimental error in the local flux.

A_x -Wall Cross-Section Area

Variations in A_x are due to (1) variations in test section internal diameter and (2) variations in the outside diameter due to machining. The machining errors were controlled by 100% inspection of test section outside diameters for conformance with allowed tolerances. The net actual variation in A_x was established by measuring wall thicknesses on 32 sections taken from seven tubes selected randomly to represent all the basic designs. From these measurements the average variation from design of wall thicknesses (4 at each section) was 3.5% with a maximum variation of 7.5%.

$\rho(T)$ - Electrical Resistivity

Variations in resistivity result from wall temperature differences due to axial changes in heat transfer coefficient. The changes in heat transfer coefficient result from the axial quality changes which can exist in a test section.

The variation in wall temperature along a test section can be bounded as follows. The minimum $(T_W - T_{SAT})$ can be taken from the fully developed boiling curve at a heat flux of 3×10^5 since heat fluxes of interest in this work were all above 3×10^5 BTU/hr ft². From Fig. 29, $(T_W - T_{SAT})_{MIN}$ is 40°F. The maximum $(T_W - T_{SAT})$ can be also taken from the fully developed boiling curve at the maximum heat flux achieved in test i.e. 3×10^6 BTU/hr ft². From Fig. 29 $(T_W - T_{SAT})_{MAX}$ equals 70°F. Hence, the maximum wall temperature difference for the composite worst case is 30°F.

Now for the 2024-T3 aluminum used, the resistivity as a function of temperature is

$$\rho(T) \text{ ohm-ft} = .1765 \times 10^{-6} \left[1 + 1.152 \times 10^{-3} T^{\circ F} \right]$$

in the range 200-500°F. Based on the nominal experimental pressure of 100 psia, (3278°F) the maximum variation in resistivity along a test section would be 2.2%

dQ - Axial Conduction

Axial conduction effects can also be bounded by a worst case analysis. The maximum axial heat transfer is given by

$$dQ_{axial} = k A_x \frac{\partial T}{\partial z}$$

where

$$k_{2024T3 \text{ aluminum}} = 80 \frac{\text{BTU}}{\text{hr ft}^{\circ F}}$$

$$A_x \text{ maximum} = 248 \times 10^{-6} \text{ ft}^2 \text{ (.3020.0 inch, .214 inch I.D.)}$$

$$\left. \frac{\partial T}{\partial x} \right)_{\text{maximum}} = \frac{30^{\circ F}}{7.5/12 \text{ ft}} = 48^{\circ F/\text{ft}} \text{ (the maximum axial temperature difference of } 30^{\circ F} \text{ can occur over a minimum distance of 7.5 in. in the peak inlet and exit designs)}$$

Hence $dQ_{\text{AXIAL MAXIMUM}} \cong 1$ BTU/hr. The minimum radial heat transfer, assuming the minimum heat flux is 1×10^5 BTU/hr ft², is about 500 BTU/hr.

Hence in the worst composite case the axial heat flow is less than .5% of the radial heat flux. This is primarily due to the thin wall test section geometry which yields large L(length)/D(wall thickness) ratios thus inhibiting axial conduction. In the immediate regions of the test section inlet and exit, the temperature gradients are probably more severe and the local flux profiles in these extreme locations may be somewhat effected by axial conduction effects.

Overall Variation

Combining the effects discussed above, and the estimate of the most probable error in local heat flux is obtained as

$$\sqrt{(3.5)^2 + (2.2)^2 + (.5)^2} \cong 4.2\%$$

48" Long Test Sections

These test sections were fabricated by coupling two shorter length together with a 1 1/2" threaded thin walled sleeve (TEST SECTION 114136) or a 1" soldered thin walled sleeve (OTHERS). Hence, at the midsection of these test sections over the sleeve length, the heat flux is slightly lower than over the remainder of the test section.

APPENDIX B

TEST SECTION ANALYSIS

The analysis of the experimental data first requires calculation of various parameters from the test section data. These parameters, which are dependent on the flux profile shape are **derived on the following pages.**

The governing heat balance expression relating heat flux and electrical heat input, applicable to a length dx of tubing is

$$\phi(x)\pi D_1 dx = I^2 dR = I^2 \frac{\int dx}{A_x(x)} \quad (B-1)$$

The assumptions inherent in this expression are

1. One dimensional (radial) heat flow
2. Adiabatic outside diameter tube wall
3. Constant radial temperature profile so that $\int (T)$ is a constant
4. No azimuthal variation in tube wall thickness so that the power is generated uniformly throughout the tube wall at any axial location.

This expression can be assumed to be applicable over the entire tube length with the additional assumption of

1. Constant tube temperature so that \int which

is temperature dependent is a constant over the entire tube length.

These assumptions are shown, in Appendix A, to be met for the data presented and analyzed in this work and hence equation (1) serves as a valid point of reference for the following derivations. In the following derivations consistency of units is assumed; hence for use in actual computations numerical factors should be inserted where appropriate to assure this consistency of units. Also for the uniform and linear flux shapes, x is used as the axial position variable, while for the cosine and peaked flux shapes, z is used as the axial position variable.

UNIFORM FLUX PROFILE

The flux shape in this case, figure 10, is simply

$$\phi(x) = \phi \quad (B-2)$$

From equation (1) we obtain

$$A_x(x) = A_x = \frac{I^2 \int}{\phi \pi D_1}$$

and by the governing assumptions we find that $A_x(x) = A_x$ and hence D_o is also constant. However it is desirable to obtain all relevant parameters in terms of experimentally determined quantities as is accomplished below

a. $\phi(x) = \phi$

$$Q(x) = \int_0^x \phi \pi D_1 dx$$

$$Q_{TOT} = \phi \pi D_1 l$$

$$\phi = \frac{Q_{TOT}}{\pi D_1 l} \quad (B-3)$$

b. $D_o(x) = D_o$

From equation (1) we obtained A_x as a constant,

hence

$$D_o = \sqrt{\frac{4}{\pi} A_x + D_1^2} \quad (B-4)$$

Now A_x is a function of the overall tube resistance R which is established to make maximum use of the available D.C. power supply. The maximum power supply available is 72 kilowatts at 24 volts and 300 amperes hence establishing the optimum tube resistance as 8.0×10^{-3} ohms.

Again from equation (1)

$$dR = \frac{\rho dx}{A_x(x)}$$

$$R = \frac{\rho l}{A_x}$$

and substituting this into equation (4) we obtain

$$D_o = \sqrt{\frac{(4)}{\pi} \frac{\rho l}{R} + D_1^2} \quad (\text{B-5})$$

c. $Q(x)$

Now $Q(x) = \int_0^x \phi(x) \pi D_1 dx$ in general. For $\phi(x) = \phi$

per equation (3) we obtain simply.

$$Q(x) = Q_{\text{TOT}} \frac{x}{l} \quad (\text{B-6})$$

COSINE FLUX PROFILE

The flux shape in this case as shown in figure 10 is

$$\phi(z) = \phi_{\text{MAX}} \cos \frac{\pi z}{L} \quad \text{for } -\frac{\ell}{2} \leq z \leq +\frac{\ell}{2} \quad (\text{B-7})$$

Note that as defined in figure 10, L represents one half wavelength of a cosine wave which is truncated at $z = \pm \ell/2$ to form a test section of physical length ℓ . Using this flux shape, equation (7) and equation (1), we derive the relevant parameters in terms of experimental quantities as follows:

a. $\phi(z)$

$$Q(z) = \int_{-\ell/2}^z \phi(z) \pi D_1 dz$$

$$Q_{\text{TOT}} = \int_{-\ell/2}^{+\ell/2} \phi_{\text{MAX}} \cos \frac{\pi z}{L} \pi D_1 dz$$

Yields

$$\phi_{\text{MAX}} = \frac{Q_{\text{TOT}}}{2D_1 L \sin \frac{\pi}{2} \frac{\ell}{L}}$$

and

$$\phi(z) = \frac{Q_{\text{TOT}}}{2D_1 L \sin \frac{\pi}{2} \frac{\ell}{L}} \cos \frac{\pi z}{L} \quad (\text{B-8})$$

This expression however contains the quantity, L, which can be expressed in terms of the physical length, ℓ , and the quantity M which is defined below as the ratio of

the maximum flux to minimum flux.

$$M = \frac{\phi_{\text{MAX}}}{\phi_{\text{MIN}}} \quad (\text{B-9})$$

and thus is a crucial variable in selection of the flux profile for experimentation.

Now from (1) we see that for D_1 , I^2 , and \int constant, $\phi(z)$ is inversely proportional to $A_x(z)$. Hence at $z = 0$ where $\phi(z)$ is maximum, $A_x(z)$ is minimum and conversely at $z = \pm \ell/2$ where $\phi(z)$ is minimum, $A_x(z)$ is maximum. This leads to the relations.

$$\phi(z) = \phi_{\text{MAX}} \cos \frac{\pi z}{L} \quad ; \quad A_x(z) = \frac{A_{\text{MIN}}}{\cos \frac{\pi z}{L}} \quad (\text{B-10a})$$

$$\text{at } z = +\ell/2 \quad \phi_{\text{MIN}} = \phi_{\text{MAX}} \cos \frac{\pi \ell}{2L} \quad \text{and} \quad A_{\text{MAX}} = \frac{A_{\text{MIN}}}{\cos \frac{\pi \ell}{2L}} \quad (\text{B-10b})$$

$$\text{Hence} \quad \cos \frac{\pi \ell}{2L} = \frac{\phi_{\text{MIN}}}{\phi_{\text{MAX}}} = \frac{A_{\text{MIN}}}{A_{\text{MAX}}} = \frac{1}{M} \quad (\text{B-10c})$$

Thus we obtain

$$L = \frac{\pi \ell/2}{\cos^{-1} 1/M} \quad (\text{B-11})$$

and using the identity, $\sin \alpha = \sqrt{1 - \cos^2 \alpha}$, we obtain

$$\sin \frac{\pi}{2} \frac{\ell}{L} = \sqrt{1 - \cos^2 \frac{\pi \ell}{2L}} = \sqrt{\frac{M^2 - 1}{M^2}} \quad (\text{B-12})$$

Substituting these values into equation (8) we obtain the desired result

$$\phi(z) = \frac{Q_{\text{TOT}}}{2D_1 L \sqrt{\frac{M^2 - 1}{M^2}}} \cos \frac{\pi z}{L} \quad (\text{B-13})$$

where L is retained for convenience and defined in equation (11).

b. $D_o(z)$

$$\text{Now } D_o(z) = \sqrt{\frac{(4)}{\pi} A_x(z) + D_i^2} \quad (\text{B-14})$$

Again from equation (1) obtain

$$R = \int_{-\ell/2}^{+\ell/2} dR = \int_{-\ell/2}^{+\ell/2} \frac{\rho dz}{A_x(z)}$$

Now substituting from equation (10) where $A_x(z)$ is defined, obtain

$$R = \int_{-\ell/2}^{+\ell/2} \frac{\rho}{A_{\text{MIN}}} \cos \frac{\pi z}{L} dz$$

$$R = \frac{2 \rho L}{A_{\text{MIN}} \pi} \sin \frac{\pi}{2} \frac{\ell}{L}$$

$$\text{or } A_x(z) = \frac{A_{\text{MIN}}}{\cos \frac{\pi z}{L}} = \frac{2 \rho L}{\pi R} \frac{\sin \frac{\pi}{2} \frac{\ell}{L}}{\cos \frac{\pi z}{L}} \quad (\text{B-15})$$

Substituting (15) into (14) we obtain the desired result

$$D_o(z) = \sqrt{\frac{(8) \rho L}{\pi^2 R} \frac{\sin \frac{\pi}{2} \frac{\ell}{L}}{\cos \frac{\pi z}{L}} + D_i^2} = \sqrt{\frac{(4) A_{\text{MIN}}}{\pi \cos \frac{\pi z}{L}} + D_i^2} \quad (\text{B-16})$$

c. $Q(z)$

$$\text{Now } Q(z) = \int_{-\ell/2}^z \pi D_1 \phi(z) dz$$

$$Q(z) = \int_{-\ell/2}^{-z} \pi D_1 \phi_{\text{MAX}} \cos \frac{\pi z}{L} dz \quad \text{for } -\ell/2 \leq z \leq 0$$

$$= \int_{-\ell/2}^{+z} \pi D_1 \phi_{\text{MAX}} \cos \frac{\pi z}{L} dz \quad \text{for } 0 \leq z \leq +\ell/2$$

Carrying out the indicated operations and substituting for

$$\phi_{\text{MAX}} = \frac{Q_{\text{TOT}}}{2D_1 L \sin \frac{\pi \ell}{2L}} \quad \text{per equation B-8}$$

and

$$\sin \frac{\pi \ell}{2L} = \sqrt{\frac{M^2 - 1}{M^2}} \quad \text{per equation B-12}$$

obtain

$$Q(z) = \frac{Q_{\text{TOT}}}{2} \left[1 - \frac{\sin \frac{\pi z}{L}}{\sqrt{\frac{M^2 - 1}{M^2}}} \right] \quad \text{for } -\frac{\ell}{2} \leq z \leq 0 \quad (\text{B-17})$$

and

$$Q(z) = \frac{Q_{\text{TOT}}}{2} \left[1 + \frac{\sin \frac{\pi z}{L}}{\sqrt{\frac{M^2 - 1}{M^2}}} \right] \quad \text{for } 0 \leq z \leq +\ell/2 \quad (\text{B-18})$$

where L is defined as equal to $\frac{\pi \ell/2}{\cos^{-1} 1/M}$ per equation (11).

LINEARLY INCREASING FLUX PROFILE

The flux shape in this case as shown in figure 10 is

$$\phi(x) = \phi_{IN} + (\phi_{OUT} - \phi_{IN}) \frac{x}{\ell} \quad \text{for } 0 \leq x \leq \ell \quad (\text{B-19})$$

Using this flux shape equation and equation (1) we obtain

a. $\phi(x)$

$$Q_{TOT} = \int_0^{\ell} \left[\phi_{IN} + (\phi_{OUT} - \phi_{IN}) \frac{x}{\ell} \right] \pi D_1 dx$$

$$Q_{TOT} = \frac{\pi D_1 \ell}{2} \left[\phi_{IN} + \phi_{OUT} \right] \quad (\text{B-20})$$

Now $M = \frac{\phi_{OUT}}{\phi_{IN}}$ for a linearly increasing flux

and hence

$$Q_{TOT} = \frac{\pi D_1 \ell}{2(1+M)} \phi_{OUT} \left[\frac{1+M}{M} \right] = \frac{\pi D_1 \ell}{2} \phi_{IN} \left[1+M \right]$$

$$\phi_{OUT} = \frac{(2Q_{TOT})}{\pi D_1 \ell} \left[\frac{M}{1+M} \right] \quad (\text{B-21})$$

$$\phi_{IN} = \frac{(2Q_{TOT})}{\pi D_1 \ell} \left[\frac{1}{1+M} \right] \quad (\text{B-22})$$

Substituting these expressions for ϕ_{IN} and ϕ_{OUT} into equation (19), we obtain the desired result

$$\phi(x) = \frac{2Q_{TOT}}{A_s} \left(\frac{1}{1+M} \right) \left[1 + (M-1) \frac{x}{\ell} \right] \quad (\text{B-23})$$

b. $D_o(x)$

$$\text{Now in general } D_o(x) = \sqrt{\frac{4}{\pi} A_x(x) + D_1^2} \quad (\text{B-24})$$

Proceeding as in the cosine tube case we obtain from equation (1) the general expression for overall tube resistance, R,

$$R = \int_0^l dR = \int_0^l \frac{\rho dx}{A_x(x)} \quad (\text{B-25})$$

Now from equation (1) we also obtain an expression for $A_x(x)$ as follows:

$$\phi(x) = \frac{I^2 \rho}{\pi D_1} \frac{1}{A_x(x)} \quad (\text{B-26})$$

$$\text{At } x = 0 \quad \phi_{IN} = \frac{I^2 \rho}{\pi D_1} \frac{1}{A_{IN}} \quad (\text{B-26a})$$

$$\text{At } x = l \quad \phi_{OUT} = \frac{I^2 \rho}{\pi D_1} \frac{1}{A_{OUT}} \quad (\text{B-26b})$$

$$\text{Hence } \frac{\phi_{IN}}{\phi_{OUT}} = \frac{A_{OUT}}{A_{IN}} = \frac{1}{M} \quad (\text{B-26c})$$

Substituting the above equations, 26a and b, into equation (1) we obtain

$$\phi(x) = \frac{I^2 \rho}{\pi D_1} \left[\frac{1}{A_{IN}} + \left(\frac{1}{A_{OUT}} - \frac{1}{A_{IN}} \right) \frac{x}{l} \right] \quad (\text{B-27})$$

Now equating the expressions for $\phi(x)$ from equations (26) and (27) obtain

$$A_x(x) = \frac{1}{\frac{1}{A_{IN}} + \left(\frac{1}{A_{OUT}} - \frac{1}{A_{IN}} \right) \frac{x}{l}} \quad (\text{B-28})$$

or utilizing equation (26c)

$$A_x(x) = \frac{A_{IN}}{1 + (M-1) \frac{x}{\ell}} \quad (B-29)$$

Now substituting the expression for $A_x(x)$, equation (29), into equation (25), we obtain

$$R = \int_0^{\ell} \frac{f(1+(M-1)\frac{x}{\ell})}{A_{IN}} dx = \frac{f\ell}{2A_{IN}} (M+1) \quad (B-30)$$

Hence

$$A_{IN} = \frac{f\ell}{2R} (M+1)$$

and from equation (29)

$$A_x(x) = \frac{f\ell (M+1)}{2R \left[1 + (M-1) \frac{x}{\ell} \right]} \quad (B-31)$$

Substituting equations (29) and (31) into the general expression for $D_o(x)$, equation (24), we obtain the desired results.

$$D_o(x) = \sqrt{\frac{2f\ell (M+1)}{\pi R \left[1 + (M-1) \frac{x}{\ell} \right]} + D_1^2} = \sqrt{\frac{(4)A_{IN}}{\pi \left[1 + (M-1) \frac{x}{\ell} \right]} + D_1^2} \quad (B-32)$$

c. $Q(x)$

$$\text{Now } Q(x) = \int_0^x \pi D_1 \phi(x) dx$$

Performing the indicated integration yields

$$\phi(x) = \frac{2Q_{TOT}}{1+M} \left[\frac{1}{\ell} + \left(\frac{M-1}{2} \right) \frac{x^2}{\ell^2} \right] \quad (B-33)$$

LINEARLY DECREASING FLUX PROFILE

The flux shape in this case is the mirror image of the linearly decreasing profile and is shown in figure 10. In this case the maximum flux occurs at the test section inlet and hence is written as

$$\phi(x) = \phi_{IN} - (\phi_{IN} - \phi_{OUT}) \frac{x}{\ell} \quad \text{for } 0 \leq x \leq \ell \quad (\text{B-34})$$

and M in this case is defined as the inverse of the linearly increasing flux case and is written as

$$M = \frac{\phi_{IN}}{\phi_{OUT}} \quad (\text{B-35})$$

These basic expressions are different from corresponding quantities of the linearly increasing flux profile and hence yield different expressions for the desired parameters as shown below.

a. $\phi(x)$

$$\begin{aligned} Q_{TOT} &= \int_0^{\ell} \left[\phi_{IN} - (\phi_{IN} - \phi_{OUT}) \frac{x}{\ell} \right] \pi D_1 dx \\ Q_{TOT} &= \frac{\pi D_1 \ell}{2} \left[\phi_{IN} + \phi_{OUT} \right] \end{aligned} \quad (\text{B-36})$$

However since $M = \frac{\phi_{IN}}{\phi_{OUT}}$, we obtain

$$Q_{TOT} = \frac{\pi D_1 \ell}{2} \phi_{IN} \left[\frac{1+M}{M} \right] = \frac{\pi D_1 \ell}{2} \phi_{IN} [1+M] \quad (\text{B-37})$$

$$\text{and } \phi_{\text{IN}} = \frac{2Q_{\text{TOT}}}{\pi D_1 l} \left(\frac{M}{1+M} \right) \quad (\text{B-38})$$

$$\phi_{\text{OUT}} = \frac{2Q_{\text{TOT}}}{\pi D_1 l} \left(\frac{1}{1+M} \right) \quad (\text{B-39})$$

Substituting these expressions for ϕ_{IN} and ϕ_{OUT} into equation (34), we obtain the desired result

$$\phi(x) = \frac{2Q_{\text{TOT}}}{A_s} \left(\frac{M}{1+M} \right) \left(1 - \left(\frac{M-1}{M} \right) \frac{x}{l} \right) \quad (\text{B-40})$$

b. $D_o(x)$

$$\text{Now in general } D_o(x) = \sqrt{\frac{4}{\pi} A_x(x) + D_1^2} \quad (\text{B-41})$$

From equation (1) obtain

$$R = \int_0^l dR = \int_0^l \frac{f dx}{A_x(x)} \quad (\text{B-42})$$

Now from equation (1), we also obtain an expression for $A_x(x)$ as follows

$$\phi(x) = \frac{I^2 f}{\pi D_1} \frac{1}{A_x(x)} \quad (\text{B-43})$$

$$\text{At } x = 0 \quad \phi_{\text{IN}} = \frac{I^2 f}{\pi D_1} \frac{1}{A_{\text{IN}}} \quad (\text{B-43a})$$

$$\text{At } x = l \quad \phi_{\text{OUT}} = \frac{I^2 f}{\pi D_1} \frac{1}{A_{\text{OUT}}} \quad (\text{B-43b})$$

Hence

$$\frac{\phi_{\text{IN}}}{\phi_{\text{OUT}}} = \frac{A_{\text{OUT}}}{A_{\text{IN}}} = M \quad (\text{B-43c})$$

Substituting the above equations, (43a) and (43b), into equation (1) we obtain

$$\varnothing(x) = \frac{I^2 f}{D_1} \left[\frac{1}{A_{IN}} + \left(\frac{1}{A_{OUT}} - \frac{1}{A_{IN}} \right) \frac{x}{L} \right] \quad (B-44)$$

Now equating the expressions for $\varnothing(x)$ from equations (43) and (44) obtain

$$A_x(x) = \frac{1}{\frac{1}{A_{IN}} + \left(\frac{1}{A_{OUT}} - \frac{1}{A_{IN}} \right) \frac{x}{L}} \quad (B-45)$$

or utilizing equation (43c)

$$A_x(x) = \frac{A_{IN}}{1 + \frac{1-M}{M} \frac{x}{L}} \quad (B-46)$$

Now substituting equation (46) into equation (42)

$$R = \int_0^L \frac{f \left(1 + \left(\frac{1-M}{M} \right) \frac{x}{L} \right)}{A_{IN}} dx = \frac{fL}{2A_{IN}} \left(\frac{M+1}{M} \right) \quad (B-47)$$

Hence

$$A_{IN} = \frac{fL}{2R} \left(\frac{M+1}{M} \right) \quad (B-48)$$

and from equation (46)

$$A_x(x) = \frac{fL \left(\frac{M+1}{M} \right)}{2R \left[1 + \left(\frac{1-M}{M} \right) \frac{x}{L} \right]} \quad (B-49)$$

Substituting equations (46) and (49) into the general expression for $D_o(x)$, equation (41), we obtain the desired results

$$D_o(x) = \sqrt{\frac{2 \rho l \left(\frac{M+1}{M}\right)}{\pi R \left[1 + \left(\frac{1-M}{M}\right) \frac{x}{l}\right]} + D_i^2} = \sqrt{\frac{4A_{IN}}{\pi \left[1 + \left(\frac{1-M}{M}\right) \frac{x}{l}\right]} + D_i^2}$$

(B-50)

c. $Q(x)$

$$\text{Now } Q(x) = \int_0^x \pi D_i \phi(x) dx$$

where per equation (40)

$$\phi(x) = \frac{2Q_{TOT}}{A_s} \left(\frac{M}{1+M}\right) \left(1 - \left(\frac{M-1}{M}\right) \frac{x}{l}\right)$$

Performing the indicated integration yields

$$Q(x) = 2Q_{TOT} \left(\frac{M}{M+1}\right) \left(\frac{x}{l} - \left(\frac{M-1}{2M}\right) \frac{x^2}{l^2}\right)$$

(B-51)

PEAKED COSINE PROFILE

To simulate an inlet or outlet flux peaking, a flux profile consisting of cosine shaped portion and an exponential portion was chosen as shown in figure 10. For the inlet flux peaked tubes, the cosine portion was established by fixing the maximum position 7.5 inches from the inlet. The exponential portion was blended into the cosine profile at 12 inches from the inlet by a suitable choice (1.33) of the constant $\frac{F}{\lambda}$ which occurs in the exponential expression for the flux. The outlet flux peaked tubes are mirror images of the inlet peaked tubes. Hence the expressions for the flux profile in the inlet peaked geometry are:

$$\phi(z) = \phi_{MAX} \cos \frac{\pi z}{L'} \quad \text{for } -\frac{l'}{2} \leq z \leq 0 \quad (\text{B-51a})$$

$$\phi(z) = \phi_{MAX} \cos \frac{\pi z}{L'} \quad \text{for } 0 \leq z \leq (l - l' - .5 l') \quad (\text{B-51b})$$

$$\begin{aligned} \phi(u) &= \phi_{u=0} \exp \left(-\frac{F u}{\lambda} \right) \\ &= \phi_{MAX} \cos \frac{\pi(l - l' - .5 l')}{L'} \exp \left(\frac{F u}{\lambda} \right) \quad \text{for } 0 \leq u \leq \lambda \end{aligned} \quad (\text{B-51c})$$

For this specific design, the break point between the cosine and exponential portions of the flux profile was

taken at 12 inches from the tube inlet and hence for the tubes under consideration:

$$M = 5.75$$

$$l = 30 \text{ inches}$$

$$L = l - 12 = 18 \text{ inches}$$

$$l' = 15 \text{ inches}$$

$$L' = \frac{\pi l'}{2 \cos^{-1} \frac{1}{M}} = 16.88 \text{ inches}$$

$$\xi = 1.33 \text{ (dimensionless)}$$

However, the derivations of relevant parameters will be carried out without the insertion of these specific numerical values to obtain more general defining equations.

a. $\phi(z \text{ and } u)$

$$\text{Now } Q(z) = \int_{-l/2}^z \phi(z) \pi D_1 dz$$

$$Q_{\text{TOT}} = \pi D_1 \left[\int_{-l/2}^0 \phi_{\text{MAX}} \cos \frac{\pi z}{L'} dz + \int_0^{l-L-.5l'} \phi_{\text{MAX}} \cos \frac{\pi z}{L'} dz + \int_0^l \phi_{\text{MAX}} \cos \frac{\pi(l-L-.5l')}{L'} \exp \left(-\left(\frac{\xi u}{l} \right) du \right) \right]$$

$$Q_{\text{TOT}} = \pi D_1 \phi_{\text{MAX}} \left[\frac{L'}{\pi} \sin \frac{\pi z}{L'} \Big|_{-l/2}^{l-L-.5l'} + \cos \frac{\pi(l-L-.5l')}{L'} \left(-\frac{l}{\xi} \right) \exp \left(-\frac{\xi u}{l} \right) \Big|_0^l \right]$$

(B-52)

$$\text{Hence } \phi_{\text{MAX}} = \frac{Q_{\text{TOT}}}{\pi D_1 C_1} \quad (\text{B-53})$$

$$\begin{aligned} \text{where } C_1 &= \left[\frac{L'}{\pi} \left(\sin \frac{\pi}{L'} (\ell - \ell' - .5\ell') + \sin \frac{\pi \ell'}{L'/2} \right) + \right. \\ &\quad \left. \cos \frac{\pi (\ell - \ell' - .5\ell')}{L'} \left(1 - \exp \left(- \xi \right) \frac{\ell'}{\xi} \right) \right] \\ &= \left[\frac{L'}{\pi} \left(\sin \frac{\pi}{L'} (\ell - \ell' - .5\ell') + \sqrt{\frac{M^2 - 1}{M^2}} \right) + \right. \\ &\quad \left. \cos \frac{\pi (\ell - \ell' - .5\ell')}{L'} \left(1 - \exp \left(- \xi \right) \frac{\ell'}{\xi} \right) \right] \quad (\text{B-54}) \end{aligned}$$

Substituting the expressions for ϕ_{MAX} back into equations (51 a, b, and c) we obtain the desired result:

$$\phi(z) = \phi_{\text{MAX}} \cos \frac{\pi z}{L'} = \frac{Q_{\text{TOT}}}{\pi D_1 C_1} \cos \frac{\pi z}{L'} \quad \text{for } -\frac{\ell'}{2} \leq z \leq 0 \quad (\text{B-55a})$$

$$\phi(z) = \phi_{\text{MAX}} \cos \frac{\pi z}{L'} = \frac{Q_{\text{TOT}}}{\pi D_1 C_1} \cos \frac{\pi z}{L'} \quad \text{for } 0 \leq z \leq \ell - \ell' - .5\ell' \quad (\text{B-55b})$$

$$\phi(u) = \phi_{\text{MAX}} \cos \frac{\pi (\ell - \ell' - .5\ell')}{L'} \exp \left(- \frac{\xi u}{\ell'} \right)$$

$$\phi(u) = \frac{Q_{\text{TOT}}}{\pi D_1 C_1} \cos \frac{\pi (\ell - \ell' - .5\ell')}{L'} \exp \left(- \frac{\xi u}{\ell'} \right) \quad \text{for } 0 \leq u \leq \ell' \quad (\text{B-55c})$$

In the above expressions the quantities L' , ℓ' , and M are derived and defined in the same manner as in the cosine flux case. Hence we obtain

$$\cos \frac{\pi \ell'}{2 L'} = \frac{Q_{\text{MIN}}}{Q_{\text{MAX}}} = \frac{A_{\text{MIN}}}{A_{\text{MAX}}} = \frac{1}{M} \quad (\text{B-57})$$

and

$$L = \frac{\pi \ell' / 2}{\arccos(1/M)} \quad (\text{B-58})$$

where MIN and MAX refer to values on the cosine portion of the profile.

b. $D_o(z \text{ and } u)$

$$\text{Now in general } D_o(z \text{ or } u) = \sqrt{\frac{4}{\pi} A_x(z \text{ or } u) + D_1^2} \quad (\text{B-59})$$

From equation (1) we obtain

$$R = \int_{-l'/2}^l dR = \int_{-l'/2}^l \frac{\int d(z \text{ or } u)}{A_x(z \text{ or } u)} \quad (\text{B-60})$$

Now over the region $-l'/2 \leq z \leq l - l' - .5l'$, $A_x(z)$ can be expressed as

$$A_x(z) = \frac{A_{\text{MIN}}}{\cos \frac{\pi z}{L'}} \quad (\text{B-61})$$

whereas over the region $0 \leq u \leq l$, $A_x(u)$ can be expressed as

$$A_x(u) = \frac{A_{\text{MIN}} / \cos \frac{\pi}{L'} (l - l' - .5l')}{\exp(-\frac{\xi u}{l})} \quad (\text{B-62})$$

Hence

$$R = \int_{-l'/2}^{l - l' - .5l'} \frac{\int}{A_{\text{MIN}}} \cos \frac{\pi z}{L'} dz + \int_0^l \frac{\int \cos \frac{\pi}{L'} (l - l' - .5l')}{A_{\text{MIN}}} \exp(-\frac{\xi u}{l}) du \quad (\text{B-63})$$

Integrating we obtain R in terms of A_{MIN} as

$$R = \frac{\int}{A_{\text{MIN}}} \left(\frac{L'}{\pi} \left(\sin \frac{\pi l'}{2L'} + \sin \frac{\pi}{L'} (l - l' - .5l') \right) + \frac{\cos \frac{\pi}{L'} (l - l' - .5l')}{\xi / l} \right) (1 - \exp(-\xi)) \quad (\text{B-64})$$

or $R = \frac{f C_1}{A_{\text{MIN}}}$ where C_1 is defined by equation (54)

$$\text{Thus } A_{\text{MIN}} = \frac{f C_1}{R} \quad (\text{B-65})$$

Hence in the range $-\ell'/2 \leq z \leq \ell - \ell' - .5 \ell'$

$$A_x(z) = \frac{A_{\text{MIN}}}{\cos \frac{\pi z}{L'}} \quad \text{where } A_{\text{MIN}} \text{ is defined by equation (65)} \quad (\text{B-66})$$

and in the range $0 \leq u \leq \ell$

$$A_x(u) = \frac{A_{\text{MIN}}}{\cos \frac{\pi}{L'} (\ell - \ell' - .5 \ell') \exp(-\frac{\xi u}{\ell'})} \quad (\text{B-67})$$

where A_{MIN} is defined by equation (65).

Hence the desired result for $D_o(z)$ can be obtained by substituting equation (61) into equation (59) obtaining

$$D_o(z) = \sqrt{\frac{4}{\pi} \frac{A_{\text{MIN}}}{\cos \frac{\pi z}{L'}} + D_1^2} \quad (\text{B-68})$$

where A_{MIN} is expressible as a function of tube parameters only (i.e. R, ℓ, ℓ', ℓ' and ξ) per equation (65).

The desired result for $D_o(u)$ can be obtained by substituting equation (62) into equation (59), obtaining

$$D_o(u) = \sqrt{\frac{4}{\pi} \frac{A_{\text{MIN}}}{\left(\cos \frac{\pi}{L'} (\ell - \ell' - .5 \ell') \exp(-\frac{\xi u}{\ell'})\right)} + D_1^2} \quad (\text{B-69})$$

where A_{MIN} is also expressed per equation (65).

c. Q (z and u)

$$\text{Now } Q(x) = \int_{\text{INLET}}^x \phi(x) \pi D_1 dx \text{ where } \phi(x) \text{ as a}$$

function of position and total power was previously derived in equation (55). Substituting this expression for ϕ and performing the indicated integrations, we obtain the desired results in the range $-\ell'/2 \leq z \leq 0$.

$$\begin{aligned} Q(z) &= \int_{-\ell'/2}^z \frac{Q_{\text{TOT}}}{\pi D_1 C_1} \pi D_1 \cos \frac{\pi z}{L'} dz \\ &= \frac{Q_{\text{TOT}} L'}{C_1 \pi} \left[\sin \frac{\pi}{2} \frac{\ell'}{L'} + \sin \frac{\pi z}{L'} \right] \\ Q(z) &= \frac{Q_{\text{TOT}} L'}{C_1 \pi} \left[\sqrt{\frac{M^2-1}{M^2}} - \sin \frac{\pi |z|}{L'} \right] \end{aligned} \quad (\text{B-70})$$

In the range $0 \leq z \leq \ell - \frac{1}{2} \ell'$

$$\begin{aligned} Q(z) &= \int_{-\ell'/2}^z \frac{Q_{\text{TOT}}}{\pi D_1 C_1} \pi D_1 \cos \frac{\pi z}{L'} dz \\ Q(z) &= \frac{Q_{\text{TOT}} L'}{C_1 \pi} \left[\sqrt{\frac{M^2-1}{M^2}} + \sin \frac{\pi z}{L'} \right] \end{aligned} \quad (\text{B-71})$$

In the range $0 \leq u \leq \ell$

$$\begin{aligned} Q(z) &= \int_{-\ell'/2}^{\ell - \frac{1}{2} \ell'} \phi(z) \pi D_1 dz + \int_0^u \phi(u) \pi D_1 du \\ Q(z) &= \frac{Q_{\text{TOT}} L'}{C_1 \pi} \left[\sin \frac{\pi(\ell - \frac{1}{2} \ell')}{L'} + \sin \frac{\pi}{2} \frac{\ell'}{L'} \right] + \quad (\text{B-72}) \\ &\quad \frac{Q_{\text{TOT}} \ell}{C_1 \xi} \left[\cos \frac{\pi(\ell - \frac{1}{2} \ell')}{L'} \left(1 - \exp \left(-\frac{\xi u}{\ell} \right) \right) \right] \end{aligned}$$

OUTLET PEAK

This flux profile is shown in figure 10. The analytic expression for the flux profile is as follows:

$$\begin{aligned} \phi(u) &= \phi_{\text{MAX}} \cos \frac{-\pi(+l - l' - .5l')}{L'} \exp\left(\xi\left(\frac{u-l'}{l}\right)\right) \\ &= \phi_{\text{MAX}} \cos \frac{\pi(l - l' - .5l')}{L'} \exp\left(\xi\left(\frac{u-l'}{l}\right)\right) \text{ for } 0 \leq u \leq l \end{aligned} \quad (\text{B-73a})$$

$$\phi(z) = \phi_{\text{MAX}} \cos \frac{\pi z}{L'} \text{ for } -(l - l' - .5l') \leq z \leq 0 \quad (\text{B-73b})$$

$$\phi(z) = \phi_{\text{MAX}} \cos \frac{\pi z}{L'} \text{ for } 0 \leq z \leq + l'/2 \quad (\text{B-73c})$$

a. $\phi(z)$

Now Q_{TOT} is expressable by equation (52) for the inlet peak case since the flux profile are mirror images.

Hence

$$\phi_{\text{MAX}} = \frac{Q_{\text{TOT}}}{\pi D_1 C_1} \text{ where } C_1 \text{ is also given by equation (54).} \quad (\text{B-74})$$

Substituting equation (74) into equations (73 a, b, and c)

we obtain

$$\phi(u) = \frac{Q_{\text{TOT}}}{\pi D_1 C_1} \cos \frac{\pi(l - l' - .5l')}{L'} \exp\left(\xi\left(\frac{u-l'}{l}\right)\right) \text{ for } 0 \leq u \leq l \quad (\text{B-75})$$

$$\phi(z) = \frac{Q_{\text{TOT}}}{\pi D_1 C_1} \cos \frac{\pi z}{L'} \text{ for } -(l - l' - .5l') \leq z \leq 0 \quad (\text{B-75b})$$

$$\phi(z) = \frac{Q_{\text{TOT}}}{\pi D_1 C_1} \cos \frac{\pi z}{L'} \text{ for } 0 \leq z \leq + l'/2 \quad (\text{B-75c})$$

b. $D_o(z \text{ and } u)$

The desired relations for tube outside diameter, $D_o(z \text{ and } u)$, are obtained in the same manner as the inlet peak case. Since the two cases are mirror images of each other

$$R = \frac{\int C_1}{A_{\text{MIN}}} \quad \text{where } C_1 \text{ is defined by equation (54)} \quad (\text{B-76})$$

$$\text{and } A_{\text{MIN}} = \frac{\int C_1}{R} \quad (\text{B-77})$$

This result may easily be **seen by direct integration.** Now in this case, the wall cross sectional areas are given by

$$A_x(u) = \frac{A_{\text{MIN}}}{\cos \frac{\pi}{L'} (\ell - \ell' - .5\ell') \exp\left(\xi\left(\frac{u-\ell'}{\ell}\right)\right)} \quad \text{for } 0 \leq u \leq \ell' \quad (\text{B-78})$$

$$A_x(z) = \frac{A_{\text{MIN}}}{\cos \frac{\pi z}{L'}} \quad \text{for } -(\ell - \ell' - .5\ell') \leq z \leq + \ell'/2 \quad (\text{B-79})$$

Hence the desired results are

$$D_o(z) = \sqrt{\frac{4}{\pi} \frac{A_{\text{MIN}}}{\cos \frac{\pi z}{L'}} + D_1^2} \quad (\text{B-80})$$

where A_{MIN} is expressible as a function of tube parameters only (i.e. $R, \ell, \ell', \ell'',$ and ξ) by equations (74 and 54).

$$\text{and } D_o(u) = \sqrt{\frac{4}{\pi} \frac{A_{\text{MIN}}}{\cos \frac{\pi}{L'} (\ell - \ell' - .5\ell') \exp\left(\xi\left(\frac{u-\ell'}{\ell}\right)\right)} + D_1^2} \quad (\text{B-81})$$

where A_{MIN} is also expressed by equations (77 and 54).

c. $Q(z \text{ and } u)$

$$\text{Now } Q(x) = \int_{\text{INLET}}^x \phi(x) \pi D_1 dx \quad \text{where}$$

$\phi(x)$ as a function of position and total power was previously derived in equation (75). Substituting this expression for ϕ and performing the indicated integrations we obtain the desired results.

In the range $0 \leq u \leq l'$

$$Q(u) = \frac{Q_{\text{TOT}}}{C_1} \cos \frac{\pi(l - l' - .5l')}{L'} \left(\frac{l'}{\xi} \right) \exp\left(\frac{\xi}{l'} (u - l') - \exp(-\xi) \right) \quad (\text{B-82a})$$

In the range $-(l - l' - .5l') \leq z \leq 0$, where z is inherently negative

$$Q(z) = \frac{Q_{\text{TOT}}}{C_1} \left(\frac{l'}{\xi} \cos \frac{\pi(l - l' - .5l')}{L'} (1 - \exp(-\xi)) + \frac{L'}{\pi} \left(\sin \frac{\pi(l - l' - .5l')}{L'} - \sin \frac{\pi|z|}{L'} \right) \right) \quad (\text{B-82b})$$

In the range $0 \leq z \leq +l'/2$, where z is positive

$$Q(z) = \frac{Q_{\text{TOT}}}{C_1} \left(\frac{l'}{\xi} \cos \frac{\pi(l - l' - .5l')}{L'} (1 - \exp(-\xi)) + \frac{L'}{\pi} \left(\sin \frac{\pi(l - l' - .5l')}{L'} + \sin \frac{\pi z}{L'} \right) \right) \quad (\text{B-82c})$$

FLUX SPIKE (COSINE SHAPED)

This flux profile is shown in Fig. 10. The analytic expression for the flux profile is as follows:

$$\phi = \phi_{\text{MIN}} \text{ for } -(l - \mathcal{L} + \frac{l'}{2}) \leq z \leq -l'/2 \quad (\text{B-83a})$$

$$\phi = \phi_{\text{MAX}} \cos \frac{\pi z}{L'} \text{ for } -\frac{l'}{2} \leq z \leq +\frac{l'}{2} \quad (\text{B-83b})$$

$$\phi = \phi_{\text{MIN}} \text{ for } +\frac{l'}{2} \leq z \leq \mathcal{L} - \frac{l'}{2} \quad (\text{B-83c})$$

a. $\phi(z)$

$$\text{Now } Q(z) = \int_{-(l - \mathcal{L} + l'/2)}^{\mathcal{L} - l'/2} \phi(z) \pi D_1 dz$$

$$\begin{aligned} \text{Hence } Q_{\text{TOT}} &= \int_{-(l - \mathcal{L} + \frac{l'}{2})}^{-l'/2} \phi_{\text{MIN}} \pi D_1 dz + \int_{-\frac{l'}{2}}^{+\frac{l'}{2}} \phi_{\text{MAX}} \cos \frac{\pi z}{L'} \pi D_1 dz \\ &+ \int_{+\frac{l'}{2}}^{+\mathcal{L} - \frac{l'}{2}} \phi_{\text{MIN}} \pi D_1 dz \end{aligned}$$

$$Q_{\text{TOT}} = \pi D_1 \phi_{\text{MIN}} [l - l'] + \phi_{\text{MAX}} 2D_1 L' \sin \frac{\pi}{2} \frac{l'}{L'}$$

$$\text{Since } M \equiv \frac{\phi_{\text{MAX}}}{\phi_{\text{MIN}}}$$

$$\text{We obtain } Q_{\text{TOT}} = \pi D_1 \phi_{\text{MAX}} \left\{ \frac{l - l'}{M} + \frac{2L'}{\pi} \sin \frac{\pi}{2} \frac{l'}{L'} \right\} \quad (\text{B-84})$$

$$\text{Let } C_7 \equiv \frac{l - l'}{M} + \frac{2L'}{\pi} \sin \frac{\pi}{2} \frac{l'}{L'}$$

$$\text{or } \frac{l - l'}{M} + \frac{2L'}{\pi} \sqrt{\frac{M^2 - 1}{M^2}} \quad (\text{per Eq. B-12}) \quad (\text{B-85})$$

Hence we obtain

$$\phi_{\text{MAX}} = \frac{Q_{\text{TOT}}}{\pi D_1 C_7} \quad (\text{B-86a})$$

$$\phi_{\text{MIN}} = \frac{Q_{\text{TOT}}}{M\pi D_1 C_7} \quad (\text{B-86b})$$

Substituting these expressions for ϕ_{MAX} and ϕ_{MIN} into Eq. (B-83) we obtain

$$\phi(z) = \frac{Q_{\text{TOT}}}{M\pi D_1 C_7} \quad \text{for} \quad -(l-x + \frac{l'}{2}) \leq z \leq -\frac{l'}{2} \quad (\text{B-87a})$$

$$\phi(z) = \frac{Q_{\text{TOT}}}{\pi D_1 C_7} \cos \frac{\pi z}{L'} \quad \text{for} \quad -\frac{l'}{2} \leq z \leq \frac{l'}{2} \quad (\text{B-87b})$$

$$\phi(z) = \frac{Q_{\text{TOT}}}{M\pi D_1 C_7} \quad \text{for} \quad +\frac{l'}{2} \leq z \leq l - \frac{l'}{2} \quad (\text{B-87c})$$

b. $D_o(z)$

The relation for the tube outside diameter, D_o , is obtained as follows. The wall cross sectional areas are given as

$$A_x(z) = \frac{A_{\text{MIN}}}{\cos \frac{\pi z}{2L'}} = MA_{\text{MIN}} \quad \text{for} \quad -(l-x + \frac{l'}{2}) \leq z \leq -l'/2$$

$$+ \frac{l'}{2} \leq z \leq l - l'/2 \quad (\text{B-88a})$$

$$A_x(z) = \frac{A_{\text{MIN}}}{\cos \frac{\pi z}{L'}} \quad -\frac{l'}{2} \leq z \leq +\frac{l'}{2} \quad (\text{B-88b})$$

Now since $R = \int_{\text{TOT}} dR = \int_{\text{TOT}} \frac{pdz}{A_x(z)}$

Substituting for $A_x(z)$ from Eq. (B-88) we obtain

$$R = \int_{-(l-l'+l'/2)}^{-l'/2} \frac{\rho dz}{MA_{\text{MIN}}} + \int_{+l'/2}^{l-l'} \frac{\rho dz}{MA_{\text{MIN}}} + \int_{-l'/2}^{+l'/2} \frac{\rho dz}{\left(\frac{A_{\text{MIN}}}{\cos \frac{\pi z}{L}}\right)}$$

$$R = \frac{\rho}{A_{\text{MIN}}} \left[\frac{(l-l')}{M} + \frac{2L'}{\pi} \sqrt{\frac{M^2-1}{M^2}} \right] \quad (\text{B-89})$$

$$\text{Hence } A_{\text{MIN}} = \frac{\rho}{R} \left[\frac{l-l'}{M} + \frac{l'}{\cos \frac{l'}{M}} \sqrt{\frac{M^2-1}{M^2}} \right] \quad (\text{B-90})$$

$$\text{Hence } D_0(z) = \sqrt{\frac{4}{\pi} MA_{\text{MIN}} + D_1^2} \quad \text{for } -(l-l'+\frac{l'}{2}) \leq z \leq -l'/2 \quad (\text{B-91a})$$

$$+ l'/2 \leq z \leq l - \frac{l'}{2}$$

$$= \sqrt{\frac{4}{\pi} \frac{A_{\text{MIN}}}{\cos \frac{\pi z}{L}} + D_1^2} \quad \text{for } -\frac{l'}{2} \leq z \leq +\frac{l'}{2} \quad (\text{B-91b})$$

where A_{MIN} is given by Eq. (B-90).

c. $Q(z)$

$$\text{Now } Q(z) = \int_{-(l-l'+l'/2)}^z \pi D_1 \phi(z) dz \quad (\text{B-92})$$

where $\phi(z)$ as a function of position and total power was previously derived in Eq. (B-83).

In the range $-(l-l'+\frac{l'}{2}) \leq z \leq -l'/2$

$$Q(z) = \int_{-(l-l'+l'/2)}^{-z} \pi D_1 \frac{Q_{\text{TOT}}}{M\pi D_1 C_7} dz$$

$$Q(z) = \frac{Q_{\text{TOT}}}{MC_7} (-z+l-l'+\frac{l'}{2}) \quad (\text{B-93a})$$

In the range $-\frac{\ell'}{2} \leq z \leq 0$

$$\begin{aligned}
 Q(z) &= \int_{-(\ell - \mathcal{L} + \ell'/2)}^{-\ell'/2} \pi D_1 \frac{Q_{TOT}}{MC_7 \pi D_1} dz + \int_{-\ell'/2}^{-z} \pi D_1 \frac{Q_{TOT}}{\pi D_1 C_7} \cos \frac{\pi z}{L'} dz \\
 &= \frac{Q_{TOT}}{MC_7} (\ell - \mathcal{L}) + \frac{Q_{TOT}}{C_7} \frac{L'}{\pi} \left[\sqrt{\frac{M^2 - 1}{M^2}} - \sin \frac{\pi |z|}{L'} \right] \quad (B-93b)
 \end{aligned}$$

In the range $0 \leq z \leq +\frac{\ell'}{2}$

$$\begin{aligned}
 Q(z) &= \frac{Q_{TOT}}{MC_7} (\ell - \mathcal{L}) + \int_{-\ell'/2}^0 \pi D_1 \frac{Q_{TOT}}{\pi D_1 C_7} \cos \frac{\pi z}{L'} dz \\
 &\quad + \int_0^z \pi D_1 \frac{Q_{TOT}}{\pi D_1 C_7} \cos \frac{\pi z}{L'} dz \\
 Q(z) &= \frac{Q_{TOT}}{MC_7} (\ell - \mathcal{L}) + \frac{Q_{TOT}}{C_7} \frac{L'}{\pi} \left[\sqrt{\frac{M^2 - 1}{M^2}} + \sin \frac{\pi z}{L'} \right] \quad (B-93c)
 \end{aligned}$$

In the range $+\frac{\ell'}{2} \leq z \leq \mathcal{L} - \frac{\ell'}{2}$

$$\begin{aligned}
 Q(z) &= \frac{Q_{TOT}}{MC_7} (\ell - \mathcal{L}) + \frac{Q_{TOT} L'}{C_7 \pi} \sqrt{\frac{M^2 - 1}{M^2}} + \int_{+\ell'/2}^z \pi D_1 \frac{Q_{TOT}}{\pi D_1 C_7} dz \\
 &= \frac{Q_{TOT}}{MC_7} (\ell - \mathcal{L} + z - \ell'/2) + \frac{Q_{TOT}}{C_7} \frac{L'}{\pi} \sqrt{\frac{M^2 - 1}{M^2}} \quad (B-93d)
 \end{aligned}$$

APPENDIX C

TEST SECTION DESIGN

The initial factor to be considered in the design of the test sections is the characteristics of the available power supply. With the 24 volt, 3000 ampere supply available, Ohms Law indicates that an overall tube resistance of 8.0×10^{-3} ohms is necessary to achieve full power of 72 kw without exceeding either the generator voltage or current limitations.

Secondly the range of mass velocity (G) to be investigated is fixed. In this investigation values of $.5 \times 10^6$, 1.0×10^6 and 2.0×10^6 were chosen to cover the range reported by previous investigators and/or selected in reactor design application. Now the dimensions, D_1 and l , are established by consideration of the limiting operating condition requiring the maximum heat input (and flux) to achieve the critical condition. Thus we take the limiting case as that of G_{MAX} (2.0×10^6), and X_{in-MIN} (about -.28 for 80 psia) which utilizing the critical heat flux correlation of Macbeth (reference 30) defines a critical heat flux ϕ_c as

$$\phi_c \cdot 10^{-6} = \frac{A + \frac{1}{4} CD_1 (G \cdot 10^{-6}) \Delta H_{SUB-IN}}{1 + C l} \quad (C-1)$$

where A and C both represent expressions which are functions of D_1 , G, and P.

A second equation defining the limits of tube geometry results from the identity $\phi_c = \frac{Q_{TOT}}{A_s}$. Substituting for A_s we obtain

$$\phi_c D_i = \frac{Q_{TOT}}{\pi l} \quad (C-2)$$

However, additional factors also limit the selection of individual values of l and D_i .

a) To simulate reactor conditions and also to avoid effects on critical heat flux resulting from very short test lengths, it is desirable that l be as large as possible, at least 20 inches or greater.

b) It is desirable to work within the limits of existing uniform flux data to provide a reference point for the nonuniform flux data obtained. This existing data can then be used as a check of uniform data obtained during this study and to provide the basis for a uniform flux correlation useful to analytic work. Hence the following restrictions on l/D ratio are in order

$$50 \leq l/D \leq 250$$

c) As reported by Bergles (reference 32) for the subcooled burnout case, small tube data deviates from the data obtained for large tubes. This probably is a consequence of the existence of considerable nonequilibrium vapor volume as the **hydraulic** diameter

becomes comparable to bubble dimensions. Although this study is concerned primarily with burnout in the quality region, nucleation can occur within the annular film. This nucleation and the present lack of definition of the mechanics of the burnout process in this case make it prudent to restrict the test section diameters to relatively large values, .150 inches or greater, to eliminate any extraneous diameter effect on the results.

d) Finally a limitation on maximum tube inside diameter is imposed by the desire to achieve maximum pump discharge pressure (270 psia) to assure adequate flow control of the loop. From the pump characteristic, the maximum flow rate allowed is about 1800 lb/hr which corresponds to a pump discharge of 260 psia. Since

$$G = \frac{W}{A_F} = \frac{W}{\frac{\pi}{4} \frac{D_i^2}{144}} \quad (C-3)$$

For $G_{MAX} = 2.0 \times 10^{-6}$, the maximum inside diameter is .410 inches.

Summarizing now we have two equations (1 and 2) and three unknowns (l , D_i and ϕ_c) with the following additional restrictions from physical grounds listed above

$$.150 \text{ inches} \leq D \leq .410 \text{ inches}$$

$$l \geq 20 \text{ inches}$$

$$50 \leq l/D \leq 250$$

From the range of values which satisfy these conditions, the following set of parameters was selected

$$D = .214 \text{ inches}$$

$$l = 30 \text{ inches}$$

and hence $l/D = 140$ and $\phi_c(\text{MAX G and } \Delta H_{\text{SUB-IN}}) = 1.8 \times 10^{-6} \text{ BTU/hr ft}^2$.

Next the degree of steepness of the test flux shapes was established. The M values (M = MAXIMUM FLUX/MINIMUM FLUX) of this study were chosen to duplicate and bracket those of other investigators.

With the conditions established above, the finished tube dimensions for the flux shapes chosen can be calculated and the test section material selected.

The tube outside diameter for aluminum and hence the required amount of wall material to be removed was less than that for A nickel and stainless steel, due to the lower value of resistivity for Aluminum 2024-T3. Since the machinability of Aluminum 2024-T3 is also good, it was selected as the working material.

The specification of the actual machined dimensions of the test sections, the outside diameter as a function of axial length, can be calculated from expressions in Appendix B. Equation (B-16) typically illustrates alternate expressions for $D_o(z)$ as a function of ρ , R and M or A_{MIN} and M. Either expression can be used for tube design.

Permissable dimensional tolerances were established by the requirement that the local flux at any point should be within 5% of the design. Since

$$dP = I^2 dR = I^2 \rho \frac{d}{A_x}$$

$$dP \propto \frac{1}{A_{x \text{ local}}}$$

Hence for locations of small wall cross section area the machining tolerance to hold $\pm 5\%$ power becomes tighter. The tolerances specified for the first batches of machined tubes reflected this fact and specified several tolerances, each one applicable over a different axial location range. However, as manufacturing techniques improved, the minimum tolerance, applicable only to the area of minimum wall thickness, was applied to the entire tube. Typically on wall thicknesses ranging from .009 inches to .044 inches, a tolerance of $\pm .001$ inches was met. This resulted in flux shapes at any point within 2 - 5% of design.

APPENDIX D

DATA REDUCTION AND ANALYSIS

The reduction of the experimental data and the computation of parameters relevant to the analytic model developed are performed by the computer program described in Appendix E. The computational methods and equations upon which this program is based are presented in this appendix in the following order

- a) INITIAL DATA
- b) PARAMETERS DERIVED FROM FIRST LAW (BASIC DATA REDUCTION)
- c) ANALYTIC MODEL
- d) ANNULAR FILM CHARACTERISTICS

a) INITIAL DATA

For each fabricated test section, the following data is available:

D_1, L, M

L, L' (applicable only to test sections with a cosine shaped portion)

L, ξ, l' (applicable only to peaked inlet, peaked outlet, or spike-cosine shaped test sections)

The following additional data is obtained from each experiment

$T_{IN} \quad E \quad P_p \text{ OUT}$

$W \quad I \quad P_{IN}$

P_{OUT}

From these data, $\Delta P = P_{IN} - P_{OUT}$ and H_{IN} are directly available.

b) PARAMETERS DERIVED FROM FIRST LAW

Using the above data, the desired parameters at the test section inlet and along the test section are calculated as follows

$$\underline{\text{TUBE INLET}} \quad X_{\text{IN}} = \frac{H_{\text{IN}} - H_{f\text{-IN}}}{H_{fg\text{-IN}}} = \frac{\Delta H_{\text{SUB-IN}}}{H_{fg\text{-IN}}}$$

AXIALLY ALONG TUBE

(q/A_x) , $(q/A)_c$, Q_x , Q_c per equations in Appendix B

$$H_x = H_{\text{IN}} + \frac{Q_x}{W}$$

$$X_x = \frac{H_x - H_{f-x}}{H_{fg-x}}$$

In addition parameters associated with the saturation location and the bubbly-annular transition point are calculated as follows

SATURATION LOCATION

$$Q_{X=0} = -\Delta H_{\text{SUB-IN}} W$$

$L_{X=0}$ is length at which $Q_x = Q_{X=0}$. This parameter is obtained by solving the relevant Q_x equation in Appendix B for the position variable having first made the substitution $Q_{X=0} = Q_x$

$$L_S = L - L_{X=0}$$

$$Q_{\text{SAT}} = \text{EI } 3.41 \text{ BTU/hr/watt} - Q_{X=0} = Q_{\text{TOT}} - Q_{X=0}$$

BUBBLY-ANNULAR TRANSITION LOCATION

The value of x at the transition location is established by repetition of calculations for increasing

distances beyond the zero quality length, $L_{x=0}$, until the preset value of quality at the transition point is attained. With x thus established at the transition location, the additional parameters below are calculated

$$Q_{ANN} = Q_{TOT} - Q_X$$

$$Q_{ANN-C} = Q_C - Q_X$$

CALCULATION OF P(X)

In all the above work, calculation of P_x is computed by the empirical formulation below. This formulation was established by calculating pressure drops using the Martinelli-Nelson model (43) for tubes representing the extreme ranges in pressure drop and mass flow experienced. These results of pressure over tube length were then fitted by two straight lines, the latter line which is applicable over the higher quality regions having the more negative slope to reflect the larger rate of pressure drop in the higher quality region. The empirical fitted results compared well with the calculated results. While this method gives pressure results which are only within $\pm 10\%$, these values are used only to obtain enthalpy, quality, and heat flux for incipient nucleation which are relatively insensitive to small changes in pressure. This procedure was adopted since the accuracy obtained was acceptable and a more complicated program for pressure calculation was therefore not needed.

For $x \leq L_{X=0}$, $P_x = P_{IN}$ (neglects single phase pressure drop)

For $L_{X=0} < x \leq 1.6 L_{X=0}$

$$P_x = P_{IN} - .750 \Delta P \left(\frac{x - L_{X=0}}{L - L_{X=0}} \right)$$

For $x > 1.6 L_{X=0}$

$$P_x = P_{BK} - (P_{BK} - P_{OUT}) \left(\frac{x - 1.6 L_{X=0}}{L - 1.6 L_{X=0}} \right)$$

where

$$P_{BK} = P_{IN} - .750 \Delta P \left(\frac{0.60 L_{X=0}}{L - L_{X=0}} \right)$$

c) ANALYTIC MODEL

The model discussed in Chapter IV requires computation of the heat flux to initiate nucleate boiling at given conditions of mass flow rate G , pressure P , quality X and tube geometry, D, L . The correlations used in this computation are

TWO PHASE HEAT TRANSFER COEFFICIENT, h

1) DENGLER-ADDOMS CORRELATION (38)

$$h = 3.5 h_L (1/X_{tt})^{+0.5} \quad \text{for } .25 < X_{tt} < 70$$

where

$$h_L = .023 \left(\frac{k_L}{D/12.0} \right) (Re)^{0.8} (Pr_L)^{0.4}$$

and

$$1/X_{tt} = \left(\frac{X}{1-X} \right)^{0.9} \left(\frac{v_v}{v_L} \right)^{0.5} \left(\frac{\mu_v}{\mu_L} \right)^{0.1}$$

2) CHEN CORRELATION (39)

$$h = h_{MAC} + h_{MIC}$$

$$h_{MAC} = 0.23 \left(\frac{k_L}{D/12.0} \right) (Re_L)^{0.8} (Pr_L)^{0.4} F$$

where

$$Re_L = \frac{G(1-X)D}{\mu_L 12.0}$$

F = function of $\frac{1}{X_{tt}}$ defined by Chen's Fig. 7.

and

$$h_{MIC} = 0.00122 \frac{k_L^{0.79} C_{PL}^{0.45} v_v^{0.24} g_o^{0.25}}{\sigma^{0.5} \mu_L^{0.29} H_{fg}^{0.24} v_l^{0.49}} (\Delta T)^{0.24} (\Delta P)^{0.75} S$$

where

$$\Delta T = T_{WALL} - T_{SAT}$$

ΔP = difference in vapor pressure corresponding to ΔT , lb_f/ft²

S = function of $Re_L F^{1.25}$ defined by Chen's Fig. 8.

BERGLES-ROHSENOW INCIPIENT HEAT FLUX FOR NUCLEATION,
 $(q/A)_1$ (35)

$$(q/A)_1 = 15.60 p^{1.156} (T_{WALL} - T_{SAT})^{2.30/p^{0.0234}}$$

The associated maximum cavity size required is obtained

as

$$r = \frac{+ \alpha + 2T_{WALL} \pm \sqrt{\frac{2\alpha\beta T_{WALL}^2}{\gamma} + 4T_{WALL}\alpha + \alpha^2}}{2\gamma - \alpha\beta}$$

where

$$\gamma = q/A/k = \text{°F/ft or °R/ft}$$

$$\alpha = \frac{h_{fg} 778}{R_g} = \text{°R} \text{ where } R_g = 85.8 \frac{1b_f \text{ ft}}{1b_m \text{ °R}}$$

$$\beta = \frac{P}{\sigma 144.0} = \frac{1}{\text{ft}}$$

d) ANNULAR FILM CHARACTERISTICS (44)

The GEAP report presents curves of $\frac{b-a}{b}$ as a function of $F'(\frac{b-a}{b})$. The film thickness, $b-a$, is thus obtained from the quantities b (radius in ft) and $F'(\frac{b-a}{b})$ where

$$F'(\frac{b-a}{b}) = \sqrt{\frac{(-\frac{dP}{dz})_{TOT-TP} \frac{b}{2.0g_o}}{\rho_L}} \left(\frac{3600 \rho_G}{G_G}\right) \left(\frac{\rho_L}{\rho_G}\right)^{1/3} \left(\frac{g\rho_L}{g_o(-\frac{dP}{dz})_{TOT-TP}}\right)^{-n}$$

where

$$n = 0 \text{ if } (-\frac{dP}{dz})_{TOT-TP} \geq \frac{g}{g_o} \rho_L$$

$$n = -1/3 \text{ if } (-\frac{dP}{dz})_{TOT-TP} < \frac{g}{g_o} \rho_L$$

Computation of the film flow rate, G_f is accomplished by the following series of equations

$$\tau_{WALL} = \left[(-\frac{dP}{dz})_{TOT-TP} - \frac{g\rho_L}{g_o} \left(1 - \frac{a^2}{b^2}\right) \right] \frac{b}{2}$$

$$y^+ = y \sqrt{\frac{\tau_{WALL} 4.17 \times 10^8}{\rho_L}} \frac{\rho_L}{\mu_L}$$

where

$$y = b-a$$

$$G_{\text{film}} = \frac{2}{b} \mu_L F(y^+)$$

where

$$\begin{aligned} F(y^+) &= 3y^+ + 2.5y^+ \ln y^+ - 64 \quad \text{for } y^+ > 30 \\ &= 12.5 - 8.05y^+ + 5y^+ \ln y^+ \quad \text{for } 5 < y^+ \leq 30 \\ &= 0.5y^{+2} \quad \text{for } y^+ \leq 5 \end{aligned}$$

The results of the GEAP report are applicable only to adiabatic conditions and hence are not strictly applicable to the conditions of the subject investigation. However, the test results were analysed based on the above equations to explore the possibility of calculating local film flow rates by this method. Since contradictory answers were obtained, the extrapolation of the equations to the test conditions was not considered reliable and hence analysis by this means was not pursued.

APPENDIX E

COMPUTER PROGRAM FOR DATA REDUCTION
AND ANALYSIS

The experimental data obtained was reduced in accordance with the equations of Appendix D by a program written in FORTRAN and run on the MIT Computation Center IBM 7090 computer.

The program consists of a main program (AXIAL) which identifies from the input the flux shape of each tube (i.e. uniform, cosine, etc.) and transfers control to one of seven subroutines, one for each flux shape, where computations are initiated. These routines (UNIFRM, COSINE, LININC, LINDEC, PKIN, PKOUT, SPKCOS) together with the subroutines for calculating the saturated liquid and evaporation enthalpy (LIQEN and EVAPEN respectively) perform calculations of desired parameters at the **critical** location and over the entire length of the test section. In addition these subroutines call the subroutines (UNIANN, COSANN, LNIANN, LNDANN, PKIANN, PKOANN, SPKANN, CSPIKE) which calculate the desired parameters at the location of the **bubbly-annular transition**.

Calculation of the annular film thickness and the film flow rate past the **bubbly-annular transition** point is initiated by the subroutine FILMER

which is also called by the seven basic subroutines (UNIFRM, COSINE, etc.). The subroutine FILMFR accomplishes this calculation by calling the subroutines listed below.

- a) Local momentum pressure gradient based on the homogeneous flow assumption (HOMMGD).
- b) Overall momentum pressure drop divided by the length yielding a linear momentum pressure gradient (GRDMOM).
- c) Fluid properties - specific volume of saturated water (SPECVL), specific volume of saturated water vapor (SPECVG), saturation temperature (SATTMP), viscosity of saturated liquid (VISCOS), saturated liquid enthalpy (LIQEN) and evaporation liquid enthalpy (EVAPEN).
- d) The Martinelli-Nelson friction pressure gradient multiplier (MNPGRD).
- e) The ratio of film thickness to tube radius for given value of Levy's universal factor F' (UNIVER).

If it is desired to exclude calculation of the film thickness and flow rate, it is sufficient to substitute dummy subroutines in place of subroutines FILMFR and GRDMOM.

The program also computes the relevant variables for the model by which the test results are analysed. These variables are (1) the change in enthalpy from the bubbly-annular transition location to the local point of interest

and (2) the ratio of the local flux to the flux required to initiate nucleation in the liquid film based on both Chen's (39) and Dengler's (38) correlations. The calculation is initiated from the subroutine FILMFR by calling subroutines BONUCF and LONUFC which perform the desired calculations respectively at the burnout location and any local position of interest. The associated subroutines used in this calculation are

- (1) Chen's two phase heat transfer coefficient (XHCHEN)
- (2) Largest pit radius needed for nucleation per the Bergles-Rohsenow theory (XRAD)
- (3) Fluid properties (in addition to those listed above under FILMFR) - thermal conductivity of saturated water (XTHCON), specific heat at constant pressure of saturated water (XCPLIQ), steam-water surface tension (XSURFT), pressure of saturated water (XSATP), saturated vapor viscosity (XVISCG)
- (4) Derived property dependent quantities - difference in vapor pressure corresponding to given water temperature difference (XDELTV), Martinelli parameter (XMTT), Chen's F factor (XFCHEN) and Chen's factor (XSCHEN).

In addition provision is available thru subroutine NFLUX2 for a revised nucleation flux criteria in those cases where the maximum available surface pit radius is less than that required by the Bergles-Rohsenow criteria. However, NFLUX2 presently exists as a dummy subroutine.

A complete listing of the fortran statements for this program is included at the end of this appendix.

A listing of the variable names and the physical parameters which they represent is presented in Tables E-1, E-2, and E-3 where Table E-2 includes specifically the variables associated with the calculation of annular film thickness and flow rate (Subroutines FILMFR, GRDMOM and other called subroutines) and Table E-3 pertains to BONUCF and LONUFC and associated subroutines.

The procedure for inputing data to run this program is as follows. Following the star data card which follows the compiled program is the first data card on which the number of individual cases to be run is punched. This number is fixed point and should be punched, right oriented, in the field 1-5. This card controls the actual number of executions of the program which should correspond to the number of cases to be reduced.

The remaining data cards directly pertain to the data for individual tubes. For uniform, cosine and linear flux shapes, five cards are required for each case. For the peaked flux shapes a sixth card is required as described below. For the cosine spike shape a seventh card is required.

- a) First card - A fixed point number, right oriented, should be punched in the field 1-5. This number identifies the flux shape according to the code;
- 1 - uniform, 2 - cosine, 3 - linear increasing,
 - 4 - linear decreasing, 5 - peaked inlet,

- 6 - peaked exit and 7-spiked cosine.
- b) Second Card - Seven floating point input variables should be punched in sequence in fields of ten each. The variables, in sequence, are TUBE, RATIOM, DIAINS, VOLTS, AMPS, ENTHIN, FLMASS. The physical parameters and units represented by these variables are listed in Table E-1. Since these variables are all floating point, they should be punched with a decimal point unless specific care is taken to right orient them in their field and provide sufficient digits to accomodate the format statements in the program. This comment applies equally to cards 3, 4, 5 and 6.
 - c) Third Card - Six floating point input variables should be punched in sequence in fields of ten each. The variables in sequence are PRESP, PRESIN, PRESOT, RESDP, TSDP, BOLOCA.
 - d) Fourth Card - Two floating point input variables should be punched in sequence in field of ten each. The variables in sequence are XLNGTH and SHUNTM.
 - e) Fifth Card - A fixed point variable JLOCAT is punched right oriented in columns 1-5, and a floating point variable QUALIA is punched in columns 6-15.
 - f) Sixth Card - Three floating point input variables should be punched in sequence in fields of ten each.

The variables in sequence are SCRPTL, ZETA and PLNGTH and are applicable only to the peaked inlet and exit flux shapes and with new definitions to the **spike cosine** shape.

- g) Seventh Card - The fixed point variable J, should be punched in format I5. This card is applicable only to **spike cosine** flux shape.

The following characteristics of the program should be noted in particular.

- 1) PRESP and RESDP are input only to maintain a complete record of the data for each tube. Since they are not used in the subsequent calculation, they can if desired be set equal to zero for convenience.
- 2) AMPS represents the tube amperage in millivolts (shunt voltage drop) and is used in conjunction with SHUNTM to calculate the tube current. SHUNTM represents the number of amperes per millivolt for the particular calibration shunt installed in the heat transfer laboratory. Since the product AMPS and SHUNTM represents tube current in amperes, the arbitrary value 1.00 can be assigned to SHUNTM if an experiment yields current directly in amperes.

A group of punched input cards for the case of an inlet peaked and a cosine spike tube are shown for illustration with the program listing.

The basis for the formulations of the subroutines for fluid properties and the subroutines MNPGRD and UNIVER are discussed below. The polynomial fits of data for subroutines below were taken from the work of Trembley (45) unless otherwise noted.

a) Subroutine SPECVL - Specific Volume of Saturated Liquid vs. Pressure

The specific volume of saturated liquid as function of pressure was obtained by fitting the Keenan and Keyes' values (46) on a power series to obtain for $P < 400$ psia,

$$v_f(P) = \sum_{i=0}^9 a_i P^i$$

where

$a_0 = 1.6401745 (10^{-2})$	$a_5 = 3.8991151 (10^{-15})$
$a_1 = 2.3289060 (10^{-5})$	$a_6 = -4.3187213 (10^{-18})$
$a_2 = -1.5364591 (10^{-7})$	$a_7 = 2.8681090 (10^{-21})$
$a_3 = 7.4158910 (10^{-10})$	$a_8 = -1.0458372 (10^{-24})$
$a_4 = -2.1694997 (10^{-12})$	$a_9 = 1.6082445 (10^{-28})$

for $P \geq 400$ psia,

$$v_f(P) = \sum_{i=0}^4 b_i P^i$$

where

$b_0 = 1.7382154 (10^{-2})$	$b_3 = 6.6669956 (10^{-13})$
$b_1 = 5.5320054 (10^{-6})$	$b_4 = -2.1537248 (10^{-17})$
$b_2 = -1.9348749 (10^{-9})$	

b) Subroutine SPECVG - Specific Volume of Saturated Vapour vs. Pressure

The specific volume of saturated vapour as a function of pressure was obtained by a power series fit of the Keenan and Keyes' values.

For $P < 200$ psia, we have

$$v_g (P) = \sum_{i=0}^{10} a_i P^i$$

where

$a_0 = 7.0026614 (10^1)$	$a_6 = 8.8808151 (10^{-9})$
$a_1 = -5.2270893 (10^0)$	$a_7 = -4.6173317 (10^{-11})$
$a_2 = 2.2026868 (10^{-1})$	$a_8 = 1.5321887 (10^{-13})$
$a_3 = -5.7651685 (10^{-3})$	$a_9 = -2.9334747 (10^{-16})$
$a_4 = 9.8819624 (10^{-5})$	$a_{10} = 2.4643861 (10^{-19})$
$a_5 = -1.1389329 (10^{-6})$	

For $200 \leq P < 400$ psia,

$$v_g (P) = \sum_{i=0}^5 b_i P^i$$

where

$b_0 = 9.1051359 (10^0)$	$b_3 = -8.6394549 (10^{-7})$
$b_1 = -7.6398584 (10^{-2})$	$b_4 = 1.1495386 (10^{-9})$
$b_2 = 3.4342061 (10^{-4})$	$b_5 = -6.3157880 (10^{-13})$

For $P \geq 400$ psia,

$$v_g (P) = \sum_{i=0}^7 c_i P^i$$

where

$$\begin{aligned}
 c_0 &= 4.2909747 (10^0) & c_4 &= 3.6138355 (10^{-11}) \\
 c_1 &= -1.6646162 (10^{-2}) & c_5 &= -1.7180116 (10^{-14}) \\
 c_2 &= 3.5532997 (10^{-5}) & c_6 &= 4.4959690 (10^{-18}) \\
 c_3 &= -4.5689872 (10^{-8}) & c_7 &= -4.9699884 (10^{-22})
 \end{aligned}$$

c) Subroutine LIQEN - Enthalpy of Saturated Liquid
vs. Pressure

The enthalpy of saturated liquid as function of pressure was obtained by a power series fit of the Keenan and Keyes' values.

For $P < 200$ psia,

$$h_f(P) = \sum_{i=0}^9 a_i P^i$$

where

$$\begin{aligned}
 a_0 &= 1.1222734 (10^2) & a_5 &= 2.1239014 (10^{-7}) \\
 a_1 &= 6.3204790 (10^0) & a_6 &= -1.0067598 (10^{-9}) \\
 a_2 &= -1.4742752 (10^{-1}) & a_7 &= 2.9480958 (10^{-12}) \\
 a_3 &= 2.5403593 (10^{-3}) & a_8 &= -4.8430355 (10^{-15}) \\
 a_4 &= -2.8788220 (10^{-5}) & a_9 &= 3.4075972 (10^{-18})
 \end{aligned}$$

For $P \geq 200$ psia,

$$h_f(P) = \sum_{i=0}^7 b_i P^i$$

where

$$\begin{aligned}
 b_0 &= 2.4510585 (10^2) & b_4 &= -6.8660980 (10^{-10}) \\
 b_1 &= 7.1675962 (10^{-1}) & b_5 &= 2.6573456 (10^{-13}) \\
 b_2 &= -9.9955201 (10^{-4}) & b_6 &= -5.5654666 (10^{-17})
 \end{aligned}$$

$$b_3 = 1.0516702 (10^{-6}) \quad b_7 = 4.8594220 (10^{-21})$$

d) Subroutine EVAPEN - Latent Heat vs. Pressure

By definition the latent heat is simply the enthalpy difference between that of the saturated vapour and that of the saturated liquid ($h_{fg} = h_g - h_f$). It was obtained by fitting the Keenan and Keyes' values on a power series.

For $P < 400$ psia,

$$h_{fg}(P) = \sum_{i=0}^9 a_i P^i$$

where

$$\begin{aligned} a_0 &= 9.9704457 (10^2) & a_5 &= -1.2499843 (10^{-9}) \\ a_1 &= -2.1762821 (10^0) & a_6 &= 1.9322768 (10^{-12}) \\ a_2 &= 1.9558791 (10^{-2}) & a_7 &= -1.8023251 (10^{-15}) \\ a_3 &= -1.2610018 (10^{-4}) & a_8 &= 9.2680092 (10^{-19}) \\ a_4 &= 5.0308804 (10^{-7}) & a_9 &= -2.0148643 (10^{-22}) \end{aligned}$$

For $P > 400$ psia,

$$h_{fg}(P) = \sum_{i=0}^4 b_i P^i$$

where

$$\begin{aligned} b_0 &= 8.9642372 (10^2) & b_3 &= -4.3416487 (10^{-8}) \\ b_1 &= -3.3549732 (10^{-1}) & b_4 &= 4.8788247 (10^{-12}) \\ b_2 &= 1.2678091 (10^{-4}) \end{aligned}$$

e) Subroutine SATTMP - Saturation Temperature vs. Pressure

The saturation temperature as function of pressure was obtained from Steltz and al. (47).

$$T = \sum_{i=0}^8 a_i P_L^i$$

where

	$0.2 \leq P < 450$ psia	$450 \leq P < 3206$ psia
P_L	$\ln(10 P)$	$\ln P = 0$
a_0	$3.5157890 (10^1)$	$1.1545164 (10^4)$
a_1	$2.4592588 (10^1)$	$-8.3860182 (10^3)$
a_2	$2.1182069 (10^0)$	$2.4777661 (10^3)$
a_3	$-3.4144740 (10^{-1})$	$-3.6344271 (10^2)$
a_4	$1.5741642 (10^{-1})$	$2.6690978 (10^1)$
a_5	$-3.1329585 (10^{-2})$	$-7.8073813 (10^{-1})$
a_6	$3.8658282 (10^{-3})$	0
a_7	$-2.4901784 (10^{-4})$	0
a_8	$6.8401559 (10^{-6})$	0

f) Subroutine VISCOS - Viscosity of Saturated Liquid and Vapour vs. Temperature

The viscosity of saturated liquid as function of temperature to 600°F was obtained by a power series fit of Wellman and Sibbitt's data. (48)

$$\mu_f = \sum_{i=0}^{10} a_i T^i$$

where

$$\begin{aligned} a_0 &= 8.0144599 (10^0) & a_6 &= 8.4382483 (10^{-13}) \\ a_1 &= -1.6728317 (10^{-1}) & a_7 &= -1.4493830 (10^{-15}) \end{aligned}$$

$$\begin{aligned}
 a_2 &= 2.0423535 (10^{-3}) & a_8 &= 1.5963800 (10^{-18}) \\
 a_3 &= -1.6324668 (10^{-5}) & a_9 &= -1.0173273 (10^{-21}) \\
 a_4 &= 8.8555744 (10^{-8}) & a_{10} &= 2.8496174 (10^{-25}) \\
 a_5 &= -3.3015965 (10^{-10})
 \end{aligned}$$

Above 600°F the viscosity was obtained by a series of straight line fits of the Wellman and Sibbitt data.

g) Subroutine MNPGRD - Martinelli-Nelson's Friction Pressure Gradient Ratio

Jones' polynomial fit (49) of Martinelli-Nelson values was used, i.e.,

$$\phi_{M-N} = \exp \sum_{i=1}^4 \sum_{j=0}^7 a_{ij} \cdot P^j \cdot X^i$$

where

$$p = P/1000$$

$$X = \ln(100x + 1)$$

J	a_{1j}	a_{2j}	a_{3j}
0	2.5448316 (10 ⁰)	-5.1756752 (10 ⁻¹)	1.0193956 (10 ⁻¹)
1	-7.8896201 (10 ⁰)	1.9550200 (10 ⁰)	-3.7233785 (10 ⁻¹)
2	1.5575870 (10 ¹)	-9.6886164 (10 ⁻¹)	-1.9025685 (10 ⁻¹)
3	-1.7340906 (10 ¹)	-4.6120079 (10 ⁰)	-2.2654839 (10 ⁰)
4	1.0409842 (10 ¹)	8.4910340 (10 ⁰)	-3.4925414 (10 ⁰)
5	-3.2044877 (10 ⁰)	-5.9583098 (10 ⁰)	2.3299085 (10 ⁰)
6	4.2484805 (10 ⁻¹)	1.8989183 (10 ⁰)	-7.2534973 (10 ⁻¹)
7	-1.0804871 (10 ⁻²)	-2.2867680 (10 ⁻¹)	8.6169847 (10 ⁻²)

j	a_{4j}
0	-8.0606798 (10^{-3})
1	2.6160876 (10^{-2})
2	6.0288725 (10^{-2})
3	-3.2426871 (10^{-1})
4	4.6553847 (10^{-1})
5	-3.0333482 (10^{-1})
6	9.3379834 (10^{-2})
7	-1.1021915 (10^{-2})

Corrected Pressure Gradient Ratio

It was recognized that the Martinelli-Nelson values of ϕ correspond to a mass velocity of about 200 lbm/sec-ft² and that the pressure gradient ratio depends not only on quality and pressure but also on the mass velocity. Jones (49) has derived a mass velocity correction factor that is valid for $G \leq 10^3$ lbm/sec-ft². This factor is function of both pressure and mass velocity and is expressed in polynomial form as

$$\Omega' = \sum_{i=0}^5 (a_i + b_i P) \cdot G_o^i$$

where

$$G_o = \ln (.0036 G + 0.2)$$

i	a	b
0	1.4012797 (10^0)	-3.8229399 (10^{-5})
1	-6.8082318 (10^{-2})	-4.5200014 (10^{-4})
2	-8.3387593 (10^{-2})	1.2278415 (10^{-4})
3	3.5640886 (10^{-2})	1.5165216 (10^{-4})
4	2.1855741 (10^{-2})	-3.4296260 (10^{-5})
5	-6.3676796 (10^{-3})	-3.2820747 (10^{-5})

But, at $G \approx 200$ at any pressure Jones predicts of value of $\Omega' = 1.4$. Since the Martinelli-Nelson pressure gradient ratios correspond to that mass velocity, Jones' correction factor should therefore be unity. **Therefore, the suggested Jones factor was normalized as**

$$\Omega = \Omega' - 0.4$$

It was found by Trembley (45) that the transition across the $G = 10^3$ boundary yielded a serious discontinuity. Hence

$$\Omega = \Omega_{G=10^3} \quad \text{for } G > 10^3 \text{ was assumed.}$$

The two-phase to liquid-phase pressure gradient ratio is therefore

$$\phi = \Omega \cdot \phi_{M-N}$$

h) Subroutine UNIVER - The relevant curves of GEAP 4615 relating the ratio film thickness/tube radius to the calculated factor F' were fit by an MIT Computational

Center Share program (50). The form of the fit is

$$\frac{b-a}{b} = \sum_{i=0}^n a_i \left(F' \left(\frac{b-a}{b}\right)\right)^{i-1}$$

i) Subroutine XTHCON - Thermal Conductivity of Saturated Liquid Water vs Temperature

The thermal conductivity of saturated liquid water was obtained by a series of straight line fits of the data of Wellman and Sibbitt (48).

j) Subroutine XCPLIQ - Constant Pressure Specific Heat of Saturated Liquid Water vs Temperature

The specific heat of saturated liquid water was obtained by a series of straight line fits of the data of Wellman and Sibbitt (48).

k) Subroutine XSURFT - Surface Tension of Saturated Water

The surface tension for saturated water as a function of pressure to 1000 psia was obtained by a power series fit on Volyak's data. (51)

$$\sigma = \sum_{i=0}^{10} a_i P^i$$

where

$$\begin{aligned}
 a_0 &= 6.3225462 (10^1) & a_6 &= 2.8461426 (10^{-13}) \\
 a_1 &= -3.2677020 (10^{-1}) & a_7 &= -3.0063514 (10^{-16}) \\
 a_2 &= 2.8126518 (10^{-3}) & a_8 &= 1.9734415 (10^{-19}) \\
 a_3 &= -1.7494856 (10^{-5}) & a_9 &= -7.3149007 (10^{-23}) \\
 a_4 &= 6.8880390 (10^{-8}) & a_{10} &= 1.1689972 (10^{-26}) \\
 a_5 &= -1.7378005 (10^{-10})
 \end{aligned}$$

Above 1000 psia (544.69°F) the surface tension was obtained by a series of straight line fits to data presented in figure E.2 of Rohsenow and Choi (52).

1) Subroutine XSATP - Saturation Pressure vs. Temperature

The saturation pressure corresponding to the temperature was obtained from Steltz et al (47) as

$$P = P_c \cdot 10^{-X}$$

where

$$\begin{aligned}
 X &= \frac{t}{T_K} \left(\frac{N_u}{D_N} \right) & P_c &= 3206.182 \\
 N_u &= A + Bt + Ct^3 + Et^4 & t &= T_c - T_K \\
 D_N &= 1 + Dt & T_c &= 647.27 \\
 & & T_K &= \frac{T - 32}{1.8} + 273.16
 \end{aligned}$$

	50 ≤ T < 200	200 < T ≤ 705
A	3.2437814	3.3463130
B	5.86826 (10 ⁻³)	4.14113 (10 ⁻²)
C	1.1702379 (10 ⁻⁸)	7.515484 (10 ⁻⁹)
D	2.1878462 (10 ⁻³)	1.3794481 (10 ⁻²)
E	0	6.56444 (10 ⁻¹¹)

m) Subroutine XVISCG - Viscosity of Saturated Vapour

For $T \leq 500^{\circ}\text{F}$, the viscosity of saturated vapour was taken from Kestin's correlation (53)

$$\mu_g(P,T) = 2.419 (10^{-4}) \left[88.020 + 0.32827 \cdot T_c + 2.1350 (10^{-4}) T_c^2 - 1.6018 (10^{-2}) (1858 - 5.90 T_c) / v_g \right]$$

where

$$T_c = (T - 32) / 1.8$$

$$v_g(P,T) = (\text{use subroutine SPECVG})$$

For $T > 500^{\circ}\text{F}$, we used Keyes' correlation as given by Quan (54)

$$\mu_g(P,T) = 2.419 (10^{-3}) \left[420 T^{1/2} (1 + 2600 T^{-1} \cdot 10^{-30 T^{-1}})^{-1} + 1.5 (10^{0.0906 / v_g - 1}) \right]$$

TABLE E-1

VARIABLE NAME	PHYSICAL PARAMETER OR DEFINING EQUATION	UNITS
<u>Input Variables</u>		
NTUBES	Number of tubes	-
MSHAPE	Index representing tube flux shape	-
TUBE	Tube identification no.	-
RATIOM	M	-
DIAINS	D _{in}	inches
VOLTS	V	volts
AMPS	a	millivolt
ENTHIN	h _{IN}	BTU/lb m
FLMASS		lb m/hr
JLOCAT	Index indicating length over which calculation of thermal and hydraulic parameters should be made.	-
PRESP	Pump outlet pressure	psia
PRESIN	P _{IN}	psia
PRESOT	P _{OUT}	psia
QUALIA	Quality at bubbly-annular transition	wt % steam
RESDP	Pressure drop across needle valve at test section inlet	psi
TSDP	ΔP	psi
BOLOCA	c	inches
XLNGTH	l	inches
SHUNTM	S	amperes/millivolt
SCRPTL	l	inches
ZETA	ξ	-
PLNGTH	l'	inches

Intermediate Computed Variables

ARG	$\arcsin \left[\pm \left(\frac{2Q_{X=0}}{Q_{TOT}-1} \right) \left(\frac{M^2-1}{M^2} \right) \right]$	-
CONSTP	C ₁	inches
COSABK	$\cos \frac{\pi}{L} (l - l' - .5 l')$	-
COSLEN	L or L'	inches
EXTRAA	SINABK + ONEMSQ	-
EXTRAB	(SCRPTL * COSABK)/ZETA	inches
EXTRAC	(POWER * COSLEN) / (CONSTP * π)	BTU/hr
EXTRAD	C ₂	-
EXTRAE	(POWER * 144.0) / (CONSTP * DIAINS * π)	BTU/hr ft ²
EXTRAF	(POWER * COSABK * SCRPTL) / (CONSTP * ZETA)	BTU/hr
EXTRAG	Unused floating point variable	
EXTRAH	DVLSPL (see FILMFR)	ft ³ /lb m
EXTRAJ	DVLSPG (see FILMFR)	ft ³ /lb m
EXTRAJ	QUALOX (see FILMFR)	wt % steam
FACMIB	$1 - \frac{\sin \frac{\pi}{L} \left \frac{c-l/2}{2} \right }{\left(\frac{M^2-1}{M^2} \right)^{1/2}}$	-
FACPLB	$1 + \frac{\sin \frac{\pi}{L} \left(\frac{c-l/2}{2} \right)}{\left(\frac{M^2-1}{M^2} \right)^{1/2}}$	-
FACTMI	$1 - \frac{\sin \frac{\pi}{L} z }{\left(\frac{M^2-1}{M^2} \right)^{1/2}}$	-
FACTPL	$1 + \frac{\sin \frac{\pi}{L} z }{\left(\frac{M^2-1}{M^2} \right)^{1/2}}$	-

Intermediate Computed Variables (Cont.)

K	Position index	-
L	Position index	-
ONEOVM	1/M	-
ONEMSQ	$(\frac{M^2-1}{M^2})^{1/2}$	-
POWOQ	$Q_{X=0}$	BTU/hr
PBREAK	P_{BK}	psia
SINABK	$\sin \frac{\pi}{L} (L - l - .5 l')$	-
SIGNZ	$\pm (\frac{M^2-1}{M^2})^{1/2} (\frac{2Q_{X=0}}{Q_{TOT}} - 1)$	-
ULOCAT	$1 - \exp(-\xi)$	-

Output Variables

AREAFL	A_F	ft ²
AREAIS	A_S	ft ²
CFXAVG	ϕ_{AVG}	BTU/hr ft ²
CFXBO	ϕ_c	BTU/hr ft ²
CFXLOX	$\phi(x)$	BTU/hr ft ²
CFXLOY	$\phi(y)$	BTU/hr ft ²
DMEFB	H_{f-c}	BTU/lb m
DMEFGB	H_{fg-c}	BTU/lb m
DMEFX	H_{f-x}	BTU/lb m
DMEFGX	H_{fg-x}	BTU/lb m

Output Variables

DMEFY	H_{f-y}	BTU/lb m
DMEFGY	H_{fg-y}	BTU/lb m
ENFPX	H_f	BTU/lb m
ENFGPX	H_{fg}	BTU/lb m
ENLOB	H_c	BTU/lb m
ENLOX	H_x	BTU/lb m
ENLOY	H_y	BTU/lb m
ENSIN	ΔH_{SUB-IN}	BTU/lb m
ENSLOB	ΔH_{SUB-C}	BTU/lb m
ENSLOX	ΔH_{SUB-X}	BTU/lb m
ENSLOY	ΔH_{SUB-Y}	BTU/lb m
P	P	psia
PANBOL	Q_{ANN-c}	BTU/hr
POWERA	Q_{ANN}	BTU/hr
POWERB	Q_c	BTU/hr
POWERT	Q_{TOT}	BTU/hr
POWERX	$Q(x)$	BTU/hr
POWERY	$Q(y)$	BTU/hr
PSATL	Q_s	BTU/hr
PSLBOL	Q_{sc}	BTU/hr
QUALOL	$L_{x=0}$	inches
QUALO4	$16.0 L_{x=0}$	inches
QUALIN	X_{IN}	wt % steam
QUALOB	X_c	wt % steam
QUALOX	$X(x)$	wt % steam
SATL	L_s	inches
U	u	inches
X	x	inches
Y	y	inches
Z	z	inches

TABLE E-2

FILMFR, GRDMOM and called subroutines

VARIABLE NAME	PHYSICAL PARAMETER OR DEFINING EQUATION	UNITS
<u>Intermediate Computed Variables</u>		
a	Distance from centerline to film-core interface	inches
b	Tube radius	inches
BMAOA	b-a/b	
COLM 1)		
COLM 2)	Intermediate variables	
COLM 3)	in the subroutine MNPGRD	
COLM 4)		
DENFO	H_f -OUT	BTU/lb m
DENFGO	H_{fg} -OUT	BTU/lb m
DP	P/1000	psia
DFMOM	$\Delta P_{TPF-MOM}$	lb _f /ft ²
DX	log (100 X +1.0)	-
DUMMY A	Linear momentum gradient	lb _f /ft ³
DUMMY B	I	-
DUMMY C	K + 1, L + 1	-
ENO	h_{OUT}	BTU/lb m
ENSO	ΔH_{OUT}	BTU/lb m
FFACTP	f/4.0	-
FILMTK	12.0(b-a)	ft
GRAVAC	g = 32.2	ft/sec ²
GRAVCS	$\epsilon_0 = 32.2$	$\frac{lb_m}{lb_f} \frac{ft}{sec^2}$
GRAVCH	$\epsilon_{00} = 4.17 \times 10^8$	$\frac{lb_m}{lb_f} \frac{ft \delta}{shr^2}$

Intermediate Computed Variables (Cont.)

GRDMT	$dP/dz_{TPF-MOM}$	lb _f /ft ³
GSUBZ	log(.0036 G/3600.0 + 0.2)	
GTOT	G	lb _m /hr ft ²
GTOTSC	G/3600.0	$\frac{lb_m}{m}$ sec-ft ²
I	3 or 2; spacing between calculations along the tube length.	inches
OMEGA	$\Omega = \Omega' - 0.4$	
OMEGAP	Ω	
PGMULT	ϕ	-
PHIMN	ϕ_{M-N}	-
PSUBL	log (10.0p)	-
QUALO	X_{OUT}	-
QUALO 4	16.0 $L_{X=0}$	inches
SUMCOL		
SUMO		
SUM 1		
SUM 2		
SUM 3		
SUM 4		
SUM 5		
T		
TERM 1	$(v_g/v_l)^{0.334}$	O_F
TERM 2	$3600.0/v_g G_G$	sec/ft
TERM 3	$\left(\frac{(-\frac{dP}{dz})_{TPF-TOT} 32.2b v_l}{2} \right)^{1/2}$	ft/sec
TERM 4	$\left(\frac{g}{\epsilon_0 v_l (-\frac{dP}{dz})_{TPF-TOT}} \right)^n$	-
FISCL	μ	lb _m /hr ft
VOLSPL	v_l	ft ³ /lb m
VOLSPG	v_g	ft ³ /lb m

TABLE E-3

BONUFC, LONUFC and called subroutines

Output Variables		
DBMAOA	$\frac{b-a}{b}$	-
DPGMLT	ϕ_{M-N}	-
DT	T	0_F
DVLSPG	v_g	ft ³ /lb m
DVLSPL	v_L	ft ³ /lb m
DVISCL	μ'	lb _m /hr ft
FACTUN	F	-
FFACT	f	-
FYPLUS	F(y ⁺)	-
GFILM	G _{FILM}	lb _m /hr ft ²
GGAS	G _G	lb _m /hr ft ²
GLIQ	G _L	lb _m /hr ft ²
GLQENT	G _{L-ENT}	lb _m /hr ft ²
GRDFS	$\frac{dP}{dz}$ SP-FRICTION	lb _f /ft ³
GRDFT	$\frac{dP}{dz}$ TPF-FRICTION	lb _f /ft ³
GRDMT	$\frac{dP}{dz}$ TPF-MOM	lb _f /ft ³
GRDTOT	$\frac{dP}{dz}$ TPF-TOT	lb _f /ft ³
PCLIQ	% LIQ	$\frac{\text{lb}_m \text{ liquid}}{\text{lb}_m \text{ total}}$
PCLENT	%E	$\frac{\text{lb}_m \text{ liquid entrained}}{\text{lb}_m \text{ liquid}}$
REYNUM	Re	-
TAUWAL	τ	lb _f /ft ²
TKINCH	b-a	inches
VALUEN	n	-
VELOC	V	ft/sec
YPLUS	y ⁺	-

VARIABLE NAME	PHYSICAL PARAMETER OR DEFINING EQUATION	UNITS
<u>INPUT VARIABLE</u>		
J	J/8 = spacing at which calculations are performed over spiked portion of test section 47 (CSPIKE)	-
<u>INTERMEDIATE AND OUTPUT VARIABLES</u>		
BERGHT	$\left(\frac{1.0}{15.6 p^{1.156}}\right)^{\frac{p \cdot 0.0234}{2.30 - p \cdot 0.0234}}$	-
BMAOA	$(q/A)_x / (q/A)_{1-CHEN}$	-
CC	$(q/A)_x / (q/A)_{1-DEGLER}$	-
CPLIQ	C _p	BTU/LEM-°F
DD	1.0/X _{tt}	-
DELTFN	h _{ANN-c}	BTU/LEM
DELTT	T _w -T _{SAT}	°F
DELTVF	ΔP corresponding to T _w -T _{SAT}	lb _f /ft ²
DTCHEN	(T _w -T _{SAT}) _{CHEN}	°F
DTDENG	(T _w -T _{SAT}) _{DEGLER}	°F
EE	F _{CHEN} 1.25 Re _L	-
FILMTK	$(1 - \frac{\bar{x}}{X})^{0.9}$	-
HCHEN	h _{CHEN}	BTU/HR FT ² °F
HDB	h _{DIFFUS-BOELTER}	BTU/HR-FT-°F
HDENG	h _{DEGLER}	BTU/HR FT ² °F
HMAC	h _{MAC} (from CHEN)	BTU/HR FT ² °F

SAMPLE INPUT DATA

Intermediate and Output Variables (Cont.)

Variable	Description	Units	PEAK INLET FLUX DISTRIBUTION - #2503						
HMIC	h_{MIC} (from CHEN)	BTU/HR FT ² F							
M	UNUSED FIXED POINT VARIABLE	-							
N	FIXED POINT INDEX FROM CSPIKE	-	5						
			2503.	5.75	.213	13.9	30.9	204.2	123.75
			281.	120.	99.	161.	21.	28.1	
NFLUX	QUALO4	inches	30.00	60.17					
QACHEN	$(q/A)_1$ -CHEN	BTU/HR FT ²	31	0.080					
QADENG	$(q/A)_1$ -DENGLER	BTU/HR FT ²	18.0	1.33	15.0				
QUALO4	$8(\ell - \ell' + \ell')$	inches							
PRNUMB	N_{PR}	-							
RADIUS	R_{MIN}	ft.							
RADMAX	Maximum pit radius available in test section	ft.							
REYNLQ	Re_L	-							
SATP	P_{SAT}	lb _F /in ²							
SCHEN	S_{CHEN}	-							
SMALLT	Intermediate variable in XSATP	-	7						
			7210.	2.27	.213	16.7	36.4	203.4	250.0
			280.	128.	35.	152.	93.	29.8	
SURFTL	σ	lb _F /ft ²	30.00	60.17					
			31	0.080					
TAUWAL	$(\mu_L/\mu_G)^{-1}$	-	6.0	0.0	1.0				
THCOND	k	BTU/HR FT ² F	1						
VISCG	μ_G	LEM/HR FT							
XTT	X_{tt}	-							
YPLUS	$(v_L/v_G)^{-5}$	-							

UNIFORM FLUX DISTRIBUTION WITH COSINE SPIKE

#7210

PROGRAM LISTING

```

DATA REDUCTION FOR NONUNIFORM AXIAL HEAT FLUX INPUT      00010
COMMON NTURFS,MSHAPF,TUBE,RATIOM,DIAINS,VOLTS,AMPS,ENTHIN,FLMASS, 00020
1 PRESO,PRESP,PREIN,PRESET,RESDP,TSDP,BOLOCA,XLNGTH,SHUNTM,P, 00030
2 DMFFX,ENFPX,DMFFGX,FNFGPX,ENSIN,QUALIN,POWER,AREAF,AREATS, 00040
3 QVALOL,SATL,PSATL,POWERB,PSLBOL,CFXAVG,CFXLX,JLOCAT,K,X, 00050
4 PRPEAK,POWERX,ENLX,ENSLOB,QUALOX,DMFFY,DMEFGY,POWQO,ONFOVM, 00060
5 COSLEN,ONFMSO,SIGNZ,ARG,Z,FACMIB,FACPLB,CFXBOL,L,Y, 00070
6 FACTMI,POWFPY,CFXLX,ENLOY,ENSLOY,QUALOY,FACTPL, 00080
7 CONSTP,SCRPTL,ZFTA,PLNGTH,J,U,ULOCAT,COSABK,SINABK,I, 00090
8 EXTRAA,EXTRAAB,EXTRAC,EXTRAD,EXTRAF,EXTRAF, 00100
9 DMEFB,DMEFGB,FNLOB,ENSLOB,QUALOB,EXTRAG,EXTRAH,EXTRAJ,EXTRAJ 00110
COMMON QUALIA,GLIO,TKINCH, 00120
1DP,DX,COLM1,COLM2,COLM3,COLM4,SUMCOL,PHIMN,GTOTSC,GSURZ,SUM0,SUM1, 00130
2SUM2,SUM3,SUM4,SUM5,OMEGAP,OMEGA,PGMULT,PSURL,T,VISCL,VOL SPL,FNO, 00140
3VOLSPG,QUALO4,POWERA,PANBOL,DENFO,DFNFGO,ENSO,QUALO,DVSPLO,DVSPGO, 00150
4GTOT,DPMOM,GRDMT,DVLSPL,DVLSPG,TERM1,TERM2,TERM3,TERM4,GGAS,DT, 00160
5VISCL,REYNUM,FFACTP,FFACT,VELOC,GRDFS,DPGMLT,GRDFT,GRDGMT,GRDTOT, 00170
6B,GRAVAC,GRAVCS,GRAVCH,VALUEN,FACTUN,BMAOA,DBMAOA,A,FILMTK,YPLUS, 00180
7TAUWAL,FYPLUS,GFILM,GLQENT,PCLIQ,PCLFNT,DUMMYA,DUMMYB,DUMMYC 00190
COMMON N,M,THCON,FCHEN,SCHFN,VISCG,CPLIQ,SURFTL, 00200
1XTT,SATP,SMALLT,DELTV,TWALL,HCHEN,HMAC,HMIC,RFYNLO,NFLUX, 00210
2 PNUMB,REGHT,HDB,HDFNG,OADFNG,OTDFNG,DLFTT,QACHEN, 00220
3 DTCHEN,RADMAX,DELTFN,RADIUS,CC,DD,FF 00230
MSHAPE VALUE INDICATES THE TUBE FLUX SHAPE,MSHAPE=1 IS UNIFORM 00240
MSHAPE=2 IS COSINE, MSHAPE=3 IS LINEAR INCREASING, AND MSHAPE=4 IS 00250
DECREASING FLUX,MSHAPE 5=PEAKED INLET, AND MSHAPE 6= PEAKED EXIT 00260
READ 505,NTURFS 00270
PRINT 505,NTURFS 00280
505 FORMAT (15) 00290
510 FORMAT (15) 00300
512 FORMAT (14),15) 00310
DO 2000 I=1,NTURFS 00320
READ 510,MSHAPE 00330
PRINT 512,MSHAPE 00340
IF (ARSE(MSHAPE-1) ) 5, 100, 5 00350
5 IF (ARSE(MSHAPE-2) ) 10, 200, 10 00360
10 IF (ARSE(MSHAPE-3) ) 15,600,15 00370
15 IF (ARSE(MSHAPE-4) ) 20,800,20 00380
20 IF (ARSE(MSHAPE-5) ) 30,1100,30 00390
20 IF (ARSE(MSHAPE-6) ) 1600,1400,1600 00400
STATEMENTS BEGINNING WITH 100 ARE FOR UNIFORM FLUX, 200 COSINE 00410
1 600 LINEAR INCREASING,800 LINEAR DECREASING,1100 PEAKED 00420
2 INLET, AND 1400 PEAKED EXIT 00430

```

```

100 CALL UNIFORM 00440
GO TO 2000 00450
200 CALL COSINE 00460
GO TO 2000 00470
600 CALL LININC 00480
GO TO 2000 00490
800 CALL LINDEC 00500
GO TO 2000 00510
1100 CALL OKIN 00520
GO TO 2000 00530
1400 CALL PKOUT 00540
GO TO 2000 00550
1600 CALL SPKCON 00560
GO TO 2000 00570
2000 CONTINUE 00580
CALL EXIT 00590
END 00600

```

```

SUBROUTINE UNIFORM 00010
COMMON NTUBES,MSHAPE,TUBE,RATIOM,DIAINS,VOLTS,AMPS,ENTHIN,FLMASS, 00020
1 PRES,PREIN,PRESET,RESDP,TSDP,BOLOCA,XLNGTH,SHUNTM,P, 00030
2 DMFFX,ENFPX,DMFFGX,FNFGPX,ENSIN,QUALIN,POWER,AREAF,AREATS, 00040
3 QVALOL,SATL,PSATL,POWERB,PSLBOL,CFXAVG,CFXLX,JLOCAT,K,X, 00050
4 PRPEAK,POWERX,ENLX,ENSLOB,QUALOX,DMFFY,DMEFGY,POWQO,ONEOVM, 00060
5 COSLEN,ONFMSO,SIGNZ,ARG,Z,FACMIB,FACPLB,CFXBOL,L,Y, 00070
6 FACTMI,POWFPY,CFXLX,ENLOY,ENSLOY,QUALOY,FACTPL, 00080
7 CONSTP,SCRPTL,ZFTA,PLNGTH,J,U,ULOCAT,COSABK,SINABK,I, 00090
8 EXTRA,EXTRAAB,EXTRAC,EXTRAD,EXTRAF,EXTRAF, 00100
9 DMEFB,DMEFGB,FNLOB,ENSLOB,QUALOB,EXTRAG,EXTRAH,EXTRAJ,EXTRAJ 00110
COMMON QUALIA,GLIO,TKINCH, 00120
1DP,DX,COLM1,COLM2,COLM3,COLM4,SUMCOL,PHIMN,GTOTSC,GSURZ,SUM0,SUM1, 00130
2SUM2,SUM3,SUM4,SUM5,OMEGAP,OMEGA,PGMULT,PSURL,T,VISCL,VOL SPL,FNO, 00140
3VOLSPG,QUALO4,POWERA,PANBOL,DENFO,DFNFGO,ENSO,QUALO,DVSPLO,DVSPGO, 00150
4GTOT,DPMOM,GRDMT,DVLSPL,DVLSPG,TERM1,TERM2,TERM3,TERM4,GGAS,DT, 00160
5VISCL,REYNUM,FFACTP,FFACT,VELOC,GRDFS,DPGMLT,GRDFT,GRDGMT,GRDTOT, 00170
6B,GRAVAC,GRAVCS,GRAVCH,VALUEN,FACTUN,BMAOA,DBMAOA,A,FILMTK,YPLUS, 00180
7TAUWAL,FYPLUS,GFILM,GLQENT,PCLIQ,PCLFNT,DUMMYA,DUMMYB,DUMMYC 00190
COMMON N,M,THCON,FCHEN,SCHFN,VISCG,CPLIQ,SURFTL, 00200
515 FORMAT (F10.0,F10.2,F10.4,4F10.1) 00200
520 FORMAT (5F10.0,1F10.2) 00210
525 FORMAT (2F10.2) 00220
530 FORMAT (15,F10.3) 00230
540 FORMAT(24H INLET LIQUID ENTHALPY = F8.2, 00240
1 25H INLET EVAP ENTHALPY =F8.2, 22H INLET SUBCOOLING =F8.2) 00250
543 FORMAT(16H INLET QUALITY = F6.3) 00260
545 FORMAT(12H FLOW AREA =3PE15.2,25H INSIDE SURFACE AREA =0PE15.4) 00270
550 FORMAT(35H LENGTH WHERE QUALITY EQUALS ZERO =F15.2, 00280
1 42H LENGTH OVER WHICH QUALITY ABOVE ZERO =F15.2) 00290
555 FORMAT(24H POWER OVER SAT LENGTH =1PE10.3,17H POWER TO BO = 00300
1 1PE10.3,26H POWER FROM SAT TO BO = 1PE10.3) 00310
560 FORMAT(20H AVG CRITICAL FLUX =1PF10.3, 00320
1 25H CRITICAL FLUX AT BO = 1PF10.3) 00330
565 FORMAT(F10.2) 00340
570 FORMAT(F10.1) 00350
575 FORMAT(2F20.2) 00360
READ 515,TUBE,RATIOM,DIAINS,VOLTS,AMPS,ENTHIN,FLMASS 00370
READ 520,PRESP,PREIN,PRESET,RESDP,TSDP,BOLOCA 00380
READ 525,XLNGTH,SHUNTM 00390
READ 530,JLOCAT,QUALIA 00400
PRINT 515,TUBE,RATIOM,DIAINS,VOLTS,AMPS,ENTHIN,FLMASS 00410
PRINT 520,PRESP,PREIN,PRESET,RESDP,TSDP,BOLOCA 00420

```

```

PRINT 575,XLNGTH,SHUNTM
PRINT 570,JLOCAT,QUALIA
100 P=PPFSIN
CALL LIOFN
DMFFX=ENFDX
CALL FVADFN
DMFFGX=FNFGDX
FNSIN=FNTHIN-DMFFX
QUALIN=ENSIN/DMFFGX
POWER=VOLTS*AMPS*3.41*SHUNTM
ARFAFL=(3.1416*DIAINS*DIAINS)/576.0
ARFAIS=(3.1416*XLNGTH*DIAINS)/144.0
QUALOL=(XLNGTH*FNSIN*FLMASS)/POWER
SATL=XLNGTH*QUALOL
PSATL=POWER*(SATL/XLNGTH)
POWERB=POWER*(BOLOCA/XLNGTH)
IF (BOLOCA-QUALOL) 750,750,755
755 IF (BOLOCA-(1.6*QUALOL)) 760,760,765
760 P=PPFSIN
GO TO 770
760 P=PPFSIN-(0.750*TSDP*(BOLOCA-QUALOL)/(XLNGTH-QUALOL))
GO TO 770
765 PRPFK=PPFSIN-(0.750*TSDP*(0.60*QUALOL)/(XLNGTH-QUALOL))
P=PRPFK-(PRPFK-PPFSIN)*(BOLOCA-(1.60*QUALOL)/(XLNGTH-
1 (1.60*QUALOL)))
770 CALL LIOFN
DMFFR=ENFDX
CALL FVADFN
DMFFGR=FNFGDX
ENLOR=FNTHIN+POWER/FLMASS
FNSLOR=ENLOR-DMFFR
QUALOR=FNSLOR/DMFFGR
145 PSLROL=PSATL-(POWER-POWERB)
150 CFXAVG=POWER/ARFAIS
CFXBO=POWER/ARFAIS
PRINT 540,DMFFX,DMFFGX,ENSIN
PRINT 543,QUALIN
PRINT 545,ARFAFL,ARFAIS
PRINT 550,QUALOL,SATL
PRINT 555,PSATL,POWERB,PSLROL
PRINT 560,CFXAVG,CFXBO
PRINT 775,P,DMFFR,DMFFGR
PRINT 785,QUALOR
775 FORMAT(17H PRESSURE AT BO =F6.1,25H SAT LJO ENTH AT BO =F8.2,
1 22H FVAP FNTH AT BO =F8.2)
780 FORMAT(13H ENTH AT RO =F8.2, 27H SURCOOLED ENTH AT BO =F8.2)
785 FORMAT(16H QUALITY AT RO =F6.3)
CALL GRDMOM
CALL UNJANN
DO 460 K=1,JLOCAT,3
156 X=K-1
IF(X=QUALOL)160,160,157
157 IF(X=(1.60*QUALOL))162,162,165
160 P=PPFSIN
GO TO 167
162 P=PPFSIN-(0.750*TSDP*(X-QUALOL)/(XLNGTH-QUALOL))
GO TO 167
165 PRPFK=PPFSIN-(0.750*TSDP*(0.60*QUALOL)/(XLNGTH-QUALOL))
166 P=PRPFK-(PRPFK-PPFSIN)*(X-(1.60*QUALOL))/
1 (XLNGTH-(1.60*QUALOL)))
167 CALL LIOFN
DMFFX=ENFDX
CALL FVADFN
DMFFGX=FNFGDX

```

```

00430
00440
00450
00460
00470
00480
00490
00500
00510
00520
00530
00540
00550
00560
00570
00580
00590
00600
00610
00620
00630
00640
00650
00660
00670
00680
00690
00700
00710
00720
00730
00740
00750
00760
00770
00780
00790
00800
00810
00820
00830
00840
00850
00860
00870
00880
00890
00900
00910
00920
00930
00940
00950
00960
00970
00980
00990
01000
01010
01020
01030
01040
01050
01060
01070

```

```

PRINT 565 *X
PRINT 570 ,P
PRINT 575,DMFFX,DMFFGX
170 CFXLOX=POWER/ARFAIS
175 POWERX=POWER*(X/XLNGTH)
180 ENLOX=FNTHIN + POWERX/FLMASS
185 ENSLOX=ENLOX-DMFFX
190 QUALOX=ENSLOX/DMFFGX
PRINT 700,POWER,POWERX,CFXLOX
PRINT 710,ENLOX
PRINT 720,FNSLOX,QUALOX
700 FORMAT(14H POWER TOTAL = E9.4/,
1 28H POWER INPUT TO POSITION X = E9.4/,
2 18H LOCAL HEAT FLUX = E11.5)
710 FORMAT(31H LOCAL ENTHALPY AT POSITION X = F8.2)
720 FORMAT(41H LOCAL SUBCOOLED ENTHALPY AT POSITION X = F8.2/,
130H LOCAL QUALITY AT POSITION X = F6.3)
CALL FILMFR
460 CONTINUE
RETURN
END
SUBROUTINE COSINE
COMMON NTUBES,MSHAPE,TUBE,RATIOM,DIAINS,VOLTS,AMPS,ENTHIN,FLMASS,
00010
00020
00030
00040
00050
00060
00070
00080
00090
00100
00110
00120
00130
00140
00150
00160
00170
00180
00190
00200
00210
00220
00230
00240
00250
00260
00270
00280
00290
00300
00310
00320
00330
00340
00350
00360
00370
00380
1 PRESP,PRESIN,PRESOT,RESDP,TSDP,BOLOCA,XLNGTH,SHUNTM,P,
2 DMEFX,ENFDX,DMFFGX,ENFGDX,FNSIN,QUALIN,POWER,ARFAFL,ARFAIS,
3 QUALOL,SATL,PSATL,POWERB,PSLROL,CFXAVG,CFXLOX,JLOCAT,K,X,
4 PRPFK,POWERX,ENLOX,ENSLOX,QUALOX,DMEFY,DMEFGY,POWER,ONEOVM,
5 COSLEN,ONEWSO,SIGNZ,ARG,Z,FACMIB,FACPLR,CFXRO,Z,Y,
6 FACTM,POWERX,CFXLOX,ENLOY,ENSLOY,QUALOY,FACTPL,
7 CONST,SCRPTL,ZFTA,PLNGTH,J,U,ULOCAT,COSABK,SINABK,I,
8 EXTRA,EXTRAB,EXTRAC,EXTRAD,EXTRAE,EXTRAF,
9 DMEFB,DMEFGB,ENLOB,FNSLOB,QUALOR,EXTRAG,EXTRAH,EXTRAJ,EXTRAJ
COMMON QUALIA,GLIO,TKINCH,
1DP,DX,COLM1,COLM2,COLM3,COLM4,SUMCOL,PHIMN,GTOTSC,GSUBZ,SUM0,SUM1,
2SUM2,SUM3,SUM4,SUM5,OMFGAP,OMFGA,PGMULT,PSURL,T,VISCL,VOLSPL,ENO,
3VOLSPG,QUALO4,POWER,ANBOL,DFNFC,DENFGO,FNSO,QUALO,DVSPL0,DVSPGO,
4GTOT,DPDMO,GRDMT,DVLSPL,DVLSPL,TERM1,TERM2,TERM3,TERM4,GGAS,DT,
5DVISCL,REYNUM,FFACTP,FFACT,VFLOC,GPDFS,DPGMLT,GRDFT,GRDMT,GRDGT,
6B,GRAVAC,GRAVCS,GRAVCH,VALUEN,FACTUN,BMAOA,DRMAOA,A,FILMTK,YPLUS,
7TAUWAL,FYPLUS,GFILM,GLQENT,PCLIO,PCLNT,DUMMYA,DUMMYB,DUMMYC
515 FORMAT (F10.0,F10.2,F10.4,4F10.1)
520 FORMAT (5F10.0, 1F10.2)
525 FORMAT (2F10.2)
530 FORMAT(15,F10.3)
540 FORMAT(24H INLET LIQUID ENTHALPY = F8.2,
1 25H INLET EVAP ENTHALPY =F8.2, 22H INLET SUBCOOLING =F8.2)
543 FORMAT(16H INLET QUALITY = F6.3)
545 FORMAT(12H FLOW AREA =3PE15.2,25H INSIDE SURFACE AREA =0PE15.4)
550 FORMAT(35H LENGTH WHERE QUALITY EQUALS ZERO =F15.2)
1 42H LENGTH OVER WHICH QUALITY ABOVE ZERO =F15.2)
555 FORMAT(24H POWER OVER SAT LENGTH =1PE10.3,17H POWER TO BO =
1 1PE10.3,26H POWER FROM SAT TO BO = 1PE10.3)
560 FORMAT(20H AVG CRITICAL FLUX =1PF10.3,
1 25H CRITICAL FLUX AT BO = 1PE10.3)
565 FORMAT(F10.2)
570 FORMAT(F10.1)
575 FORMAT(2F20.2)
READ 515,TUBE,RATIOM,DIAINS,VOLTS,AMPS,ENTHIN,FLMASS
READ 520,PRESP,PRESIN,PRESOT,RESDP,TSDP,BOLOCA

```

115

```

READ 525,XLNGTH,SHUNTM
READ 530,JLOCAT,QUALIA
PRINT 515,TURF,PAT10M,DIAINS,VOLTS,AMPS,FNTHIN,FLMASS
PRINT 520,PPESD,PPESIN,PPESOT,PPESD,TSDP,ROLOCA
PRINT 525,XLNGTH,SHUNTM
PRINT 530,JLOCAT,QUALIA
P=PPESIN
CALL LIQFN
DMFFY=FNFPX
CALL FVAFEN
DMFFGY=FNFGPX
FNSIN=FNTHIN/DMFFY
QUALIN=FNSIN/DMFFGY
POWERT=VOLTS*AMPS*3.41*SHUNTM
ARFAFL=(3.1416*DIAINS*DIAINS)/(576.0)
ARFAIS=(3.1416*XLNGTH*DIAINS)/144.0
225 POWQO=-FNSIN*FLMASS
230 ONEFOVM=1.0/PAT10M
235 COSLEN=(1.5708*XLNGTH)/ACOS(ONEFOVM)
240 ONEMSQ=SQRT( (PAT10M**2-1.0) / PAT10M**2 )
IF (1.0-(2.0*POWQO/POWERT) ) 255, 255, 245
245 SIGNZ=ONEMSQ*(1.0-(2.0*POWQO/POWERT) )
GO TO 275
255 SIGNZ=ONEMSQ*( (2.0*POWQO/POWERT) -1.0 )
260 APO=ASINE(SIGNZ)
265 Z=COSLEN*APO/3.1416
270 QUALOL=(XLNGTH/2.0)*Z
GO TO 290
275 APO=ASINE(SIGNZ)
280 Z=COSLEN*APO/3.1416
285 QUALOL=(XLNGTH/2.0)*Z
290 SATL=POWERT-POWQO
IF (ROLOCA-(XLNGTH/2.0)) 325, 325, 340
325 FACPLR=(1.0-(SINE( (3.1416*(XLNGTH/2.0)-ROLOCA) )/COSLEN)/
ONEMSQ)
335 POWERR=(POWERT*FACPLR)/2.0
IF (ROLOCA-QUALOL) 750, 750, 755
755 IF (ROLOCA-(1.6*QUALOL)) 760, 760, 765
765 P=PPESIN
GO TO 770
770 P=PPESIN-(0.750*TSDP*(ROLOCA-QUALOL)/(XLNGTH-QUALOL))
GO TO 770
775 P=PPESIN-(0.750*TSDP*(0.60*QUALOL)/(XLNGTH-QUALOL))
P=PPFAK-((PPFAK-PPESOT)*(ROLOCA-(1.60*QUALOL))/(XLNGTH-
(1.60*QUALOL)))
780 CALL LIQFN
DMFFR=FNFPX
CALL FVAFEN
DMFFGR=FNFGPX
ENSLOR=FNTHIN+POWERR/FLMASS
ENSLOR=ENSLOR-DMFFR
QUALOR=ENSLOR/DMFFGR
338 CFXBO=144.0*(POWERT/(2.0*DIAINS*COSLEN*ONEMSQ))*
ICOSF(3.1416*(XLNGTH/2.0)-ROLOCA)/COSLEN)
340 PSLROL=POWERR-POWQO
GO TO 350
345 FACPLR=(1.0+(SINE( (3.1416*(ROLOCA-(XLNGTH/2.0) )/COSLEN)
)/ONEMSQ) )
345 POWERR=(POWERT*FACPLR)/2.0
IF (ROLOCA-QUALOL) 850, 850, 855
855 IF (ROLOCA-(1.6*QUALOL)) 860, 860, 865
860 P=PPESIN
GO TO 870
860 P=PPESIN-(0.750*TSDP*(ROLOCA-QUALOL)/(XLNGTH-QUALOL))

```

```

00390
00400
00410
00420
00430
00440
00450
00460
00470
00480
00490
00500
00510
00520
00530
00540
00550
00560
00570
00580
00590
00600
00610
00620
00630
00640
00650
00660
00670
00680
00690
00700
00710
00720
00730
00740
00750
00760
00770
00780
00790
00800
00810
00820
00830
00840
00850
00860
00870
00880
00890
00900
00910
00920
00930
00940
00950
00960
00970
00980
00990
01000
01010
01020
01030

```

```

GO TO 870
865 P=PPFAK-((PPFAK-PPESOT)*(ROLOCA-(1.60*QUALOL))/(XLNGTH-
1 (1.60*QUALOL)))
870 CALL LIQFN
DMFFR=FNFPX
CALL FVAFEN
DMFFGR=FNFGPX
ENLOB=FNTHIN+POWERR/FLMASS
ENSLOR=ENLOB-DMFFR
QUALOR=ENSLOR/DMFFGR
348 CFXBO=144.0*(POWERT/(2.0*DIAINS*COSLEN*ONEMSQ))*
ICOSF(3.1416*(ROLOCA-(XLNGTH/2.0) )/COSLEN )
350 PSLROL=POWERR-POWQO
353 CFXAVG=POWERT/AREAIS
PRINT 540,DMFFY,DMFFGY,FNSIN
PRINT 543, QUALIN
PRINT 545, ARFAFL, AREAIS
PRINT 550, QUALOL, SATL
PRINT 555, PSATL, POWERR, PSLROL
PRINT 560, CFXAVG, CFXRO
PRINT 775, P, DMFFR, DMFFGR
PRINT 780, ENSLOR, ENSLOR
PRINT 785, QUALOR
775 FORMAT(17H PRESSURE AT BO =F6.1,25H SAT LIQ ENTH AT BO =F8.2,
1 22H EVAP FNTH AT RO =F8.2)
780 FORMAT(13H FNTH AT RO =F8.2, 27H SUBCOOLED ENTH AT BO =F8.2)
785 FORMAT(16H QUALITY AT RO =F6.3)
CALL GDDMMO
CALL COSANN
DO 460 L=1,JLOCAT,3
360 Y=L-1
IF (Y-QUALOL) 370, 370, 365
365 IF (Y-(1.6*QUALOL) ) 375, 375, 380
370 P=PPESIN
GO TO 390
375 P=PPESIN-(0.750*TSDP*(Y-QUALOL)/(XLNGTH-QUALOL) )
GO TO 390
380 P=PPESIN-(0.750*TSDP*(0.60*QUALOL)/(XLNGTH-QUALOL) )
385 P=PPFAK-((PPFAK-PPESOT)*(Y-(1.60*QUALOL))/
1 (XLNGTH-(1.60*QUALOL)))
390 CALL LIQFN
DMFFY=FNFPX
CALL FVAFEN
DMFFGY=FNFGPX
PRINT 565,Y
PRINT 570, P
PRINT 575,DMFFY,DMFFGY
IF (Y-(XLNGTH/2.0) )400,400,428
400 FACTMI=(1.0-(SINE( (3.1416*( XLNGTH/2.0)-Y) )
1/COSLEN) )/ONEMSQ)
410 POWERY=(POWERT*FACTMI)/2.0
412 CFXLOY=144.0*(POWERT/(2.0*DIAINS*COSLEN*ONEMSQ))*
ICOSF(3.1416*( XLNGTH/2.0)-Y)/COSLEN)
415 ENLOY=FNTHIN+(POWERT*FACTMI)/(2.0*FLMASS)
420 ENSLOY=ENLOY-DMFFY
425 QUALOX=ENSLOR/DMFFGY
GO TO 455
428 FACTPL=(1.0+(SINE( (3.1416*(Y-(XLNGTH/2.0) ) )
1/COSLEN) )/ONEMSQ)
430 POWERY=(POWERT*FACTPL)/2.0
433 CFXLOY=144.0*(POWERT/(2.0*DIAINS*COSLEN*ONEMSQ))*
ICOSF(3.1416*(Y-(XLNGTH/2.0) )/COSLEN)
435 ENLOY=FNTHIN+(POWERT*FACTPL)/(2.0*FLMASS)
440 ENSLOY=ENLOY-DMFFY

```

```

01040
01050
01060
01070
01080
01090
01100
01110
01120
01130
01140
01150
01160
01170
01180
01190
01200
01210
01220
01230
01240
01250
01260
01270
01280
01290
01300
01310
01320
01330
01340
01350
01360
01370
01380
01390
01400
01410
01420
01430
01440
01450
01460
01470
01480
01490
01500
01510
01520
01530
01540
01550
01560
01570
01580
01590
01600
01610
01620
01630
01640
01650
01660
01670
01680

```

```

450 QUALOX=FNSLOY/DMEFGY 01690
455 CONTINUE 01700
PRINT 700,POWERPT,POWERY,CFXLOY 01710
PRINT 710,ENLOY 01720
PRINT 720,FNSLOY,QUALOX 01730
700 FORMAT(14H POWER TOTAL = F9.4/,
1 28H POWER INPUT TO POSITION X = E9.4/,
2 18H LOCAL HEAT FLUX = F11.5) 01760
710 FORMAT(31H LOCAL ENTHALPY AT POSITION7X = F8.7) 01770
720 FORMAT(41H LOCAL SUBCOOLED ENTHALPY AT POSITION X = F8.2/,
130H LOCAL QUALITY AT POSITION X = F6.3) 01780
CALL FILMFO 01790
460 CONTINUE 01800
PFTURN 01810
END 01830

SURROUTINF LININC 01290
COMMON NTUBFS,MSHAPE,TUBE,RATIOM,DIAINS,VOLTS,AMPS,ENTHIN,FLMASS, 01300
1 PRFSP,PRE SIN,PRE SOT,RES DP,TS DP,BOLOCA,XLNGTH,SHUNT M,P, 01310
2 DMFFX,ENFPX,DMEFGX,ENFGPX,FNSIN,QUALIN,POWER T,ARE AFL,ARE AIS, 01320
3 QUALOL,SATL,PSATL,POWERB,PSLBOL,CFXAVG,CFXLOX,JLOCAT,K,X, 01330
4 PBRFAK,POWFPX,ENLOX,ENSLQX,QUALOX,DMEFY,DMEFGY,POWQO,ONEOVM, 01340
5 COSLEN,ONFMSO,SIGNZ,ARG,Z,FACMIB,FACPLB,CFXBO,L,Y, 01350
6 FACTMI,POWERY,CFXLOY,ENLOY,ENSLQY,QUALQY,FACTPL, 01360
7 CONSTP,SCRPTL,ZETA,PLNGTH,J,U,ULOCAT,COSABK,SINABK,I, 01370
8 FXTAAA,FXTBAB,FXTAC,FXTAD,FXTAE,FXTAF, 01380
9 DMFFB,DMEFGB,FNLOB,FNSLOB,QUALOB,EXTRAG,EXTRAH,EXTRAJ,EXTRAJ 01390
COMMON QUALIA,GLIQ,TKINCH, 01400
1DP,DX,COLM1,COLM2,COLM3,COLM4,SUMCOL,PHIMN,GTOTSC,GSUBZ,SUM0,SUM1, 01410
2SUM2,SUM3,SUM4,SUM5,OMEGAP,OMEGA,PGMULT,PSUBL,T,VISCL,VOL SPL,FNO, 01420
3VOLSPG,QUALQ4,POWPA,PANBOL,DENFO,DENFGO,ENSO,QUALO,DVSPLO,DVSPGO, 01430
4GTOT,DPMOM,GRDMT,DVLSPL,DVLSPG,TERM1,TERM2,TERM3,TERM4,GGAS,DT, 01440
5DVISCL,REYNUM,FFACTP,FFACT,VELOC,GRDFS,DPGMLT,GRDFT,DGRDMT,GRDLOT, 01450
6R,GRAVAC,GRAVCS,GRAVCH,VALUEN,FACTUN,RMAOA,DBMAOA,A,FILMTK,YPLUS, 01460
7TAUWAL,FYPLUS,GFILM,GLQENT,PCLIQ,PCLFNT,DUMMYA,DUMMYB,DUMMYC 01470
515 FORMAT (F10.0,F10.2,F10.4,4F10.1) 01480
520 FORMAT (5F10.0,1F10.2) 01490
525 FORMAT (2F10.2) 01500
530 FORMAT(15,F10.3) 01510
540 FORMAT(24H INLET LIQUID ENTHALPY = F8.2,
1 25H INLET FVAP ENTHALPY =F8.2, 22H INLET SUBCOOLING =F8.2) 01520
545 FORMAT(16H INLET QUALITY = F6.3) 01530
545 FORMAT(12H FLOW AREA =3PE15.2,25H INSIDE SURFACE AREA =0PE15.4) 01540
550 FORMAT(35H LENGTH WHERE QUALITY EQUALS ZERO =F15.2,
1 47H LENGTH OVER WHICH QUALITY ABOVE ZERO =F15.2) 01550
555 FORMAT(24H POWER OVER SAT LENGTH =1PE10.3,17H POWER TO BO =
1 1PE10.3,26H POWER FROM SAT TO BO = 1PE10.2) 01560
560 FORMAT(20H AVG CRITICAL FLUX =1PE10.3,
1 25H CRITICAL FLUX AT BO = 1PE10.3) 01610
565 FORMAT(F10.2) 01620
570 FORMAT(F10.1) 01630
575 FORMAT(2F20.2) 01640
READ 515,TURE,RATIOM,DIAINS,VOLTS,AMPS,ENTHIN,FLMASS 01650
READ 520,PRFSP,PRE SIN,PRE SOT,RES DP,TS DP,BOLOCA 01660
READ 525,XLNGTH,SHUNT M 01670
READ 530,JLOCAT,QUALIA 01680
PRINT 515,TUBE,RATIOM,DIAINS,VOLTS,AMPS,ENTHIN,FLMASS 01690
PRINT 520,PRE SIN,PRE SOT,RES DP,TS DP,BOLOCA 01700
PRINT 525,XLNGTH,SHUNT M 01710
PRINT 530,JLOCAT,QUALIA 01720

```

```

100 P=PRFSIN 01730
CALL LIQEN 01740
DMFFX=FNFPX 01750
CALL FVAPFN 01760
DMEFGX=ENFGPX 01770
FNSIN=FNTHIN-DMEFX 01780
QUALIN=ENSIN/DMEFGX 01790
POWER T=VOLTS*AMPS*3.41*SHUNT M 01800
ARE AFL=(3.1416*DIAINS*DIAINS)/576.0 01810
ARE AIS=(3.1416*XLNGTH*DIAINS)/144.0 01820
POWQO=-(ENSIN*FLMASS) 01830
QUADA=(RATIOM-1.00)/(2.00*XLNGTH) 01840
QUADC=-(XLNGTH*(RATIOM+1.00)*POWQO)/(2.00*POWER T) 01850
QUALOL=(-1.00+(AR SF(SQRTF(1.00-4.00*QUADA*QUADC)))/(2.00*QUADA) 01860
SATL=XLNGTH-QUALOL 01870
PSATL=POWER T-POWQO 01880
POWERFR=(POWER T*2.00)/(RATIOM+1.00)*(BOLOCA/XLNGTH) 01890
1 *(BOLOCA*BOLOCA*(RATIOM-1.00)/(XLNGTH*XLNGTH*2.00)) 01900
IF (BOLOCA-QUALOL) 750,750,755 01910
755 IF (BOLOCA-(1.6*QUALOL)) 760,760,765 01920
750 P=PRE SIN 01930
GO TO 770 01940
760 P=PRFSIN- (0.750*TS DP*(BOLOCA-QUALOL)/(XLNGTH-QUALOL)) 01950
GO TO 770 01960
765 PBRFAK=PRE SIN-(0.750*TS DP*(0.60*QUALOL)/(XLNGTH-QUALOL)) 01970
P=PRE SIN-((PBRFAK-PRE SOT)*(BOLOCA-(1.60*QUALOL))/(XLNGTH-
1 (1.60*QUALOL))) 01980
770 CALL LIQEN 02000
DMEFB=ENFPX 02010
CALL FVAPFN 02020
DMFFGB=ENFGPX 02030
ENLOB=ENTHIN+POWERFR/FLMASS 02040
ENSLQB=ENLOB-DMEFB 02050
QUALOR=FNSLOB/DMEFGB 02060
CFXBO=(2.0*POWER T)/(APE AIS*(1.00+RATIOM)) 02070
1 *(1.00+(BOLOCA*(RATIOM-1.00))/XLNGTH) 02080
PSLROL=POWERFR-POWQO 02090
CFXAVG=POWER T/ARE AIS 02100
PRINT 540,DMEFX,DMEFGB,FNSIN 02110
PRINT 543, QUALIN 02120
PRINT 545,ARE AFL,ARE AIS 02130
PRINT 550,QUALOL,SATL 02140
PRINT 555 , PSATL, POWERB, PSLBOL 02150
PRINT 560,CFXAVG,CFXBO 02160
PRINT 775,P,DMEFB,DMEFGB 02170
PRINT 780,ENLOB,ENSLQB 02180
PRINT 785,QUALOR 02190
775 FORMAT(17H PRESSURE AT BO =F6.1,25H SAT LIQ ENTH AT BO =F8.2,
1 22H FVAP FNTH AT BO =F8.2) 02200
780 FORMAT(13H ENTH AT BO =F8.2, 27H SUBCOOLED ENTH AT BO =F8.2) 02220
785 FORMAT(16H QUALITY AT BO =F6.3) 02230
CALL GRDMOM 02240
CALL LNIANN 02250
DO 460 K=1,JLOCAT,3 02260
156 X=K-1 02270
IF(X=QUALOL)160,160,157 02280
157 IF(X-(1.60*QUALOL)) 162,162,165 02290
160 P=PRFSIN 02300
GO TO 167 02310
162 P=PRE SIN-(0.750*TS DP*(X-QUALOL)/(XLNGTH-QUALOL)) 02320
GOTO 167 02330
165 PBRFAK=PRE SIN-(0.750*TS DP*(0.60*QUALOL)/(XLNGTH-QUALOL)) 02340
166 P=PRE SIN-((PBRFAK-PRE SOT)*(X-(1.60*QUALOL))
1 (XLNGTH-(1.60*QUALOL))) 02350
167 CALL LIQEN 02360

```

```

DMFFX=ENFPX
CALL EVAPEN
DMFFGX=ENFGGX
PRINT 565,X
PRINT 570,P
PRINT 575,DMFFX,DMFFGX
CFXLOX=((2.0*POWER2)/(ARFAIS*(RATIO+1.00)))
1 *I,20+(X*(RATIO-1.00)/XLNGTH)
POWERX=((POWER*2.0)/(RATIO+1.00))*(X/XLNGTH+((X*X*(RATIO-1.00)
1)/(XLNGTH*XLNGTH*2.0)))
180 ENLOX=FNTHIN + POWERX/FLMASS
185 ENSLOX=ENLOX-DMFFX
190 QUALOX=ENSLGX/DMFFGX
PRINT 700,POWER,POWERX,CFXLOX
PRINT 710,ENLOX
PRINT 720,ENSLOX,QUALOX
700 FORMAT(14H POWER TOTAL = F9.4/,
1 2H INLET HEAT FLUX = F11.5)
710 FORMAT(13H LOCAL ENTHALPY AT POSITION 7X = F8.2)
720 FORMAT(14H LOCAL SUBCOOLED ENTHALPY AT POSITION X = F8.2/,
13H LOCAL QUALITY AT POSITION X = F6.3)
460 CALL FLMOP
CONTINUE
RETURN
END
02380
02390
02400
02410
02420
02430
02440
02450
02460
02470
02480
02490
02500
02510
02520
02530
02540
02550
02560
02570
02580
02590
02600
02610
02620
02630
02640
02650
02660
02670
02680
02690
02700
02710
02720
02730
02740
02750
02760
02770
02780
02790
02800
02810
02820
02830
02840
02850
02860
02870
02880
02890
02900
02910
02920
02930
02940
02950
02960

```

```

565 FORMAT(F10.2)
570 FORMAT(F10.1)
575 FORMAT(2F20.2)
READ 515,TURF,RATIO,DIAINS,VOLTS,AMPS,FNTHIN,FLMASS
PFAD 520,PPESP,PPRESIN,PPRESOT,RESDP,TSDP,ROLOCA
RFAD 525,XLNGTH,SHUNTM
PFAD 530,JLOCAT,QUALIA
PRINT 515,TURF,RATIO,DIAINS,VOLTS,AMPS,FNTHIN,FLMASS
PRINT 520,PPESP,PPRESIN,PPRESOT,RESDP,TSDP,ROLOCA
PRINT 525,XLNGTH,SHUNTM
PRINT 530,JLOCAT,QUALIA
100 P=PPRESIN
CALL LIQFN
DMFFX=ENFPX
CALL EVAPEN
DMFFGX=ENFGGX
ENSIN=FNTHIN-DMFFX
QUALIN=ENSIN/DMFFGX
POWER=VOLTS*AMPS*3.41*SHUNTM
AREAF=(3.1416*DIAINS*DIAINS)/576.0
ARFAIS=(3.1416*XLNGTH*DIAINS)/144.0
POWOO=(ENSIN*FLMASS)
QUADA=(RATIO-1.00)/(2.00*XLNGTH*RATIO)
QUADC=(XLNGTH*(RATIO+1.00)*POWOO)/(2.00*POWER*RATIO)
QUALOL=(1.00-(ARF(SQRT(1.00-4.00*QUADA*QUADC))))
1/(2.00*QUADA)
SATL=XLNGTH-QUALOL
PSATL=POWER-POWOO
POWER=((POWER*2.00*RATIO)/(RATIO+1.00))*
1((BOLOCA/XLNGTH)-(ROLOCA*BOLOCA*(RATIO-1.00))/(XLNGTH
2*XLNGTH*2.00*RATIO))
IF (BOLOCA-QUALOL) 750,750,755
755 IF (BOLOCA-(1.6*QUALOL)) 760,760,765
750 P=PPRESIN
GO TO 770
760 P=PPRESIN-(0.750*TSDP*(BOLOCA-QUALOL)/(XLNGTH-QUALOL))
GO TO 770
765 PBRFAK=PPRESIN-(0.750*TSDP*(0.60*QUALOL)/(XLNGTH-QUALOL))
P=PBRFAK-(PBRFAK-PPRESOT)*(BOLOCA-(1.60*QUALOL))/(XLNGTH-
1(1.60*QUALOL))
770 CALL LIQFN
DMFFB=ENFBX
CALL EVAPFN
DMFFGB=ENFGB
FNLOB=FNTHIN+POWER/FLMASS
FNSLOR=FNLOB-DMFFB
QUALOB=ENSLOR/DMFFGB
CFXRO=((2.0*POWER*RATIO)/(ARFAIS*(1.00+RATIO)))*
1(1.00-(BOLOCA*(RATIO-1.00))/(XLNGTH*RATIO))
PSLROL=POWER-POWOO
CFXAVG=POWER/ARFAIS
PRINT 540,DMFFX,DMFFGX,ENSIN
PRINT 543,QUALIN
PRINT 545,AREAF,ARFAIS
PRINT 550,QUALOL,SATL
PRINT 555,PSATL,POWER,PSLROL
PRINT 560,CFXAVG,CFXRO
PRINT 775,P,DMFFB,DMFFGB
PRINT 780,FNLOB,FNSLOR
PRINT 785,QUALOR
775 FORMAT(17H PRESSURE AT BO =F6.1,25H SAT LIQ ENTH AT BO =F8.2,
1 22H EVAP ENTH AT RO =F8.2)
780 FORMAT(13H FNTH AT RO =F8.2, 27H SUBCOOLED ENTH AT RO =F8.2)
785 FORMAT(16H QUALITY AT RO =F6.3)
CALL GRDMOM
02970
02980
02990
03000
03010
03020
03030
03040
03050
03060
03070
03080
03090
03100
03110
03120
03130
03140
03150
03160
03170
03180
03190
03200
03210
03220
03230
03240
03250
03260
03270
03280
03290
03300
03310
03320
03330
03340
03350
03360
03370
03380
03390
03400
03410
03420
03430
03440
03450
03460
03470
03480
03490
03500
03510
03520
03530
03540
03550
03560
03570
03580
03590
03600
03610

```

188

```

CALL LNDANN
DO 460 K=1,JLOCAT,3
156 X=K-1
IF(X-QUALOL)160,160,157
157 IF(X-(1.60*QUALOL))162,162,165
160 P=PPRESIN
GO TO 167
162 P=PPRESIN-(0.750*TSDP*(X-QUALOL)/(XLNGTH-QUALOL))
GO TO 167
164 PRPFAK=PPRESIN-(0.750*TSDP*(0.60*QUALOL)/(XLNGTH-QUALOL))
166 P=PRPFAK-((PRPFAK-PPRESIN)*(X-(1.60*QUALOL)))/(
1 (XLNGTH-(1.60*QUALOL)))
167 CALL LINDEN
DMFFX=FNFDPX
CALL FVAPFN
DMFFGX=FNFDPX
PRINT 565,X
PRINT 570,P
PRINT 575,DMFFX,DMFFGX
CFXLOX=((2.0*POWER**RAT10M)/(APEAIS*(1.00+RAT10M)))*
1(1.00-(X*(RAT10M-1.00)))/(XLNGTH*RAT10M)
DMFFOX=((POWER**RAT10M)/(RAT10M+1.00))*((X/XLNGTH)
1-(X*(RAT10M-1.00)))/(XLNGTH*XLNGTH*2.00*RAT10M)
187 FNLOX=FNTHIN + DMFFOX/FLMASS
185 FNSLOX=FNLOX-DMFFX
190 QUALOX=FNSLOX/DMFFGX
PRINT 700,POWER,DMFFOX,CFXLOX
PRINT 710,FNLOX
PRINT 720,FNSLOX,QUALOX
710 FORMAT(14H POWER TOTAL = E9.4/,
1 2RH POWER INPUT TO POSITION X = F9.4/,
2 18H LOCAL HEAT FLUX = E11.5)
710 FORMAT(31H LOCAL ENTHALPY AT POSITION X = F8.2)
720 FORMAT(41H LOCAL SURCOOLED ENTHALPY AT POSITION X = F8.2/,
10H LOCAL QUALITY AT POSITION X = F6.3)
CALL FILMFO
460 CONTINUE
RETURN
END

```

```

03620
03630
03640
03650
03660
03670
03680
03690
03700
03710
03720
03730
03740
03750
03760
03770
03780
03790
03800
03810
03820
03830
03840
03850
03860
03870
03880
03890
03900
03930
03940
03950
03960
03970
03980
03990
04000

```

```

SUBROUTINE PKIN
COMMON NTUBES,MSHAPE,TUBE,RAT10M,DIAINS,VOLTS,AMPS,ENTHIN,FLMASS,
1 PRESIN,PPRESIN,PRESOT,PPRESOT,TSDP,BOLOCA,XLNGTH,SHUNTM,P,
2 DMFFX,FNFDPX,DMFFGX,FNFDPX,FNSIN,QUALIN,POWER,AREAF,AREAIS,
3 QUALOL,SATL,PSATL,POWERB,PSLROL,CFXAVG,CFXLOX,JLOCAT,K,X,
4 PRPFAK,DMFFOX,FNLOX,FNSLOX,QUALOX,DMFFY,DMFFGY,POWOO,ONEOVM,
5 COSLEN,ONEMSQ,SINZ,ARG,Z,FACTM,FACTPL,CFXBO,L,Y,
6 FACTM,POWERF,CFXLOY,FNLOY,FNSLOY,QUALOY,FACTPL,
7 CONSTP,SCRPTL,ZFTA,PLNGTH,J,U,JLOCAT,COSABK,SINABK,I,
8 EXTRAA,FXTRAB,FXTRAC,FXTRAD,EXTRAE,EXTRAF,EXTRAG,
9 DMFFB,DMFFGB,FNLOB,FNSLOB,QUALOB,EXTRAG,EXTRAH,EXTRAJ,EXTRAJ
COMMON QUALIA,GLIO,TKINCH,
1DP,DX,COLM1,COLM2,COLM3,COLM4,SUMCOL,PHIMN,GTOTSC,GSUB2,SUM0,SUM1,
2SUM2,SUM3,SUM4,SUM5,DFEGAP,OMEGA,PGMULT,PSURL,T,VISCL,VOLSP,ENO,
3VOLSPG,QUALO4,POWERPA,PANBOL,DEFNO,DEFNGO,ENSO,QUALO,DVSPLO,DVSPGO,
4GTOT,DPMMO,GRDMT,DVLSPL,DVLSPG,TERM1,TERM2,TERM3,TERM4,GGAS,DT,
5NVISCL,REFNUM,FFACT,FFACT,VFLOC,GRDPS,DRGMLT,GRDFT,DGRDMT,GRDTOT,
6R,CPAVAC,CPAVCS,CPAVCH,VALUEN,FACTUN,RMAOA,DRMAOA,A,FILMTK,YPLUS,
7TAUWAL,FYPLUS,GFILM,GLQENT,PCLIQ,PCLFNT,DUMMYA,DUMMYB,DUMMYC
515 FORMAT (F10.0,F10.2,F10.4,4F10.1)
00010
00020
00030
00040
00050
00060
00070
00080
00090
00100
00110
00120
00130
00140
00150
00160
00170
00180
00190
00210

```

```

520 FORMAT (5F10.0, 1F10.2)
525 FORMAT (2F10.2)
530 FORMAT(15,F10.3)
540 FORMAT(24H INLET LIQUID ENTHALPY = F8.2,
1 25H INLET EVAP ENTHALPY =F8.2, 22H INLET SUBCOOLING =F8.2)
543 FORMAT(16H INLET QUALITY = F6.3)
545 FORMAT(12H FLOW AREA =3PE15.2,25H INSIDE SURFACE ARFA =0PE15.4)
550 FORMAT(95H LENGTH WHFRE QUALITY EQUALS ZFRO =F15.2,
1 42H LENGTH OVER WHICH QUALITY ABOVE ZERO =F15.2)
555 FORMAT(24H POWER OVER SAT LENGTH =1PE10.3,17H POWER TO BO =
1 1PE10.3,26H POWER FROM SAT TO BO = 1PE10.3)
560 FORMAT(20H AVG CRITICAL FLUX =1PE10.3,
1 25H CRITICAL FLUX AT BO = 1PE10.3)
565 FORMAT(F10.2)
570 FORMAT(F10.1)
575 FORMAT(2F20.2)
580 FORMAT (3F10.2)
READ 515,TURB,RAT10M,DIAINS,VOLTS,AMPS,ENTHIN,FLMASS
READ 520,PRESIN,PRESOT,RESDP,TSDP,BOLOCA
READ 525,XLNGTH,SHUNTM
READ 530,JLOCAT,QUALIA
READ 580,SCRPTL,ZETA,PLNGTH
PRINT 515,TURB,RAT10M,DIAINS,VOLTS,AMPS,ENTHIN,FLMASS
PRINT 520,PRESIN,PRESOT,RESDP,TSDP,BOLOCA
PRINT 525,XLNGTH,SHUNTM
PRINT 530,JLOCAT,QUALIA
PRINT 580,SCRPTL,ZETA,PLNGTH
P=PPRESIN
CALL LINDEN
DMFFY=FNFDPX
CALL FVAPFN
DMFFGY=FNFDPX
FNSIN=FNTHIN-DMFFY
QUALIN=FNSIN/DMFFGY
POWER=VOLTS*AMPS*3.41*SHUNTM
AREAF=(3.1416*DIAINS*DIAINS)/(576.0)
AREAIS=(3.1416*XLNGTH*DIAINS)/144.0
225 POWOO =-FNSIN*FLMASS
230 ONEOVM =1.0/RAT10M
COSLEN = (1.5708*PLNGTH) /ACOS(ONEOVM)
240 ONEMSQ = SORTF( (RAT10M**2 -1.0) / RAT10M**2 )
SINABK=SINF(3.1416*(XLNGTH-SCRPTL-(.500*PLNGTH)))/COSLEN)
COSABK=COSF(3.1416*(XLNGTH-SCRPTL-(.500*PLNGTH)))/COSLEN)
EXTRAA=SINABK+ONEMSQ
EXTRAB=(SCRPTL-COSARK)/ZFTA
CONSTP=((COSLEN*EXTRAA)/3.1416)+(EXTRAB*(1.00-EXP(-ZFTA) ) )
EXTRAC=(POWER/COSLEN)/(3.1416*CONSTP)
EXTRAD=1.0+(((COSLEN*EXTRAA)/3.1416)-(CONSTP*POWOO/POWER))/EXTRAB)
EXTRAE=(144.0*POWER)/(CONSTP*DIAINS*3.1416)
IF (POWOO-(EXTRAC*ONEMSQ)) 245,245,255
245 SINZ=ONEMSQ-(POWOO/EXTRAC)
ARG=ASINF(SINZ)
Z=COSLEN*ARG/3.1416
QUALOL=(PLNGTH/2.00)-Z
GO TO 270
255 IF (POWOO-(EXTRAC*(ONEMSQ+SINABK))) 260,260,265
260 SINZ = -(ONEMSQ-(POWOO/EXTRAC))
ARG=ASINF(SINZ)
Z=COSLEN*ARG/3.1416
QUALOL=(PLNGTH/2.00)+Z
GO TO 270
265 U=(SCRPTL/ZETA)*LOGF(EXTRAD)
QUALOL=XLNGTH-SCRPTL+U
270 SATL=XLNGTH-QUALOL
PSATL=POWER-POWOO
06220
06230
06240
06250
06260
06270
06280
06290
06300
06310
06320
06330
06340
06350
06360
06370
06380
06390
06400
06410
06420
06430
06440
06450
06460
06470
06480
06490
06500
06510
06520
06530
06540
06550
06560
06570
06580
06590
06600
06610
06620
06630
06640
06650
06660
06670
06680
06690
06700
06710
06720
06730
06740
06750
06760
06770
06780
06790
06800
06810
06820
06830
06840
06850
06860

```

```

IF (BOLOCA-(PLNGTH/2.00)) 275,275,280
275 POWFRB=EXTRAC*(ONEMSQ-SINF(3.1416*((PLNGTH/2.00)-
1*ROLOCA)/COSLEN))
IF (ROLOCA-QUALOL) 760,750,755
755 IF (BOLOCA-(1.6*QUALOL)) 760,760,765
750 P=PPRESIN
GO TO 770
760 P=PPRESIN-(0.750*TSDP*(BOLOCA-QUALOL)/(XLNGTH-QUALOL))
GO TO 770
765 PRRFAK=PPRESIN-(0.750*TSDP*(0.60*QUALOL)/(XLNGTH-QUALOL))
P=PBRFAK-((PRRFAK-PPRESOT)*(BOLOCA-(1.60*QUALOL))/(XLNGTH-
1 (1.60*QUALOL)))
770 CALL LIQEN
DMFFR=FNF PX
CALL EVAPFN
DMFFGB=ENFGPX
ENLOB=ENTHIN+POWERB/FLMASS
FNSLOB=ENLOB-DMEFB
QUALOR=ENSLOB/DMEFGB
CFXRO =EXTRAF*COSF(3.1416*((PLNGTH/2.00)-
1*ROLOCA)/COSLEN)
GO TO 350
280 IF (ROLOCA-(XLNGTH-SCRPTL)) 285,285,290
285 POWFRB=EXTRAC*(ONEMSQ+SINF(3.1416*(
1*ROLOCA-(PLNGTH/2.00))/COSLEN))
IF (ROLOCA-QUALOL) 850,850,855
855 IF (BOLOCA-(1.6*QUALOL)) 860,860,865
850 P=PPRESIN
GO TO 870
860 P=PPRESIN-(0.750*TSDP*(BOLOCA-QUALOL)/(XLNGTH-QUALOL))
GO TO 870
865 PBRFAK=PPRESIN-(0.750*TSDP*(0.60*QUALOL)/(XLNGTH-QUALOL))
P=PBRFAK-((PBRFAK-PPRESOT)*(BOLOCA-(1.60*QUALOL))/(XLNGTH-
1 (1.60*QUALOL)))
870 CALL LIQFN
DMFFR=FNF PX
CALL EVAPFN
DMFFGB=ENFGPX
FNLOR=ENTHIN+POWERB/FLMASS
FNSLOR=FNLOR-DMEFB
QUALOR=FNSLOR/DMEFGB
CFXBO =EXTRAE*COSF(3.1416*(
1*ROLOCA-(PLNGTH/2.00))/COSLEN)
GO TO 350
290 POWFRB=(POWER/CONSTP)*((COSLEN*EXTRAA/3.1416)+EXTRAR*(1.00-
1*XPFI (-ZETA)*(BOLOCA-(XLNGTH-SCRPTL))/SCRPTL))
IF (BOLOCA-QUALOL) 950,950,955
955 IF (BOLOCA-(1.6*QUALOL)) 960,960,965
950 P=PPRESIN
GO TO 970
960 P=PPRESIN-(0.750*TSDP*(BOLOCA-QUALOL)/(XLNGTH-QUALOL))
GO TO 970
965 PBRFAK=PPRESIN-(0.750*TSDP*(0.60*QUALOL)/(XLNGTH-QUALOL))
P=PBRFAK-((PBRFAK-PPRESOT)*(BOLOCA-(1.60*QUALOL))/(XLNGTH-
1 (1.60*QUALOL)))
970 CALL LIQFN
DMFFR=FNF PX
CALL EVAPFN
DMFFGB=ENFGPX
ENLOB=ENTHIN+POWERB/FLMASS
FNSLOB=ENLOB-DMEFB
QUALOR=FNSLOB/DMEFGB
CFXRO =EXTRAF*COSASK*FXPF( (-ZETA)*(
1*ROLOCA-(XLNGTH-SCRPTL))/SCRPTL)
350 PSLBOL =POWFRB-POWOD

```

```

00870
00880
00890
00900
00910
00920
00930
00940
00950
00960
00970
00980
00990
01000
01010
01020
01030
01040
01050
01060
01070
01080
01090
01100
01110
01120
01130
01140
01150
01160
01170
01180
01190
01200
01210
01220
01230
01240
01250
01260
01270
01280
01290
01300
01310
01320
01330
01340
01350
01360
01370
01380
01390
01400
01410
01420
01430
01440
01450
01460
01470
01480
01490
01500
01510

```

```

353 CFXAVG = POWER / AREAIS
01520
PRINT 540,DMEFY,DMEFGY,ENSIN 01530
PRINT 543, QUALIN 01540
PRINT 545, AREAFL,AREAIS 01550
PRINT 550,QUALOL, SATL 01560
PRINT 555,PSATL, POWERB, PSLBOL 01570
PRINT 560,CFXAVG,CFXBO 01580
PRINT 775,P,DMEFB,DMEFGB 01590
PRINT 780,FNLOR,ENSLOB 01600
PRINT 785,QUALOR 01610
775 FORMAT(17H PRESSURE AT BO =F6.1,25H SAT LIQ ENTH AT BO =F8.2,
1 22H EVAP ENTH AT BO =F8.2) 01620
780 FORMAT(13H ENTH AT BO =F8.2, 27H SUBCOOLED ENTH AT BO =F8.2) 01630
785 FORMAT(16H QUALITY AT BO =F6.3) 01640
CALL GRDMOM 01650
CALL PKIANN 01660
DO 460 L=1,JLOCAT,2 01670
360 Y=L-1 01680
IF (Y - QUALOL) 370, 370, 365 01690
365 IF (Y -(1.6*QUALOL)) 375, 375, 380 01700
370 P = PRESIN 01710
GO TO 390 01720
375 P=PRESTN-(0.750*TSDP*(Y-QUALOL)/(XLNGTH-QUALOL)) 01730
GO TO 390 01740
380 PBREAK=PRESTN-(0.750*TSDP*(0.60*QUALOL)/(XLNGTH-QUALOL)) 01750
385 P=PBREAK-((PBRFAK-PPRESOT)*(Y-(1.60*QUALOL))/
1 (XLNGTH-(1.60*QUALOL))) 01760
390 CALL LIQFN 01770
DMFFY=FNF PX 01780
CALL EVAPFN 01790
DMEFGY=ENFGPY 01800
PRINT 565,Y 01810
PRINT 570, P 01820
PRINT 575,DMEFY,DMEFGY 01830
IF (Y-(PLNGTH/2.0)) 400,400,410 01840
400 POWERY=EXTRAC*(ONEMSQ-SINF(3.1416*((PLNGTH/2.00)-
1Y )/COSLEN)) 01850
CFXLOY=EXTRAF*COSF(3.1416*((PLNGTH/2.00)-
1Y )/COSLEN) 01860
GO TO 435 01870
410 IF (Y-(XLNGTH-SCRPTL)) 415,415,425 01880
415 POWERY=EXTRAC*(ONEMSQ+SINF(3.1416*(
1Y -(PLNGTH/2.00))/COSLEN)) 01890
CFXLOY=EXTRAE*COSF(3.1416*(
1Y -(PLNGTH/2.00))/COSLEN) 01900
GO TO 435 01910
425 POWERY=(POWER/CONSTP)*((COSLEN*EXTRAA/3.1416)+EXTRAR*(1.00-
1*XPFI (-ZETA)*(Y -(XLNGTH-SCRPTL))/SCRPTL)) 01920
CFXLOY=EXTRAE*COSASK*FXPF( (-ZETA)*(
1Y -(XLNGTH-SCRPTL))/SCRPTL) 01930
435 ENLOY=ENTHIN+(POWERY/FLMASS) 01940
440 ENSLOY=ENLOY-DMEFY 01950
450 QUALOX=ENSLOY/DMEFGY 01960
455 CONTINUE 01970
PRINT 700,POWER,POWERY,CFXLOY 01980
PRINT 710,ENLOY 01990
PRINT 720,FNSLOY,QUALOX 02000
700 FORMAT(14H POWER TOTAL = E9.4/,
1 28H POWER INPUT TO POSITION X = E9.4/,
2 18H LOCAL HEAT FLUX = E11.5) 02010
710 FORMAT(31H LOCAL ENTHALPY AT POSITION X = F8.2) 02020
720 FORMAT(41H LOCAL SUBCOOLED ENTHALPY AT POSITION X = F8.2/,
130H LOCAL QUALITY AT POSITION X = F6.3) 02030
CALL FILMFR 02040
460 CONTINUE 02050
02060
02070
02100
02110
02120
02130
02140
02150
02160

```

105

```

RETURN
END

SURROUTINE PKOUT
COMMON NTUBFS,MSHAPF,TUBE,RATION,DIAINS,VOLTS,AMPS,ENTHIN,FLMASS,
1 PPFSP,PPFSIN,PPFSOT,RESDD,TSDD,BOLOCA,XLNGTH,SHUNTM,P,
2 DMFFX,FNFPX,DMFFGX,FNFGPX,ENSIN,QUALIN,POWER,AREAF,AREATS,
3 QUALOL,SATL,PSATL,POWERR,PSLROL,CFXAVG,CFXLOX,JLOCAT,K,X,
4 PRRFAK,POWEPX,FNLOX,FNSLOX,QUALOX,DMFFY,DMFFGY,POWOO,ONFOVM,
5 COSLEN,ONFMSQ,SIGNZ,ARG,Z,FACMIR,FACPLB,CFXBO,L,Y,
6 FACMI,POWERY,CFXLOY,FNLOY,FNSLOY,QUALOY,FACTPL,
7 CONSTP,SCRPTL,ZFTA,PLNGTH,J,U,ULOCAT,COSABK,STNARK,I,
8 EXTRAA,EXTRAR,EXTRAC,EXTRAD,EXTRAF,EXTRAF,
9 DMFFB,DMFFGB,ENLOB,FNSLOB,QUALOB,EXTRAG,EXTRAH,EXTRAJ,EXTRAJ
COMMON QUALIA,GLI,TKINCH,
1DP,DX,COLM1,COLM2,COLM3,COLM4,SUMCOL,PHIMN,GTOTSC,GSUBZ,SUM0,SUM1,
2SUM2,SUM3,SUM4,SUM5,DMFFAP,DMFFGA,PGMULT,PSURL,T,VISCL,VOLSP,ENO,
3VOLSPG,QUALO,POWFA,PANBOL,DFNFO,DFNFGO,FNSO,QUALO,DVSPLO,DVSPGO,
4GTOT,DPMMV,GRDMT,DVLSPL,DVLSPG,TERM1,TERM2,TERM3,TERM4,GGAS,DT,
5DVISCL,RYENUM,FFACTP,FFACT,VELOC,GRDES,DPGMLT,GRDFT,GRDMT,GRDGT,
6R,GRAVAC,GRAVCH,VALUEN,FACTUN,BMAOA,DBMAOA,A,FLMTK,YPLUS,
7TAUVAL,FYPLUS,GFILY,GLOENT,PCLIO,PCLFNT,DUMMYA,DUMMYB,DUMMYC
515 FORMAT (F10.2,F10.2,F10.4,F10.1)
520 FORMAT (5F10.2,1F10.2)
525 FORMAT (2F10.2)
530 FORMAT (15,F10.3)
540 FORMAT (24H INLET LIQUID ENTHALPY = F8.2,
1 25H INLET FVAP ENTHALPY = F8.2, 22H INLET SUBCOOLING = F8.2)
543 FORMAT (16H INLET QUALITY = F6.3)
545 FORMAT (12H FLOW AREA = 3PE15.2, 25H INSIDE SURFACE AREA = 0PE15.4)
550 FORMAT (35H LENGTH WHERE QUALITY EQUALS ZFRO = F15.2,
1 42H LENGTH OVER WHICH QUALITY ABOVE ZERO = F15.2)
555 FORMAT (24H POWER OVER SAT LENGTH = 1PE10.3, 17H POWER TO BO =
1 1PE10.3, 26H POWER FROM SAT TO BO = 1PE10.3)
560 FORMAT (27H AVG CRITICAL FLUX = 1PF10.3,
1 25H CRITICAL FLUX AT BO = 1PF10.3)
565 FORMAT (F10.2)
570 FORMAT (F10.1)
575 FORMAT (2F20.2)
580 FORMAT (3F10.2)
DEAD 515,TURF,RATION,DIAINS,VOLTS,AMPS,ENTHIN,FLMASS
DEAD 520,PPFSP,PPFSIN,PPFSOT,RESDD,TSDD,BOLOCA
DEAD 525,XLNGTH,SHUNTM
DEAD 530,JLOCAT,QUALIA
DEAD 540,SCRPTL,ZFTA,PLNGTH
DOINT 515,TURF,DIAINS,DIAINS,VOLTS,AMPS,ENTHIN,FLMASS
DOINT 520,PPFSP,PPFSIN,PPFSOT,RESDD,TSDD,BOLOCA
DOINT 525,XLNGTH,SHUNTM
DOINT 530,JLOCAT,QUALIA
DOINT 540,SCRPTL,ZFTA,PLNGTH
P=PPFSIN
CALL LIQFN
DMFFY=FNFPX
CALL FVAPFN
DMFFGY=FNFGPX
FNSIN=ENTHIN-DMFFY
QUALIN=FNSIN/DMFFGY
POWER=VOLTS*AMPS*3.41*SHUNTM
AREAF=(3.1416*DIAINS*DIAINS)/(576.0)
AREATS=(3.1416*XLNGTH*DIAINS)/144.0

```

02170
02180

00010
00020
00030
00040
00050
00060
00070
00080
00090
00100
00110
00120
00130
00140
00150
00160
00170
00180
00190
00200
00210
00220
00230
00240
00250
00260
00270
00280
00290
00300
00310
00320
00330
00340
00350
00360
00370
00380
00390
00400
00410
00420
00430
00440
00450
00460
00470
00480
00490
00500
00510
00520
00530
00540
00550
00560
00570
00580

```

225 POWOO = -FNSIN*FLMASS
230 ONFOVM = 1.0/RATION
COSLEN = (1.5708*PLNGTH) / ACOS(ONEOVM)
240 ONFMSQ = SQRT( (RATIOM**2 - 1.0) / RATIOM**2 )
SINARK = SIN(3.1416*(XLNGTH-SCRPTL-(.500*PLNGTH))/COSLEN)
COSABK = COS(3.1416*(XLNGTH-SCRPTL-(.500*PLNGTH))/COSLEN)
EXTRAA = SINARK+ONFMSQ
EXTRAB = (SCRPTL*COSABK)/ZETA
CONSTP = ((COSLEN*EXTRAA)/(3.1416) + (EXTRAB*(1.00-EXPF(-ZFTA) ) ) )
EXTRAF = (144.0*POWERT)/(CONSTP*DIAINS*3.1416)
JLOCAT = 1.00-EXPF(-ZFTA)
EXTRAF = (POWER*(COSABK*SCRPTL)/(CONSTP*ZETA)
IF (POWOO-(EXTRAF*ULOCAT)) 245,245,255
245 U = SCRPTL+(SCRPTL/ZFTA)*LOG((POWOO/EXTRAF)+EXPF(-ZETA))
QUALOL = U
GO TO 270
255 IF (POWOO-((POWER/CONSTP)*((EXTRAB*ULOCAT)+(COSLEN*SINARK/
13.1416)))) 260,260,265
260 SINZ = SINARK + ((3.1416/COSLEN)*((EXTRAB*ULOCAT) - (CONSTP*POWOO/
1POWERT) ) )
ARG=ASIN(SINZ)
Z=COSLEN*ARG/3.1416
QUALOL=XLNGTH-(PLNGTH/2.00)-Z
GO TO 270
265 SINZ = -SINARK - ((3.1416/COSLEN)*((EXTRAB*ULOCAT) - (CONSTP*POWOO/
1POWERT) ) )
ARG=ASIN(SINZ)
Z=COSLEN*ARG/3.1416
QUALOL=XLNGTH-(PLNGTH/2.00)+Z
270 SATL=XLNGTH-QUALOL
PSATL=POWERT-POWOO
IF (BOLOCA-SCRPTL) 275,275,280
275 POWERR=EXTRAF*(EXPF(ZETA*(
1BOLOCA-SCRPTL)/SCRPTL)-EXPF(-ZETA))
IF (BOLOCA-QUALOL) 750,750,755
755 IF (BOLOCA-(1.6*QUALOL)) 760,760,765
750 P=PRESIN
GO TO 770
760 P=PRESIN-(0.750*TSDD*(BOLOCA-QUALOL)/(XLNGTH-QUALOL))
GO TO 770
765 PRRFAK=PRESIN-(0.750*TSDD*(0.60*QUALOL)/(XLNGTH-QUALOL))
P=PBRFAK-(PBRFAK-PRESOT)*(BOLOCA-(1.60*QUALOL))/(XLNGTH-
1(1.60*QUALOL))
770 CALL LIQFN
DMFFB=FNFPX
CALL FVAPFN
DMFFGB=FNFGPX
FNLOB=ENTHIN+POWERR/FLMASS
FNSLOB=FNLOB-DMFFB
QUALOB=FNSLOB/DMFFGB
CFXRO=EXTRAF*COSABK*(EXPF(ZFTA*(
1BOLOCA-SCRPTL)/SCRPTL))
GO TO 350
280 IF (BOLOCA-(XLNGTH-(PLNGTH/2.00))) 285,285,290
285 POWERR = (POWER/CONSTP)*((EXTRAB*ULOCAT) + ((COSLEN/3.1416)*(
1SINARK-SIN((3.1416/COSLEN)*(XLNGTH-(PLNGTH/2.00)-BOLOCA) ) ) ) )
IF (BOLOCA-QUALOL) 850,850,855
855 IF (BOLOCA-(1.6*QUALOL)) 860,860,865
850 P=PRESIN
GO TO 870
860 P=PRESIN-(0.750*TSDD*(BOLOCA-QUALOL)/(XLNGTH-QUALOL))
GO TO 870
865 PRRFAK=PRESIN-(0.750*TSDD*(0.60*QUALOL)/(XLNGTH-QUALOL))
P=PBRFAK-(PBRFAK-PRESOT)*(BOLOCA-(1.60*QUALOL))
1/(XLNGTH-(1.60*QUALOL))

```

00590
00600
00610
00620
00630
00640
00650
00660
00670
00680
00690
00700
00710
00720
00730
00740
00750
00760
00770
00780
00790
00800
00810
00820
00830
00840
00850
00860
00870
00880
00890
00900
00910
00920
00930
00940
00950
00960
00970
00980
00990
01000
01010
01020
01030
01040
01050
01060
01070
01080
01090
01100
01110
01120
01130
01140
01150
01160
01170
01180
01190
01200
01210
01220
01230

```

870 CALL LIOFN
DMFFR=ENFPX
CALL EVAPFN
DMFFGR=ENFGPX
FNLOB=FNTHIN+POWER/FLMASS
FNSLOB=FNSLOB-DMFFR
QUALOR=FNSLOB/DMFFGR
CFXBO=EXTRAF*COSF((3.1416/COSLEN)*(XLNGTH-(PLNGTH/2.00)-BOLOCA)
GO TO 350
290 POWER=(POWER/CONSTP)*((EXTRAB*ULOCAT)+(COSLEN/3.1416)*
1SINARK+SINF((3.1416/COSLEN)*(BOLOCA-(XLNGTH-(PLNGTH/2.00))))
2))
IF (BOLOCA-QUALOR) 950,950,955
955 IF (BOLOCA-(1.6*QUALOR)) 960,960,965
960 D=PRESIN
GO TO 970
967 D=PRESIN-(0.750*TSDP*(BOLOCA-QUALOR)/(XLNGTH-QUALOR))
GO TO 970
965 DRPEAK=PRESIN-(0.750*TSDP*(0.60*QUALOR)/(XLNGTH-QUALOR))
D=DRPEAK-((DRPEAK-PRESOT)*(BOLOCA-(1.60*QUALOR)/(XLNGTH-
1(1.60*QUALOR))))
970 CALL LIOFN
DMFFR=ENFPX
CALL EVAPFN
DMFFGR=ENFGPX
FNLOB=FNTHIN+POWER/FLMASS
FNSLOB=FNSLOB-DMFFR
QUALOR=FNSLOB/DMFFGR
CFXBO=EXTRAF*COSF((3.1416/COSLEN)*(BOLOCA-(XLNGTH-(PLNGTH/2.00)
1))
350 PSLOL=POWER-POWER
353 CFXAVG=POWER/AREAFS
PRINT 540,DMFFY,DMFFGY,ENSIN
PRINT 543,QUALIN
PRINT 545,AREAF,AREAFS
PRINT 550,QUALOR,SATL
PRINT 555,PSATL,POWERB,PSLOL
PRINT 560,CFXAVG,CFXBO
PRINT 775,D,DMFFB,DMFFGB
PRINT 780,ENLOB,FNSLOB
PRINT 785,QUALOR
775 FORMAT(17H PRESSURE AT BO =F6.1,25H SAT LIO ENTH AT BO =F8.2,
1 22H EVAP FNTH AT BO =F8.2)
780 FORMAT(17H FNTH AT BO =F8.2, 27H SUBCOOLED ENTH AT BO =F8.2)
785 FORMAT(16H QUALITY AT BO =F6.3)
CALL GROUND
CALL PKOANN
DO 460 L=1,JLOCAT,2
360 Y=L-1
IF (Y=QUALOR) 370, 370, 365
365 IF (Y-(1.4*QUALOR)) 375, 375, 380
370 D=PRESIN
GO TO 390
375 D=PRESIN-(0.750*TSDP*(Y-QUALOR)/(XLNGTH-QUALOR))
GO TO 390
380 DRPEAK=PRESIN-(0.750*TSDP*(0.60*QUALOR)/(XLNGTH-QUALOR))
D=DRPEAK-((DRPEAK-PRESOT)*(Y-(1.60*QUALOR))/(
1(XLNGTH-(1.60*QUALOR))))
390 CALL LIOFN
DMFFY=ENFPX
CALL EVAPFN
DMFFGY=ENFGPX
PRINT 545,Y
PRINT 570,D
PRINT 575,DMFFY,DMFFGY

```

```

01240
01250
01260
01270
01280
01290
01300
01310
01320
01330
01340
01350
01360
01370
01380
01390
01400
01410
01420
01430
01440
01450
01460
01470
01480
01490
01500
01510
01520
01530
01540
01550
01560
01570
01580
01590
01600
01610
01620
01630
01640
01650
01660
01670
01680
01690
01700
01710
01720
01730
01740
01750
01760
01770
01780
01790
01800
01810
01820
01830
01840
01850
01860
01870
01880

```

```

IF (Y-SCRPTL) 400,400,410
400 POWERY=EXTRAF*(FXPF(ZETA*(
1Y -SCRPTL)/SCRPTL)-EXPF(-ZFTA))
CFXLOY=EXTRAF*COSARK*(FXPF(ZFTA*(
1Y -SCRPTL)/SCRPTL))
GO TO 435
410 IF (Y-(XLNGTH-(PLNGTH/2.00))) 415,415,425
415 POWERY=(POWER/CONSTP)*((EXTRAB*ULOCAT)+(COSLEN/3.1416)*
1SINARK-SINF((3.1416/COSLEN)*(XLNGTH-(PLNGTH/2.00)-Y
1))
CFXLOY=EXTRAF*COSF((3.1416/COSLEN)*(XLNGTH-(PLNGTH/2.00)-Y
1))
GO TO 435
425 POWERY=(POWER/CONSTP)*((EXTRAB*ULOCAT)+(COSLEN/3.1416)*
1SINARK+SINF((3.1416/COSLEN)*(Y -(XLNGTH-(PLNGTH/2.00)
1))
CFXLOY=EXTRAF*COSF((3.1416/COSLEN)*(Y -(XLNGTH-(PLNGTH/2.00)
1))
435 FNLOY=FNTHIN+(POWER/FLMASS)
440 FNSLOY=FNLOY-DMFFY
450 QUALOX=FNSLOY/DMFFGY
455 CONTINUE
PRINT 700,POWER,POWERY,CFXLOY
PRINT 710,FNLOY
PRINT 720,FNSLOY,QUALOX
700 FORMAT(14H POWER TOTAL = F9.4/,
1 28H POWER INPUT TO POSITION X = E9.4/,
2 18H LOCAL HEAT FLUX = F11.5)
710 FORMAT(31H LOCAL ENTHALPY AT POSITION X = F8.7)
720 FORMAT(41H LOCAL SURCOOLED ENTHALPY AT POSITION X = F8.2/,
130H LOCAL QUALITY AT POSITION X = F6.3)
CALL FILMER
460 CONTINUE
RETURN
END
SUBROUTINE SPKCO5
COMMON NTURFS,MSHAPE,TUBE,RATION,DIAINS,VOLTS,AMPS,ENTHIN,FLMASS,
1 PRESO,PRESIN,PRESOT,RESPD,TSDP,BOLOCA,XLNGTH,SHUNTM,P,
2 DMFFX,ENFPX,DMFFGX,ENFGPX,ENSIN,QUALIN,POWER,AREAF,AREAFS,
3 QUALOR,SATL,PSATL,POWERB,PSLOL,CFXAVG,CFXLOX,JLOCAT,K,X,
4 DRPEAK,POWERX,FNSLOX,FNSLOY,QUALOX,DMFFY,DMFFGY,POWERB,DMFFOB,
5 COSLEN,ONEMSQ,SIGNZ,ARG,Z,FACMIR,FACPLB,CFXBO,L,Y,
6 FACTM,POWERY,CFXLOY,FNLOY,FNSLOY,QUALOY,FACTPL,
7 CONSTP,SCRPTL,ZFTA,PLNGTH,J,U,ULOCAT,COSARK,SINARK,I,
8 EXTRA,EXTRAB,EXTRAC,EXTRAD,EXTRAF,EXTRAG,
9 DMFFR,DMFFGR,FNSLOB,FNSLOB,QUALOB,EXTRAG,EXTRAH,EXTRAJ,EXTRAJ
COMMON QUALIA,GLIO,TKINCH,
1 DP,DX,COLM1,COLM2,COLM3,COLM4,SUMCOL,PHIMN,GTOTSC,GSUBZ,SUM0,SUM1,
2 SUM2,SUM3,SUM4,SUM5,OMEGAP,OMEGA,PGMULT,PSURL,T,VISCL,VOLSPL,FNO,
3 VOLSPG,QUALO4,POWER4,PANBOL,DENFO,DFNFGO,ENSO,QUALO,DVSPLO,DVSPGO,
4 GTOT,DPMM,GRMT,DVLSPL,DVLSPL,TERM1,TERM2,TERM3,TERM4,GGAS,DT,
5 VISCL,PFYNUM,FFACT,FFACT,VFLOC,GNFS,DPGMLT,SPDET,DPDMT,DPDTOT,
6 B,GRAVAC,GRAVCS,GRAVCH,VALUEN,FACTUN,BMAOA,DBMAOA,A,FILMTK,YPLUS,
7 AUWAL,FYPLUS,GFILM,CLDENT,PCLIO,PCLFNT,DUMMYA,DUMMYC
COMMON N,M,THCON,FCHEN,SCHFN,VISCG,CPLIO,SURFTL,
1 XTT,SATP,SMALL,DELTV,TWALL,HCHEN,HMAC,HMIC,REYNLO,NFLUX,
2 PRNUMB,BERGH,HDDB,HDENG,QADENG,DTDENG,DELTT,QACHEN,
3 DTCHFN,RADMAX,DELTFN,RADIUS,CC,DD,FF
515 FORMAT (F10.0,F10.2,F10.4,F10.1)
520 FORMAT (5F10.0, 1F10.2)
525 FORMAT (2F10.2)

```

```

01890
01900
01910
01920
01930
01940
01950
01960
01970
01980
01990
02000
02010
02020
02030
02040
02050
02060
02070
02080
02090
02100
02110
02140
02150
02160
02170
02180
02190
02200
02210
00020
00030
00040
00050
00060
00070
00080
00090
00100
00110
00120
00130
00140
00150
00160
00170
00180
00190
00200
00210
00220
00230
00240
00250
00260

```

530	FORMAT(15,F10.3)	00270	GO TO 270	00920
535	FORMAT(15)	00280		00930
540	FORMAT(24H INLET LIQUID ENTHALPY = F8.2,	00290	Z=ULOCAT+((POW00-(EXTRAB*2.0*ONEMSO))/EXTRAA)	00940
1	25H INLET EVAP ENTHALPY =F8.2, 22H INLET SUBCOOLING =F8.2)	00300	QUALOL=ULOCAT+Z	00950
543	FORMAT(16H INLET QUALITY = F6.3)	00310	SATL=XLNGTH-QUALOL	00960
545	FORMAT(12H FLOW AREA =3PE15.2,25H INSIDE SURFACE AREA =0PE15.4)	00320	PSATL=POWFRT-POW00	00970
550	FORMAT(35H LENGTH WHERE QUALITY EQUALS ZERO =F15.2,	00330	IF (ROLOCA -(XLNGTH-SCDPTL)) 275,275,280	00980
1	42H LENGTH OVER WHICH QUALITY ABOVE ZERO =F15.2)	00340	POWFRB=EXTRAA*ROLOCA	00990
555	FORMAT(24H POWER OVER SAT LENGTH =1PE10.3,17H POWER TO BO =	00350	IF (ROLOCA-QUALOL) 750,750,755	01000
1	1PE10.3,26H POWER FROM SAT TO BO = 1PE10.3)	00360	IF (ROLOCA-(1.6*QUALOL)) 760,760,765	01010
560	FORMAT(20H AVG CRITICAL FLUX =1PF10.3,	00370	P=PPFSIN	01020
1	25H CRITICAL FLUX AT BO = 1PF10.3)	00380	GO TO 770	01030
565	FORMAT(F10.2)	00390	P=PPRESIN-(0.750*TSDP*(BOLOCA-QUALOL)/(XLNGTH-QUALOL))	01040
570	FORMAT(F10.1)	00400	GO TO 770	01050
575	FORMAT(F20.2)	00410	765 PRPFAK=PPFSIN-(0.750*TSDP*(0.60*QUALOL)/(XLNGTH-QUALOL))	01060
580	FORMAT(F30.2)	00420	P=PRBREAK-((PRPFAK-PPFSOT)*(BOLOCA-(1.60*QUALOL))/(XLNGTH-	01070
		00430	1 (1.60*QUALOL)))	01080
	READ 515,TURF,RATION,DIAINS,VOLTS,AMPS,ENTHIN,FLMASS	00440	770 CALL LIOFN	01090
	READ 520,PPESP,PPFSIN,PPFSOT,PPESDP,TSDP,BOLOCA	00450	DMEFB=ENFPX	01100
	READ 525,XLNGTH,SHUNTM	00460	CALL EVAPFN	01110
	READ 530,ULOCAT,QUALIA	00470	DMEFGR=ENFGPX	01120
	READ 540,SCDPTL,ZETA,PLNGTH	00480	ENLOB=ENTHIN+POWERB/FLMASS	01130
	READ 545,J	00490	ENSLOR=ENLOB/DMEFB	01140
	DDINT 515,TURF,RATION,DIAINS,VOLTS,AMPS,ENTHIN,FLMASS	00500	QUALOR=ENSLOR/DMEFGR	01150
	DDINT 520,PPESP,PPFSIN,PPFSOT,PPESDP,TSDP,BOLOCA	00510	CFXBO=EXTRAF/RATION	01160
	DDINT 525,XLNGTH,SHUNTM	00520	GO TO 350	01170
	DDINT 530,ULOCAT,QUALIA	00530	280 IF (BOLOCA-ULOCAT) 285,285,290	01180
	DDINT 540,SCDPTL,ZETA,PLNGTH	00540	285 POWERR=(EXTRAA*(XLNGTH-SCDPTL))+	01190
	DDINT 545,J	00550	1 (EXTRAB*(ONFMSO-SINF(3.1416*(ULOCAT-BOLOCA)/COSLFN)))	01200
	P=PPFSIN	00560	IF (BOLOCA-QUALOL) 850,850,855	01210
	CALL LIOFN	00570	855 IF (ROLOCA-(1.6*QUALOL)) 860,860,865	01220
	DMEFB=ENFPX	00580	860 P=PPRESIN	01230
	CALL EVAPFN	00590	GO TO 870	01240
	DMEFGR=ENFGPX	00600	P=PPRESIN-(0.750*TSDP*(BOLOCA-QUALOL)/(XLNGTH-QUALOL))	01250
	ENSIN=ENTHIN/DMEFB	00610	GO TO 870	01260
	QUALIN=ENSIN/DMEFGR	00620	865 PRPFAK=PPRESIN-(0.750*TSDP*(0.60*QUALOL)/(XLNGTH-QUALOL))	01270
	POWERT=VOLTS*AMPS*3.61*SHUNTM	00630	P=PRBREAK-((PRPFAK-PPFSOT)*(BOLOCA-(1.60*QUALOL))	01280
	APFAFL=(3.1416*DIAINS*DIAINS)/(576.0)	00640	1/(XLNGTH-(1.60*QUALOL)))	01290
	APFAIS=(3.1416*XLNGTH*DIAINS)/144.0	00650	870 CALL LIOFN	01300
225	POW00=-ENSIN*FLMASS	00660	DMEFB=ENFPX	01310
230	ONFOVM=1./RATION	00670	CALL EVAPFN	01320
	COSLFN=(1.5708*PLNGTH)/ACOSF(ONFOVM)	00680	DMEFGR=ENFGPX	01330
240	ONFMSO=SQRTF((RATION**2-1.0)/RATION**2)	00690	ENLOB=ENTHIN+POWFRB/FLMASS	01340
	CONSTP=(XLNGTH-PLNGTH)/RATION+(2.0*COSLFN-ONFMSO/	00700	ENSLOR=ENLOB/DMEFB	01350
	1 3.1416)	00710	QUALOR=ENSLOR/DMEFGR	01360
	EXTRAA=POWFRT/(RATION*CONSTP)	00720	CFXBO=EXTRAE*COSF(3.1416*(ULOCAT-BOLOCA)/COSLFN)	01370
	EXTRAB=POWERT*(COSLFN)/(CONSTP*3.1416)	00730	GO TO 350	01380
	ULOCAT=XLNGTH-SCDPTL+(PLNGTH/2.0)	00740	290 IF (BOLOCA-(ULOCAT+(PLNGTH/2.0))) 295,295,300	01390
	EXTRAF=(144.0*POWFRT)/(CONSTP*DIAINS*3.1416)	00750	295 POWERR=(EXTRAA*(XLNGTH-SCDPTL))+	01400
	IF (POW00-(EXTRAA*(XLNGTH-SCDPTL))) 245,245,255	00760	1 (EXTRAB*(ONFMSO+SINF(3.1416*(BOLOCA-ULOCAT)/COSLFN)))	01410
245	Z=ULOCAT-(POW00/EXTRAA)	00770	IF (ROLOCA-QUALOL) 950,950,955	01420
	QUALOL=ULOCAT-Z	00780	950 P=PPRESIN	01430
	GO TO 270	00790	GO TO 970	01440
255	IF (POW00-(EXTRAA*(XLNGTH-SCDPTL)))+(EXTRAB*ONEMSO	00800	960 P=PPRESIN-(0.750*TSDP*(BOLOCA-QUALOL)/(XLNGTH-QUALOL))	01450
1))) 260,260,265	00810	GO TO 970	01460
260	SINZ=((POW00-(EXTRAA*(XLNGTH-SCDPTL)))/EXTRAB)+ONEMSO	00820	965 PRPFAK=PPRESIN-(0.750*TSDP*(0.60*QUALOL)/(XLNGTH-QUALOL))	01470
	ARG=ASINF(SINZ)	00830	P=PRBREAK-((PRPFAK-PPFSOT)*(BOLOCA-(1.60*QUALOL))	01480
	Z=COSLFN*ARG/3.1416	00840	1 (1.60*QUALOL)))	01490
	QUALOL=ULOCAT-Z	00850	970 CALL LIOFN	01500
	GO TO 270	00860	DMEFB=ENFPX	01510
265	IF (POW00-(EXTRAA*(XLNGTH-SCDPTL)))+(EXTRAB*ONEMSO	00870	CALL EVAPFN	01520
1	*2.0))) 266,266,268	00880	DMEFGR=ENFGPX	01530
266	SINZ=((POW00-(EXTRAA*(XLNGTH-SCDPTL)))/EXTRAB)-ONEMSO	00890	ENLOB=ENTHIN+POWERB/FLMASS	01540
	ARG=ASINF(SINZ)	00900	ENSLOR=ENLOB/DMEFB	01550
	Z=COSLFN*ARG/3.1416	00910	QUALOR=ENSLOR/DMEFGR	01560
	QUALOL=ULOCAT+Z			

```

CFXRO =FXTRAF*COSF(3.1416*(BOLOCA-ULOCAT)/COSLEN)
GO TO 350
300 POWFR=EXTRAA*(BOLOCA-PLNGTH)+(EXTRAR*2.0*ONFMSQ)
IF (BOLOCA-QUALOL) 305,305,310
310 IF (BOLOCA-(1.6*QUALOL)) 315,315,320
305 P=PPFSIN
GO TO 325
315 P=PPFSIN-(0.750*TSOP*(BOLOCA-QUALOL)/(XLNGTH-QUALOL))
GO TO 325
320 P=PBFAK-PPFSIN-(0.750*TSOP*(0.60*QUALOL)/(XLNGTH-QUALOL))
P=PBFAK-((PBFAK-PPFSOT)*(BOLOCA-(1.60*QUALOL))/(XLNGTH-
1 (1.60*QUALOL)))
325 CALL LIQFN
DMFFR=FMFDX
CALL EVAPFN
DMFFGR=FMFGDX
FNLOB=FNTHIN+POWFR/FLMASS
FNSLOB=FNLOB-DMFFR
QUALOR=FNSLOB/DMFFGR
CFXRO=FXTRAF/RATION
350 PSLBOL=POWFR-POWQ
353 CFXAVG = POWER / AFAIS
PRINT 540,DMFFY,DMFFGY,ENSIN
PRINT 543, QUALIN
PRINT 545, AFAFL, AFAIS
PRINT 550,QUALOL, SATL
PRINT 555,PSATL, POWERB, PSLBOL
PRINT 560,CFXAVG,CFXRO
PRINT 775,P,DMFFR,DMFFGB
PRINT 780,FNLOB,FNSLOB
PRINT 785,QUALOR
775 FORMAT(17H PRESSURE AT BO =F6.1,25H SAT LIQ ENTH AT RO =F8.2,
1 22H EVAP ENTH AT RO =F8.2)
780 FORMAT(13H ENTH AT RO =F8.2, 27H SUBCOOLED ENTH AT BO =F8.2)
785 FORMAT(16H QUALITY AT RO =F6.3)
CALL GPMOM
CALL SPMXMM
DO 460 L=1,JLOCAT,3
360 Y=L-1
363 IF (Y-(XLNGTH-SCRPTL)) 362,359,359
365 IF (N) 364,364,361
361 IF (Y-(XLNGTH-SCRPTL+PLNGTH)) 460,460,362
364 CALL CSPIKE
GO TO 460
362 IF (Y-QUALOL) 370,370,365
365 IF (Y-(1.6*QUALOL)) 375, 375, 380
370 P = PPFSIN
GO TO 390
375 P=PPFSIN-(0.750*TSOP*(Y-QUALOL)/(XLNGTH-QUALOL))
GO TO 390
380 P=PBFAK-PPFSIN-(0.750*TSOP*(0.60*QUALOL)/(XLNGTH-QUALOL))
385 P=PBFAK-((PBFAK-PPFSOT)*(Y-(1.60*QUALOL))/(
1 (XLNGTH-(1.60*QUALOL)))
390 CALL LIQFN
DMFFY=FMFDX
CALL EVAPFN
DMFFGY=FMFGDX
PRINT 565,Y
PRINT 570, P
PRINT 575,DMFFY,DMFFGY
IF (Y -(XLNGTH-SCRPTL))400,400,410
400 POWFR=EXTRAA*Y
CFXLOY=EXTRAF/RATION
GO TO 435
410 IF (Y -ULOCAT) 415,415,435

```

```

01570
01580
01590
01600
01610
01620
01630
01640
01650
01660
01670
01680
01690
01700
01710
01720
01730
01740
01750
01760
01770
01780
01790
01800
01810
01820
01830
01840
01850
01860
01870
01880
01890
01900
01910
01920
01930
01940
01950
01960
01965
01970
01980
01985
01990
02000
02010
02020
02030
02040
02050
02060
02070
02080
02090
02100
02110
02120
02130
02140
02150
02160
02170
02180
02190

```

```

415 POWFRY = (EXTRAA*(XLNGTH-SCRPTL))+
1 (EXTRAB*(ONFMSQ-SINF(3.1416*(ULOCAT-Y
)/COSLEN)))
CFXLOY=EXTRAF*COSF(3.1416*(ULOCAT-Y)/COSLEN)
GO TO 435
425 IF (Y -(ULOCAT+(PLNGTH/2.0)))430,430,433
430 POWERY = (EXTRAA*(XLNGTH-SCRPTL))+
1 (EXTRAB*(ONFMSQ-SINF(3.1416*(Y
-ULOCAT)/COSLEN)))
CFXLOY=EXTRAF*COSF(3.1416*(Y
-ULOCAT)/COSLEN)
GO TO 435
433 POWFRY=EXTRAA*(Y -PLNGTH)+(EXTRAR*2.0*ONFMSQ)
CFXLOY=EXTRAF/RATION
435 ENLOY=FNTHIN+(POWERY/FLMASS)
440 ENSLOY=ENLOY-DMFFY
450 QUALOX=ENSLOY/DMFFGY
455 CONTINUE
PRINT 700,POWER,POWFRY,CFXLOY
PRINT 710,ENLOY
PRINT 720,ENSLOY,QUALOX
700 FORMAT(14H POWER TOTAL = E9.4/,
1 28H POWER INPUT TO POSITION X = E9.4/,
2 18H LOCAL HEAT FLUX = E11.5)
710 FORMAT(31H LOCAL ENTHALPY AT POSITION TX = F8.2)
720 FORMAT(41H LOCAL SUBCOOLED ENTHALPY AT POSITION X = F8.2/,
130H LOCAL QUALITY AT POSITION X = F6.3)
CALL FILMR
460 CONTINUE
N=0
RETURN
END
02200
02210
02220
02230
02240
02250
02260
02270
02280
02290
02300
02310
02320
02330
02340
02350
02360
02370
02380
02390
02400
02410
02420
02430
02440
02450
02460
02470
SURROUTINE CSPIKE
COMMON NTUBES,MSHAPE,TUBE,RATION,DIAINS,VOLTS,AMPS,ENTHIN,FLMASS,
1 PRFSP,PPFSIN,PPFSOT,PPFSOP,TSOP,BOLOCA,XLNGTH,SHUNTM,P,
2 DMFFX,ENFPX,DMFFGX,ENFGPX,ENSIN,QUALIN,POWER,AFAFL,AFAIS,
3 QUALOL,SATL,PSATL,POWERB,PSLBOL,CFXAVG,CFXLOA,JLOCAT,K,X,
4 PBFAK,POWFR,FNLOB,FNSLOB,QUALOX,DMFFY,DMFFGY,POWQ,ONFOVM,
5 COSLEN,ONFMSQ,SIGNZ,ARG,Z,FACMIB,FACPLB,CFXBO,L,Y,
6 FACTMI,POWERY,CFXLOY,ENLOY,FNSLOY,QUALOY,FACTPL,
7 CONST,SCRPTL,ZETA,PLNGTH,J,U,ULOCAT,COSABK,SINABK,I,
8 EXTRAA,EXTRAR,FXTRAC,FXTRAD,EXTRAF,FXTRAF,
9 DMFFB,DMFFGR,FNLOB,FNSLOB,QUALOB,EXTRAG,FXTRAH,EXTRAI,FXTRAJ
COMMON QUALIA,GLIO,TKINCH,
1 DP,DX,COLM1,COLM2,COLM3,COLM4,SUMCOL,PHIMN,GTOTSC,GSUBZ,SUM0,SUM1,
2 SUM2,SUM3,SUM4,SUM5,OMEGAP,OMEGA,PGMULT,PSURL,T,VISCL,VOLSPL,ENO,
3 VOLSPLG,QUALO4,POWERA,PANBOL,DFNO,DFNFGO,ENSO,QUALO,DVSPLO,DVSPGO,
4 GTOT,DPMOM,GRDNT,DVLSPL,DVLSPLG,TERM1,TERM2,TERM3,TERM4,GGA5,DT,
5 DVISCL,REYNUM,FFACT,FFACT,VFLOC,GRDFS,DPGMLT,GPDEF,DGRDNT,GRDTOT,
6 B,GRAVAC,GRAVCS,GRAVCH,VALUEN,FACTUN,BMAOA,DBMAOA,A,FILMTK,YPLUS,
7 TAUWAL,FYPLUS,GFILM,GLQENT,PCLIQ,PCLFNT,DUMMYA,DUMMYB,DUMMYC
COMMON N,M,THCOND,FCHEN,SCHEM,VISCG,CPLIO,SURFTL,
1 XTT,SATP,SMALLT,DELTVP,TWALL,HCHEN,HMAC,HMIC,PFYNLO,NFLUX,
2 PRNUMB,BERHT,HDB,HDENG,QADENG,DTDENG,DELTT,QACHEN,
3 DTCHEN,RADMAX,DELTEN,RADIUS,CC,DD,EE
364 QUALO4=R.0*(XLNGTH-SCRPTL+PLNGTH)
NFLUX=QUALO4
K=R.0*(XLNGTH-SCRPTL)
DO 459 N=K,NFLUX,J
ZFTA=N
Y=ZFTA/R.0
362 IF (Y-QUALOL) 370,370,365
00010
00020
00030
00040
00050
00060
00070
00080
00090
00100
00110
00120
00130
00140
00150
00160
00170
00180
00190
00200
00210
00220
00230
00240
00250
00260
00270
00280
00290

```

17

```

365 IF (Y - (1.6*QUALOL) ) 375, 375, 380
370 D = PRESIN
GO TO 390
375 P=PPRESIN-(0.750*TSDP*(Y-QUALOL)/(XLNGTH-QUALOL) )
GO TO 390
380 PRRFAK=PPRESIN-(0.750*TSDP*(0.60*QUALOL)/(XLNGTH-QUALOL) )
385 P=PRRFAK-((PRRFAK-PPRESOT)*(Y-(1.60*QUALOL)))/
1 (XLNGTH-(1.60*QUALOL))
390 CALL LIQEN
DMFFY=FNFPX
CALL EVAPEN
DMFFGY=ENFGPX
PRINT 565,Y,P,DMFFY,DMFFGY
565 FORMAT(4F20.3)
IF (Y -(XLNGTH-SCPPTL))400,400,410
400 POWFOY=EXTDAA*Y
CFXLOY=EXTDAA/RATIOM
GO TO 435
410 IF (Y -ULOCAT) 415,415,425
415 POWFXY=(EXTRA*(XLNGTH-SCPPTL))+
1 (EXTRAB*(ONEMSO-SINF(3.1416*(ULOCAT-Y )/COSLEN))
CFXLOY=EXTRA*COSEF(3.1416*(ULOCAT-Y )/COSLEN)
GO TO 435
425 IF (Y -(ULOCAT+(PLNGTH/2.0)))430,430,435
430 POWFXY=(EXDAA*(XLNGTH-SCPPTL))+
1 (EXTRAB*(ONEMSO+SINF(3.1416*(Y-ULOCAT )/COSLEN))
CFXLOY=EXTRA*COSEF(3.1416*(Y -ULOCAT)/COSLEN)
GO TO 435
435 POWFXY=EXTDAA*(Y -PLNGTH)+(EXTRA*2.0*ONEMSO)
CFXLOY=EXTDAA/RATIOM
435 ENLOY=ENTHIN+(POWFRX/FLMASS)
440 ENSLOY=ENLOY-DMFFY
450 QUALOX=ENSLOY/DMFFGY
455 CONTINUE
PRINT 700,POWFR,POWFRY,CFXLOY
PRINT 710,ENLOY
PRINT 720,ENSLOY,QUALOX
700 FORMAT(14H POWFR TOTAL = F9.4/,
1 28H POWFR INPUT TO POSITION X = E9.4/,
2 18H LOCAL HEAT FLUX = F11.5)
710 FORMAT(31H LOCAL ENTHALPY AT POSITION X = F8.2)
720 FORMAT(41H LOCAL SUBCOOLED ENTHALPY AT POSITION X = F8.2/,
130H LOCAL QUALITY AT POSITION X = F6.3)
CALL FILMED
450 CONTINUE
RETURN
END

```

```

SUBROUTINE UMIANN
COMMON NTUBES,MSHAPE,TUBE,RATIOM,DIAINS,VOLTS,AMPS,ENTHIN,FLMASS,
1 PRES,PPRESIN,PPRESOT,PPRES,TSDP,ROLOCA,XLNGTH,SHUNTM,P,
2 DMFFX,ENFPX,DMFFGX,ENFGPX,ENSIN,QUALIN,POWFR,AREAF,AREAS,
3 QUALOL,SATL,PSATL,POWFRB,PSLBOL,CFXAVG,CFXLOX,JLOCAT,K,X,
4 PRRFAK,POWFRX,ENLOY,ENSLOY,QUALOX,DMFFY,DMFFGY,POWOB,ONEOVM,
5 COSLEN,ONEMSO,SIGNZ,ARG,Z,FACMI,FACEPL,CFXBO,L,Y,
6 FACMI,POWFRY,CFXLOY,ENLOY,ENSLOY,QUALOY,FACTPL,
7 CONSTP,SCPPTL,ZFTA,PLNGTH,J,U,ULOCAT,COSABK,STNABK,I,
8 EXTRA,EXTDAA,EXTDAB,EXTDAB,EXTDAB,EXTDAB,EXTDAB,EXTDAB,
9 DMFFY,DMFFGX,ENLOY,ENSLOY,QUALOB,EXTRAG,EXTRAH,EXTRAJ,EXTRAJ
COMMON QUALIA,GLIO,TKINCH,

```

```

00300
00310
00320
00330
00340
00350
00360
00370
00380
00390
00400
00410
00420
00430
00440
00450
00460
00470
00480
00490
00500
00510
00520
00530
00540
00550
00560
00570
00580
00590
00600
00610
00620
00630
00640
00650
00660
00670
00680
00690
00700
00710
00720
00730
00740
00750
00760
00010
00020
00030
00040
00050
00060
00070
00080
00090
00100
00110
00120

```

```

1DP,DX,COLM1,COLM2,COLM3,COLM4,SUMCOL,PHIMN,GTOTSC,GSUBZ,SUMO,SUM1,
2SUM2,SUM3,SUM4,SUM5,OMEGAP,OMEGA,PGMULT,PSURL,T,VISCL,VOLSPL,ENO,
3VOLSPG,QUALO4,POWERA,PANBOL,DENFO,DENFGO,ENSO,QUALO,DVSPLO,DVSPGO,
4GTOT,DPMOM,GRDMT,DVLSPL,DVLSPG,TERM1,TERM2,TERM3,TERMA,GGAS,DT,
5DVISCL,REYNUM,FFACTP,FFACT,VELOC,GRDFS,DPGMLT,GRDFT,DGRDMT,GRDTOT,
6B,GRAVAC,GRAVCS,GRAVCH,VALUFN,FACTUN,BMAOA,DBMAOA,A,FILMTK,YPLUS,
7TAUWAL,FYPLUS,GFILM,GLQENT,PCLTO,PCLFNT,DUMMYA,DUMMYB,DUMMYC
QUALO4=16.0*QUALOL
I=QUALO4
DO 451 K=1,1000,1
DUMMYC=K+1
X=DUMMYC/16.0
IF (X-QUALOL)160,160,157
157 IF (X-(1.60*QUALOL) ) 162,162,165
160 P=PRESIN
GO TO 167
162 P=PRESIN-(0.750*TSDP*(X-QUALOL)/(XLNGTH-QUALOL))
GO TO 167
165 PRRFAK=PPRESIN-(0.750*TSDP*(0.60*QUALOL) / (XLNGTH-QUALOL))
166 P=PRRFAK-((PRRFAK-PPRESOT)*(X-(1.60*QUALOL)))/
1 (XLNGTH-(1.60*QUALOL))
167 CALL LIQEN
DMFFX=FNFPX
CALL EVAPEN
DMFFGX=ENFGPX
170 CFXLOX=POWFR/AREAS
175 POWFRX=POWFR*(X/XLNGTH)
180 ENLOY=ENTHIN + POWFRX/FLMASS
185 ENSLOY=ENLOY-DMFFX
190 QUALOX=ENSLOY/DMFFGX
455 IF (QUALOX-QUALIA) 451,453,453
451 CONTINUE
453 POWFR=POWFR-POWFRX
PANBOL=POWFR-POWFRX
PRINT 721,X,P
PRINT 722,DMFFX,DMFFGX
PRINT 723,POWERA,PANBOL
PRINT 700,POWFR,POWFRX,CFXLOX
PRINT 710,ENLOY
PRINT 720,ENSLOY,QUALOX
700 FORMAT(14H POWFR TOTAL = E9.4/,
1 28H POWER INPUT TO POSITION X = E9.4/,
2 18H LOCAL HEAT FLUX = F11.5)
710 FORMAT(31H LOCAL ENTHALPY AT POSITION X = F8.2)
720 FORMAT(41H LOCAL SUBCOOLED ENTHALPY AT POSITION X = F8.2/,
130H LOCAL QUALITY AT POSITION X = F6.3)
721 FORMAT(51H CONDITIONS AT SLUG ANNULAR TRANSITION POSITION =F8.1,
1 14H PRESSURE =F8.1)
722 FORMAT(18H LIQUID ENTHALPY =F8.2,19H EVAP ENTHALPY =F8.2)
723 FORMAT(28H POWER OVER ANNULAR REGION =1PE10.3,
1 45H POWER FROM SLUG ANNULAR TRANSITION TO RO =1PE10.3)
RETURN
END

```

```

SUBROUTINE COSANN
COMMON NTUBES,MSHAPE,TUBE,RATIOM,DIAINS,VOLTS,AMPS,ENTHIN,FLMASS,
1 PRES,PPRESIN,PPRESOT,PPRES,TSDP,ROLOCA,XLNGTH,SHUNTM,P,
2 DMFFX,ENFPX,DMFFGX,ENFGPX,ENSIN,QUALIN,POWFR,AREAF,AREAS,
3 QUALOL,SATL,PSATL,POWFRB,PSLBOL,CFXAVG,CFXLOX,JLOCAT,K,X,
4 PRRFAK,POWFRX,ENLOY,ENSLOY,QUALOX,DMFFY,DMFFGY,POWOB,ONEOVM,

```

```

00130
00140
00150
00160
00170
00180
00190
00200
00210
00220
00240
00250
00260
00270
00280
00290
00300
00310
00320
00330
00340
00350
00360
00400
00410
00420
00430
00440
00450
00460
00470
00480
00490
00500
00510
00520
00530
00540
00550
00560
00570
00580
00590
00600
00610
00620
00630
00640
00650
00660
00670
00680
00690
00660
00670
00680
00690
00700
00710
00720
00730
00740
00750
00760
00010
00020
00030
00040
00050
00060
00070
00080
00090
00100
00110
00120
00010
00020
00030
00040
00050
00060

```

```

5 COSLEN,ONEMSQ,SIGNZ,ARG,Z,FACMIB,FACPLB,CFXBO,L,Y,
6 FACTMI,POWERF,CFXLOY,ENLOY,ENSLOY,QUALOY,FACTPL,
7CONSTP,SCRPTL,ZETA,PLNGTH,J,U,ULOCAT,COSABK,SINABK,I,
8 EXTRA,EXTRAR,EXTRAC,EXTRAD,EXTRAF,EXTRAF,
9DMEFB,DMEFGB,ENLOB,ENSLOB,QUALOB,EXTRAG,EXTRAH,EXTRAI,EXTRAJ
COMMON QUALIA,GLIO,TKINCH,
1DP,DX,COLM1,COLM2,COLM3,COLM4,SUMCOL,PHIMN,GTOTSC,GSURZ,SUMO,SUM1,
2SUM2,SUM3,SUM4,SUM5,OMEGAP,OMEGA,PGMULT,PSUBL,T,VISCL,VOLSPL,ENO,
3VOLSPG,QUALO4,POWERA,PANBOL,DENFO,DENFGO,ENSO,QUALO,DVSPLO,DVSPGO,
4GTOT,DPMM,GRDMT,DVLSPL,DVLSPG,TERM1,TERM2,TERM3,TERM4,GGAS,DT,
5DVISCL,REYNUM,FFACTP,FFACT,VFLOC,GRDFS,DPGMLT,GRDFT,DGRDMT,GRDTOT,
6B,GRAVAC,GRAVCS,GRAVCH,VALUEN,FACTUN,BMAOA,DBMAOA,A,FILMTK,YPLUS,
7TAUWAL,FYPLUS,GFILM,GFLOENT,PCLIQ,PCLFNT,DUMMYA,DUMMYB,DUMMYC
QUALO4=16.0*QUALOL
T=QUALO4
DO 451 L=1,10000,1
DUMMYC=L+1
Y=DUMMYC/16.0
IF (Y - QUALOL) 370, 370, 365
365 IF (Y - (1.6*QUALOL) ) 375, 375, 380
370 P = PRESIN
GO TO 390
375 P=PRESIN-(0.750*TSDP*(Y-QUALOL)/(XLNGTH-QUALOL) )
GO TO 390
380 PRRFAK=PRESIN-(0.750*TSDP*(0.60*QUALOL)/(XLNGTH-QUALOL) )
385 P=PRRFAK-(PRRFAK-PRESOT)*(Y-(1.60*QUALOL))/
1 (XLNGTH-(1.60*QUALOL))
390 CALL LIOFN
DMEFY=ENFPX
CALL EVAPEN
DMEFGY=ENFGPX
IF (Y-(XLNGTH/2.0) )400,400,428
400 FACTMI=(1.0-(SINF( 3.1416*( XLNGTH/2.0)-Y) )
1/COSLEN) /ONEMSQ
410 POWERY=(POWERF*FACTMI) / 2.0
415 CFXLOY=144.0*(POWERF/(2.0*DIAINS*COSLEN*ONEMSQ))*
1COSF(3.1416*( XLNGTH/2.0)-Y)/COSLEN
415 ENLOY = ENTHIN + (POWER*FACTMI) / (2.0 * FLMASS)
420 ENSLOY=ENLOY-DMEFY
425 QUALOX=ENSLOY/DMEFGY
GO TO 455
428 FACTPL=(1.0+(SINF( 3.1416*(Y-(XLNGTH/2.0) ) )
1/COSLEN) )/ONEMSQ
430 POWERY = (POWERF*FACTPL) / 2.0
435 CFXLOY=144.0*(POWERF/(2.0*DIAINS*COSLEN*ONEMSQ))*
1COSF(3.1416*(Y-(XLNGTH/2.0) )/COSLEN
435 ENLOY = ENTHIN + ( POWER* FACTPL) / ( 2.0 * FLMASS)
440 ENSLOY=ENLOY-DMEFY
450 QUALOX=ENSLOY/DMEFGY
455 IF(QUALOX-QUALIA) 451,453,453
451 CONTINUE
453 POWERA=POWERF-POWERY
PANBOL=POWERR-POWERY
PRINT 721,Y,P
PRINT 722,DMEFY,DMEFGY
PRINT 723,POWERA,PANBOL
PRINT 700,POWERF,POWERY,CFXLOY
PRINT 710,ENLOY
PRINT 720,ENSLOY,QUALOX
700 FORMAT(14H POWER TOTAL = E9.4/,
1 2RH POWER INPUT TO POSITION X = E9.4/,
2 1RH LOCAL HEAT FLUX = E11.5)
710 FORMAT(31H LOCAL ENTHALPY AT POSITION X = F8.2)
720 FORMAT(41H LOCAL SURCOOLED ENTHALPY AT POSITION X = F8.2/,
130H LOCAL QUALITY AT POSITION X = F6.3)

```

```

00070
00080
00090
00100
00110
00120
00130
00140
00150
00160
00170
00180
00190
00200
00210
00220
00240
00250
00260
00270
00280
00290
00300
00310
00320
00330
00340
00350
00360
00370
00380
00390
00400
00410
00420
00430
00440
00450
00460
00470
00480
00490
00500
00510
00520
00530
00540
00550
00560
00570
00580
00590
00600
00610
00620
00630
00640
00670
00680
00690
00700

```

```

721 FORMAT(51H CONDITIONS AT SLUG ANNULAR TRANSITION POSITION =F8.1,
1 14H PRSSURF =F8.1)
722 FORMAT(18H LIQUID ENTHALPY =F8.2,19H EVAP ENTHALPY =F8.2)
723 FORMAT(28H POWER OVER ANNULAR REGION =IPE10.3,
1 45H POWER FROM SLUG ANNULAR TRANSITION TO BO =IPE10.3)
RETURN
END
00710
00720
00730
00740
00750
00760
00770
SURROUTINE LNIANN
COMMON NTUBES,MSHAPE,TUBE,RATION,DIAINS,VOLTS,AMPS,ENTHIN,FLMASS,
1 PREFP,PRESIN,PRESOT,RESDP,TSDP,BOLOCA,XLNGTH,SHUNT,P,
2 DMEFX,ENFPX,DMEFGX,ENFGPX,ENSIN,QUALIN,POWER,AREAPL,AREAS,
3 QUALOL,SATL,PSATL,POWERB,PSLBOL,CFXAVG,CFXLOX,JLOGAT,K,X,
4PBREAK,POWERX,ENLOX,ENSLOX,QUALOX,DMEFY,DMEFGY,POWER,ONEOVM,
5 COSLEN,ONEMSQ,SIGNZ,ARG,Z,FACMIB,FACPLB,CFXBO,L,Y,
6 FACTMI,POWERY,CFXLOY,ENLOY,ENSLOY,QUALOY,FACTPL,
7CONSTP,SCRPTL,ZETA,PLNGTH,J,U,ULOCAT,COSABK,SINABK,I,
8 EXTRA,EXTRAR,EXTRAC,EXTRAD,EXTRAF,EXTRAF,
9DMEFB,DMEFGB,ENLOB,ENSLOB,QUALOB,EXTRAG,EXTRAH,EXTRAI,EXTRAJ
COMMON QUALIA,GLIO,TKINCH,
1DP,DX,COLM1,COLM2,COLM3,COLM4,SUMCOL,PHIMN,GTOTSC,GSUBZ,SUMO,SUM1,
2SUM2,SUM3,SUM4,SUM5,OMEGAP,OMEGA,PGMULT,PSUBL,T,VISCL,VOLSPL,ENO,
3VOLSPG,QUALO4,POWERA,PANBOL,DENFO,DENFGO,ENSO,QUALO,DVSPLO,DVSPGO,
4GTOT,DPMM,GRDMT,DVLSPL,DVLSPG,TERM1,TERM2,TERM3,TERM4,GGAS,DT,
5DVISCL,REYNUM,FFACTP,FFACT,VFLOC,GRDFS,DPGMLT,GRDFT,DGRDMT,GRDTOT,
6B,GRAVAC,GRAVCS,GRAVCH,VALUEN,FACTUN,BMAOA,DBMAOA,A,FILMTK,YPLUS,
7TAUWAL,FYPLUS,GFILM,GFLOENT,PCLIQ,PCLFNT,DUMMYA,DUMMYB,DUMMYC
QUALO4=16.0*QUALOL
I=QUALO4
DO 451 K=1,10000,1
DUMMYC=K+1
X=DUMMYC/16.0
IF (X-QUALOL)160,160,157
157 IF (X-(1.60*QUALOL) ) 162,162,165
160 P=PRESIN
GO TO 167
162 P=PRESIN-(0.750*TSDP*(X-QUALOL)/(XLNGTH-QUALOL) )
GOTO 167
165 PRRFAK=PRESIN-(0.750*TSDP*(0.60*QUALOL)/(XLNGTH-QUALOL) )
166 P=PRRFAK-(PRRFAK-PRESOT)*(X-(1.60*QUALOL))/
1 (XLNGTH-(1.60*QUALOL))
167 CALL LIOFN
DMEFX=ENFPX
CALL EVAPEN
DMEFGX=ENFGPX
CFXLOX=((2.0*POWERF)/(AREAS*(RATIO+1.00)))
1 *(1.00+((X*(RATIO-1.00))/XLNGTH))
POWERX=((POWERF*2.00)/(RATIO+1.00))*(X/XLNGTH+((X*(RATIO-1.00)
1 )/(XLNGTH*XLNGTH*2.00)))
180 ENLOX=ENTHIN + POWERX/FLMASS
185 ENSLOX=ENLOX-DMEFX
190 QUALOX=ENSLOX/DMEFGX
455 IF(QUALOX-QUALIA) 451,453,453
451 CONTINUE
453 POWERA=POWERF-POWERX
PANBOL=POWERR-POWERX
PRINT 721,X,P
PRINT 722,DMEFX,DMEFGX
PRINT 723,POWERA,PANBOL
PRINT 700,POWERF,POWERX,CFXLOX
PRINT 710,ENLOX
PRINT 720,ENSLOX,QUALOX
01440
01450
01460
01470
01480
01490
01500
01510
01520
01530
01540
01550
01560
01570
01580
01590
01600
01610
01620
01630
01640
01650
01670
01680
01690
01700
01710
01720
01730
01740
01750
01760
01770
01780
01790
01800
01810
01820
01830
01840
01850
01860
01870
01880
01890
01900
01910
01920
01930
01940
01950
01960

```

```

700 FORMAT(14H POWER TOTAL = F9.4/,
1 28H POWER INPUT TO POSITION X = E9.4/,
2 18H LOCAL HEAT FLUX = F11.5)
710 FORMAT(31H LOCAL ENTHALPY AT POSITION X = F8.2)
720 FORMAT(41H LOCAL SUBCOOLED ENTHALPY AT POSITION X = F8.2/,
130H LOCAL QUALITY AT POSITION X = F6.3)
721 FORMAT(51H CONDITIONS AT SLUG ANNULAR TRANSITION POSITION =F8.1,
1 14H PRESSURE =F8.1)
722 FORMAT(18H LIQUID ENTHALPY =F8.2,19H EVAP ENTHALPY =F8.2)
723 FORMAT(28H POWER OVER ANNULAR REGION =1PE10.3,
1 45H POWER FROM SLUG ANNULAR TRANSITION TO BO =1PE10.3)
RETURN
END

SUBROUTINE LNDANN
COMMON NTUBES,MSHAPE,TUBE,RATIOM,DIAINS,VOLTS,AMPS,ENTHIN,FLMASS,
1 PDESP,PREFSIN,PREFOT,PRESDP,TSDP,BOLOCA,XLNGTH,SHUNTM,P,
2 DMEFX,ENFPX,DMEFGX,ENFGPX,ENSIN,QUALIN,POWER,AREAF,AREAIS,
3 QUALOL,SATL,PSATL,POWERB,PSLBOL,CFXAVG,CFXLOX,JLOCAT,K,X,
4 PRRFAK,POWERX,FNLOX,FNSLOX,QUALOX,DMEFY,DMEFGY,POWER,ONFOVM,
5 COSLEN,ONEMSO,SIGNZ,ARG,Z,FACMIR,FACPLR,CFXRO,L,Y,
6 FACTMI,POWERY,CFXLOY,FNLOY,FNSLOY,QUALOY,FACTPL,
7 CONST,SCPTL,ZFTA,PLNGTH,J,U,ULOCAT,COSARK,SINARK,I,
8 EXTRA,EXTRAB,EXTRAC,EXTRAD,EXTRAE,EXTRAF,
9 DMEFB,DMEFGB,ENLOB,ENSOB,QUALOB,EXTRAG,EXTRAH,EXTRAI,EXTRAJ
COMMON QUALTA,GLIQ,TKINCH,
1P,DX,COLM1,COLM2,COLM3,COLM4,SUMCOL,PHIMN,GTOTSC,GSURZ,SUM0,SUM1,
2SUM2,SUM3,SUM4,SUM5,OMEGAP,OMEGA,PGMULT,PSUBL,T,VISCL,VOLSP,ENO,
3VOLSPG,QUALO4,POWERA,PANBOL,DFNFO,DENFGO,ENSO,QUALO,DVSPLO,DVSPGO,
4GTOT,DPMOM,GRDMT,DVLSPL,DVLSPG,TERM1,TERM2,TERM3,TERM4,GGAS,DT,
5DVISCL,REYNUM,FFACTP,FFACT,VFLOC,GRDFS,DPGMLT,GRDFT,DGRDMT,GRDGT,
6R,GRAVAC,GRAVCS,GRAVCH,VALUEN,FACTUN,BMAOA,DBMAOA,A,FILMTK,YPLUS,
7TAUWAL,FYPLUS,GFILM,GLENT,PCLIQ,PCLFNT,DUMMYA,DUMMYR,DUMMYC
QUALO4=16.0*QUALOL
I=QUALO4
DO 451 K=I,10000,1
DUMMYC=K+1
X=DUMMYC/16.0
IF(X=QUALOL)160,160,157
IF(X=(1.60*QUALOL))162,162,165
157 P=PREFSIN
GO TO 167
160 P=PREFSIN-(0.750*TSDP*(X-QUALOL)/(XLNGTH-QUALOL))
GO TO 167
165 PRRFAK=PREFSIN-(0.750*TSDP*(0.60*QUALOL)/(XLNGTH-QUALOL))
166 P=PRRFAK-(PRRFAK-PRESOT)*(X-(1.60*QUALOL))/
1 (XLNGTH-(1.60*QUALOL))
167 CALL LIOFN
DMEFX=ENFPX
CALL EVAPFN
DMEFGX=ENFGPX
CFXLOX=((2.0*POWER*RATIOM)/(AREAF*(1.00+RATIOM)))*
1 (1.00-(X*(RATIOM-1.00))/(XLNGTH*RATIOM))
POWERX=((POWER*2.00*RATIOM)/(RATIOM+1.00))*(X/XLNGTH)
1-(X*X*(RATIOM-1.00))/(XLNGTH*XLNGTH*2.00*RATIOM)
180 FNLOX=ENTHIN + POWERX/FLMASS
185 FNSLOX=FNLOX-DMEFX
190 QUALOX=FNSLOX/DMEFGX
455 IF(QUALOX=QUALIA)451,453,453
451 CONTINUE
453 POWERA=POWER-PPOWERX
PANROL=POWERB-PPOWERX

```

```

01990
02000
02010
02020
02030
02040
02050
02060
02070
02080
02090

```

```

00780
00790
00800
00810
00820
00830
00840
00850
00860
00870
00880
00890
00900
00910
00920
00930
00940
00950
00960
00970
00980
00990

```

```

01010
01020
01030
01040
01050
01060
01070
01080
01090
01100
01110
01120
01130
01140
01150
01160
01170
01180
01190
01200
01210
01220
01230
01240

```

```

PRINT 721,X,P
PRINT 722,DMEFX,DMEFGX
PRINT 723,POWERA,PANBOL
PRINT 700,POWER,POWERX,CFXLOX
PRINT 710,FNLOX
PRINT 720,FNSLOX,QUALOX
700 FORMAT(14H POWER TOTAL = E9.4/,
1 28H POWER INPUT TO POSITION X = E9.4/,
2 18H LOCAL HEAT FLUX = F11.5)
710 FORMAT(31H LOCAL ENTHALPY AT POSITION X = F8.2)
720 FORMAT(41H LOCAL SUBCOOLED ENTHALPY AT POSITION X = F8.2/,
130H LOCAL QUALITY AT POSITION X = F6.3)
721 FORMAT(51H CONDITIONS AT SLUG ANNULAR TRANSITION POSITION =F8.1,
1 14H PRESSURE =F8.1)
722 FORMAT(18H LIQUID ENTHALPY =F8.2,19H EVAP ENTHALPY =F8.2)
723 FORMAT(28H POWER OVER ANNULAR REGION =1PE10.3,
1 45H POWER FROM SLUG ANNULAR TRANSITION TO BO =1PE10.3)
RETURN
END

```

```

01250
01260
01270
01280
01290
01300
01330
01340
01350
01360
01370
01380
01390
01400
01410
01420
01430

```

```

SUBROUTINE PKIANN
COMMON NTUBES,MSHAPE,TUBE,RATIOM,DIAINS,VOLTS,AMPS,ENTHIN,FLMASS,
1 PDESP,PREFSIN,PREFOT,PRESDP,TSDP,BOLOCA,XLNGTH,SHUNTM,P,
2 DMEFX,ENFPX,DMEFGX,ENFGPX,ENSIN,QUALIN,POWER,AREAF,AREAIS,
3 QUALOL,SATL,PSATL,POWERB,PSLBOL,CFXAVG,CFXLOX,JLOCAT,K,X,
4 PRRFAK,POWERX,FNLOX,FNSLOX,QUALOX,DMEFY,DMEFGY,POWER,ONFOVM,
5 COSLEN,ONEMSO,SIGNZ,ARG,Z,FACMIR,FACPLR,CFXRO,L,Y,
6 FACTMI,POWERY,CFXLOY,FNLOY,FNSLOY,QUALOY,FACTPL,
7 CONST,SCPTL,ZFTA,PLNGTH,J,U,ULOCAT,COSARK,SINARK,I,
8 EXTRA,EXTRAB,EXTRAC,EXTRAD,EXTRAE,EXTRAF,
9 DMEFB,DMEFGB,ENLOB,ENSOB,QUALOB,EXTRAG,EXTRAH,EXTRAI,EXTRAJ
COMMON QUALTA,GLIQ,TKINCH,
1P,DX,COLM1,COLM2,COLM3,COLM4,SUMCOL,PHIMN,GTOTSC,GSURZ,SUM0,SUM1,
2SUM2,SUM3,SUM4,SUM5,OMEGAP,OMEGA,PGMULT,PSUBL,T,VISCL,VOLSP,ENO,
3VOLSPG,QUALO4,POWERA,PANBOL,DFNFO,DENFGO,ENSO,QUALO,DVSPLO,DVSPGO,
4GTOT,DPMOM,GRDMT,DVLSPL,DVLSPG,TERM1,TERM2,TERM3,TERM4,GGAS,DT,
5DVISCL,REYNUM,FFACTP,FFACT,VFLOC,GRDFS,DPGMLT,GRDFT,DGRDMT,GRDGT,
6R,GRAVAC,GRAVCS,GRAVCH,VALUEN,FACTUN,BMAOA,DBMAOA,A,FILMTK,YPLUS,
7TAUWAL,FYPLUS,GFILM,GLENT,PCLIQ,PCLFNT,DUMMYA,DUMMYR,DUMMYC
QUALO4=16.0*QUALOL
I=QUALO4
DO 451 L=I,10000,1
DUMMYC=L+1
Y=DUMMYC/16.0
IF(Y=QUALOL)370,370,365
IF(Y=(1.6*QUALOL))375,375,380
370 P=PREFSIN
GO TO 390
375 P=PREFSIN-(0.750*TSDP*(Y-QUALOL)/(XLNGTH-QUALOL))
GO TO 390
380 PRRFAK=PREFSIN-(0.750*TSDP*(0.60*QUALOL)/(XLNGTH-QUALOL))
385 P=PRRFAK-(PRRFAK-PRESOT)*(Y-(1.60*QUALOL))/
1 (XLNGTH-(1.60*QUALOL))
390 CALL LIOFN
DMEFY=ENFPX
CALL EVAPFN
DMEFGY=ENFGPX
IF(Y=(PLNGTH/2.0))400,400,410
POWERY=EXTRAC*(ONEMSO-SINF(3.1416*((PLNGTH/2.00)-
1Y
)/COSLEN))
CFXLOY=EXTRAF*COSF(3.1416*((PLNGTH/2.00)-
1Y
)/COSLEN)

```

```

02880
02890
02900
02910
02920
02930
02940
02950
02960
02970
02980
02990
03000
03010
03020
03030
03040
03050
03060
03070
03080
03090
03110
03120
03130
03140
03150
03160
03170
03180
03190
03200
03210
03220
03230
03240
03250
03260
03270
03280

```

```

GO TO 435
410 IF (Y-(XLNGTH-SCRPTL)) 415,415,425
415 POWFRY=EXTRAC*(ONFMSQ+SINF(3.1416*(
  1Y -(PLNGTH/2.00))/COSLEN) )
  CFXYLOY=EXTRAF*COSE(3.1416*(
  1Y -(PLNGTH/2.00))/COSLEN)
GO TO 435
425 POWFRY=(POWER/CONSTP)*((COSLEN*EXTRAA/3.1416)+EXTRAR*(1.00-
  1EXPF((-ZETA)*(Y -(XLNGTH-SCRPTL))/SCRPTL)))
  CFXYLOY=EXTRAE*COSEABK*EXPF((-ZETA)*(
  1Y -(XLNGTH-SCRPTL))/SCRPTL)
435 ENLOY=FNTIN+(POWER/FLMASS)
440 ENSLOY=ENLOY-DMEFGY
450 QVALOX=ENSLOY/DMEFGY
455 IF(QVALOX-QUALIA) 451,453,453
451 CONTINUE
453 POWERA=POWER-POWERY
  PANROL=POWERB-POWERY
  PRINT 721,Y,P
  PRINT 722,DMEFY,DMEFGY
  PRINT 723,POWERA,PANROL
  PRINT 700,POWER,POWERY,CFXYLOY
  PRINT 710,ENLOY
  PRINT 720,ENSLOY,QVALOX
700 FORMAT(14H POWER TOTAL = F9.4/,
  1 28H POWER INPUT TO POSITION X = E9.4/,
  2 18H LOCAL HEAT FLUX = E11.5)
710 FORMAT(31H LOCAL ENTHALPY AT POSITION7X = F8.2)
720 FORMAT(41H LOCAL SURCOOLED ENTHALPY AT POSITION X = F8.2/,
  130H LOCAL QUALITY AT POSITION X = F6.3)
721 FORMAT(51H CONDITIONS AT SLUG ANNULAR TRANSITION POSITION =F8.1,
  1 14H PRESSURE =F8.1)
722 FORMAT(18H LIQUID ENTHALPY =F8.2,19H EVAP ENTHALPY =F8.2)
723 FORMAT(28H POWER OVER ANNULAR REGION =1PE10.3,
  1 45H POWER FROM SLUG ANNULAR TRANSITION TO BO =1PE10.3)
  OFTURM
  END
SUBROUTINE PKOAMM
COMMON NTUBES,MSHAPE,TUBE,RATIOM,DIAINS,VOLTS,AMPS,ENTHIN,FLMASS,
  1 PRES,PREIN,PRESOT,PESDP,TSDP,BOLOCA,XLNGTH,SHUNT,P,
  2 DMEFX,ENFPX,DMEFGX,ENFGPX,ENFIN,QUALIN,POWER,AREAF,AREAS,
  3 QVALOL,SATL,PSATL,POWERB,PSLBOL,CFXAVG,CFXLOX,JLOCAT,K,X,
  4 PBRFAK,POWERX,ENLOX,ENSLOX,QVALOX,DMEFY,DMEFGY,POWOB,ONEOVM,
  5 COSLEN,ONFMSQ,SIGNZ,ARG,Z,FACMIB,FACPLB,CFXBO,L,Y,
  6 FACTMI,POWFRY,CFXYLOY,ENLOY,ENSLOY,QVALOY,FACTPL,
  7 CONST,SCRPTL,ZETA,PLNGTH,J,U,ULOCAT,COSABK,SINABK,I,
  8 EXTRAA,EXTRAR,EXTRAC,EXTRAQ,EXTRAF,EXTRAG,
  9 DMFFB,DMFFGR,ENLOB,ENSLOB,QVALOB,EXTRAG,EXTRAH,EXTRAJ,EXTRAJ
  COMMON QUALIA,GLIQ,TKINCH,
  1DP,DX,COLM1,COLM2,COLM3,COLM4,SUMCOL,PHIMN,GTOTSC,GSUBZ,SUM0,SUM1,
  2SUM2,SUM3,SUM4,SUM5,OMEGAP,OMEGA,PGMULT,PSUBL,T,AVISCL,VOLSPL,ENO,
  3VOLSPL,QVALO4,POWERA,PANBOL,DENFQ,ENSO,QVALO,DVSPLO,DVSPGO,
  4GTOT,DPMOV,GPDMT,DVLSPL,DVLSPG,TERM1,TERM2,TERM3,TERM4,GGAS,DT,
  5DVISCL,RFYNUM,FFACTP,FFACT,VFLOC,GRDPS,DRGMLT,GRDFT,GRDMT,GRDOT,
  6R,CPAVAC,CPAVS,GRAVCH,VALUFN,FACTUN,BMAOA,DBMAOA,A,FLMTR,YPLUS,
  7TAUWAL,FYPLUS,GFILP,GLQENT,PCLIQ,PCLFNT,DUMMYA,DUMMYB,DUMMYC
  QVALO4=16.0*QVALOL
  I=QVALO4
  DO 451 L=1,1000,1
  DUMMYC=L+1
  Y=DUMMYC/16.0

```

```

03290
03300
03310
03320
03330
03340
03350
03360
03370
03380
03390
03400
03410
03420
03430
03440
03450
03460
03470
03480
03490
03500
03510
03520
03550
03560
03570
03580
03590
03600
03610
03620
03630
03640
02100
02110
02120
02130
02140
02150
02160
02170
02180
02190
02200
02210
02220
02230
02240
02250
02260
02270
02280
02290
02300
02310

```

```

IF (Y + QVALOL) 370, 370, 365
365 IF (Y -(1.6*QVALOL) ) 375, 375, 380
370 P = PRESIN
GO TO 390
375 P=PRFSIN-(0.750*TSDP*(Y-QVALOL)/(XLNGTH-QVALOL) )
GO TO 390
380 PBRFAK=PRFSIN-(0.750*TSDP*(0.60*QVALOL)/(XLNGTH-QVALOL) )
385 P=PBRFAK-((PBRFAK-PRESOT)*(Y-(1.60*QVALOL))/
  1 (XLNGTH-(1.60*QVALOL)))
390 CALL LTOEN
  DMFFY=ENFPX
  CALL EVAPEN
  DMEFGY=ENFGPX
  IF (Y-SCRPTL) 400,400,410
400 POWERY=EXTRAF*(EXPF(ZETA*(
  1Y -SCRPTL)/SCRPTL)-EXPF(-ZETA))
  CFXYLOY=EXTRAE*COSEABK*(EXPF(ZETA*(
  1Y -SCRPTL)/SCRPTL))
GO TO 435
410 IF (Y-(XLNGTH-(PLNGTH/2.00))) 415,415,425
415 POWERY = (POWER/CONSTP)*((EXTRAB*ULOCAT) + ((COSLEN/3.1416)*(
  1SINABK-SINF(3.1416/COSLEN)*(XLNGTH-(PLNGTH/2.00)-Y ) ) ) )
  CFXYLOY=EXTRAF*COSE((3.1416/COSLEN)*(XLNGTH-(PLNGTH/2.00)-Y ) )
GO TO 435
425 POWERY = (POWER/CONSTP)*((EXTRAB*ULOCAT) + ((COSLEN/3.1416)*(
  1SINABK+SINF(3.1416/COSLEN)*(Y -(XLNGTH-(PLNGTH/2.00) ) ) ) )
  2 ) )
  CFXYLOY=EXTRAF*COSE((3.1416/COSLEN)*(Y -(XLNGTH-(PLNGTH/2.00) )
  1 ) )
435 ENLOY=FNTIN+(POWER/FLMASS)
440 ENSLOY=ENLOY-DMEFGY
450 QVALOX=ENSLOY/DMEFGY
455 IF(QVALOX-QUALIA) 451,453,453
451 CONTINUE
453 POWERA=POWER-POWERY
  PANROL=POWERB-POWERY
  PRINT 721,Y,P
  PRINT 722,DMEFY,DMEFGY
  PRINT 723,POWERA,PANBOL
  PRINT 700,POWER,POWERY,CFXYLOY
  PRINT 710,ENLOY
  PRINT 720,ENSLOY,QVALOX
700 FORMAT(14H POWER TOTAL = E9.4/,
  1 28H POWER INPUT TO POSITION X = E9.4/,
  2 18H LOCAL HEAT FLUX = E11.5)
710 FORMAT(31H LOCAL ENTHALPY AT POSITION7X = F8.2)
720 FORMAT(41H LOCAL SURCOOLED ENTHALPY AT POSITION X = F8.2/,
  130H LOCAL QUALITY AT POSITION X = F6.3)
721 FORMAT(51H CONDITIONS AT SLUG ANNULAR TRANSITION POSITION =F8.1,
  1 14H PRESSURE =F8.1)
722 FORMAT(18H LIQUID ENTHALPY =F8.2,19H EVAP ENTHALPY =F8.2)
723 FORMAT(28H POWER OVER ANNULAR REGION =1PE10.3,
  1 45H POWER FROM SLUG ANNULAR TRANSITION TO BO =1PE10.3)
  RETURN
  END
SUBROUTINE SPKANN
COMMON NTUBES,MSHAPE,TUBE,RATIOM,DIAINS,VOLTS,AMPS,ENTHIN,FLMASS,
  1 PRES,PREIN,PRESOT,PESDP,TSDP,BOLOCA,XLNGTH,SHUNT,P,
  2 DMEFX,ENFPX,DMEFGX,ENFGPX,ENFIN,QUALIN,POWER,AREAF,AREAS,
  3 QVALOL,SATL,PSATL,POWERB,PSLBOL,CFXAVG,CFXLOX,JLOCAT,K,X,
  4 PBRFAK,POWERX,ENLOX,ENSLOX,QVALOX,DMEFY,DMEFGY,POWOB,ONEOVM,

```

```

02330
02340
02350
02360
02370
02380
02390
02400
02410
02420
02430
02440
02450
02460
02470
02480
02490
02500
02510
02520
02530
02540
02550
02560
02570
02580
02590
02600
02610
02620
02630
02640
02650
02660
02670
02680
02690
02700
02710
02720
02730
02740
02770
02780
02790
02800
02810
02820
02830
02840
02850
02860
02870
00010
00020
00030
00040
00050
00060

```

```

5 COSLEN,ONEMSO,SIGNZ,ARG,Z,FACMI,FACPL,CFXRO,L,Y,
6 FACTMI,POWERY,CFXLOY,FNLOY,ENSLLOY,QUALOY,FACTPL,
7 CONSTP,SCRPTL,ZETA,PLNGTH,J,U,ULOCAT,COSABK,SINARK,I,
8 EXTPAA,FXTRAP,FXTRAC,EXTRAD,FXTRAF,FXTRAF,
9 DMEFB,DMEFGA,FNLOB,ENSLQB,QUALOB,EXTRAG,EXTRAH,EXTRAJ,EXTRAJ
COMMON QUALIA,GLIO,TKINCH,
1DP,DX,COLM1,COLM2,COLM3,COLM4,SUMCOL,PHIMN,GTOTSC,GSUBZ,SUM0,SUM1,
2SUM2,SUM3,SUM4,SUM5,OMEGAP,OMEGA,PGMULT,PSUBL,T,VISCL,VOLSPL,FNO,
3VOLSPG,QUALO4,POWER4,PANROL,DEFNO,DEFNO,ENSO,QUALO,DVSPLO,DVSPGO,
4GTOT,DPDMOM,GRDMT,DVLSPL,DVLSPG,TERM1,TERM2,TERM3,TERM4,GGAS,DT,
5DVISCL,REYNUM,FFACTP,FFACT,VFLQC,GRDFS,DRGMLT,GRDFT,GRDRT,GRDTOT,
6R,GRAVAC,GRAVCS,GRAVCH,VALUEN,FACTUN,RMAOA,DBMAOA,A,FILMTK,YPLUS,
7TAUWAL,FYPLUS,GFILM,GLOENT,PCLIO,PCLNT,DUMMYA,DUMMYB,DUMMYC
COMMON N,M,THCOND,FCHEN,SCHEM,VISCG,CPLIO,SURFTL,
1XTT,SATP,SMALLT,DELTVP,TWALL,HCHFN,HMAC,HMIC,RFYNLO,NFLUX,
2 PRNUMB,BERGH,HTB,HDFNG,QADENG,DTDENG,DELTT,QACHEN,
3 DTCHEN,RADMAX,DELTFN,RADIUS,CC,DD,FF
QUALO4=16.0*QUALOL
I=ROLOCA
DO 451 L=1,1000,1
DUMMYC=L+1
Y=DUMMYC/16.0
IF (Y - QUALOL) 370, 370, 365
365 IF (Y - (1.6*QUALOL)) 375, 375, 380
370 P = PRESIN
GO TO 300
375 P=PRESIN-(0.750*TSDP*(Y-QUALOL)/(XLNGTH-QUALOL))
GO TO 300
380 P=PRFAK=PRESIN-(0.750*TSDP*(0.60*QUALOL)/(XLNGTH-QUALOL))
385 P=PRFAK-((PRFAK-PRESOT)*(Y-(1.60*QUALOL))/(
1 (XLNGTH-(1.60*QUALOL))))
390 CALL LIQEN
DMEFY=ENFDX
CALL EVAPEN
YVFFGY=FNFGPX
IF (Y - (XLNGTH-SCRPTL))400,400,410
400 POWERY=EXTPAA*Y
CFXLOY=EXTRAF/PATIOM
GO TO 435
410 IF (Y -ULOCAT) 415,415,425
415 POWERY=(EXTPAA*(XLNGTH-SCRPTL))+
1 (EXTPAA*(ONEMSO-SINF(3.1416*(ULOCAT-Y)/(COSLFN)))
CFXLOY=EXTRAF*(COSF(3.1416*(ULOCAT-Y)/(COSLFN))
GO TO 435
425 IF (Y - (ULOCAT+(PLNGTH/2.0)))430,430,433
430 POWERY=(EXTPAA*(XLNGTH-SCRPTL))+
1 (EXTPAA*(ONEMSO+SINF(3.1416*(Y-ULOCAT)/(COSLFN)))
CFXLOY=EXTRAF*(COSF(3.1416*(Y-ULOCAT)/(COSLFN))
GO TO 435
435 POWERY=EXTPAA*(Y -PLNGTH)+(EXTPAA*2.0*ONEMSO)
CFXLOY=EXTRAF/PATIOM
435 FNLOY=FNTHIM*(POWERY/FLMASS)
440 ENSLOY=FNLOY-DMEFY
450 QUALOX=FNLSLOY/DMEFGY
455 IF (QUALOX-QUALIA) 451,453,453
451 CONTINUE
455 POWER4=POWERP-POWERY
PANROL=POWERB-POWERY
PRINT 721,Y,P
PRINT 722,DMEFY,DMEFGY
PRINT 723,POWER4,PANROL
PRINT 700,POWERP,POWERY,CFXLOY
PRINT 710,FNLOY
PRINT 720,ENSLLOY,QUALOX
700 FORMAT(14H POWER TOTAL = F9.4/,
00070
00080
00090
00100
00110
00120
00130
00140
00150
00160
00170
00180
00190
00200
00210
00220
00230
00240
00250
00260
00270
00280
00290
00300
00310
00320
00330
00340
00350
00360
00370
00380
00390
00400
00410
00420
00430
00440
00450
00460
00470
00480
00490
00500
00510
00520
00530
00540
00550
00560
00570
00580
00590
00600
00610
00620
00630
00640
00650
00660
00670
00680
00690
00700
00710

```

```

1 28H POWER INPUT TO POSITION X = E9.4/,
2 14H LOCAL HEAT FLUX = E11.5)
710 FORMAT(31H LOCAL ENTHALPY AT POSITION(X = F8.2)
720 FORMAT(41H LOCAL SUBCOOLED ENTHALPY AT POSITION X = F8.2/,
130H LOCAL QUALITY AT POSITION X = F6.3)
721 FORMAT(51H CONDITIONS AT SLUG ANNULAR TRANSITION POSITION =F8.1,
1 14H PRESSURE =F9.1)
722 FORMAT(18H LIQUID ENTHALPY =F8.2,19H EVAP ENTHALPY =F8.2)
723 FORMAT(28H POWER OVER ANNULAR REGION =1PE10.3,
1 45H POWER FROM SLUG ANNULAR TRANSITION TO BO =1PE10.3)
RETURN
END
SUBROUTINE BONUCF
COMMON NTUBES,MSHAPE,TUBE,PATIOM,DIAINS,VOLTS,AMPS,ENTHIN,FLMASS,
1 PRESO,PRESIN,PRESOT,PRESDP,TSDB,BOLOCA,XLNGTH,SHUNTM,P,
2 DMEFX,ENFDX,DMEFGX,ENFGPX,ENSIN,QUALIN,POWERP,APFAFL,APFAIS,
3 QUALOL,SATL,PSATL,POWERB,PSLROL,CFXAVG,CFXLOX,JLOCAT,K,X,
4 PRFAK,POWERX,FNLOB,ENSLQX,QUALOX,DMEFY,DMEFGY,POWERD,ONFOVM,
5 COSLEN,ONEMSO,SIGNZ,ARG,Z,FACMI,FACPL,CFXRO,L,Y,
6 FACTMI,POWERY,CFXLOY,ENSLLOY,QUALOY,FACTPL,
7 CONSTP,SCRPTL,ZETA,PLNGTH,J,U,ULOCAT,COSABK,SINARK,I,
8 EXTRAH,EXTRAH,EXTRAC,FXTRAD,FXTRAF,FXTRAF,
9 DMEFB,DMEFGA,ENLOB,ENSLQB,QUALOB,EXTRAG,EXTRAH,EXTRAJ,EXTRAJ
COMMON QUALIA,GLIO,TKINCH,
1DP,DX,COLM1,COLM2,COLM3,COLM4,SUMCOL,PHIMN,GTOTSC,GSUBZ,SUM0,SUM1,
2SUM2,SUM3,SUM4,SUM5,OMEGAP,OMEGA,PGMULT,PSUBL,T,VISCL,VOLSPL,FNO,
3VOLSPG,QUALO4,POWER4,PANROL,DEFNO,DEFNO,ENSO,QUALO,DVSPLO,DVSPGO,
4GTOT,DPDMOM,GRDMT,DVLSPL,DVLSPG,TERM1,TERM2,TERM3,TERM4,GGAS,DT,
5DVISCL,REYNUM,FFACTP,FFACT,VFLQC,GRDFS,DRGMLT,GRDFT,GRDRT,GRDTOT,
6R,GRAVAC,GRAVCS,GRAVCH,VALUEN,FACTUN,RMAOA,DBMAOA,A,FILMTK,YPLUS,
7TAUWAL,FYPLUS,GFILM,GLOENT,PCLIO,PCLNT,DUMMYA,DUMMYB,DUMMYC
COMMON N,M,THCOND,FCHEN,SCHEM,VISCG,CPLIO,SURFTL,
1XTT,SATP,SMALLT,DELTVP,TWALL,HCHFN,HMAC,HMIC,RFYNLO,NFLUX,
2 PRNUMB,BERGH,HTB,HDFNG,QADENG,DTDENG,DELTT,QACHEN,
3 DTCHEN,RADMAX,DELTFN,RADIUS,CC,DD,FF
IF (ROLOCA-QUALOL) 750,750,755
755 IF (ROLOCA-(1.6*QUALOL)) 760,760,765
750 P=PRESIN
GO TO 770
760 P=PRESIN-(0.750*TSDP*(ROLOCA-QUALOL)/(XLNGTH-QUALOL))
GO TO 770
765 PBREAK=PRESIN-(0.750*TSDP*(0.60*QUALOL)/(XLNGTH-QUALOL))
P=PBREAK-((PBREAK-PRESOT)*(ROLOCA-(1.60*QUALOL))/(XLNGTH-
1 (1.60*QUALOL)))
770 QUALOX=QUALOR
IF (QUALOX) 780,780,775
775 CALL XXXT
CALL SATTMP
CALL VISCSO
CALL XTHCON
CALL XCPLIO
CALL XSURFT
CALL EVAPEN
CALL SPECVG
CALL SPECVL
PRNUMB=CPLIO*VISCL/THCOND
A=(P**0.234)
SUM1=A/(7.30-A)
BERGH=((1.0/(15.6*(P**1.156)))**SUM1)
REYNUM=(GTOT*DIAINS)/(12.0*VISCL)
HDB=0.023*THCOND*(12.0/DIAINS)*(REYNUM**0.8)*(PRNUMB**0.4)
00720
00730
00740
00750
00760
00770
00780
00790
00800
00810
00820
00830
00810
00820
00830
00840
00850
00860
00870
00880
00890
00900
00910
00920
00930
00940
00950
00960
00970
00980
00990
01000
01010
01020
01030
01040
01050
01060
01070
01080
01090
01100
01110
01120
01130
01140
01150
01160
01170
01180
01190
01200
01210
01220
01230
01240
01250
01260
01270
01280
01290
01300
01310
01320
01330
01340
01350
01360
01370
01380
01390
01400
01410
01420
01430
01440
01450
01460
01470
01480
01490
01500

```

```

HDFNG=3.5*HDR/(XTT**0.5)
R=(2.30/(2.30-A))
QADENG=(BERGHT*(HDFNG** B))
DTDFNG=QADENG/HDFNG
100 PRINT 100,HDFNG,QADENG,DTDFNG
FORMAT(9H H DENG =E15.5,25H NUCL FLUX DENG=BERGLES =F15.5,
1 24H TWALL MINUS TSAT DENG =F15.5)
DELTT=DTDFNG
CALL XHCHFN
GO TO 10
5 CALL XHCHFN
10 QACHEN=(BERGHT*(HCHFN** B))
DTCHEN=QACHEN/HCHFN
PRINT 200,DTCHEN,DELTT,HCHFN,QACHEN
FORMAT(10H DT CHFN =F10.5,14H DT PREVIOUS =F10.5,
1 9H H CHFN =F10.5, 23H NUC FLUX CHFN=BERGLES=F10.5)
IF(ABS(DTCHFN-DELTT)-0.05) 40,40,20
20 DELTT=DTCHEN
GO TO 5
40 RADMAX=.0000575
CALL XRAD
IF (RADIUS-RADMAX) 50,50,60
50 CALL NFLUX2
CONTINUE
BMAOA=CFXRO/QACHEN
CC=CFXRO/QADENG
DELTFN=(POWERB-(POWERF-POWERPA))/FLMASS
PRINT 3000,DELTFN,BMAOA,CC
3000 FORMAT(40H DELTA ENTHALPY ANNULAR TRANS TO LOCAL =F9.2,
1 37H LOCAL FLUX OVER FLUX FOR NUCLFATION=F8.2,
2 13H RATIO DENG =F8.2)
700 CONTINUE
RETURN
END
00490
00500
00510
00520
00530
00540
00550
00560
00570
00580
00590
00600
00610
00620
00630
00640
00650
00660
00670
00680
00690
00700
00710
00720
00730
00740
00750
00760
00770
00780
00790
00810
00820
00010
00020
00030
00040
00050
00060
00070
00080
00090
00100
00110
00120
00130
00140
00150
00160
00170
00180
00190
00200
00210
00220
00230
00240
00250
00260
00270

```

```

CALL XCPLIQ
CALL XSURFT
CALL FVAPFN
CALL SPECVC
CALL SPECVL
PRNUMR= CPLIQ*VISCL/THCOND
A=(P**0.234)
SUM1=A/(2.30-A)
BERGHT=((1.0/(15.6*(P**1.156)))*SUM1)
REYNUM=(GTOT*DIAINS)/(12.0*VISCL)
HDB=0.023*THCOND*(12.0/DIAINS)*(REYNUM**0.8)*(PRNUM**0.4)
HDFNG=3.5*HDR/(XTT**0.5)
R=(2.30/(2.30-A))
QADENG=(BERGHT*(HDENG** B))
DTDFNG=QADENG/HDFNG
PRINT 100,HDFNG,QADENG,DTDFNG
100 FORMAT(9H H DENG =E15.5,25H NUCL FLUX DENG=BERGLES =F15.5,
1 24H TWALL MINUS TSAT DENG =E15.5)
DELTT=DTDFNG
CALL XHCHFN
GO TO 10
5 CALL XHCHFN
10 QACHEN=(BERGHT*(HCHFN** B))
DTCHEN=QACHEN/HCHFN
PRINT 200,DTCHEN,DELTT,HCHFN,QACHEN
FORMAT(10H DT CHFN =F10.5,14H DT PREVIOUS =F10.5,
1 9H H CHFN =E10.5, 23H NUC FLUX CHFN=BERGLES=F10.5)
IF(ABS(DTCHFN-DELTT)-0.05) 40,40,20
20 DELTT=DTCHFN
GO TO 5
40 RADMAX=.0000575
CALL XRAD
IF (RADIUS-RADMAX) 50,50,60
50 CALL NFLUX2
CONTINUE
IF(ABS(MSHAPE-1)) 900,905,900
900 IF(ABS(MSHAPE-2)) 910,915,910
910 IF(ABS(MSHAPE-3)) 920,905,920
920 IF(ABS(MSHAPE-4)) 925,905,925
925 IF(ABS(MSHAPE-5)) 930,915,930
930 IF(ABS(MSHAPE-6)) 940,915,940
940 IF(ABS(MSHAPE-7)) 915,915,915
905 BMAOA=CFXLOX/QACHEN
CC=CFXLOX/QADENG
DELTFN=(POWERX-(POWERF-POWERB))/FLMASS
GO TO 1000
915 BMAOA=CFXLOY/QACHEN
CC=CFXLOY/QADENG
DELTFN=(POWERX-(POWERF-POWERB))/FLMASS
1000 PRINT 3000,DELTFN,BMAOA,CC
3000 FORMAT(40H DELTA ENTHALPY ANNULAR TRANS TO LOCAL =F9.2,
1 37H LOCAL FLUX OVER FLUX FOR NUCLFATION=F8.2,
2 13H RATIO DENG =F8.2)
RETURN
END
SURROUTINE XRAD
COMMON NTUBES,MSHAPE,TUBE,RATIOM,DIAINS,VOLTS,AMPS,ENTHIN,FLMASS,
1 PRES,PRESIN,PRESOT,RESOP,TSDP,BOLOCA,XLNGTH,SHUNTM,P,
2 DMEFX,ENFPX,DMEFGX,FNFGPX,ENSIN,QUALIN,POWER,AREAF,AREAIS,
3 QUALOL,SATL,PSATL,POWERB,PSLBOL,CFXAVG,CFXLOX,JLOCAT,K,X,
4 PBREAK,POWERX,FNLOX,ENSLOX,QUALOX,DMEFY,DMEFGY,POWER,ONEOVM,
5 COSLEN,ONFNSO,STGZ,APGZ,FACMIB,FACPLB,CFXRO,L,Y,
6 FACTM,POWERY,CFXLOY,ENLOY,ENLOY,QUALY,FACTPL,
7 CONSTD,SCRPTL,ZFTA,PLNGTH,J,U,ULOCAT,COSABK,S,NABK,I,
8 FXTDAA,FXTDAB,FXTDPC,FXTDPA,FXTDPA,FXTDPA,
9 DMEFB,DMEFGB,FNLOB,FNSLOB,QUALOB,EXTRAG,EXTRAH,EXTRAJ,EXTRAJ
COMMON QUALI,CLIQ,TKINCH,
1 DD,DX,COLM1,COLM2,COLM3,COLM4,SUMCOL,PHIWN,GTOT,SC,GSURZ,SUM0,SUM1,
2 SUM2,SUM3,SUM4,SUM5,OMEGAP,OMEGA,PGMULT,PSURL,T,VISCL,VOLSPL,ENO,
3 VOLSPL,QUALO4,POWERPA,ANBOL,DEFNO,DEFNO,ENSO,QUALO,DVSPLO,DVSPGO,
4 GTOT,DDMOM,GRDPT,DVLSPL,DVLSPL,TERM1,TERM2,TERM3,TERM4,GGAS,DT,
5 DVISCL,REYNUM,FFACTD,VFLOC,GRDPS,DPGMLT,GRDPT,DGRDPT,GRDPT,
6 GRAVAC,GRAVCS,GRAVCH,VALUEN,FACTUN,BMAOA,DBMAOA,A,FILMT,K,YPLUS,
7 TAUWAL,FYPLUS,GFILM,GLQENT,PLIQ,PLENT,DUMMYA,DUMMYB,DUMMYC
COMMON N,M,THCOND,FCHEN,SCHEM,VISCG,CPLIQ,SURFTL,
1 XTT,SAIT,SMALLT,DELTV,THALL,HCHFN,HMAC,HMIC,REYNLO,NFLUX,
2 PRNUMR,BERGHT,HDR,HDFNG,QADENG,DTDFNG,DELTT,QACHEN,
3 DTCHEN,RADMAX,DELTFN,RADIUS,CC,DD,FF
00280
00290
00300
00310
00320
00330
00340
00350
00360
00370
00380
00390
00400
00410
00420
00430
00440
00450
00460
00470
00480
00490
00500
00510
00520
00530
00540
00550
00560
00570
00580
00590
00600
00610
00620
00630
00640
00650
00660
00670
00680
00690
00700
00710
00720
00730
00740
00750
00760
00770
00780
00790
00800
00810
00820
00010
00020
00030
00040
00050
00060
00070
00080
00090
00100

```

```

5 COSLEN,ONEMSO,SIGNZ,ARG,Z,FACMIB,FACPLB,CFXR0,L,Y,
6 FACTMI,POWERY,CFXLOY,ENLOY,ENSL0Y,QUAL0Y,FACTPL,
7CONSTP,SCRPTL,ZETA,PLNGTH,J,U,ULOCAT,COSABK,SINABK,I,
8 EXTRA,EXTRAB,EXTRAC,EXTRAD,EXTRAE,EXTRAF,
9DMEFB,DMEFCB,ENLOB,ENSL0B,QUAL0B,EXTRAG,EXTRAH,EXTRAJ,EXTRAJ
COMMON QUALIA,GLIO,TKINCH,
1DP,DX,COLM1,COLM2,COLM3,COLM4,SUMCOL,PHIMN,GTOTSC,GSUBZ,SUM0,SUM1,
2SUM2,SUM3,SUM4,SUM5,OMEGAP,OMEGA,PGMULT,PSURL,T,VISCL,VOLSPL,ENO,
3VOLSPG,QUAL04,POWER4,PANBOL,DEFNO,DEFNGO,ENSO,QUAL0,DVSPLO,DVSPGO,
4GTOT,DPMOM,GRDMT,DVLSPL,DVLSPG,TERM1,TERM2,TERM3,TERM4,GGAS,DT,
5DVISCL,REYNUM,FFACTP,FFACT,VLOC,GRDFS,DPGMLT,GRDFT,DGRDMT,GRDTOT,
6B,GRAVAC,GRAVCS,GRAVCH,VALUEN,FACTUN,BMAOA,DBMAOA,A,FILMTK,YPLUS,
7TAUWAL,FYPLUS,GFILM,GLQENT,PCLIO,PCLNT,DUMMYA,DUMMYB,DUMMYC
COMMON N,M,THCOND,FCHEN,SCHEN,VISCG,CPLIO,SURFTL,
1XTT,SATP,SMALLT,DELTV,TWALL,HCHEN,HMAC,HMIC,REYNLO,NFLUX,
2 PRNUMB,BERGH,HDENG,QADENG,DTDENG,DELTT,QACHEN,
3 DTCHEN,RADMAX,DELTFN,RADIUS,CC,DD,EE
A=FNFGPX*77.0/85.5
R=(P*144.0)/SURFTL
DX=QACHEN/THCOND
TWALL=DTDENG+T*460.0
COLM1=2.0*A*R*TWALL*TWALL/DX
COLM2=4.0*TWALL*A
COLM3=A*A
SUM1=A*(2.0*TWALL)
SUM2=COLM1+COLM2+COLM3
SUM3=(2.0*DX)-(A*R)
RADIUS=(SUM1-SQRT(SUM2))/SUM3
PRINT 20,RADIUS
FORMAT(4H LARGEST RADIUS(FT) NEEDED FOR NUCLEATIONS$DENG=E10.4)
DX=QACHEN/THCOND
TWALL=DELTT+T*460.0
COLM1=2.0*A*R*TWALL*TWALL/DX
COLM2=4.0*TWALL*A
COLM3=A*A
SUM1=A*(2.0*TWALL)
SUM2=COLM1+COLM2+COLM3
SUM3=(2.0*DX)-(A*R)
RADIUS=(SUM1-SQRT(SUM2))/SUM3
PRINT 10,RADIUS
FORMAT(4H LARGEST RADIUS(FT) NEEDED FOR NUCLATIONS$SCHEN=E10.4)
2FTUOH
END

```

```

00070
00080
00090
00100
00110
00120
00130
00140
00150
00160
00170
00180
00190
00200
00210
00220
00230
00330
00340

```

```

00350
00360
00370
00380
00390
00400
00410
00420
00430
00440
00460
00470

```

```

SUBROUTINE XHCHFN
COMMON NTUBES,MSHAP,TUBE,RATIOM,DIAINS,VOLTS,AMPS,ENTHIN,FLMASS,
1 PRES,PRESEN,PRESOT,PESDP,TSDP,BOLOCA,XLNGTH,SHUNTM,P,
2 DMEFX,ENFPX,DMEFGX,ENFGPX,ENSIN,QUALIN,POWER,AREAF,AREATS,
3 QUALOL,SATL,PSATL,POWERB,PSLBOL,CFXAVG,CFXLOX,JLOCAT,K,X,
4PBREK,POWERX,ENLOX,ENSL0X,QUAL0X,DMEFY,DMEFGY,POWOO,ONEOVM,
5 COSLEN,ONEMSO,SIGNZ,ARG,Z,FACMIB,FACPLB,CFXR0,L,Y,
6 FACTMI,POWERY,CFXLOY,ENLOY,ENSL0Y,QUAL0Y,FACTPL,
7CONSTP,SCRPTL,ZETA,PLNGTH,J,U,ULOCAT,COSABK,SINABK,I,
8 EXTRA,EXTRAB,EXTRAC,EXTRAD,EXTRAE,EXTRAF,
9DMEFB,DMEFCB,ENLOB,ENSL0B,QUAL0B,EXTRAG,EXTRAH,EXTRAJ,EXTRAJ
COMMON QUALIA,GLIO,TKINCH,
1DP,DX,COLM1,COLM2,COLM3,COLM4,SUMCOL,PHIMN,GTOTSC,GSUBZ,SUM0,SUM1,
2SUM2,SUM3,SUM4,SUM5,OMEGAP,OMEGA,PGMULT,PSURL,T,VISCL,VOLSPL,ENO,
3VOLSPG,QUAL04,POWER4,PANBOL,DEFNO,DEFNGO,ENSO,QUAL0,DVSPLO,DVSPGO,
4GTOT,DPMOM,GRDMT,DVLSPL,DVLSPG,TERM1,TERM2,TERM3,TERM4,GGAS,DT,
5DVISCL,REYNUM,FFACTP,FFACT,VLOC,GRDFS,DPGMLT,GRDFT,DGRDMT,GRDTOT,
6B,GRAVAC,GRAVCS,GRAVCH,VALUEN,FACTUN,BMAOA,DBMAOA,A,FILMTK,YPLUS,

```

```

00010
00020
00030
00040
00050
00060
00070
00080
00090
00100
00110
00120
00130
00140
00150
00160
00170
00180
00190
00200
00210
00220
00230
00240
00250
00260
00270
00280
00290
00300

```

```

7TAUWAL,FYPLUS,GFILM,GLQENT,PCLIO,PCLNT,DUMMYA,DUMMYB,DUMMYC
COMMON N,M,THCOND,FCHEN,SCHEN,VISCG,CPLIO,SURFTL,
1XTT,SATP,SMALLT,DELTV,TWALL,HCHEN,HMAC,HMIC,REYNLO,NFLUX,
2 PRNUMB,BERGH,HDENG,QADENG,DTDENG,DELTT,QACHEN,
3 DTCHEN,RADMAX,DELTFN,RADIUS,CC,DD,EE
CALL XDELTV
CALL XFCFHN
REYNLO=(GTOT*DIAINS*(1.0-QUAL0X))/(12.0*VISCL)
CALL XSCHFN
HMAC=0.023*(REYNLO**0.8)*(PRNUMB**0.4)*THCOND*FCHEN
1 *(12.0/DIAINS)
TERM1=(THCOND**0.70)*(CPLIO**0.45)*(VOLSPG**0.24)*
1 (4.17E+8**0.25)
TERM2=(SURFTL**0.5)*(VISCL**0.29)*(ENFGPX**0.24)*
1 (VOLSP**0.49)
TERM3=SCHEM*0.00122*(TERM1/TERM2)
HMIC=TERM3*(DELTT**0.24)*(ABS(DELTV)**0.75)
HCHEN=HMAC+HMIC
PRINT 100,T,VISCL,THCOND,CPLIO,SURFTL,VISCG
PRINT 150,P,ENFGPX,VOLSPG,VOLSPL
PRINT 200,SATP,DELTV,PRNUMB,XTT,FCHEN,SCHEN,REYNLO
PRINT 300,HMAC,HMIC,HCHEN
100 FORMAT(8H SATTMP=E10.4, 7H VISCL=E10.4, 8H THCOND=E10.4,
1 7H CPLIO=E10.4, 8H SURFTL=E10.4, 7H VISCG=E10.4)
150 FORMAT(4H P =E10.4,9H ENFGPX =E10.4,9H VOLSPG =E10.4,
1 9H VOLSPL =F10.4)
200 FORMAT(6H SATP=E10.4,8H DELTV=E10.4,8H PRNUMB=E10.4,
1 5H XTT=E10.4,7H FCHEN=E10.4, 7H SCHEN=E10.4,8H REYNLO=E10.4)
300 FORMAT(6H HMIC=E10.4,6H HMIC=E10.4,7H HCHEN=E10.4 )
RETURN
END

```

```

00190
00200
00210
00220
00230
00240
00250
00270
00275
00280
00290
00300
00310
00320
00330
00340
00360
00370
00380
00390
00400
00410
00420
00430
00431
00440
00450
00460
00470
00480

```

```

SUBROUTINE XTHCON
COMMON NTUBES,MSHAP,TUBE,RATIOM,DIAINS,VOLTS,AMPS,ENTHIN,FLMASS,
1 PRES,PRESEN,PRESOT,PESDP,TSDP,BOLOCA,XLNGTH,SHUNTM,P,
2 DMEFX,ENFPX,DMEFGX,ENFGPX,ENSIN,QUALIN,POWER,AREAF,AREATS,
3 QUALOL,SATL,PSATL,POWERB,PSLBOL,CFXAVG,CFXLOX,JLOCAT,K,X,
4PBREK,POWERX,ENLOX,ENSL0X,QUAL0X,DMEFY,DMEFGY,POWOO,ONEOVM,
5 COSLEN,ONEMSO,SIGNZ,ARG,Z,FACMIB,FACPLB,CFXR0,L,Y,
6 FACTMI,POWERY,CFXLOY,ENLOY,ENSL0Y,QUAL0Y,FACTPL,
7CONSTP,SCRPTL,ZETA,PLNGTH,J,U,ULOCAT,COSABK,SINABK,I,
8 EXTRA,EXTRAB,EXTRAC,EXTRAD,EXTRAE,EXTRAF,
9DMEFB,DMEFCB,ENLOB,ENSL0B,QUAL0B,EXTRAG,EXTRAH,EXTRAJ,EXTRAJ
COMMON QUALIA,GLIO,TKINCH,
1DP,DX,COLM1,COLM2,COLM3,COLM4,SUMCOL,PHIMN,GTOTSC,GSUBZ,SUM0,SUM1,
2SUM2,SUM3,SUM4,SUM5,OMEGAP,OMEGA,PGMULT,PSURL,T,VISCL,VOLSPL,ENO,
3VOLSPG,QUAL04,POWER4,PANBOL,DEFNO,DEFNGO,ENSO,QUAL0,DVSPLO,DVSPGO,
4GTOT,DPMOM,GRDMT,DVLSPL,DVLSPG,TERM1,TERM2,TERM3,TERM4,GGAS,DT,
5DVISCL,REYNUM,FFACTP,FFACT,VLOC,GRDFS,DPGMLT,GRDFT,DGRDMT,GRDTOT,
6B,GRAVAC,GRAVCS,GRAVCH,VALUEN,FACTUN,BMAOA,DBMAOA,A,FILMTK,YPLUS,
7TAUWAL,FYPLUS,GFILM,GLQENT,PCLIO,PCLNT,DUMMYA,DUMMYB,DUMMYC
COMMON N,M,THCOND,FCHEN,SCHEN,VISCG,CPLIO,SURFTL,
1XTT,SATP,SMALLT,DELTV,TWALL,HCHEN,HMAC,HMIC,REYNLO,NFLUX,
2 PRNUMB,BERGH,HDENG,QADENG,DTDENG,DELTT,QACHEN,
3 DTCHEN,RADMAX,DELTFN,RADIUS,CC,DD,EE
CALL SATTMP
IF(T=0.0) 10,20,20
20 IF(T=130.0) 30,40,40
40 IF(T=180.0) 50,60,60
60 IF(T=250.0) 70,80,80
80 IF(T=320.0) 90,100,100
100 IF(T=380.0) 110,120,120

```

```

00010
00020
00030
00040
00050
00060
00070
00080
00090
00100
00110
00120
00130
00140
00150
00160
00170
00180
00190
00200
00210
00220
00230
00240
00250
00260
00270
00280
00290
00300

```

```

120 1F(T=500,0) 130,140,140
140 1F(T=550,0) 150,140,140
160 1F(T=600,0) 170,180,180
180 1F(T=650,0) 190,200,200
200 1F(T=690,0) 210,210,220
10 THCOND=(.700E-3*T)+.302
  RETURN
30 THCOND=(.486E-3*T)+.315
  RETURN
50 THCOND=(.266E-3*T)+.3426
  RETURN
70 THCOND=(.0834E-3*T)+.376
  RETURN
90 THCOND=.3960
  RETURN
110 THCOND=(-.1595E-3*T)+.447
  RETURN
130 THCOND=(-.318E-3*T)+.504
  RETURN
150 THCOND=(-.496E-3*T)+.5974
  RETURN
170 THCOND=(-.655E-3*T)+.6849
  RETURN
190 THCOND=(-.931E-3*T)+.8504
  RETURN
210 THCOND=(-1.5E-3*T)+1.22
  RETURN
220 THCOND=.1854
  RETURN
  END

```

```

SURROUTINE XCPLIQ
LIMITS ON THIS SURROUTINE ARE 32 DEG F (CPLIQ =1.000)
AND 690 DEG F (CPLIQ =2.09) DATA FROM WFLLMAN THESIS
COMMON NTURFS,MSHAPF,TUBE,RATIOM,DIAINS,VOLTS,AMPS,ENTHIN,FLMASS,
1  PPFSP,PPFSIN,PPFSOT,RESDP,TSDD,BOLOCA,XLNGTH,SHUNTM,P,
2  DMFFX,ENFPX,DMFFGX,ENFGPX,ENFSIN,QUALIN,POWER,ARFAFL,ARFAIS,
3  QUALOL,SATL,PSATL,POWERB,PSLBOL,CFXAVG,CFXLOX,JLOCAT,K,X,
4  DRRFAK,POWERX,ENLOX,ENSLOX,QUALOX,DMFFY,DMFFGY,POWQQ,ONEOVM,
5  COSLEN,ONEMSO,SIGNZ,ARG,Z,FACMIR,FACPLB,CFXBO,L,Y,
6  FACTMI,POWERY,CFXLOY,ENLOY,ENSLOY,QUALOY,FACPL,
7  CONSTP,SCRPTL,ZFTA,PLNGTH,J,U,ULOCAT,COSABK,SINABK,I,
8  EXTRAA,EXTRAB,EXTRAC,EXTRAD,EXTRAF,EXTRAJ,
9  DMFFB,DMFFGR,FNLOB,FNSLOB,QUALOB,EXTRAG,EXTRAH,EXTRAJ,EXTRAJ
COMMON QUALIA,GLIQ,TKINCH,
10P,DX,COLM1,COLM2,COLM3,COLM4,SUMCOL,PHIMN,GTOTSC,GSUBZ,SUM0,SUM1,
2SUM2,SUM3,SUM4,SUM5,OMEGAP,OMEGA,PGMULT,PSUBL,T,VISCL,VOLSPL,ENO,
3VOLSPG,QUALQ4,POWER4,PANBOL,DFNFO,DEFNGO,ENSO,QUALQ,DVSPLO,DVSPGO,
4GTOT,DPMM,GRDMT,DVLSPL,DVLSPL,TERM1,TERM2,TERM3,TERM4,GGAS,DT,
5VISCL,REYNUM,FFACTP,FFACT,VELOC,GRDFS,DPGLT,GRDFT,GRDGT,GRDGT,
6R,GRAVAC,GRAVCS,GRAVCH,VALUEN,FACTUN,BMAOA,DBMAOA,A,FILMTK,YPLUS,
7AUWAL,FYPLUS,GFILM,GLQENT,PCLIQ,PCLNT,DUMMYA,DUMMYB,DUMMYC
COMMON N,M,THCOND,FCHEN,SCHEM,VISCG,CPLIQ,SURFTL,
1XTT,SATP,SMALLT,DELTVP,TWALL,HCHFN,HMAC,HMIC,FFYNLO,NFLUX,
2  PRNUMB,BERGHT,HDB,HDENG,QADENG,DTDFNG,DELTT,QACHEN,
3  DTCHFN,RADMAX,DELTFN,RADIUS,CC,DD,FF
CALL SATTMP
1F(T=160,0) 17,20,20
20 1F(T=240,0) 30,40,40
40 1F(T=320,0) 50,60,60
60 1F(T=450,0) 70,80,80
80 1F(T=500,0) 90,100,100

```

```

00310
00320
00330
00340
00350
00360
00370
00380
00390
00400
00410
00420
00430
00440
00450
00460
00470
00480
00490
00500
00510
00520
00530
00540
00550
00560
00570
00580
00590
00600

```

```

00010
00020
00030
00040
00050
00060
00070
00080
00090
00100
00110
00120
00130
00140
00150
00160
00170
00180
00190
00200
00210
00220
00230
00240
00250
00260
00270
00280
00290
00300
00310

```

```

100 1F(T=550,0) 110,120,120
120 1F(T=600,0) 130,140,140
140 1F(T=630,0) 140,160,160
160 1F(T=650,0) 170,170,180
10 CPLIQ =1.000
  RETURN
30 CPLIQ =(1.5E-4*T)+.076
  RETURN
50 CPLIQ =(2.8E-4*T)+.043
  RETURN
70 CPLIQ =(6.61E-4*T)+.823
  RETURN
90 CPLIQ =(1.90E-4*T)+.536
  RETURN
110 CPLIQ =(24.8E-4*T)-.056
  RETURN
130 CPLIQ =(40.0E-4*T)-.890
  RETURN
150 CPLIQ =(66.67E-4*T)-2.50
  RETURN
170 CPLIQ =(190.0E-4*T)-10.24
  RETURN
180 CPLIQ =2.09
  RETURN
  END

```

```

SURROUTINE XSURFT
COMMON NTUBES,MSHAPF,TUBE,RATIOM,DIAINS,VOLTS,AMPS,ENTHIN,FLMASS,
1  PRES,PREIN,PREOT,RESDP,TSDD,BOLOCA,XLNGTH,SHUNTM,P,
2  DMFFX,ENFPX,DMFFGX,ENFGPX,ENFSIN,QUALIN,POWER,ARFAFL,ARFAIS,
3  QUALOL,SATL,PSATL,POWERB,PSLBOL,CFXAVG,CFXLOX,JLOCAT,K,X,
4  DRRFAK,POWERX,ENLOX,ENSLOX,QUALOX,DMFFY,DMFFGY,POWQQ,ONEOVM,
5  COSLEN,ONEMSO,SIGNZ,ARG,Z,FACMIR,FACPLB,CFXBO,L,Y,
6  FACTMI,POWERY,CFXLOY,ENLOY,ENSLOY,QUALOY,FACPL,
7  CONSTP,SCRPTL,ZFTA,PLNGTH,J,U,ULOCAT,COSABK,SINABK,I,
8  EXTRAA,EXTRAB,EXTRAC,EXTRAD,EXTRAF,EXTRAJ,EXTRAJ,EXTRAJ,EXTRAJ
9  DMFFB,DMFFGR,FNLOB,FNSLOB,QUALOB,EXTRAG,EXTRAH,EXTRAJ,EXTRAJ
COMMON QUALIA,GLIQ,TKINCH,
10P,DX,COLM1,COLM2,COLM3,COLM4,SUMCOL,PHIMN,GTOTSC,GSUBZ,SUM0,SUM1,
2SUM2,SUM3,SUM4,SUM5,OMEGAP,OMEGA,PGMULT,PSUBL,T,VISCL,VOLSPL,ENO,
3VOLSPG,QUALQ4,POWER4,PANBOL,DFNFO,DEFNGO,ENSO,QUALQ,DVSPLO,DVSPGO,
4GTOT,DPMM,GRDMT,DVLSPL,DVLSPL,TERM1,TERM2,TERM3,TERM4,GGAS,DT,
5VISCL,REYNUM,FFACTP,FFACT,VELOC,GRDFS,DPGLT,GRDFT,GRDGT,GRDGT,
6R,GRAVAC,GRAVCS,GRAVCH,VALUEN,FACTUN,BMAOA,DBMAOA,A,FILMTK,YPLUS,
7AUWAL,FYPLUS,GFILM,GLQENT,PCLIQ,PCLNT,DUMMYA,DUMMYB,DUMMYC
COMMON N,M,THCOND,FCHEN,SCHEM,VISCG,CPLIQ,SURFTL,
1XTT,SATP,SMALLT,DELTVP,TWALL,HCHFN,HMAC,HMIC,FFYNLO,NFLUX,
2  PRNUMB,BERGHT,HDB,HDENG,QADENG,DTDFNG,DELTT,QACHEN,
3  DTCHFN,RADMAX,DELTFN,RADIUS,CC,DD,EE
IF(P=1000,0) 5,5,10
5 CONTINUE
SUM1=+.6.3225462F+1-3.2677020E-1*P+.2.8126518E-3*(P**2)
1 -1.7494856F-5*(P**3) +6.8880390E-8*(P**4)
2 -1.7378005F-10*(P**5) +2.8461426F-13*(P**6)
3 -3.0063514E-16*(P**7) +1.9734415E-19*(P**8)
4 -7.3149007E-23*(P**9) +1.1689972E-26*(P**10)
SURFTL=SUM1*2.24E-6*2.54*12.0
  RETURN
10 CALL SATTMP
1F(T=610,0) 15,15,20
15 SUM1=33.8-(6.45*LOGF(T))
SURFTL=FXPF(SUM1)

```

```

00320
00330
00340
00350
00360
00370
00380
00390
00400
00410
00420
00430
00440
00450
00460
00470
00480
00490
00500
00510
00520
00530
00540
00550
00560

```

```

00010
00020
00030
00040
00050
00060
00070
00080
00090
00100
00110
00120
00130
00140
00150
00160
00170
00180
00190
00200
00210
00220
00230
00240
00250
00260
00270
00280
00290
00300
00310
00320
00330
00340
00350
00360

```

```

RETURN
20 SUM1=4.5-(11.1*LOGF(T))
SUFPTL=FXPF(SUM1)
RETURN
END

```

```

00370
00380
00390
00400
00410

```

```

SURROUTINE XSATP
COMMON NTUBFS,MSHAPF,TUBE,RATION,DIAINS,VOLTS,AMPS,ENTHIN,FLMASS,
1 PRES,PRFSIN,PRESET,RESOP,TSOP,BOLCA,XLNGLH,SHUNTM,P,
2 DMEFX,ENFPX,DMEFGX,ENFGPX,ENFSIN,QUALIN,POWER,AREAF,AREATS,
3 QVALOL,SATL,PSATL,POWERB,PSLBOL,CFXAVG,CFXLOX,JLOCAT,K,X,
4 PBRFAK,POWERX,ENLOX,ENSLGX,QUALGX,DMEFY,DMEFGY,POWER,ONEOVM,
5 COSLEN,ONEMSO,SIGNZ,ARG,Z,FACMIB,FACPLB,CFXBO,L,Y,
6 FACTMI,POWERY,CFXLOY,ENLOY,ENSLGY,QUALGY,FACTPL,
7 CONSTP,SCRPTL,ZETA,PLNGLH,J,U,ULOCAT,COSABK,SINABK,I,
8 EXTRAA,EXTRAP,EXTRAC,EXTRAD,EXTRAF,EXTRAF,
9 DMEFB,DMEFGB,ENLOB,ENSLGB,QUALGB,EXTRAG,EXTRAH,EXTRAJ,EXTRAJ
COMMON QUALIA,GLIQ,TKINCH,
10P,DX,COLM1,COLM2,COLM3,COLM4,SUMCOL,PHIMN,GTOTSC,GSUBZ,SUM0,SUM1,
2SUM2,SUM3,SUM4,SUM5,OMEGAP,OMEGA,PGMULT,PSURL,T,VISCL,VOLSPL,ENO,
3VOLSPG,QUALQ4,POWERA,PANBOL,DEFNO,DEFNGO,ENSO,QUALQ,DVSPLO,DVSPGO,
4GTOT,DPMM,GPDMT,DVLSPL,DVLSPG,TERM1,TERM2,TERM3,TERM4,GGAS,DT,
5DVISCL,REYNUM,FFACTP,FFACT,VFLQC,GRDFS,DPGMLT,GRDFT,GRDGMT,GRDTOT,
6GRAVAC,GRAVCS,GRAVCH,VALUEN,FACTUN,BMAOA,DBMAOA,A,FILMTK,YPLUS,
7TAUWAL,FYPLUS,GFILM,GLQENT,PCLIQ,PCLFNT,DUMMYA,DUMMYB,DUMMYC
COMMON N,M,THCOND,FCHEN,SCHEN,VISCG,CPLIQ,SURFTL,
1XTT,SATP,SMALLT,DELTV,TWALL,HCHEN,HMAC,HMIC,REYNLO,NFLUX,
2 PRNUMB,BERGH,HD,HDENG,QADENG,DTDFNG,DELTT,QACHEN,
3 DTCHFN,RADMAX,DELTFN,RADIUS,CC,DD,FE
COLM1=647.27
COLM2=((T-32.0)/1.8)+273.16
SMALLT=COLM1-COLM2
SUM4=3206.182
IF (T-200.0) 5,5,10
SUM1=1.0+(SMALLT*2.1878462E-3)
SUM2=3.247814+(SMALLT*5.86*26F-3)+(SMALLT*SMALLT*
1 SMALLT*1.7702270E-9)
GO TO 15
SUM1=1.0+(SMALLT*1.3794481E-2)
SUM2=3.2463130+(SMALLT*4.14113F-2)
1 SUM3=((SMALLT**3)*7.515494E-9)+((SMALLT**4)*6.56444E-11)
SUM4=(SMALLT*SUM2)/(COLM2*SUM1)
SATP=SUM4/(1.7*10**SUM3)
RETURN
END

```

```

00010
00020
00030
00040
00050
00060
00070
00080
00090
00100
00110
00120
00130
00140
00150
00160
00170
00180
00190
00200
00210
00220
00230
00240
00250
00260
00270
00280
00290
00300
00310
00320
00330
00340
00350
00360
00370
00380
00390

```

```

2SUM2,SUM3,SUM4,SUM5,OMEGAP,OMEGA,PGMULT,PSURL,T,VISCL,VOLSPL,ENO,
3VOLSPG,QUALQ4,POWERA,PANBOL,DEFNO,DEFNGO,ENSO,QUALQ,DVSPLO,DVSPGO,
4GTOT,DPMM,GPDMT,DVLSPL,DVLSPG,TERM1,TERM2,TERM3,TERM4,GGAS,DT,
5DVISCL,REYNUM,FFACTP,FFACT,VFLQC,GRDFS,DPGMLT,GRDFT,GRDGMT,GRDTOT,
6GRAVAC,GRAVCS,GRAVCH,VALUEN,FACTUN,BMAOA,DBMAOA,A,FILMTK,YPLUS,
7TAUWAL,FYPLUS,GFILM,GLQENT,PCLIQ,PCLFNT,DUMMYA,DUMMYB,DUMMYC
COMMON N,M,THCOND,FCHEN,SCHEN,VISCG,CPLIQ,SURFTL,
1XTT,SATP,SMALLT,DELTV,TWALL,HCHEN,HMAC,HMIC,REYNLO,NFLUX,
2 PRNUMB,BERGH,HD,HDENG,QADENG,DTDFNG,DELTT,QACHEN,
3 DTCHFN,RADMAX,DELTFN,RADIUS,CC,DD,FE
CALL SATTMP
GSURZ=(T-32.0)/1.8
CALL SPECVG
IF (T-500.0) 5,5,10
5 COLM1=2.13*OF-4*(GSUBZ*GSUBZ)
COLM2=(1858.0-(5.00*GSUBZ))/VOLSPG
COLM3=88.020+(.22827*GSUBZ)
VISCG=2.419F-4*(COLM3+COLM1-(1.6018E-2*COLM2))
RETURN
10 SUM1=4.70*SQRTF(T)
TERM1=-30.0/T
SUM2=10.0**TERM1
SUM3=1.0+(2600.0/T)*SUM2
TERM2=0.0906/VOLSPG
SUM5=(10.00**TERM2)-1.0)
SUM4=1.5*SUM5
VISCG=2.419F-3*(SUM1/SUM2)+SUM4)
RETURN
END

```

```

00140
00150
00160
00170
00180
00190
00200
00210
00220
00230
00240
00250
00260
00270
00280
00290
00300
00310
00320
00330
00340
00350
00360
00370
00380
00390
00400

```

```

SURROUTINE XFLTV
COMMON NTUBFS,MSHAPF,TUBE,RATION,DIAINS,VOLTS,AMPS,ENTHIN,FLMASS,
1 PRES,PRFSIN,PRESET,RESOP,TSOP,BOLCA,XLNGLH,SHUNTM,P,
2 DMEFX,ENFPX,DMEFGX,ENFGPX,ENFSIN,QUALIN,POWER,AREAF,AREATS,
3 QVALOL,SATL,PSATL,POWERB,PSLBOL,CFXAVG,CFXLOX,JLOCAT,K,X,
4 PBRFAK,POWERX,ENLOX,ENSLGX,QUALGX,DMEFY,DMEFGY,POWER,ONEOVM,
5 COSLEN,ONEMSO,SIGNZ,ARG,Z,FACMIB,FACPLB,CFXBO,L,Y,
6 FACTMI,POWERY,CFXLOY,ENLOY,ENSLGY,QUALGY,FACTPL,
7 CONSTP,SCRPTL,ZETA,PLNGLH,J,U,ULOCAT,COSABK,SINABK,I,
8 EXTRAA,EXTRAP,EXTRAC,EXTRAD,EXTRAF,EXTRAF,
9 DMEFB,DMEFGB,ENLOB,ENSLGB,QUALGB,EXTRAG,EXTRAH,EXTRAJ,EXTRAJ
COMMON QUALIA,GLIQ,TKINCH,
10P,DX,COLM1,COLM2,COLM3,COLM4,SUMCOL,PHIMN,GTOTSC,GSUBZ,SUM0,SUM1,
2SUM2,SUM3,SUM4,SUM5,OMEGAP,OMEGA,PGMULT,PSURL,T,VISCL,VOLSPL,ENO,
3VOLSPG,QUALQ4,POWERA,PANBOL,DEFNO,DEFNGO,ENSO,QUALQ,DVSPLO,DVSPGO,
4GTOT,DPMM,GPDMT,DVLSPL,DVLSPG,TERM1,TERM2,TERM3,TERM4,GGAS,DT,
5DVISCL,REYNUM,FFACTP,FFACT,VFLQC,GRDFS,DPGMLT,GRDFT,GRDGMT,GRDTOT,
6GRAVAC,GRAVCS,GRAVCH,VALUEN,FACTUN,BMAOA,DBMAOA,A,FILMTK,YPLUS,
7TAUWAL,FYPLUS,GFILM,GLQENT,PCLIQ,PCLFNT,DUMMYA,DUMMYB,DUMMYC
COMMON N,M,THCOND,FCHEN,SCHEN,VISCG,CPLIQ,SURFTL,
1XTT,SATP,SMALLT,DELTV,TWALL,HCHEN,HMAC,HMIC,REYNLO,NFLUX,
2 PRNUMB,BERGH,HD,HDENG,QADENG,DTDFNG,DELTT,QACHEN,
3 DTCHFN,RADMAX,DELTFN,RADIUS,CC,DD,FE
CALL SATTMP
TWALL=DELTT+T
T=TWALL
CALL XSATP
CALL SATTMP
DELTV=(SATP-P)*144.0
RETURN
END

```

```

00010
00020
00030
00040
00050
00060
00070
00080
00090
00100
00110
00120
00130
00140
00150
00160
00170
00180
00190
00200
00210
00220
00230
00240
00250
00260
00270
00280
00290
00300
00310

```

```

SURROUTINE XVISCG
COMMON NTUBFS,MSHAPF,TUBE,RATION,DIAINS,VOLTS,AMPS,ENTHIN,FLMASS,
1 PRES,PRFSIN,PRESET,RESOP,TSOP,BOLCA,XLNGLH,SHUNTM,P,
2 DMEFX,ENFPX,DMEFGX,ENFGPX,ENFSIN,QUALIN,POWER,AREAF,AREATS,
3 QVALOL,SATL,PSATL,POWERB,PSLBOL,CFXAVG,CFXLOX,JLOCAT,K,X,
4 PBRFAK,POWERX,ENLOX,ENSLGX,QUALGX,DMEFY,DMEFGY,POWER,ONEOVM,
5 COSLEN,ONEMSO,SIGNZ,ARG,Z,FACMIB,FACPLB,CFXBO,L,Y,
6 FACTMI,POWERY,CFXLOY,ENLOY,ENSLGY,QUALGY,FACTPL,
7 CONSTP,SCRPTL,ZETA,PLNGLH,J,U,ULOCAT,COSABK,SINABK,I,
8 EXTRAA,EXTRAP,EXTRAC,EXTRAD,EXTRAF,EXTRAF,
9 DMEFB,DMEFGB,ENLOB,ENSLGB,QUALGB,EXTRAG,EXTRAH,EXTRAJ,EXTRAJ
COMMON QUALIA,GLIQ,TKINCH,
10P,DX,COLM1,COLM2,COLM3,COLM4,SUMCOL,PHIMN,GTOTSC,GSUBZ,SUM0,SUM1,

```

```

00010
00020
00030
00040
00050
00060
00070
00080
00090
00100
00110
00120
00130

```

```

SUBROUTINE XXTT
COMMON NTURFS,MESHAPF,TUBE,RATION,DIAINS,VOLTS,AMPS,ENTHIN,FLMASS,
1 PRESF,PRESIN,PRESOT,RESDP,TSDP,BOLOCA,XLNGTH,SHUNTM,P,
2 DMEFX,ENFPX,DMEFGX,ENFGPX,ENSIN,QUALIN,POWERF,AREAF,AREAS,
3 QVALOL,SATL,PSATL,POWERB,PSLROL,CFXAVG,CFXLX,JLOCAT,K,X,
4 PPRFAK,POWERX,FNLOX,FNSLOX,QUALOX,DMEFY,DMEFGY,POWOG,ONEOVM,
5 COSLFN,ONEMSO,SIGNZ,ARG,Z,FACMIB,FACPLB,CFXBO,L,Y,
6 FACTMI,POWERY,CFXLOY,FNLOY,FNSLOY,QUALOY,FACTPL,
7 CONSTP,SCRPTL,ZETA,PLNGTH,J,U,ULOCAT,COSABK,SINABK,I,
8 EXTRA,EXTRAP,EXTRAC,EXTRAD,EXTRAE,EXTRAF,
9 DMEFB,DMEFGB,FNLOB,FNSLOB,QUALOB,EXTRAG,EXTRAH,EXTRAJ,EXTRAJ
COMMON QUALIA,GLIQ,TKINCH,
1DP,DX,COLM1,COLM2,COLM3,COLM4,SUMCOL,PHIMN,GTOTSC,GSURZ,SUM0,SUM1,
2SUM2,SUM3,SUM4,SUM5,OMEGAP,OMEGA,PGMULT,PSURL,T,VISCL,VOLSPL,ENO,
3VOLSPG,QUALO4,POWERA,PANBOL,DEFNO,DEFNGO,ENSO,QUALO,DVSPLO,DVSPGO,
4GTOT,DPMOM,GRDMT,DVLSPL,DVLSPG,TERM1,TERM2,TERM3,TERM4,GGAS,DT,
5DVISCL,REYNUM,FFACTP,FFACT,VELOC,GRDFS,DPGMLT,GRDFT,DGRDMT,GRDTOT,
6B,GRAVAC,GRAVCS,GRAVCH,VALUEN,FACTUN,BMAOA,DBMAOA,A,FILMTK,YPLUS,
7TAUWAL,FYPLUS,GFILM,GLQENT,PCLIQ,PCLFNT,DUMMYA,DUMMYB,DUMMYC
COMMON N,M,THCOND,FCHEN,SCHFN,VISCG,CPLIQ,SURFTL,
1XTT,SATP,SMALLT,DELTVP,TWALL,HCHEN,HMAC,HMIC,RFYNLO,NFLUX,
2 PRNUMB,BERGH,HD,HDENG,QADENG,DTDENG,DELTT,QACHEN,
3 DTCHEN,RADMAX,DELTEN,RADIUS,CC,DD,FE
FILMTK=((1,000-QVALOX)/QVALOX)**.9)
CALL SPECVG
CALL SPECVL
YPLUS=((VOLSPL/VOLSPG)**.5)
CALL VISCG
CALL XVISCG
TAUWAL=((VISCL/VISCG)**.1)
PRINT 10,QVALOX,FILMTK,YPLUS,TAUWAL
FORMAT(9H QVALOX =F10.4,19H QVAL RATIO **,.9 =F10.4,
119H DVOL RATIO **,.5 =F10.4,20H VISCG RATIO **,.1 =F10.4)
XTT=FILMTK*YPLUS*TAUWAL
RETURN
END

```

```

SUBROUTINE XFCHEN
LIMITS ON THIS SUBROUTINE ARE 1/XTT GREATER THAN .1(IF GREATER THAN
1.?) AND (1./XTT) LESS THAN 100(IF LESS THAN 70)
COMMON NTURFS,MESHAPF,TUBE,RATION,DIAINS,VOLTS,AMPS,ENTHIN,FLMASS,
1 PRESF,PRESIN,PRESOT,RESDP,TSDP,BOLOCA,XLNGTH,SHUNTM,P,
2 DMEFX,ENFPX,DMEFGX,ENFGPX,ENSIN,QUALIN,POWERF,AREAF,AREAS,
3 QVALOL,SATL,PSATL,POWERB,PSLROL,CFXAVG,CFXLX,JLOCAT,K,X,
4 PPRFAK,POWERX,FNLOX,FNSLOX,QUALOX,DMEFY,DMEFGY,POWOG,ONEOVM,
5 COSLFN,ONEMSO,SIGNZ,ARG,Z,FACMIB,FACPLB,CFXBO,L,Y,
6 FACTMI,POWERY,CFXLOY,FNLOY,FNSLOY,QUALOY,FACTPL,
7 CONSTP,SCRPTL,ZETA,PLNGTH,J,U,ULOCAT,COSABK,SINABK,I,
8 EXTRA,EXTRAP,EXTRAC,EXTRAD,EXTRAE,EXTRAF,
9 DMEFB,DMEFGB,FNLOB,FNSLOB,QUALOB,EXTRAG,EXTRAH,EXTRAJ,EXTRAJ
COMMON QUALIA,GLIQ,TKINCH,
1DP,DX,COLM1,COLM2,COLM3,COLM4,SUMCOL,PHIMN,GTOTSC,GSUBZ,SUM0,SUM1,
2SUM2,SUM3,SUM4,SUM5,OMEGAP,OMEGA,PGMULT,PSUBL,T,VISCL,VOLSPL,ENO,
3VOLSPG,QUALO4,POWERA,PANBOL,DEFNO,DEFNGO,ENSO,QUALO,DVSPLO,DVSPGO,
4GTOT,DPMOM,GRDMT,DVLSPL,DVLSPG,TERM1,TERM2,TERM3,TERM4,GGAS,DT,
5DVISCL,REYNUM,FFACTP,FFACT,VELOC,GRDFS,DPGMLT,GRDFT,DGRDMT,GRDTOT,
6B,GRAVAC,GRAVCS,GRAVCH,VALUEN,FACTUN,BMAOA,DBMAOA,A,FILMTK,YPLUS,
7TAUWAL,FYPLUS,GFILM,GLQENT,PCLIQ,PCLFNT,DUMMYA,DUMMYB,DUMMYC
COMMON N,M,THCOND,FCHEN,SCHFN,VISCG,CPLIQ,SURFTL,
1XTT,SATP,SMALLT,DELTVP,TWALL,HCHEN,HMAC,HMIC,RFYNLO,NFLUX,
2 PRNUMB,BERGH,HD,HDENG,QADENG,DTDENG,DELTT,QACHEN,
3 DTCHEN,RADMAX,DELTEN,RADIUS,CC,DD,FE
EE=(FCHEN**1.25)*REYNLO
IF(EE-20000.0) 10,20,20
20 IF(EE-70000.0) 30,40,40
40 IF(EE-450000.0) 50,60,60
SCHEN=.80
RETURN
30 SCHEN=.15/(EE**.204)
RETURN
50 SCHEN=4800.0/(FF**.825)
RETURN
60 SCHEN=.10
RETURN
END

```

```

1XTT,SATP,SMALLT,DELTVP,TWALL,HCHEN,HMAC,HMIC,RFYNLO,NFLUX,
2 PRNUMB,BERGH,HD,HDENG,QADENG,DTDENG,DELTT,QACHEN,
3 DTCHEN,RADMAX,DELTEN,RADIUS,CC,DD,FE
CALL XXTT
ND=1.0/XTT
IF(DD-.10) 10,20,20
20 IF(DD-.33) 30,40,40
40 IF(DD-1.5) 50,60,60
60 IF(DD-1000.0) 70,70,70
10 FCHEN=1.0
RETURN
30 FCHEN=2.17*(DD**.336)
RETURN
50 FCHEN=2.785*(DD**.561)
RETURN
70 FCHEN=2.511*(DD**.716)
RETURN
80 FCHFN=344.0
PRINT 90,FCHFN
90 FORMAT(48H QVALOX(1/XTT) TOO LARGE EXCEEDS ALLOWED LIMITS =E10.4)
RETURN
END

```

```

SUBROUTINE XSCHFN
LIMITS ON THIS SUBROUTINE ARE EE GREATER THAN 2E+6 (S=.80)
AND FF LESS THAN 1E+6 (S=.1)
COMMON NTURFS,MESHAPF,TUBE,RATION,DIAINS,VOLTS,AMPS,ENTHIN,FLMASS,
1 PRESF,PRESIN,PRESOT,RESDP,TSDP,BOLOCA,XLNGTH,SHUNTM,P,
2 DMEFX,ENFPX,DMEFGX,ENFGPX,ENSIN,QUALIN,POWERF,AREAF,AREAS,
3 QVALOL,SATL,PSATL,POWERB,PSLROL,CFXAVG,CFXLX,JLOCAT,K,X,
4 PPRFAK,POWERX,FNLOX,FNSLOX,QUALOX,DMEFY,DMEFGY,POWOG,ONEOVM,
5 COSLFN,ONEMSO,SIGNZ,ARG,Z,FACMIB,FACPLB,CFXBO,L,Y,
6 FACTMI,POWERY,CFXLOY,FNLOY,FNSLOY,QUALOY,FACTPL,
7 CONSTP,SCRPTL,ZETA,PLNGTH,J,U,ULOCAT,COSABK,SINABK,I,
8 EXTRA,EXTRAP,EXTRAC,EXTRAD,EXTRAE,EXTRAF,
9 DMEFB,DMEFGB,FNLOB,FNSLOB,QUALOB,EXTRAG,EXTRAH,EXTRAJ,EXTRAJ
COMMON QUALIA,GLIQ,TKINCH,
1DP,DX,COLM1,COLM2,COLM3,COLM4,SUMCOL,PHIMN,GTOTSC,GSUBZ,SUM0,SUM1,
2SUM2,SUM3,SUM4,SUM5,OMEGAP,OMEGA,PGMULT,PSUBL,T,VISCL,VOLSPL,ENO,
3VOLSPG,QUALO4,POWERA,PANBOL,DEFNO,DEFNGO,ENSO,QUALO,DVSPLO,DVSPGO,
4GTOT,DPMOM,GRDMT,DVLSPL,DVLSPG,TERM1,TERM2,TERM3,TERM4,GGAS,DT,
5DVISCL,REYNUM,FFACTP,FFACT,VELOC,GRDFS,DPGMLT,GRDFT,DGRDMT,GRDTOT,
6B,GRAVAC,GRAVCS,GRAVCH,VALUEN,FACTUN,BMAOA,DBMAOA,A,FILMTK,YPLUS,
7TAUWAL,FYPLUS,GFILM,GLQENT,PCLIQ,PCLFNT,DUMMYA,DUMMYB,DUMMYC
COMMON N,M,THCOND,FCHEN,SCHFN,VISCG,CPLIQ,SURFTL,
1XTT,SATP,SMALLT,DELTVP,TWALL,HCHEN,HMAC,HMIC,RFYNLO,NFLUX,
2 PRNUMB,BERGH,HD,HDENG,QADENG,DTDENG,DELTT,QACHEN,
3 DTCHEN,RADMAX,DELTEN,RADIUS,CC,DD,FE
EE=(FCHEN**1.25)*REYNLO
IF(EE-20000.0) 10,20,20
20 IF(EE-70000.0) 30,40,40
40 IF(EE-450000.0) 50,60,60
SCHEN=.80
RETURN
30 SCHEN=.15/(EE**.204)
RETURN
50 SCHEN=4800.0/(FF**.825)
RETURN
60 SCHEN=.10
RETURN
END

```

00230
00240
00250
00260
00270
00280
00290
00300
00320
00330
00340
00350
00360
00370
00380
00390
00410
00420
00010
00020
00030
00040
00050
00060
00070
00080
00090
00100
00110
00120
00130
00140
00150
00160
00170
00180
00190
00200
00210
00220
00230
00240
00250
00260
00270
00280
00290
00300
00310
00320
00330
00340
00350
00360
00370
00380
00390
00010
00020
00030
00040
00050
00060
00070
00080
00090
00100
00110
00120
00130
00140
00150
00160
00170
00180
00190
00200
00210
00220
00230
00240
00250
00260
00270
00280
00290
00300
00310
00320
00330
00340
00350
00360
00370
00380
00390

```

SURROUTINE NFLUX2
COMMON NTURFS,MSHAPF,TUBE,RATIOM,DIAINS,VOLTS,AMPS,ENTHIN,FLMASS,
1  PPFSD,PPFSIN,PPFSOT,PPFSDP,TSDD,POLOCA,XLNGTH,SHUNTM,D,
2  DMFFX,FNFDX,DMFFGX,FNFGPX,ENSIN,QUALIN,POWER,AREAF,AREAFS,
3  QVALOL,SATL,PSATL,POWFR,PSLRLO,CFXAVG,CFXLOX,JLOCAT,K,X,
4  PRPEAK,POWFRX,ENLOX,ENSLOX,QVALOX,DMEFY,DMEFGY,POWQ,ONEOVM,
5  COSLEN,ONEMSO,SIGNZ,ARG,Z,FACMIB,FACPLB,CFXBO,L,Y,
6  FACTM1,POWFRY,CFXLOY,ENLOY,ENSLOY,QVALOY,FACTPL,
7  CONSTP,SCPTL,ZFTA,PLNGTH,J,U,ULOCAT,COSABK,SINABK,I,
8  EXTPAA,EXTPAP,EXTPAC,EXTPAD,EXTPAF,EXTRAF,
9  DWFFB,DWFFG,ENLOB,ENSLOB,QVALOB,EXTRAG,EXTRAH,EXTRAJ,EXTRAJ
COMMON QUALTA,GLIO,TKINCH,
10P,DX,COLM1,COLM2,COLM3,COLM4,SUMCOL,PHIMN,GTOTSC,GSUBZ,SUM0,SUM1,
2SUM2,SUM3,SUM4,SUM5,OMEGAP,OMEGA,PGMULT,PSURL,T,VISCL,VOLSPL,FNO,
3VOLSPO,QVALO4,POWPA,PANROL,DEFNO,DEFNO,ENSO,QVALO,DVSPLO,DVSPGO,
4GTOT,DPDMO,GRDNT,DVLSPL,DVLSPO,TERM1,TERM2,TERM3,TERM4,GGAS,DT,
5DVISCL,REYNUM,FFACTP,FFACT,VELOC,GRDFS,DPGMLT,GRDFT,DGRDNT,GRDTOT,
6GRAVAC,GRAVCS,GRAVCH,VALUEN,FACTUN,RMAOA,DBMAOA,A,FILMTK,YPLUS,
7TAUWAL,FYPLUS,GFILM,GLOFNT,PCLIO,PCLFNT,DUMMYA,DUMMYB,DUMMYC
COMMON M,T,THCOND,FCHEN,SCHEM,VISCG,CPLIO,SURFTL,
1XIT,SATP,SMALLT,DELTV,TWALL,HCHEN,HMAC,HMIC,REYNLO,NFLUX,
2  PRNUMB,BRGHT,HDB,HDENG,QADENG,DTDFNG,DELTT,QACHEN,
3  DTCHEN,RADMAX,DELTFN,RADIUS,CC,DD,FF
RETURN
END

SURROUTINE FILMER
COMMON NTURFS,MSHAPF,TUBE,RATIOM,DIAINS,VOLTS,AMPS,ENTHIN,FLMASS,
1  PPFSD,PPFSIN,PPFSOT,PPFSDP,TSDD,POLOCA,XLNGTH,SHUNTM,D,
2  DMFFX,FNFDX,DMFFGX,FNFGPX,ENSIN,QUALIN,POWER,AREAF,AREAFS,
3  QVALOL,SATL,PSATL,POWFR,PSLRLO,CFXAVG,CFXLOX,JLOCAT,K,X,
4  PRPEAK,POWFRX,ENLOX,ENSLOX,QVALOX,DMEFY,DMEFGY,POWQ,ONEOVM,
5  COSLEN,ONEMSO,SIGNZ,ARG,Z,FACMIB,FACPLB,CFXBO,L,Y,
6  FACTM1,POWFRY,CFXLOY,ENLOY,ENSLOY,QVALOY,FACTPL,
7  CONSTP,SCPTL,ZFTA,PLNGTH,J,U,ULOCAT,COSABK,SINABK,I,
8  EXTPAA,EXTPAP,EXTPAC,EXTPAD,EXTPAF,EXTRAF,
9  DWFFB,DWFFG,ENLOB,ENSLOB,QVALOB,EXTRAG,EXTRAH,EXTRAJ,EXTRAJ
COMMON QUALTA,GLIO,TKINCH,
10P,DX,COLM1,COLM2,COLM3,COLM4,SUMCOL,PHIMN,GTOTSC,GSUBZ,SUM0,SUM1,
2SUM2,SUM3,SUM4,SUM5,OMEGAP,OMEGA,PGMULT,PSURL,T,VISCL,VOLSPL,FNO,
3VOLSPO,QVALO4,POWPA,PANROL,DEFNO,DEFNO,ENSO,QVALO,DVSPLO,DVSPGO,
4GTOT,DPDMO,GRDNT,DVLSPL,DVLSPO,TERM1,TERM2,TERM3,TERM4,GGAS,DT,
5DVISCL,REYNUM,FFACTP,FFACT,VELOC,GRDFS,DPGMLT,GRDFT,DGRDNT,GRDTOT,
6GRAVAC,GRAVCS,GRAVCH,VALUEN,FACTUN,RMAOA,DBMAOA,A,FILMTK,YPLUS,
7TAUWAL,FYPLUS,GFILM,GLOFNT,PCLIO,PCLFNT,DUMMYA,DUMMYB,DUMMYC
COMMON M,T,THCOND,FCHEN,SCHEM,VISCG,CPLIO,SURFTL,
1XIT,SATP,SMALLT,DELTV,TWALL,HCHEN,HMAC,HMIC,REYNLO,NFLUX,
2  PRNUMB,BRGHT,HDB,HDENG,QADENG,DTDFNG,DELTT,QACHEN,
3  DTCHEN,RADMAX,DELTFN,RADIUS,CC,DD,FF
IF(ARSE(MSHADF-1)) 90,905,900
907 IF(ARSE(MSHADF-2)) 910,915,910
910 IF(ARSE(MSHADF-3)) 920,905,920
920 IF(ARSE(MSHADF-4)) 925,905,925
925 IF(ARSE(MSHADF-5)) 930,915,930
930 IF(ARSE(MSHADF-6)) 940,915,940
940 IF(ARSE(MSHADF-7)) 915,915,915
915 IF(POWFR-10,0) 1,1,2
915 IF(POWFR-10,0) 1,1,2
1  CALL BONUCF
GO TO 180
2  IF(QVALOX-QVALTA) 180,3,3

```

```

3  CALL BONUCF 00350
4  CALL SPFCVL 00360
   DVLSPL=VOLSPL 00370
   CALL SPFCVG 00380
   DVLSPO=VOLSPO 00390
   TERM1=(DVLSPO/DVLSPL)**.333 00400
   GGAS=QVALOX*GTOT 00410
   GLIO=(1.00-QVALOX)*GTOT 00420
   TERM2=3600.0/(DVLSPO*GGAS) 00430
   CALL SATTMP 00440
   CALL VISCS 00450
   DVISCL=VISCL 00460
   NT=T 00470
   REYNUM=(GTOT*DIAINS)/(DVISCL*12.0) 00480
   IF(REYNUM-2500.0)5,5,10 00490
5  FFACTP=16.0/REYNUM 00500
   GO TO 15 00510
10 FFACTD=0.046/(REYNUM**0.7) 00520
15 FFACT=4.0*FFACTD 00530
   VFLOC=(GTOT*DVLSPL)/3600.0 00540
   GRDFS=-FFACT*VFLOC*VELOC/(2.0*32.2*(DIAINS/12.0)*DVLSPL) 00550
   CALL MNPGRD 00560
   DPGMLT=ABS(PGMULT) 00570
   GRDFT=GRDFS*DPGMLT 00580
   IF(EXTRAJ-0.0) 23,21,23 00590
21 DGRDNT=-ARSE(DUMMYA) 00600
   GO TO 28 00610
23 CALL HOMMGD 00620
   DGRDNT=-ARSE(GRDNT) 00630
28 IF(DGRDNT+99000.0) 26,26,27 00640
26 DGRDNT=0.0 00650
27 CONTINUE 00660
24 GRDTOT=GRDFT+DGRDNT 00670
   R=(DIAINS/12.0)/2.0 00680
   GRAVAC=32.2 00690
   GRAVCS=32.2 00700
   PRINT 100,DPGMLT,DGRDNT,GRDFT,GRDTOT 00710
   PRINT 110,GGAS,GLIO 00720
   PRINT 120,DVLSPL,DVLSPO,DT,DVISCL 00730
   PRINT 130,REYNUM,FFACT,VELOC,GRDFS,FFACTP 00740
   TERM3=SQRT(ABS((GRDTOT*B*32.2*DVLSPL)/2.0)) 00750
   IF(-GRDTOT-(GRAVAC/(GRAVCS*DVLSPL))) 25,20,20 00760
20 VALUEN=0.0 00770
   GO TO 30 00780
25 VALUEN=-0.333 00790
30 TERM4=((GRAVAC/(GRAVCS*DVLSPL*(-GRDTOT)))*VALUEN) 00800
   FACTUN=TERM1*TERM2*TERM3*TERM4 00810
   PRINT 135,TERM1,TERM2,TERM3,TERM4 00820
   CALL UNIVER 00830
   DRMAOA=RMAOA 00840
   A=R*(1.00-ARSE(DBMAOA)) 00850
   FILMTK=BMAOA*R 00860
   TKINCH=(R/2.0)*(1-GRDTOT-(1.00-((A*A)/(R*R)))*(GRAVAC/(GRAVCS*DVLSPL))) 00870
   TAUWAL=(R/2.0)*(1-GRDTOT-(1.00-((A*A)/(R*R)))*(GRAVAC/(GRAVCS*DVLSPL))) 00880
   YPLUS=((R-A)/(DVLSPL*DVISCL))*(SQRT(TAUWAL*DVLSPL*4.17E+8)) 00900
   IF(YPLUS-5.7)40,40,35 00910
35 IF(YPLUS-30.0)45,45,50 00920
40 FYPLUS=0.5*YPLUS*YPLUS 00930
   GO TO 55 00940
45 FYPLUS=12.5-(8.05*YPLUS)+(5.0*YPLUS*LOGF(YPLUS)) 00950
   GO TO 55 00960
50 FYPLUS=(3.0*YPLUS)+(2.5*YPLUS*LOGF(YPLUS))-64.0 00970
55 GFILM=(2.0*DVISCL*FYPLUS)/R 00980
   GLOFNT=GLIO-GFILM 00990

```

```

PCLIO=GLIO/GTOT
PCLFNT=GLQFNT/GLIO
60 EXTRAJ=QUALOX
70 EXTRAI=DVLSPG
EXTRAH=DVLSPL
PRINT 140,VALUFN,FACTUN,DBMAOA
PRINT 150,TAUWAL,YPLUS,FYPLUS
PRINT 160,TKINCH,GFILM,GLQFNT
PRINT 170,PCLIO,PCLFNT
100 FORMAT(10H DPGMLT =F8.1,10H DGRDMT =F8.1,10H GRDFT =F8.1,
111H GRDTOT =F8.1)
110 FORMAT(7H GGAS =IPE10.3,8H GLIO =IPE10.3)
120 FORMAT(9H DVLSPL =F8.4,11H DVLSPG =F8.4,7H DT =F8.2,
111H DVISCL =F8.3)
120 FORMAT(9H REYNUM =IPE8.2,10H FFACT =0PF8.5,10H VELOC =F8.2,
110H GRDFS =F8.2,11H FFACTP =F8.5)
135 FORMAT(8H TERM1 =F10.4,9H TERM2 =F10.6,9H TERM3 =F10.3,
10H TERM4 =F10.4)
140 FORMAT(9H VALUFN =F8.3,11H FACTUN =F8.4,11H DBMAOA =F8.4)
150 FORMAT(9H TAUWAL =F10.2,9H YPLUS =IPE10.3,11H FYPLUS =IPE10.3)
160 FORMAT(9H TKINCH =F10.4,9H GFILM =IPE10.2,10H GLQFNT =IPE10.2)
170 FORMAT(26H PERCENT LIQUID OF TOTAL =F10.2)
180 CONTINUE
      RETURN
      END

SUBROUTINE MOMMGN
COMMON NTUBES,MSHAPE,TUBE,RATIOM,DIAINS,VOLTS,AMPS,ENTHIN,FLMASS,
1 PRES,PREIN,PRESOT,RESDP,TSDP,BOLOCA,XLNGTH,SHUNTM,P,
2 DMEFX,ENFPX,DMEFGX,ENFGPX,ENSIN,QUALIN,POWERT,AREAF,AREAIS,
3 QVALOL,SATL,PSATL,POWERB,PSLROL,CFXAVG,CFXLOA,JLOCAT,K,X,
4 PRFAK,POWFPX,ENLOX,ENSLQ,QUALOX,DMEFY,DMEFGY,POWOB,DFVOVM,
5 COSLFN,ONEMSO,SIGNZ,ARG,Z,FACMR,FACPLB,CFXRO,L,Y,
6 FACTMI,POWERY,CFXLOY,ENLOY,ENSLQ,QUALQY,FACTPL,
7 CONSTP,SCRPTL,ZFTA,PLNGTH,J,U,ULOCAT,COSABK,STNABK,I,
8 EXTRA,EXTRAH,EXTRAC,EXTRAD,EXTRAF,EXTRAF,
9 DMEFB,DMEFGB,ENLOB,FNSLOB,QUALOB,EXTRAG,EXTRAH,EXTRAJ,EXTRAJ
COMMON QUALIA,GLIO,TKINCH,
10P,DX,COLM1,COLM2,COLM3,COLM4,SUMCOL,PHIMN,GTOTSC,GSUBZ,SUMO,SUM1,
2SUM2,SUM3,SUM4,SUM5,OMEGA,OMEGA,PGMULT,PSURL,T,VISCL,VOLSP,FNO,
3VOLSPG,QUALCA,POWERA,PANBOL,DFNFO,DFNFGO,FNSO,QUALO,DVSPLO,DVSPGO,
4GTOT,DPMMOM,GRDMT,DVLSPL,DVLSPG,TERM1,TERM2,TERM3,TERM4,GGAS,DT,
5DVISCL,REYNUM,FFACTP,FFACT,VELOC,GRDFS,DPGMLT,GRDFT,DGRDMT,GRDTOT,
6R,GRAVAC,GRAVCS,GRAVCH,VALUEN,FACTUN,BMAOA,DBMAOA,A,FILMTK,YPLUS,
7TAUWAL,FYPLUS,GFILM,GLQFNT,PCLIO,PCLFNT,DUMMYA,DUMMYB,DUMMYC
COMMON N,V,THCOND,FCHEN,SCHEM,VISCG,CPLIO,SUPFTL,
1XIT,SATP,SMALLT,DFLTP,FWALL,HCHEN,MMAC,MMIC,REYNLO,NFLUX,
2DNUMR,REFRHT,HDR,DFENG,OADENG,DTDENG,DFLTT,QACHEN,
3DTCHEN,PANMAX,DELTFN,ADJUS,CC,DD,FF
GTOT=FLMASS/ARFAFL
DPMMOM=((GTOT*GTOT)/4.17E+8)*
1 ((DVLSPL*(1.00-QUALOX+QUALOX*(DVLSPG/DVLSPL)))
2 -(EXTRAH*(1.00-EXTRAJ+EXTRAJ*(EXTRAJ/EXTRAH))) ) )
IF(MSHAPE=4) 5,5,10
5 I=1
DUMMYB=I
GO TO 15
10 IF (MSHAPE=7) 11,12,12
12 IF(Y=(XLNGTH-SCRPTL)) 5,5,13
13 IF(Y=(XLNGTH-SCRPTL+PLNGTH)) 14,14,16
14 ZFTA=.1

```

```

01000
01010
01020
01030
01040
01050
01060
01070
01080
01090
01100
01110
01120
01130
01140
01150
01160
01170
01180
01190
01200
01210
01220
01230
01240
01250

```

```

NUMMYB=ZFTA/8.0
GO TO 15
16 DUMMYB=Y-(XLNGTH-SCRPTL+PLNGTH)
GO TO 15
11 I=2
NUMMYB=I
15 GRDMT=DPMMOM/(DUMMYB/12.0)
PRINT 20,DUMMYB,EXTRAJ,EXTRAJ,EXTRAH
20 FORMAT(9H DUMMYB =F6.2,27H QUALOX CONTROL VOL INLET =F8.2,
1 27H DVLSPG CONTROL VOL INLET =F8.4,
2 27H DVLSPL CONTROL VOL INLET =F8.4)
RETURN
END

SURROUTINE GRDMOM
COMMON NTUBES,MSHAPE,TUBE,RATIOM,DIAINS,VOLTS,AMPS,ENTHIN,FLMASS,
1 PRES,PREIN,PRESOT,RESDP,TSDP,BOLOCA,XLNGTH,SHUNTM,P,
2 DMEFX,ENFPX,DMEFGX,ENFGPX,ENSIN,QUALIN,POWERT,AREAF,AREAIS,
3 QVALOL,SATL,PSATL,POWERB,PSLROL,CFXAVG,CFXLOA,JLOCAT,K,X,
4 PRFAK,POWFPX,ENLOX,ENSLQ,QUALOX,DMEFY,DMEFGY,POWOB,DFVOVM,
5 COSLFN,ONEMSO,SIGNZ,ARG,Z,FACMR,FACPLB,CFXRO,L,Y,
6 FACTMI,POWERY,CFXLOY,ENLOY,ENSLQ,QUALQY,FACTPL,
7 CONSTP,SCRPTL,ZFTA,PLNGTH,J,U,ULOCAT,COSABK,STNABK,I,
8 EXTRA,EXTRAH,EXTRAC,EXTRAD,EXTRAF,EXTRAF,
9 DMEFB,DMEFGB,ENLOB,FNSLOB,QUALOB,EXTRAG,EXTRAH,EXTRAJ,EXTRAJ
COMMON QUALIA,GLIO,TKINCH,
10P,DX,COLM1,COLM2,COLM3,COLM4,SUMCOL,PHIMN,GTOTSC,GSUBZ,SUMO,SUM1,
2SUM2,SUM3,SUM4,SUM5,OMEGA,OMEGA,PGMULT,PSURL,T,VISCL,VOLSP,FNO,
3VOLSPG,QUALCA,POWERA,PANBOL,DFNFO,DFNFGO,FNSO,QUALO,DVSPLO,DVSPGO,
4GTOT,DPMMOM,GRDMT,DVLSPL,DVLSPG,TERM1,TERM2,TERM3,TERM4,GGAS,DT,
5DVISCL,REYNUM,FFACTP,FFACT,VELOC,GRDFS,DPGMLT,GRDFT,DGRDMT,GRDTOT,
6R,GRAVAC,GRAVCS,GRAVCH,VALUEN,FACTUN,BMAOA,DBMAOA,A,FILMTK,YPLUS,
7TAUWAL,FYPLUS,GFILM,GLQFNT,PCLIO,PCLFNT,DUMMYA,DUMMYB,DUMMYC
ENQ=ENTHIN+(POWERT/FLMASS)
D=PPRESOT
CALL LIOEN
DFNFO=ENFPX
CALL EVAPEN
DFNFGO=ENFGPX
ENSO=ENQ-DENFO
QUALO=ENSO/DENFGO
CALL SPECVL
DVSPLO=VOLSP
CALL SPECVG
DVSPGO=VOLSPG
GTOT=FLMASS/ARFAFL
DPMMOM=((GTOT*GTOT*DVSPLO)/4.17E+8)*((1.00-QUALO)+(QUALO*(DVSPGO/DV
1SPLO))-1.00)
DUMMYA=(-DPMMOM)/(XLNGTH/12.0)
PRINT 175,DUMMYA
175 FORMAT(38H DGRMT BASED ON LINEAR MOM GRADIFT =F12.1)
RETURN
END

SURROUTINE MNPGRD
LIMITS ON THE APPLICATION OF THIS SUBROUTINE ARE 70PERCENT QUALITY
1 AND 2500 PSIA PRESSURE
COMMON NTUBES,MSHAPE,TUBE,RATIOM,DIAINS,VOLTS,AMPS,ENTHIN,FLMASS,
1 PRES,PREIN,PRESOT,RESDP,TSDP,BOLOCA,XLNGTH,SHUNTM,P,

```

```

00355
00360
00370
00380
00390
00400
00410
00420
00430
00440
00450
00460
00470
00010
00020
00030
00040
00050
00060
00070
00080
00090
00100
00110
00120
00130
00140
00150
00160
00170
00180
00190
00200
00210
00220
00230
00240
00250
00260
00270
00280
00290
00300
00310
00320
00330
00340
00360
00370
00010
00020
00030
00040
00050

```

```

2 DMFFX,DMFFX,DMFFGX,DMFFGX,FMSIN,QUALIN,POWER,APFAFL,APFAIS, 00060
3 QUALOL,SATL,PSATL,POWFRP,PSI,ROL,CFXAVG,CFXLOX,JLOCAT,K,X, 00070
4 4PREFAX,POWFRX,FNLOX,ENSLX,QUALOX,DMFFY,DMFFGY,POWOO,ONFOVM, 00080
5 COSLEN,ONFMSQ,SIGNZ,ARG,Z,FACMIB,FACPLR,CFXRO,L,Y, 00090
6 FACTMI,POWERY,CFXLOY,FNLOY,FNSLOY,QUALOY,FACTPL, 00100
7 CONSTP,SCRPTL,ZETA,PLNGTH,J,U,ULOCAT,COSABK,SINABK,I, 00110
8 EXTRAA,EXTRAB,EXTRAC,EXTRAD,EXTRAE,EXTRAF, 00120
9 DMFFB,DMFFGB,ENLOB,ENSLB,QUALOB,EXTRAG,EXTRAH,EXTRAJ,EXTRAJ 00130
COMMON QUALIA,GLIO,TKINCH, 00140
1DP,DX,COLM1,COLM2,COLM3,COLM4,SUMCOL,PHIMN,GTOTSC,GSUBZ,SUM0,SUM1, 00150
2SUM2,SUM3,SUM4,SUM5,OMEGAP,OMEGA,PGMULT,PSUBL,T,VISCL,VOLSPL,ENO, 00160
3VOLSPL,QUALO4,POWEP,ANROL,DFNFO,DFNFG,ENSO,QUALO,NSPLO,DVSPG, 00170
4GTOT,DPMM,GRDMT,DVLSPL,DVLSPL,TERM1,TERM2,TERM3,TERM4,GGAS,DT, 00180
5DVISCL,REYNUM,FFACT,FFACT,VFLC,GRDFS,DPGLT,GRDFT,DGRDMT,GRDTOT, 00190
6R,GRAVAC,GRAVCS,GRAVCH,VALUEN,FACTUN,RMAOA,DBMAOA,A,FILMTK,YPLUS, 00200
7TAUWAL,FYPLUS,GFILY,GLQENT,PCLIQ,PCLFNT,DUMMYA,DUMMYB,DUMMYC 00210
DP=PI/1000,0 00220
DX=LOGE(1.0,0,QUALOX+1.0) 00230
COLM1=(DX)*(2.5448216-7.8896201*DP+1.5575870E+1*(DP*DP) 00240
1 -1.7340006E+1*(DP*DP*DP)+1.0409842E+1*(DP*DP*DP*DP) 00250
2 -3.2744877*(DP*DP*DP*DP*DP)+6.7484805E-1*(DP*DP*DP*DP*DP*DP) 00260
3 -1.0804871E-2*(DP*DP*DP*DP*DP*DP*DP) 00270
COLM2=(DX*DX)*(5.1756752E-1+1.9550200*DP-9.6886164E-1*(DP*DP) 00280
1 -4.6120070*(DP*DP*DP)+8.491074*(DP*DP*DP*DP) 00290
2 -5.948309*(DP*DP*DP*DP*DP)+1.8989183*(DP*DP*DP*DP*DP*DP) 00300
3 -2.284780E-1*(DP*DP*DP*DP*DP*DP*DP) 00310
COLM3=(DX*DX*DX)*(1.0199966E-1-3.7233785E-1*(DP*DP) 00320
1 -1.9025688E-1*(DP*DP*DP)+2.2654839*(DP*DP*DP) 00330
2 -2.402541*(DP*DP*DP*DP)+2.329908*(DP*DP*DP*DP*DP) 00340
3 -7.253497E-1*(DP*DP*DP*DP*DP*DP)+8.6169847E-2*(DP*DP*DP*DP*DP*DP 00350
4 *DP*DP) 00360
COLM4=(DX*DX*DX*DX)*(-8.0606798E-3+(2.6160876E-2*DP) 00370
1 +6.0288725E-2*(DP*DP)-3.2426871E-1*(DP*DP*DP) 00380
2 +4.6553847E-1*(DP*DP*DP*DP)-3.0333482E-1*(DP*DP*DP*DP*DP) 00390
3 +9.379894E-2*(DP*DP*DP*DP*DP*DP)-1.1021915E-2*(DP*DP*DP*DP*DP*DP 00400
4 *DP*DP) 00410
SUMCOL=COLM1+COLM2+COLM3+COLM4 00420
PHIMN=FXPF(SUMCOL) 00430
GTOTSC=GTOT/3600,0 00440
IF(GTOTSC=1000,0) 00450
5 GSURZ=LOGE(1.0,0036*GTOTSC+0.2) 00460
GO TO 15 00470
17 GSUR7=LOGE(1.0,0036*1000.0+0.2) 00480
15 SUM0=1.4712797-3.8229399E-5*P 00490
SUM1=(-8.9082318E-2-4.5200014E-4*P)*(GSUBZ) 00500
SUM2=(-8.2387803E-2+1.2278415E-4*P)*(GSUBZ*GSUBZ) 00510
SUM3=(3.8640886E-2+1.6165216E-4*P)*(GSUBZ*GSUBZ*GSURZ) 00520
SUM4=(2.1855741E-2-3.4296260E-5*P)*(GSUBZ*GSUBZ*GSURZ*GSUBZ) 00530
SUM5=(-6.3676796E-3-3.2820747E-5*P) 00540
1*(GSUBZ*GSUBZ*GSURZ*GSURZ*GSURZ) 00550
OMEGAP=SUM0+SUM1+SUM2+SUM3+SUM4+SUM5 00560
OMEGAP=OMEGAP,0.4 00570
PGMULT=OMEGA*PHIMN 00580
PFTUDN 00590
END 00600

SURROUTINE UNIVER 00020
COMMON NTUBES,MSHAPE,TUBE,RATIOM,DIAINS,VOLTS,AMPS,ENTHIN,FLMASS, 00030
1 PDESQ,PREFIN,PDESOT,PESDP,TSDD,ROLOCA,XLNGTH,SHUNTM,P, 00040
2 DMFFX,DMFFX,DMFFGX,DMFFGX,FMSIN,QUALIN,POWER,APFAFL,AREAIS, 00050
3 QUALOL,SATL,PSATL,POWFRP,PSI,ROL,CFXAVG,CFXLOX,JLOCAT,K,X, 00060
4 4PREFAX,POWFRX,FNLOX,ENSLX,QUALOX,DMFFY,DMFFGY,POWOO,ONFOVM, 00070
5 COSLEN,ONFMSQ,SIGNZ,ARG,Z,FACMIB,FACPLR,CFXRO,L,Y, 00080
6 FACTMI,POWERY,CFXLOY,FNLOY,FNSLOY,QUALOY,FACTPL, 00090
7 CONSTP,SCRPTL,ZETA,PLNGTH,J,U,ULOCAT,COSABK,SINABK,I, 00090
8 EXTRA,EXTRAB,EXTRAC,EXTRAD,EXTRAE,EXTRAF, 00090
9 DMFFB,DMFFGB,ENLOB,ENSLB,QUALOB,EXTRAG,EXTRAH,EXTRAJ,EXTRAJ
COMMON QUALIA,GLIO,TKINCH,
1DP,DX,COLM1,COLM2,COLM3,COLM4,SUMCOL,PHIMN,GTOTSC,GSUBZ,SUM0,SUM1,
2SUM2,SUM3,SUM4,SUM5,OMEGAP,OMEGA,PGMULT,PSUBL,T,VISCL,VOLSPL,ENO,
3VOLSPL,QUALO4,POWEP,ANROL,DFNFO,DFNFG,ENSO,QUALO,NSPLO,DVSPG,
4GTOT,DPMM,GRDMT,DVLSPL,DVLSPL,TERM1,TERM2,TERM3,TERM4,GGAS,DT,
5DVISCL,REYNUM,FFACT,FFACT,VFLC,GRDFS,DPGLT,GRDFT,DGRDMT,GRDTOT,
6R,GRAVAC,GRAVCS,GRAVCH,VALUEN,FACTUN,RMAOA,DBMAOA,A,FILMTK,YPLUS,
7TAUWAL,FYPLUS,GFILY,GLQENT,PCLIQ,PCLFNT,DUMMYA,DUMMYB,DUMMYC
IF (P=400,0) 5, 10,10
5 VOLSPL=1.6401745E-2+2.3289060E-5*P-1.5364591E-7*(P*P)

```

```

5 COSLEN,ONFMSQ,SIGNZ,ARG,Z,FACMIB,FACPLR,CFXRO,L,Y, 00070
6 FACTMI,POWERY,CFXLOY,FNLOY,FNSLOY,QUALOY,FACTPL, 00080
7 CONSTP,SCRPTL,ZETA,PLNGTH,J,U,ULOCAT,COSABK,SINABK,I, 00090
8 EXTRA,EXTRAB,EXTRAC,EXTRAD,EXTRAE,EXTRAF,
9 DMFFB,DMFFGB,ENLOB,ENSLB,QUALOB,EXTRAG,EXTRAH,EXTRAJ,EXTRAJ
COMMON QUALIA,GLIO,TKINCH,
1DP,DX,COLM1,COLM2,COLM3,COLM4,SUMCOL,PHIMN,GTOTSC,GSUBZ,SUM0,SUM1,
2SUM2,SUM3,SUM4,SUM5,OMEGAP,OMEGA,PGMULT,PSUBL,T,VISCL,VOLSPL,ENO,
3VOLSPL,QUALO4,POWEP,ANROL,DFNFO,DFNFG,ENSO,QUALO,NSPLO,DVSPG,
4GTOT,DPMM,GRDMT,DVLSPL,DVLSPL,TERM1,TERM2,TERM3,TERM4,GGAS,DT,
5DVISCL,REYNUM,FFACT,FFACT,VFLC,GRDFS,DPGLT,GRDFT,DGRDMT,GRDTOT,
6R,GRAVAC,GRAVCS,GRAVCH,VALUEN,FACTUN,RMAOA,DBMAOA,A,FILMTK,YPLUS,
7TAUWAL,FYPLUS,GFILY,GLQENT,PCLIQ,PCLFNT,DUMMYA,DUMMYB,DUMMYC 00190
FOR N=0 REFER TO FIGURE 6 GFAP4615
C FOR N=-0.333 REFER TO FIGURE 7 GFAP 4615
C IF(FACTUN=.250) 2,30,30
2 IF (VALUEN - 0.0) 7,9,7
7 IF (FACTUN-.046) 25,10,10
9 IF(FACTUN-.030) 20,5,5
5 RMAOA=+.94236102E-1-.73440465E+1*FACTUN+.18204540E+3*(FACTUN**2)
1 -1.13413306E+4*(FACTUN**3) -.55976792E+3*(FACTUN**4)
2 +.49524361E+5*(FACTUN**5) -.18569737E+6*(FACTUN**6)
3 -.56878649E+5*(FACTUN**7) +.73045481E+7*(FACTUN**8)
4 -.10236661E+8*(FACTUN**9) +.36205309E+8*(FACTUN**10)
5 -.13312636E+9*(FACTUN**11) -.44616646E+9*(FACTUN**12)
6 +.68296456E+10*(FACTUN**13) -.19259604E+11*(FACTUN**14)
7 +.12745609E+11*(FACTUN**15)
GO TO 35
10 RMAOA=.97900332E-1-.11388222E2*FACTUN+.38794992E3*(FACTUN**2)
1 -.48776956E4*(FACTUN**3)+.19313986E5*(FACTUN**4)
2 +.66295982E5*(FACTUN**5)-.12967244E6*(FACTUN**6)
3 -.53197482E7*(FACTUN**7)+.20432942E8*(FACTUN**8)
GO TO 35
20 RMAOA=.0022
GO TO 35
25 RMAOA=.0159
GO TO 35
30 RMAOA=.250
35 RFTUPN
END

SURROUTINE SPFCVL
COMMON NTUBES,MSHAPE,TUBE,RATIOM,DIAINS,VOLTS,AMPS,ENTHIN,FLMASS, 00020
1 PDESQ,PREFIN,PDESOT,PESDP,TSDD,ROLOCA,XLNGTH,SHUNTM,P, 00030
2 DMFFX,DMFFX,DMFFGX,DMFFGX,FMSIN,QUALIN,POWER,APFAFL,AREAIS, 00040
3 QUALOL,SATL,PSATL,POWFRP,PSI,ROL,CFXAVG,CFXLOX,JLOCAT,K,X, 00050
4 4PREFAX,POWFRX,FNLOX,ENSLX,QUALOX,DMFFY,DMFFGY,POWOO,ONFOVM, 00060
5 COSLEN,ONFMSQ,SIGNZ,ARG,Z,FACMIB,FACPLR,CFXRO,L,Y, 00070
6 FACTMI,POWERY,CFXLOY,FNLOY,FNSLOY,QUALOY,FACTPL, 00080
7 CONSTP,SCRPTL,ZETA,PLNGTH,J,U,ULOCAT,COSABK,SINABK,I, 00090
8 EXTRA,EXTRAB,EXTRAC,EXTRAD,EXTRAE,EXTRAF,
9 DMFFB,DMFFGB,ENLOB,ENSLB,QUALOB,EXTRAG,EXTRAH,EXTRAJ,EXTRAJ
COMMON QUALIA,GLIO,TKINCH,
1DP,DX,COLM1,COLM2,COLM3,COLM4,SUMCOL,PHIMN,GTOTSC,GSUBZ,SUM0,SUM1,
2SUM2,SUM3,SUM4,SUM5,OMEGAP,OMEGA,PGMULT,PSUBL,T,VISCL,VOLSPL,ENO,
3VOLSPL,QUALO4,POWEP,ANROL,DFNFO,DFNFG,ENSO,QUALO,NSPLO,DVSPG,
4GTOT,DPMM,GRDMT,DVLSPL,DVLSPL,TERM1,TERM2,TERM3,TERM4,GGAS,DT,
5DVISCL,REYNUM,FFACT,FFACT,VFLC,GRDFS,DPGLT,GRDFT,DGRDMT,GRDTOT,
6R,GRAVAC,GRAVCS,GRAVCH,VALUEN,FACTUN,RMAOA,DBMAOA,A,FILMTK,YPLUS,
7TAUWAL,FYPLUS,GFILY,GLQENT,PCLIQ,PCLFNT,DUMMYA,DUMMYB,DUMMYC
IF (P=400,0) 5, 10,10
5 VOLSPL=1.6401745E-2+2.3289060E-5*P-1.5364591E-7*(P*P)

```

```

1 +7.415801E-10*(D*D*D*D) -2.1604007E-10*(D*D*D*D)
2 +3.9001151E-14*(D*D*D*D*D*D) -4.318721E-14*(D*D*D*D*D*D)
3 +2.8681700E-21*(D*D*D*D*D*D*D*D) -1.0458277E-24*(D*D*D*D*D*D*D*D)
4 +1.679244E-28*(D*D*D*D*D*D*D*D*D*D)
PRTURN
10 VOLSPLE=1.7292164E-7 +5.5320054E-6*D -1.924874E-9*(D*D)
1 +5.6659056E-17*(D*D*D) -2.1537248E-17*(D*D*D*D)
PRTURN
END

```

```

SUBROUTINE SPECVC
COMMON NTUBES,MSHAP,TUBE,RAT,ION,DIAINS,VOLTS,AMPS,ENTHIN,FLMASS,
1 DPFSD,DPFSIN,DPFSOT,DPESDP,TSDD,ROLOCA,XLNGTH,SHUNTM,P,
2 DMFEF,DMFEFX,DMFEFG,DMFGPX,FNSIN,QUALIN,POWER,AREAF,AREAIS,
3 QUALOL,SATL,PSATL,POWER,PSLRPL,CFXAVG,CFXLOX,JLOCAT,K,X,
4 DRDFAK,DMFEFX,FNLOX,FNSLOX,QUALOX,DMFEY,DMFEFY,POWQO,DMFOVM,
5 COSLEN,DMFMSQ,SIGNZ,ARG,Z,FACMIR,FACPLB,CFXBO,L,Y,
6 FACMTI,DMFEY,CFXLOY,FNLOY,FNSLOY,QUALOY,FACPL,
7 CONSTP,SCPTL,ZETA,PLNGTH,J,U,ULOCAT,COSABK,SINABK,I,
8 EXTRAA,EXTRAB,EXTRAC,EXTRAD,EXTRAF,EXTRAF,
9 DMFEFB,DMFEGB,FNLOB,FNSLOB,QUALOB,EXTRAG,EXTRAH,EXTRAJ,EXTRAJ
COMMON QUALIA,GLIO,TKINCH,
10P,DX,COLM1,COLM2,COLM3,COLM4,SUMCOL,PHIMN,GTOTSC,GSUBZ,SUM0,SUM1,
2SUM2,SUM3,SUM4,SUM5,OMFGAP,OMFGA,PGMULT,PSURL,T,VISCL,VOLSPLE,ENO,
3VOLSPG,QUALO4,POWER4,PANROL,DFNFO,DFNFGO,ENSO,QUALO,DVSPLO,DVSPGO,
4GTOT,DMOM,GRDNT,DVLSPL,DVLSPG,TERM1,TERM2,TERM3,TERM4,GGAS,DT,
5DVISCL,REFNUM,FFACTP,FFACT,VELOC,GPDES,DPGMLT,GRDFT,GRDNT,GRDNT,
6GRAVAC,GRAVCS,GRAVCH,VALUEN,FACTUN,RYAOA,DBMAOA,A,FILMTK,YPLUS,
7TAUWAL,FYPLUS,GFILM,GLENT,PCLIO,PCLNT,DUMMYA,DUMMYB,DUMMYC
IF (D-200.0) 5,10,10

```

```

5 VOLSPG=7.026614E+1 -5.2270993*D +2.2026868E-1*(D*D)
1 -E.747148E-2*(D*D*D) +0.8910424E-5*(D*D*D*D)
2 -1.138220E-6*(D*D*D*D*D) +8.8808151E-9*(D*D*D*D*D*D)
3 -4.617321E-11*(D*D*D*D*D*D*D) +1.5321887E-13*(D*D*D*D*D*D*D*D)
4 -2.023474E-14*(D*D*D*D*D*D*D*D*D) +2.4643841E-10*(D*D*D*D*D*D*D*D)
5 D*D*D*D)
PRTURN
10 IF (D-400.0) 15, 20,20
15 VOLSPG=0.1051259 -7.6398584E-2*D +3.4342061E-4*(D*D)
1 -8.4904540E-7*(D*D*D) +1.1495386E-9*(D*D*D*D)
2 -4.3157880E-12*(D*D*D*D)
PRTURN
20 VOLSPG=4.220747 -1.5646152E-2*D +3.552997E-5*(D*D)
1 -4.5490977E-9*(D*D*D) +3.613935E-11*(D*D*D*D)
2 -1.7182114E-14*(D*D*D*D*D) +4.4080400E-18*(D*D*D*D*D*D)
3 -4.0690904E-22*(D*D*D*D*D*D*D)
PRTURN
END

```

```

SUBROUTINE SATTM
LIMITS ON THE APPLICATION OF THIS SUBROUTINE ARE ABOVE .2PSIA
AND BELOW 3276.8 PSIA
COMMON NTUBES,MSHAP,TUBE,RAT,ION,DIAINS,VOLTS,AMPS,ENTHIN,FLMASS,
1 DPFSD,DPFSIN,DPFSOT,DPESDP,TSDD,ROLOCA,XLNGTH,SHUNTM,P,
2 DMFEF,DMFEFX,DMFEFG,DMFGPX,FNSIN,QUALIN,POWER,AREAF,AREAIS,
3 QUALOL,SATL,PSATL,POWER,PSLRPL,CFXAVG,CFXLOX,JLOCAT,K,X,
4 DRDFAK,DMFEFX,FNLOX,FNSLOX,QUALOX,DMFEY,DMFEFY,POWQO,DMFOVM,
5 COSLEN,DMFMSQ,SIGNZ,ARG,Z,FACMIR,FACPLB,CFXBO,L,Y,
6 FACMTI,DMFEY,CFXLOY,FNLOY,FNSLOY,QUALOY,FACPL,

```

```

00020
00030
00040
00050
00060
00070
00080

```

```

7CONSTP,SCPTL,ZETA,PLNGTH,J,U,ULOCAT,COSABK,SINABK,I,
8 EXTRAA,EXTRAB,EXTRAC,EXTRAD,EXTRAF,EXTRAF,
9 DMFEFB,DMFEGB,FNLOB,FNSLOB,QUALOB,EXTRAG,EXTRAH,EXTRAJ,EXTRAJ
COMMON QUALIA,GLIO,TKINCH,
10P,DX,COLM1,COLM2,COLM3,COLM4,SUMCOL,PHIMN,GTOTSC,GSUBZ,SUM0,SUM1,
2SUM2,SUM3,SUM4,SUM5,OMFGAP,OMFGA,PGMULT,PSURL,T,VISCL,VOLSPLE,ENO,
3VOLSPG,QUALO4,POWER4,PANROL,DFNFO,DFNFGO,ENSO,QUALO,DVSPLO,DVSPGO,
4GTOT,DMOM,GRDNT,DVLSPL,DVLSPG,TERM1,TERM2,TERM3,TERM4,GGAS,DT,
5DVISCL,REFNUM,FFACTP,FFACT,VELOC,GPDES,DPGMLT,GRDFT,GRDNT,GRDNT,
6GRAVAC,GRAVCS,GRAVCH,VALUEN,FACTUN,RYAOA,DBMAOA,A,FILMTK,YPLUS,
7TAUWAL,FYPLUS,GFILM,GLENT,PCLIO,PCLNT,DUMMYA,DUMMYB,DUMMYC
10 IF (D-450.0) 15,20,20
15 PSURL=LOGF(10.0*D)
T=3.5157890E+1 +2.4592588E+1*PSURL +2.1182069*(PSURL**2)
1 -3.4144740E-1*(PSURL**3) +1.5741642E-1*(PSURL**4)
2 -3.1329585E-2*(PSURL**5) +3.8658282E-3*(PSURL**6)
3 -2.4001784E-4*(PSURL**7) +6.8401540E-6*(PSURL**8)
PRTURN
20 PSURL=LOGF(D)
T=+1.1545164E+4 -8.3860197E+3*PSURL +2.4777661E+9*(PSURL**2)
1 -3.6344271E+7*(PSURL**3) +2.6690978E+1*(PSURL**4)
2 -7.8073813E-1*(PSURL**5)
PRTURN
END

```

```

SUBROUTINE VISCOS
COMMON NTUBES,MSHAP,TUBE,RAT,ION,DIAINS,VOLTS,AMPS,ENTHIN,FLMASS,
1 DPFSD,DPFSIN,DPFSOT,DPESDP,TSDD,ROLOCA,XLNGTH,SHUNTM,P,
2 DMFEF,DMFEFX,DMFEFG,DMFGPX,FNSIN,QUALIN,POWER,AREAF,AREAIS,
3 QUALOL,SATL,PSATL,POWER,PSLRPL,CFXAVG,CFXLOX,JLOCAT,K,X,
4 DRDFAK,DMFEFX,FNLOX,FNSLOX,QUALOX,DMFEY,DMFEFY,POWQO,DMFOVM,
5 COSLEN,DMFMSQ,SIGNZ,ARG,Z,FACMIR,FACPLB,CFXBO,L,Y,
6 FACMTI,DMFEY,CFXLOY,FNLOY,FNSLOY,QUALOY,FACPL,
7 CONSTP,SCPTL,ZETA,PLNGTH,J,U,ULOCAT,COSABK,SINABK,I,
8 EXTRAA,EXTRAB,EXTRAC,EXTRAD,EXTRAF,EXTRAF,
9 DMFEFB,DMFEGB,FNLOB,FNSLOB,QUALOB,EXTRAG,EXTRAH,EXTRAJ,EXTRAJ
COMMON QUALIA,GLIO,TKINCH,
10P,DX,COLM1,COLM2,COLM3,COLM4,SUMCOL,PHIMN,GTOTSC,GSUBZ,SUM0,SUM1,
2SUM2,SUM3,SUM4,SUM5,OMFGAP,OMFGA,PGMULT,PSURL,T,VISCL,VOLSPLE,ENO,
3VOLSPG,QUALO4,POWER4,PANROL,DFNFO,DFNFGO,ENSO,QUALO,DVSPLO,DVSPGO,
4GTOT,DMOM,GRDNT,DVLSPL,DVLSPG,TERM1,TERM2,TERM3,TERM4,GGAS,DT,
5DVISCL,REFNUM,FFACTP,FFACT,VELOC,GPDES,DPGMLT,GRDFT,GRDNT,GRDNT,
6GRAVAC,GRAVCS,GRAVCH,VALUEN,FACTUN,RYAOA,DBMAOA,A,FILMTK,YPLUS,
7TAUWAL,FYPLUS,GFILM,GLENT,PCLIO,PCLNT,DUMMYA,DUMMYB,DUMMYC
CALL SATTM
IF (T-600.0) 5,5,10
5 CONTINUE
VISCL=8.0144599 -1.6728317E-1*T +2.0423535E-3*(T*T)
1 -1.6324668E-5*(T*T*T) +8.8555744E-8*(T*T*T*T)
2 -3.301594E-10*(T*T*T*T*T) +8.4382483E-13*(T*T*T*T*T*T)
3 -1.4493840E-15*(T*T*T*T*T*T*T) +1.5963800E-18*(T*T*T*T*T*T*T*T)
4 -1.0173273E-21*(T*T*T*T*T*T*T*T*T)
5 +2.8496174E-25*(T*T*T*T*T*T*T*T*T*T)
PRTURN
10 IF (T-642.5) 15,20,20
20 IF (T-675.0) 25,30,30
30 IF (T-690.0) 35,35,40
15 VISCL=5100-.00050*T
PRTURN
25 VISCL=.6310-.00069*T
PRTURN
35 VISCL=.9985-.00123*T

```

```

00010
00020
00030
00040
00050
00060
00070
00080
00090
00100
00110
00120
00130
00140
00150
00160
00170
00180
00190
00200
00210
00220
00230
00240
00250
00260
00270
00280
00290
00300
00310
00320
00330
00340
00350

```

```

RETURN
VISCL=,1480
RETURN
END

SUBROUTINE EVADEN
COMMON NTUBES,MSHAPE,TUBE,RATION,DIAINS,VOLTS,AMPS,ENTHIN,FLMASS,
1 PDES,PFESIN,PRESOT,PRESDP,TSDD,BOLUCA,XLNGLTH,SHUNTM,P,
2 DMEFX,ENFDX,DMFFGX,ENFGPX,FNSIN,QUALIN,POWER,AREAF,AREFIS,
3 QUALOL,SATL,PSATL,POWERB,PSLROL,CFXAVG,CFXLOX,JLOCAT,K,X,
4 DBREAK,POWERX,ENLOX,ENSLGX,QUALGX,DMFFY,DMFFGY,POWOO,DFEOMV,
5 COSLEN,OMESON,SIGNZ,ARGZ,FACMI,FACEB,CFXR,LY,
6 FACTM,POWERY,CFXLOY,FNLOY,ENSLGY,QUALGY,FACTPL,
7 CONSTD,SCOOTL,ZETA,PLNGTH,J,U,JLOCAT,COSABK,SINABK,I,
8 EXTOAA,EXTDAB,EXTRAC,EXTDAD,EXTRAF,EXTRAF,
9 DMFFB,DMFFCB,ENLOB,ENSLOB,QUALOB,EXTRAG,EXTRAH,EXTRAJ,EXTRAJ
COMMON QUALIA,GLIO,TKINCH,
1DP,DX,COLM1,COLM2,COLM3,COLM4,SUMCOL,PHIMN,GTOTSC,GSURZ,SUMO,SUM1,
2SUM2,SUM3,SUM4,SUM5,OMEGAP,OMEGA,PGMULT,PSUBL,T,VISCL,VOLSPL,ENO,
3VOLSPL,QUALO4,POWER4,PANROL,DFENFO,DFENFGO,ENSO,QUALO,DVSPLD,DVSPGO,
4GTOT,DPMON,GRDMT,DVLSPL,DVLSPL,TERM1,TERM2,TERM3,TERM4,GGAS,DT,
5DVISCL,PFYNUM,FFACTD,FFACT,VELOC,GRDFS,DRDMLT,GRDFT,DRDMT,GRDGT,
6R,GRAVAC,GRAVCS,GRAVCH,VALUEN,FACTUN,BMADA,DBMADA,A,FILMTK,YPLUS,
7TAUWAL,FYPLUS,GFILM,GLENT,PCLIO,PCLENT,DUMMYA,DUMMYB,DUMMYC
COMMON N,M,THCOND,FCHEN,SCHEN,VISCG,CPLIO,SURFTL,
1XTT,SATP,SMALLT,DELTV,THALL,HCHEN,HMAC,HMIC,PFYNLO,NFLUX,
2 DPNUM,PRDGH,HDR,HDENG,ADENG,DTDENG,DELTT,QACHEN,
3 DTCHEN,PDNMAX,DELTFN,RADIUS,CC,DD,FF
IF(D=200,?) 5,5,10
ENFGPX=9.970467E2 -2.1762821*P +1.9558701E-2*(P**2)
1 -1.2610018E-4*(P**3) +5.0208804E-7*(P**4) -1.2499843E-9*(P**5)
2 +1.9922768E-12*(P**6) -1.8022251E-15*(P**7)
3 +0.2680009E-19*(P**8) -2.0148442E-22*(P**9)
RETURN
END

1 ENFGPX=R.9642772E-3,3549732E-1*P+1.2678091E-4*(P**2)
1 -4.2616487E-8*(P**3)+4.8788247E-12*(P**4)
RETURN
END

```

```

00360
00370
00380
00390
SUBROUTINE LIQEN
COMMON NTUBES,MSHAPE,TUBE,RATION,DIAINS,VOLTS,AMPS,ENTHIN,FLMASS,
1 PDES,PFESIN,PRESOT,PRESDP,TSDD,BOLUCA,XLNGLTH,SHUNTM,P,
2 DMEFX,ENFDX,DMFFGX,ENFGPX,FNSIN,QUALIN,POWER,AREAF,AREFIS,
3 QUALOL,SATL,PSATL,POWERB,PSLROL,CFXAVG,CFXLOX,JLOCAT,K,X,
4 DBREAK,POWERX,ENLOX,ENSLGX,QUALGX,DMFFY,DMFFGY,POWOO,DFEOMV,
5 COSLEN,OMESON,SIGNZ,ARGZ,FACMI,FACEB,CFXR,LY,
6 FACTM,POWERY,CFXLOY,FNLOY,ENSLGY,QUALGY,FACTPL,
7 CONSTD,SCOOTL,ZETA,PLNGTH,J,U,JLOCAT,COSABK,SINABK,I,
8 EXTOAA,EXTDAB,EXTRAC,EXTDAD,EXTRAF,EXTRAF,
9 DMFFB,DMFFCB,ENLOB,ENSLOB,QUALOB,EXTRAG,EXTRAH,EXTRAJ,EXTRAJ
COMMON QUALIA,GLIO,TKINCH,
1DP,DX,COLM1,COLM2,COLM3,COLM4,SUMCOL,PHIMN,GTOTSC,GSUBZ,SUMO,SUM1,
2SUM2,SUM3,SUM4,SUM5,OMEGAP,OMEGA,PGMULT,PSUBL,T,VISCL,VOLSPL,ENO,
3VOLSPL,QUALO4,POWER4,PANROL,DFENFO,DFENFGO,ENSO,QUALO,DVSPLD,DVSPGO,
4GTOT,DPMON,GRDMT,DVLSPL,DVLSPL,TERM1,TERM2,TERM3,TERM4,GGAS,DT,
5DVISCL,PFYNUM,FFACTD,FFACT,VELOC,GRDFS,DRDMLT,GRDFT,DRDMT,GRDGT,
6R,GRAVAC,GRAVCS,GRAVCH,VALUEN,FACTUN,BMADA,DBMADA,A,FILMTK,YPLUS,
7TAUWAL,FYPLUS,GFILM,GLENT,PCLIO,PCLENT,DUMMYA,DUMMYB,DUMMYC
COMMON N,M,THCOND,FCHEN,SCHEN,VISCG,CPLIO,SURFTL,
1XTT,SATP,SMALLT,DELTV,THALL,HCHEN,HMAC,HMIC,PFYNLO,NFLUX,
2 DPNUM,PRDGH,HDR,HDENG,ADENG,DTDENG,DELTT,QACHEN,
3 DTCHEN,PDNMAX,DELTFN,RADIUS,CC,DD,FF
IF(D=200,?) 5,5,10
ENFDX = 1.1222734E2 + 6.2204700*P -1.4742752E-1*(P**2)
1 +2.5403592E-3 *(P**3) -2.8788220E-5*(P**4) +2.1239014E-7*(P**5)
2 -1.0067508E-9*(P**6) +2.9480958E-12*(P**7)
3 -4.8430355E-15*(P**8) +2.4075927E-18*(P**9)
RETURN
10 ENFDX = 2.4510585E2 +7.1675967E-1*P -9.9955201E-4*(P**2)
1 +1.0516707E-6*(P**3) -6.8660980E-10*(P**4) +2.6573456E-13*(P**5)
2 -5.5654666E-17*(P**6) +4.8594220E-21*(P**7)
RETURN
END
TOTAL 0034

```

150

APPENDIX F
 TABULATION OF THE DATA

Flux Shape*	Test Section	M Value/ Critical Location (In. from Inlet)	D_{IN} (Inches) / \pm Variation in Critical Loc. (Inches)	L (Inches) / P_c (psia)	W (lb/hr) / X_o	P_{IN} (psia) / $(q/A)_c$ (BTU/hr ft ²)	P_{EXIT} (psia) / Q_{crit} (BTU/hr)	ΔP_{TS} (psi) / X_{exit}	H_{INLET} (BTU/LEM) / ΔH_{ANN-C} (BTU/LEM)	ΔH_{INLET} (BTU/LEM) / $(q/A)_c / (q/A)_1$ based on h_{tp} DENG	M at spike / $(q/A)_c / (q/A)_1$ based on h_{tp} CHEN	L' spike (In.) / Second Failure Loc. (In. from Inlet)	$(L - \bar{x})$ spike (In. from Inlet) / \pm Variation of Third Failure Location (Inches)
1	109.0	1.00 29.5	.214 .1	30.0 105.6	121.0 .568	130.0 .616E 06	105.0 .8628E 05	25.0 .582	104.2 417.4	-214.5 5.4	11.7	C.	0.
1	137.0	1.00 29.5	.211 .2	30.0 110.5	121.5 .537	127.0 .645E 06	110.0 .8905E 05	17.0 .552	59.8 393.9	-257.1 6.2	13.0	C.	0.
1	136.0	1.00 29.6	.211 .1	30.0 100.4	122.0 .557	120.0 .576E 06	100.0 .7973E 05	20.0 .568	149.1 412.0	-163.3 4.6	9.8	C.	0.
1	116.0	1.00 29.5	.212 0.	30.0 117.4	125.0 .593	135.0 .600E 06	117.0 .8328E 05	18.0 .606	177.3 441.4	-144.5 5.0	11.9	C.	0.
1	138.0	1.00 29.9	.211 0.	30.0 88.1	122.0 .597	110.0 .547E 06	88.0 .7570E 05	22.0 .599	205.0 447.8	-100.7 3.2	7.3	C.	0.
1	115.0	1.00 29.5	.211 .2	30.0 107.4	124.0 .555	127.0 .522E 06	107.0 .7207E 05	20.0 .566	223.1 408.1	-93.8 4.4	9.5	C.	0.
1	117.0	1.00 29.7	.210 .1	30.0 112.3	120.0 .603	132.0 .518E 06	112.0 .7124E 05	20.0 .611	252.4 449.4	-67.6 4.1	9.8	C.	0.
2	205.0	2.27 19.6	.214 .6	30.0 112.1	125.0 .183	115.0 .608E 06	105.0 .7283E 05	10.0 .394	68.4 89.2	-240.7 25.4	40.4	C.	0.
2	206.0	2.27 23.5	.214 .3	30.0 110.0	125.0 .363	119.0 .514E 06	106.0 .7188E 05	19.0 .477	149.9 245.3	-161.9 9.3	15.3	C.	0.
2	208.0	2.27 26.9	.214 .6	30.0 87.5	125.0 .512	103.0 .410E 06	85.0 .7300E 05	18.0 .558	203.4 376.7	-97.3 3.3	6.2	0.	0.
2	207.0	2.27 29.5	.214 .1	30.0 98.4	125.6 .632	118.0 .327E 06	98.0 .7764E 05	20.0 .639	247.2 477.9	-63.9 2.0	4.9	C.	0.

2	337.0	4.03 29.4	.211 .2	30.0 92.7	121.5 .602	111.0 .276E 06	92.0 .9355E 05	19.0 .609	65.8 453.1	-240.6 1.7	3.9	0.	0.
2	313.0	4.03 29.5	.211 .2	30.0 94.6	121.5 .614	116.0 .259E 06	94.0 .9019E 05	22.0 .620	104.2 462.5	-205.6 1.6	3.7	20.5	0.
2	339.0	4.03 27.2	.213 .2	30.0 92.2	124.4 .553	111.0 .387E 06	89.0 .8254E 05	22.0 .590	153.8 409.5	-152.6 2.8	5.9	0.	0.
2	314.0	4.03 29.3	.210 .2	30.0 92.7	120.0 .631	112.0 .254E 06	92.0 .8233E 05	20.0 .639	176.9 478.5	-130.2 1.4	3.5	27.9	.4
2	340.0	4.03 28.9	.213 0.	30.0 95.9	123.8 .624	113.0 .271E 06	95.0 .8138E 05	18.0 .636	203.5 473.8	-104.3 1.6	4.0	0.	0.
2	324.0	4.03 28.9	.211 .2	30.0 96.0	122.0 .618	115.0 .259E 06	95.0 .7709E 05	20.0 .629	223.5 466.3	-85.6 1.4	3.8	27.4	.1
2	325.0	4.03 29.1	.211 .3	30.0 93.8	121.5 .629	114.0 .236E 06	93.0 .7384E 05	21.0 .637	254.0 476.6	-54.4 1.3	3.3	0.	0.
2	510.0	5.75 19.9	.214 .2	30.0 97.2	125.6 .304	104.0 .775E 06	86.0 .8549E 05	18.0 .622	74.3 194.3	-227.1 15.1	23.4	20.9	0.
2	511.0	5.75 24.3	.214 .2	30.0 104.8	125.6 .417	115.0 .487E 06	100.0 .7404E 05	15.0 .496	149.9 292.6	-159.2 6.8	11.7	0.	0.
2	512.0	5.75 22.6	.215 .2	30.0 100.5	126.3 .337	108.0 .526E 06	95.0 .6837E 05	13.0 .445	149.9 223.8	-154.4 9.3	14.9	0.	0.
2	513.0	5.75 20.1	.214 1.1	30.0 104.2	125.0 .425	115.0 .557E 06	95.0 .8152E 05	20.0 .626	200.4 298.2	-108.7 9.9	17.2	0.	0.
2	514.0	5.75 23.2	.214 .4	30.0 91.4	125.6 .460	105.0 .542E 06	85.0 .7398E 05	20.0 .563	202.3 330.5	-59.8 5.5	9.7	0.	0.
2	515.0	5.75 26.1	.214 .2	30.0 98.2	125.6 .601	115.0 .401E 06	95.0 .7748E 05	20.0 .647	254.6 453.1	-54.5 2.7	6.2	0.	0.
3	1202.0	2.27 29.7	.214 .1	30.0 111.2	125.0 .336	117.0 .673E 06	111.0 .6829E 05	6.0 .345	64.1 221.7	-246.3 13.7	22.2	0.	0.
3	1208.0	2.27 29.7	.214 .1	30.0 97.2	125.0 .419	107.0 .650E 06	97.0 .6593E 05	10.0 .428	149.5 295.4	-154.1 8.1	13.9	0.	0.
3	1209.0	2.27 29.9	.215 0.	30.0 100.1	126.3 .523	115.0 .659E 06	100.0 .7095E 05	15.0 .526	203.5 383.7	-105.6 6.3	12.4	0.	0.
3	1210.0	2.27 29.7	.214 .2	30.0 95.2	125.0 .583	113.0 .659E 06	95.0 .7091E 05	18.0 .592	254.7 437.5	-53.1 4.8	10.6	0.	0.
4	1260.0	2.27 29.6	.214 .2	30.0 97.3	125.0 .615	116.0 .430E 06	97.0 .9693E 05	19.0 .622	74.4 463.9	-235.4 2.7	6.5	0.	0.
4	1259.0	2.27 29.5	.214 .2	30.0 97.5	125.0 .619	118.0 .355E 06	97.0 .8834E 05	21.0 .629	149.1 467.1	-162.0 2.4	5.9	0.	0.
4	1258.0	2.27 29.7	.214 0.	30.0 103.3	125.0 .671	125.0 .359E 06	103.0 .8714E 05	22.0 .876	202.7 510.1	-112.9 2.1	6.0	0.	0.
4	1257.0	2.27	.214	30.0	125.0	120.0	98.0	22.0	257.6	-54.8			

	29.7	0.	98.2	.668	.353E 06	.7973E 05	.673	508.4	1.8	5.1	C.	C.	
3	1501.0	5.75 29.6	.213 .3	30.C 96.4	123.8 .27C	100.0 .714E 06	95.8 .5905E 05	5.0 .202	69.2 166.2	-229.3 15.9	24.2	C.	C.
3	1503.0	5.75 29.8	.214 0.	30.C 101.2	125.0 .398	110.0 .773E 06	101.0 .6386E 05	9.0 .405	147.9 277.5	-157.8 11.0	18.5	C.	C.
3	1504.0	5.75 29.8	.214 .1	30.0 93.2	125.0 .563	109.0 .9C1E 06	93.0 .7451E 05	16.0 .571	206.5 421.4	-58.5 6.5	13.7	C.	C.
3	1505.0	5.75 29.5	.215 .4	30.C 103.4	126.3 .490	117.C .749E 06	103.0 .6284E 05	14.0 .508	253.2 356.4	-57.3 7.9	15.0	C.	C.
4	1560.0	5.75 17.0	.215 .5	30.C 107.3	126.3 .372	116.0 .617E 06	96.0 .9574E 05	20.0 .601	72.3 252.1	-237.5 10.4	17.3	C.	0.
4	1550.0	5.75 28.3	.213 .4	30.C 96.4	123.8 .629	116.0 .240E 06	95.0 .8893E 05	21.0 .645	151.0 476.1	-158.8 1.4	3.5	C.	0.
4	1551.0	5.75 28.8	.214 .5	30.C 103.C	125.C .675	124.0 .221E 06	102.0 .8775E 05	22.0 .685	206.1 513.8	-108.9 1.2	3.4	0.	C.
4	1552.0	5.75 28.3	.214 .3	30.C 103.4	125.C .675	124.0 .223E 06	102.0 .8245E 05	22.0 .691	253.2 515.5	-61.8 1.2	3.4	C.	C.
5	2502.0	5.75 9.8	.215 .2	30.C 108.5	126.3 .122	110.0 .110E 06	91.0 .9059E 05	19.0 .560	73.9 36.5	-231.8 67.1	112.4	C.	C.
5	2503.0	5.75 28.1	.213 .5	30.C 100.6	123.8 .677	120.0 .242E 06	99.0 .8813E 05	21.0 .696	204.2 517.8	-108.2 1.3	3.8	C.	C.
6	2552.0	5.75 25.1	.214 .3	30.0 103.9	125.0 .310	109.0 .916E 06	98.0 .7705E 05	11.0 .435	67.6 200.5	-237.4 18.9	29.8	C.	C.
6	2553.0	5.75 28.0	.214 .3	30.0 95.0	125.C .602	112.0 .572E 06	93.0 .8179E 05	19.0 .635	205.4 454.8	-101.7 3.7	8.3	C.	C.
1	132.0	1.00 29.8	.213 .2	30.C 70.C	248.8 .408	127.0 .103E 07	67.0 .1435E 06	58.0 .414	70.6 260.8	-246.3 3.1	4.9	29.528.500	
1	129.0	1.00 29.5	.213 0.	30.C 68.8	247.5 .374	123.0 .9C1E 06	67.0 .1257E 06	56.C .385	112.0 231.6	-202.4 3.C	4.8	C.	0.
1	139.0	1.00 29.8	.210 .1	30.0 64.9	241.5 .423	129.0 .9C4E 06	64.0 .1245E 06	65.0 .439	150.7 279.4	-167.4 2.3	3.6	C.	C.
1	140.0	1.00 29.8	.210 0.	30.C 63.6	241.5 .429	128.0 .757E 06	63.0 .1099E 06	65.0 .433	205.7 275.6	-111.8 7.C	3.2	0.	C.
1	131.0	1.00 29.5	.210 0.	30.C 68.3	241.5 .456	132.0 .758E 06	67.0 .1044E 06	65.0 .465	260.6 300.7	-59.4 1.9	3.1	C.	C.
2	201.0	2.27 22.3	.213 .3	30.C 98.1	247.5 .237	123.0 .106E 07	63.0 .1385E 06	60.0 .493	68.4 128.1	-246.C 9.6	14.7	C.	C.
2	209.0	2.27 23.3	.214 .2	30.0 97.6	250.C .35C	132.0 .101E 07	77.0 .1392E 06	55.0 .474	150.7 221.0	-169.3 5.6	9.C	C.	C.
2	210.0	2.27 29.6	.214 .1	30.C 70.3	250.C .492	135.0 .530E 06	69.0 .1297E 06	66.0 .497	204.2 331.2	-117.C 1.2	2.1	C.	C.
2	211.0	2.27 29.5	.214 0.	30.C 68.5	250.C .487	135.0 .464E 06	67.0 .1162E 06	68.0 .493	252.6 326.5	-69.2 1.1	1.9	C.	C.
2	310.0	4.03 24.0	.211 0.	30.C 93.7	244.C .322	128.0 .952E 06	67.0 .1435E 06	61.0 .428	71.0 196.0	-246.5 5.8	9.1	C.	C.
2	333.0	4.03 27.6	.210 .4	30.0 76.0	241.5 .45C	131.0 .664E 06	65.0 .1538E 06	66.0 .485	72.5 299.0	-246.9 7.C	3.3	C.	C.

2	308.0	4.03 25.8	.211 .2	30.0 85.3	243.0 .405	133.0 .837E 06	67.0 .1451E 06	66.0 .472	101.3 261.8	-219.3 3.2	5.3	C.	C.
2	331.0	4.03 26.0	.211 .2	30.0 82.3	243.0 .435	137.0 .769E 06	66.0 .1375E 06	71.0 .494	151.8 283.4	-171.2 2.5	4.3	C.	C.
2	311.0	4.03 28.0	.210 0.	30.0 76.4	240.0 .476	137.0 .540E 06	69.0 .1317E 06	68.0 .500	176.5 319.7	-146.5 1.4	2.5	C.	C.
2	332.0	4.03 28.9	.213 .2	30.0 70.9	247.5 .473	136.0 .415E 06	67.0 .1247E 06	69.0 .484	205.5 313.7	-116.9 1.0	1.7	C.	C.
2	336.0	4.03 29.5	.213 .3	30.0 68.5	248.8 .472	135.0 .315E 06	67.0 .1112E 06	68.0 .476	255.4 312.2	-66.4 .7	1.3	C.	C.
2	309.0	4.03 28.0	.212 .1	30.0 71.9	246.3 .450	134.0 .432E 06	66.0 .1065E 06	68.0 .469	262.5 296.1	-58.7 1.2	1.9	27.5	2
2	501.0	5.75 22.6	.212 .6	30.0 97.0	245.0 .290	125.0 .110E 07	64.0 .1418E 06	61.0 .424	73.9 172.1	-241.7 7.7	12.0	C.	C.
2	507.0	5.75 22.1	.214 .7	30.0 96.4	251.3 .335	132.0 .109E 07	65.0 .1373E 06	66.0 .472	150.7 207.3	-169.3 6.4	10.1	C.	C.
2	504.0	5.75 22.4	.214 .2	30.0 95.3	251.3 .381	135.0 .102E 07	70.0 .1311E 06	65.0 .500	204.6 245.9	-117.2 4.9	8.1	C.	C.
2	508.0	5.75 29.0	.214 .3	30.0 71.1	250.0 .515	138.0 .328E 06	68.0 .1226E 06	70.0 .523	255.1 350.6	-68.5 .7	1.3	C.	C.
3	1204.0	2.27 29.3	.213 .5	30.0 64.9	248.8 .382	120.0 .117E 07	62.0 .1189E 06	58.0 .402	153.0 239.5	-159.4 3.5	5.4	C.	C.
3	1205.0	2.27 29.8	.214 .1	30.0 75.6	250.0 .410	125.0 .111E 07	75.0 .1122E 06	50.0 .415	203.9 267.6	-111.7 3.6	5.8	C.	C.
3	1207.0	2.27 29.9	.214 0.	30.0 65.3	250.0 .461	132.0 .108E 07	65.0 .1090E 06	67.0 .464	253.9 304.4	-66.1 2.5	4.1	C.	C.
4	1271.0	2.27 26.4	.214 1.4	30.0 78.6	250.0 .380	130.0 .757E 06	66.0 .1505E 06	64.0 .442	68.9 238.8	-249.8 2.9	4.6	C.	C.
4	1252.0	2.27 25.5	.214 1.0	30.0 81.7	250.0 .379	131.0 .759E 06	66.0 .1536E 06	65.0 .459	71.9 238.7	-247.5 3.2	5.1	C.	C.
4	1253.0	2.27 29.9	.214 0.	30.0 65.3	250.0 .447	135.0 .576E 06	65.0 .1313E 06	70.0 .449	151.0 287.9	-170.8 1.4	2.3	C.	C.
4	1254.0	2.27 29.8	.214 0.	30.0 63.8	250.0 .501	138.0 .576E 06	63.0 .1306E 06	75.0 .505	205.5 333.1	-120.1 1.1	2.0	C.	C.
4	1255.0	2.27 29.8	.214 0.	30.0 70.5	250.0 .508	140.0 .530E 06	70.0 .1203E 06	70.0 .510	254.3 343.3	-70.5 1.1	2.1	C.	C.
3	1502.0	5.75 29.5	.213 .3	30.0 70.0	248.8 .285	102.0 .141E 07	57.0 .1179E 06	45.0 .302	71.8 166.3	-228.2 6.8	9.9	C.	C.
3	1507.0	5.75 29.8	.214 .1	30.0 59.4	250.0 .326	105.0 .126E 07	58.0 .1040E 06	47.0 .334	149.8 193.5	-152.3 4.2	6.1	C.	C.
3	1508.0	5.75	.214	30.0	250.0	123.0	64.0	59.0	206.5	-107.9			

7-17-72

-173-

		29.7	0.	65.2	.425	.138E 07	.1141E 06	.435	277.1	3.6	5.7	C.	C.
3	1509.0	5.75 29.7	.213 .1	30.0 64.0	248.8 .42C	125.0 .121E 07	63.0 .1005E 06	62.0 .428	252.0 270.4	-63.6 3.2	5.0	C.	C.
4	1553.0	5.75 11.8	.214 1.6	30.0 121.4	250.0 .096	129.0 .119E 07	64.0 .1450E 06	65.0 .423	71.9 12.4	-246.2 36.2	61.5	C.	C.
4	1554.0	5.75 29.2	.214 .4	30.0 69.5	250.0 .506	140.0 .349E 06	67.0 .1453E 06	73.0 .513	150.3 339.4	-174.5 .7	1.3	C.	C.
4	1555.0	5.75 28.2	.213 .1	30.0 73.3	248.8 .489	140.0 .359E 06	68.0 .1311E 06	72.0 .505	202.4 326.7	-122.4 .9	1.5	C.	C.
4	1556.0	5.75 28.6	.213 .5	30.0 70.8	248.8 .489	140.0 .307E 06	67.0 .1166E 06	73.0 .500	255.1 324.9	-69.7 .7	1.2	C.	C.
5	2504.0	5.75 11.8	.215 .5	30.0 115.6	252.5 .066	120.0 .124E 07	62.0 .1320E 06	58.0 .359	69.3 -12.4	-243.1 50.1	84.0	C.	C.
5	2506.0	5.75 29.3	.213 .3	30.0 70.2	247.5 .500	140.0 .325E 06	68.0 .1292E 06	72.0 .506	208.7 334.4	-116.1 .7	1.3	C.	C.
6	2551.0	5.75 24.2	.215 .3	30.0 146.3	252.5 .139	153.0 .152E 07	131.0 .1198E 06	22.0 .268	81.7 47.9	-250.5 40.8	72.4	C.	C.
6	2556.0	5.75 24.4	.213 .3	30.0 88.6	247.5 .347	127.0 .158E 01	65.0 .1241E 06	62.0 .480	203.4 214.8	-113.5 8.0	12.6	C.	C.
1	142.0	1.00 29.8	.209 0.	30.0 128.3	478.0 .210	192.0 .148E 07	105.0 .2029E 06	87.0 .215	80.5 92.9	-271.2 7.3	11.9	C.	C.
1	135.0	1.00 29.6	.210 0.	30.0 112.3	480.0 .264	193.0 .162E 07	106.0 .2232E 06	87.0 .275	81.4 128.5	-270.8 5.2	8.3	C.	C.
1	130.0	1.00 29.5	.212 .5	30.0 115.9	492.5 .268	195.0 .142E 07	112.0 .1981E 06	83.0 .278	149.9 132.4	-203.2 4.7	7.5	C.	C.
1	141.0	1.00 29.8	.210 0.	30.0 111.8	483.0 .316	217.0 .134E 07	110.0 .1848E 06	107.0 .321	206.3 164.2	-156.6 3.4	5.6	C.	C.
1	133.0	1.00 29.4	.213 .4	30.0 123.1	495.0 .320	217.0 .124E 07	120.0 .1724E 06	97.0 .329	253.4 172.2	-109.5 3.5	5.8	27.515.0	
2	213.0	2.27 21.6	.214 .5	30.0 166.6	500.0 .087	185.0 .168E 07	108.0 .2150E 06	77.0 .240	86.4 4.5	-262.1 28.6	50.1	C.	C.
2	212.0	2.27 26.9	.214 .4	30.0 146.3	500.0 .233	215.0 .116E 07	115.0 .2065E 06	100.0 .284	146.1 108.5	-216.0 6.0	10.1	C.	C.
2	202.0	2.27 27.9	.212 .9	30.0 130.1	490.0 .320	223.0 .104E 07	115.0 .2017E 06	108.0 .349	205.2 171.6	-160.1 3.2	5.3	C.	C.
2	203.0	2.27 23.1	.213 .1	30.0 153.7	495.0 .242	217.0 .128E 07	113.0 .1751E 06	104.0 .339	253.2 117.9	-109.7 6.8	11.5	C.	C.
2	329.0	4.03 25.9	.212 .4	30.0 150.6	490.0 .221	197.0 .132E 07	108.0 .2344E 06	89.0 .288	80.5 105.7	-273.5 7.5	12.8	C.	C.
2	330.0	4.03 22.0	.212 .1	30.0 173.4	493.5 .181	207.0 .172E 07	114.0 .2154E 06	93.0 .315	149.3 77.4	-209.5 14.7	26.0	25.8	.6

174

2	327.0	4.03 25.1	.213 .4	30.0 148.6	495.0 .277	215.0 .124E 07	115.0 .2013E 06	100.0 .341	202.8 144.5	-159.3 5.3	9.1	0.	0.
2	328.0	4.03 23.9	.212 .3	30.0 153.8	490.0 .274	225.0 .124E 07	115.0 .1778E 06	110.0 .351	255.5 141.4	-110.6 5.6	9.6	0.	0.
2	506.0	5.75 16.3	.215 .1	30.0 155.0	505.0 -0.059	155.0 .159E 07	95.0 .1984E 06	60.0 .170	62.5 0.	-270.8 0.	0.	0.	0.
2	516.0	5.75 22.5	.214 .4	30.0 156.1	502.5 .117	178.0 .166E 07	105.0 .2150E 06	73.0 .233	80.9 27.8	-264.2 19.5	36.6	0.	0.
2	505.0	5.75 21.8	.214 1.2	30.0 174.6	500.0 .172	207.0 .174E 07	113.0 .2123E 06	94.0 .305	151.6 69.7	-207.2 15.8	28.3	0.	0.
2	502.0	5.75 23.3	.212 0.	30.0 163.6	490.0 .242	219.0 .143E 07	114.0 .1956E 06	105.0 .335	203.6 119.3	-160.1 8.2	14.2	0.	0.
2	503.0	5.75 22.0	.213 .0	30.0 161.6	495.0 .239	215.0 .146E 07	113.0 .1811E 06	102.0 .346	247.0 118.0	-115.1 8.4	14.4	21.0	0.
3	1211.0	2.27 29.8	.214 .1	30.0 117.8	500.0 .187	158.0 .206E 07	103.0 .2091E 06	55.0 .192	60.7 80.7	-274.2 10.4	17.0	0.	0.
3	1212.0	2.27 29.8	.214 .1	30.0 114.8	502.5 .252	185.0 .109E 07	109.0 .1932E 06	76.0 .260	150.0 123.4	-198.5 6.7	10.6	0.	0.
3	1213.0	2.27 29.9	.214 0.	30.0 102.0	500.0 .293	200.0 .176E 07	101.0 .1775E 06	99.0 .295	206.2 146.5	-149.1 4.4	7.0	0.	0.
3	1200.0	2.27 29.8	.214 .1	30.0 116.7	500.0 .316	215.0 .167E 07	115.0 .1694E 06	100.0 .322	253.6 168.5	-108.5 4.5	7.4	0.	0.
4	1250.0	2.27 28.9	.214 .8	30.0 120.6	500.0 .259	200.0 .109E 07	112.0 .2378E 06	88.0 .276	75.1 124.1	-200.2 3.9	6.3	0.	0.
4	1251.0	2.27 29.7	.215 .1	30.0 118.2	505.0 .311	215.0 .976E 00	116.0 .2214E 06	99.0 60.316	149.7 162.6	-212.4 2.7	4.5	0.	0.
4	1256.0	2.27 29.5	.214 .3	30.0 123.1	500.0 .342	227.0 .930E 00	120.0 .2081E 06	107.0 60.349	202.9 186.0	-164.0 2.4	4.1	0.	0.
3	1500.0	5.75 29.9	.214 0.	30.0 83.0	500.0 .086	110.0 .188E 07	73.0 .1552E 06	37.0 .089	53.7 3.7	-252.0 13.4	23.5	0.	0.
3	1510.0	5.75 29.9	.214 0.	30.0 120.8	500.0 .218	170.0 .217E 07	104.0 .1786E 06	66.0 .220	148.4 104.2	-192.8 9.5	15.4	0.	0.
3	1511.0	5.75 29.8	.214 .1	30.0 115.9	500.0 .281	192.0 .215E 07	113.0 .1775E 06	79.0 .287	205.8 145.4	-145.9 6.7	10.7	0.	0.
3	1512.0	5.75 29.9	.213 0.	30.0 113.8	495.0 .298	203.0 .153E 07	113.0 .1584E 06	90.0 .300	252.2 155.8	-104.9 5.5	8.8	0.	0.
4	1557.0	5.75 22.4	.214 .8	30.0 161.7	500.0 .216	210.0 .116E 07	118.0 .2489E 06	92.0 .309	84.8 100.5	-275.3 7.5	12.8	0.	0.
5	2505.0	5.75 19.9	.213 .4	30.0 173.4	495.0 .241	225.0 .103E 07	121.0 .2042E 06	104.0 .347	205.2 118.8	-160.9 6.4	11.1	0.	0.

2
3

5	2501.0	5.75 10.9	.214 .1	30.0 155.0	500.0 -.068	155.0 .201E 07	93.0 .1855E 06	62.0 .175	77.8 0.	-255.4 0.	0.	C.	C.
6	2555.0	5.75 27.0	.214 .2	30.0 143.9	500.0 .221	187.0 .154E 07	110.0 .1716E 06	77.0 .273	203.2 107.3	-146.2 8.3	14.0	C.	0.
6	2554.0	5.75 22.3	.214 .1	30.0 105.0	500.0 -.054	105.0 .210E 07	74.0 .1562E 06	33.0 .088	49.3 0.	-757.8 0.	C.	C.	0.
8	0326.0	4.03 28.4	.214 .1	30.0 67.3	249.8 .450	133.0 .405E 06	62.0 .1090E 06	51.0 .465	253.2 297.7	-67.4 1.0	4.17 1.7	.085 0	20.0 0
8	0345.0	4.03 20.4	.214 .0	30.0 112.2	250.0 .281	140.0 .430E 07	90.0 .1255E 06	50.0 .466	205.5 192.8	-119.3 37.5	4.17 60.0	.50 0	20.0 0
8	0343.0	4.03 27.2	.215 .1	30.0 76.8	252.5 .408	137.0 .235E 07	70.0 .1205E 06	60.0 .450	204.0 276.1	-116.6 7.9	4.52 12.7	.50 0	27.0 0
8	0344.0	4.03 28.1	.2117 .1	30.0 61.0	244.0 .400	135.0 .156E 07	60.0 .1198E 06	75.0 .471	202.5 297.0	-113.8 4.7	*** 7.3	1.5 0	27.0 0
7	7210.0	1.00 29.8	.2130 .0	30.0 35.9	250.0 .500	128.0 .871E 06	35.0 .1247E 06	93.0 .505	203.4 318.7	-114.1 .88	2.27 1.4	1.0 0	24.0 0
7	7510.0	1.00 24.6	.214 .2	30.0 59.1	250.0 .332	122.0 .408E 07	36.0 .1138E 06	86.0 .451	198.4 188.9	-115.3 13.4	5.75 19.2	1.0 0	24.0 0
7	7710.0	1.00 24.6	.213 .2	30.0 58.4	250.0 .330	120.0 .481E 07	36.0 .1125E 06	85.0 .450	202.3 188.5	-110.1 15.4	7.0 21.9	1.0 0	24.0 0
7	7250.0	1.00 29.7	.2125 .2	30.0 38.4	250.0 .518	132.0 .821E 06	37.0 .1300E 06	95.0 .525	203.5 336.5	-116.5 1.4	2.27 8.3	5.0 0	22.0 0
7	7550.0	1.00 25.7	.212 .2	30.0 55.9	250.0 .352	115.0 .239E 07	36.0 .1109E 06	79.0 .445	203.5 213.4	-105.6 6.6	5.75 9.4	5.0 0	22.0 0
7	7750.0	1.00 25.9	.211 .0	30.0 57.7	250.0 .345	115.0 .228E 07	37.0 .1061E 06	78.0 .426	206.1 210.3	-103.0 6.6	7.0 9.5	5.0 0	22.0 0
7	7290.0	1.00 29.8	.211 .0	30.0 39.0	250.0 .506	135.0 .733E 06	38.0 .1283E 06	97.0 .510	205.0 384.6	-116.8 .77	2.27 1.2	9.0 0	20.0 0
48" LONG TUBES													
1	114136	1.00 47.6	.212 .1	48.0 39.0	250.0 .484	140.0 .4915E 06	38.0 .1091E 06	102.0 .489	254.2 300.4	-70.6 56			.87
1	139135	1.00 47.8	.210 .1	48.0 38.7	240.0 .494	138.0 .5382E 06	38.0 .1184E 06	100.0 .498	206.1 310.1	-117.5 .61			.95
1	128110	1.00 47.8	.212 .2	48.0 92.1	125.0 .637	117.0 .3453E 06	92.0 .7687E 05	25.0 .641	251.3 481.6	-59.2 1.8	4.5	47.5	
DATA TAKEN WITH OSCILLATORY INSTABILITY PRESENT													
1	107.0	1.00 27.0	.213 0.0	30.0 95.0	250.0	95.0 .427E 06	95.0 .595E 05	0 .017	71.8	-222.7			17.0
1	108.0	1.00 28.3	.214 .7	30.0	250.0	170.0 .834E 06	155.0 .1168E 06	15.0 .245	88.8	-252.3			
1	120.0	1.00 29.9	.2115 .1	30.0 181.2	244.0 .374	209.0 .1014E 07	181.0 .1404E 06	28.0 .376	90.8	-268.7	25.0	12.8	
1	128.0	1.00 29.8	.211 .0	30.0	243.0	193.0 .8620E 06	170.0 .1190E 06	23.0 .321	124.3	-228.2			
1	111.0	1.00 29.6	.213 .1	30.0	250.0	175.0 .725E 06	147.0 .1010E 06	28.0 .345	162.7	-180.9			
1	119.0	1.00 29.6	.2135 .1	30.0	249.0	225.0 .9900E 06	195.0 .1380E 06	30.0 .425	175.8	-190.3			
1	118.0	1.00 29.6	.2135 .2	30.0 190.5	249.0 .414	218.0 .8362E 06	190.0 .1168E 06	29.0 .422	238.7	-124.7			
1	112.0	1.00 28.1	.2135 1.6	30.0	500.0	187.0 .1110E 07	169.0 .1550E 06	18.0 .118	99.4	-250.0			
1	122.0	1.00 29.8	.2105 .0	30.0	483.0	211.0 .1125E 07	187.0 .1560E 06	24.0 .086	104.8	-255.3	4.9		
1	113.0	1.00 25.8	.212 3.7	30.0	500.0	209.0 .9760E 06	191.0 .1355E 06	18.0 .063	144.1	-215.6			
1	128.0	1.00	.211	30.0	486.0	210.0 .1262E 07	181.0 .1745E 06	29.0 .148	114.6	-245.2			
FAST TRANSIENT TEST													
2	513.0	5.75 20.1	.214 1.1	30.0 104.2	125.0 .425	115.0 .7339E 06	95.0 .8152E 05	20.0 .626	200.4 296.2	-108.7 9.9	17.2		
*Axial Flux Distribution													
1 - Uniform													
2 - Cosine													
3 - Linear Increasing													
4 - Linear Decreasing													
5 - Peak Inlet													
6 - Peak Exit													
7 - Uniform with Cosine Spike													
8 - Cosine with Stepped Spike													
**Second Thermal Failure													
***5.14 to 4.54													

-116-

BIBLIOGRAPHY

1. DeBortoli, R.A., S.J. Green, B.W. LeTourneau, M. Troy and A. Weiss, "Forced-Convection Heat Transfer Burnout Studies for Water in Rectangular Channels and Round Tubes at Pressure Above 500 psi," Report WAPD-188, Bettis Atomic Power Laboratory (1958).
2. DeBortoli, R.A., J.D. Roarty, and A. Weiss, "Additional Burnout Data for a Rectangular Channel Having a Cosine Axial Heat Flux," WAPD-TH-227, August 23, 1956.
3. Weiss, A., "Hot Patch Burnout Tests in a 0.097 in. x 1 in. x 27 in. long Rectangular Channel at 2000 Psia," WAPD-TH-338, August 7, 1957.
4. Bell, D.W., "Correlation of Burnout Heat-Flux Data at 2000 Psia," NSE, 7, 245-251 (1960).
5. Swenson, H.S., J.R. Carver and R. Kakarala, "The Influence of Axial Heat Flux Distribution on the Departure from Nucleate Boiling in a Water Cooled Tube," ASME Paper 62-WA-297, Nov. 1962.
6. Janssen, E., J.A. Kervinen, "Burnout Conditions for Non-uniformly Heated Rod in Annular Geometry Water at 1000 Psia," GEAP-3755, APED, General Electric Co., San Jose, Calif., June 1963.
7. Casterline, J. and B. Matzner, "Burnout in Long Vertical Tubes with Uniform and Cosine Heating Using Water at 1000 Psia," Columbia Univ., Eng. Res. Labs., Topical Report, #41, Task XVI of Contract AT(30-3)-187, July 27, 1964. See also AEC Report TID-21031.
8. Schaefer, J.W. and J.R. Jack, "Investigation of Forced-Convection Nucleate Boiling of Water for Nozzle Cooling at Very High Heat Fluxes," NASA TND-1214, May 1962.
9. Lee, D.H. and J.D. Obertelli, "An Experimental Investigation of Forced Convection Burnout in High Pressure Water: Part II, Preliminary Results for Round Tubes with Non-Uniform Axial Heat Flux Distribution," AEEW-R309, November 1963.
10. Lee, D.H., "An Experimental Investigation of Forced Convection Burnout in High Pressure Water: Part III, Long Tubes with Uniform and Non-Uniform Axial Heating," AEEW-R355, March 1965.
11. Bertoletti, S., G. Gaspari, C. Lombardi and R. Zavattarelli, "Critical Heat Flux Data for Fully Developed Flow of Steam Water Mixtures in Round Vertical Tubes with Non-Uniform Axial Power Distribution," CISE-R74, April 1963.

12. Silvestri, M., "Two Phase Flow Problems," Report EUR 352.e, EURATOM, Brussels, Belgium, 1963.
13. Styrikovich, M.A., Z.L. Miropolsky and Shen Chzhao-Yuan, "The Effect of Non-Uniformity of Heating Along a Length of Pipe on the Magnitude of Critical Heat Fluxes," (Doklady) of the Academy of Sciences, USSR, No. 4, 859-862, 139 (1961). See AEC-TR-4961.
14. Duke, E., "Burnout and Heat Transfer Correlations for Once Through Superheat at Low Flow with an Exponential Source," ANS Meeting, June 1964, Paper AED-CONF. 1964-081-8.
15. Non-Uniform Heat Generation Experimental Program, Quarterly Progress Report No. 7, BAW-3238-7, January-March 1965.
16. Becker, K. et al., "The Influence of Non-Uniform Axial Heat Flux Distribution on the Burnout Conditions in Round Ducts," Report in Progress, AB Atomenergi, Sweden.
17. Becker, K. and P. Persson, "An Analysis of Burnout Conditions for Flow of Boiling Water in Vertical Round Ducts," ASME Trans. Series C, 86, 3, 393-407 63-HT-25, August 1964.
18. Isbin, H.S. et al., "A Model for Correlating Two Phase, Steam-Water Burnout Heat Transfer Fluxes," Jour. of Heat Transfer, Trans. ASME, Series C, 23, 149 May 1961.
19. Tong, L., H. Currin, P. Larsen and O. Smith, "Influence of Axial Non-Uniform Heat Flux on DNB," WCAP-2767, April 1965. See also AIChE paper, No. 17, Eighth National Heat Transfer Conf., Los Angeles, August 1965.
20. Milloti, S., "A Survey of Burnout Correlations as Applied to Water-Cooled Nuclear Reactors," SM Thesis, Dept. of Nuc. Eng., Penn. State Univ., September 1964.
21. Suo, M. et al., "Investigation of Boiling Flow Regimes and Critical Heat Flux," Dynatech Report No. 517, NYO-3304-3, March 1965.
22. Lopina, R.F., "Two-Phase Critical Heat Flux to Low Pressure Water Flowing in Small Diameter Tubes," SM Thesis, Dept. of Mech. Eng., MIT, June 1965.
23. Haberstroh, R. and P. Griffith, "The Transition from the Annular to the Slug Flow Regime in Two-Phase Flow," Contract No. AT(30-1)-3301, Technical Report 5003-28, Dept. of Mech. Eng., MIT, June 1964.
24. Baker, O., "Simultaneous Flow of Oil and Gas," Oil and Gas Jour., 53, 185 (1954).
25. Lowdermilk, W.H. and W.F. Weiland, "Some Measurements of Boiling Burnout," NACA-RM-E54 K10, (1955).

26. Jens, W.H. and P.A. Lottes, "Two-Phase Pressure Drop and Burnout Using Water Flowing in Round and Rectangular Channels," ANL-4915, October 1952.
27. Lowdermilk, W.H., C.D. Lanzo and B.L. Siegel, "Investigation of Boiling Burnout and Flow Stability for Water Flowing in Tubes," NACA-TN 4382, September 1958.
28. Becker, K.M., "Measurements of Burnout Conditions for Flow of Boiling Water in Vertical Round Ducts," AE-87 (1962).
29. VonGlahn, U., "An Empirical Correlation of Critical Boiling Heat Flux in Forced Flow Upward Through Uniformly Heated Tubes", NASA TMD-1285, September 1962.
30. MacBeth, R.V., "Burnout Analysis, Part 4: Application of a Local Condition Hypothesis to World Data for Uniformly Heated Round Tubes and Rectangular Channels," AEEW-R267, August 1963.
31. Maulbetsch, J.S., "A Study of System-Induced Instabilities in Forced-Convection Flows with Subcooled Boiling," Contract AF 49(638)-1468, Report No. 5382-35, Dept. of Mech. Eng., MIT, April 15, 1965.
32. Bergles, A.E. and W.M. Rohsenow, "Forced Convection Surface Boiling Heat Transfer and Burnout in Tubes of Small Diameter," Contract AF 19(604)-7344, Report No. 8767-21, Dept. of Mech. Eng., MIT, May 25, 1962.
33. Fauske, H.K., "Two-Phase Critical Flow," Notes from Special Summer Program on Two-Phase Gas-Liquid Flow, MIT, July 1964.
34. Hewitt, G. et al., "Burnout and Nucleation in Climbing Film Flow," AERE-R4374, August 1963.
35. Bergles, A.E. and Rohsenow, W.M., "The Determination of Forced Convection Surface-Boiling Heat Transfer," Jour. of Heat Transfer, 86, Series C, No. 3, 365-372 (Paper 63-HT-22) August 1964.
36. Jens, W.H. and P.A. Lottes, ANL-4627, May 1951.
37. Bernath, L. and Begell, W., "Forced Convection, Local Boiling Heat Transfer in Narrow Annuli," Chem. Eng. Prog. 55 Symposium Series, No. 29, 59-65 (1959).
38. Dengler, C.E. and J.N. Addoms, Chem. Eng. Prog. Symp. Series 52, 18, 95-103 (1956).
39. Chen, J.C., "A Correlation for Boiling Heat Transfer to Saturated Fluids in Convective Flow," ASME Paper No. 63-HT-34, ASME-AIChE Heat Transfer Conf., Boston, August 1963.

40. Brown, W., MechE Thesis, Dept. of Mech. Eng., MIT (in progress - to be completed February 1966).
41. Hewitt, G. et al., "Burnout and Film Flow in the Evaporation of Water in Tubes, : AERE-R 4864, March 1965.
42. Waters, E. et al., "Experimental Observations of Upstream Boiling Burnout," AIChE Paper No. 7, ASME-AIChE Heat Transfer Conf., Boston, August 1963.
43. Martinelli, R.C. and Nelson, D.B., "Prediction of Pressure Drop During Forced-Circulation Boiling of Water", Trans. ASME, 70, August 1948.
44. Levy, S., "Prediction of Two-Phase Annular Flow with Liquid Entrainment", APED-4615, May 1964.
45. Trembley, P., Priv. Comm., MIT, Nuc. Eng. Dept. (1965).
46. Keenan, J.H. and F.G. Keyes, "Thermodynamic Properties of Steam", Wiley (1962 ed).
47. Steltz, W.G., "The Formulation of Steam Properties for Digital Computer Application," Trans. ASME, Paper No. 57-A-109 (1958).
48. Wellman and Sibbitt, "Heat Transfer Properties of Water", Combustion, April 1955.
49. Jones, A.B. and D.G. Dight, "Hydrodynamic Stability of a Boiling Channel, Part 2", KAPL-2208, Knolls Atomic Power Laboratory (1962).
50. Kadakia, P.L., "SI PYFT-TO FIT POLYNOMIAL OF DEGREE 15 (MAX)," MIT Share Program No. 1421, January 3, 1962.
51. Volyak, L.D., "Temperature Dependence of the Surface Tension of Water," Doklady Akad. Nauk. S.S.S.R. 74, 307-10 (1950).
52. Rohsenow, W. and H. Choi, Heat Mass and Momentum Transfer Prentice-Hall Inc. (1961).
53. Kestin, J. and P.D. Richardson, "The Viscosity of Superheated Steam up to 275°C. A Refined Determination," Trans. ASME, Paper No. 62-WA-172 (1963).
54. Quan, D., "Properties of Superheated Steam" Nuclear-13, Orenda Engines Limited, Malton, Ont., December 1959.

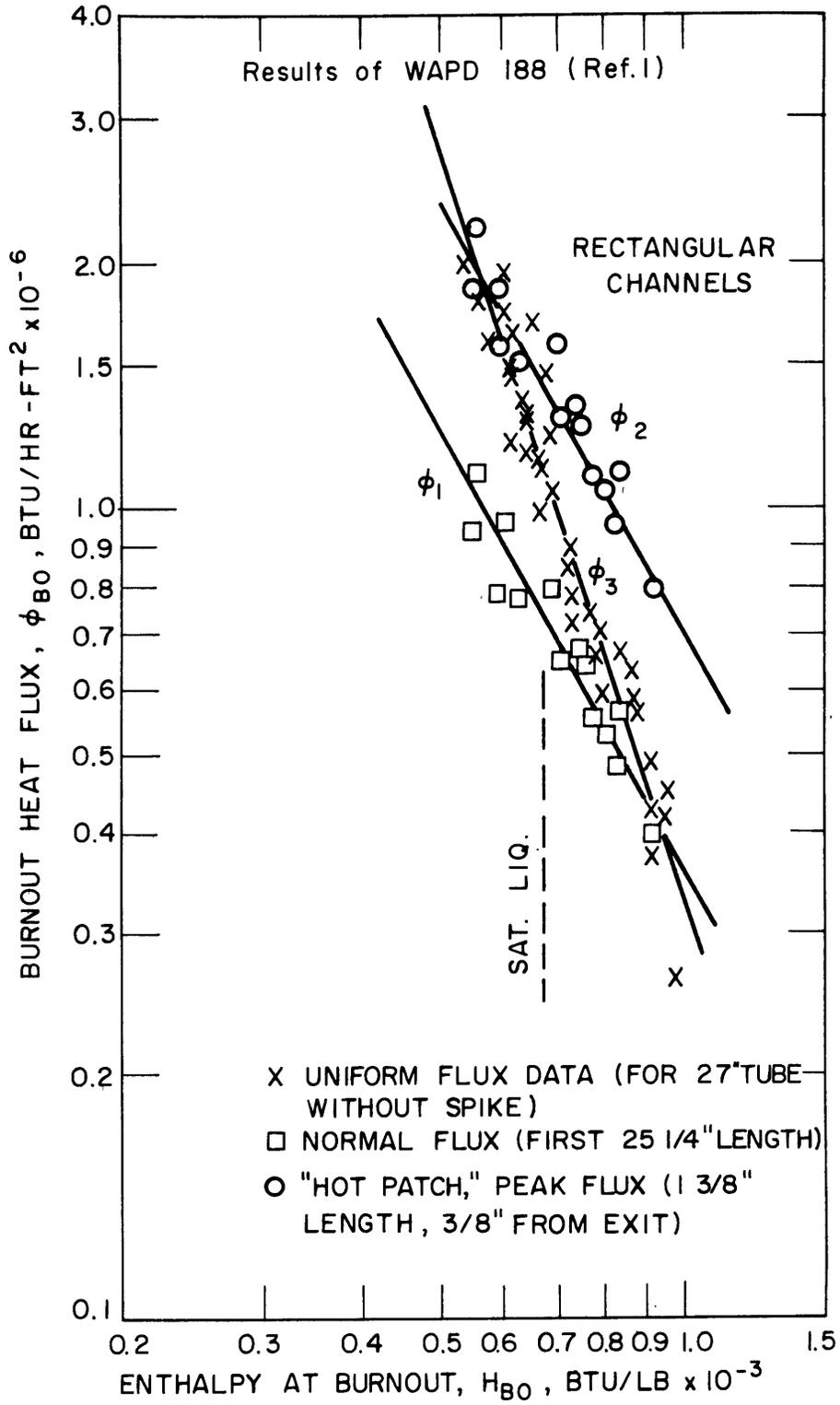


FIGURE I. EFFECT OF LOCAL HEAT FLUX SPIKE ON BURNOUT

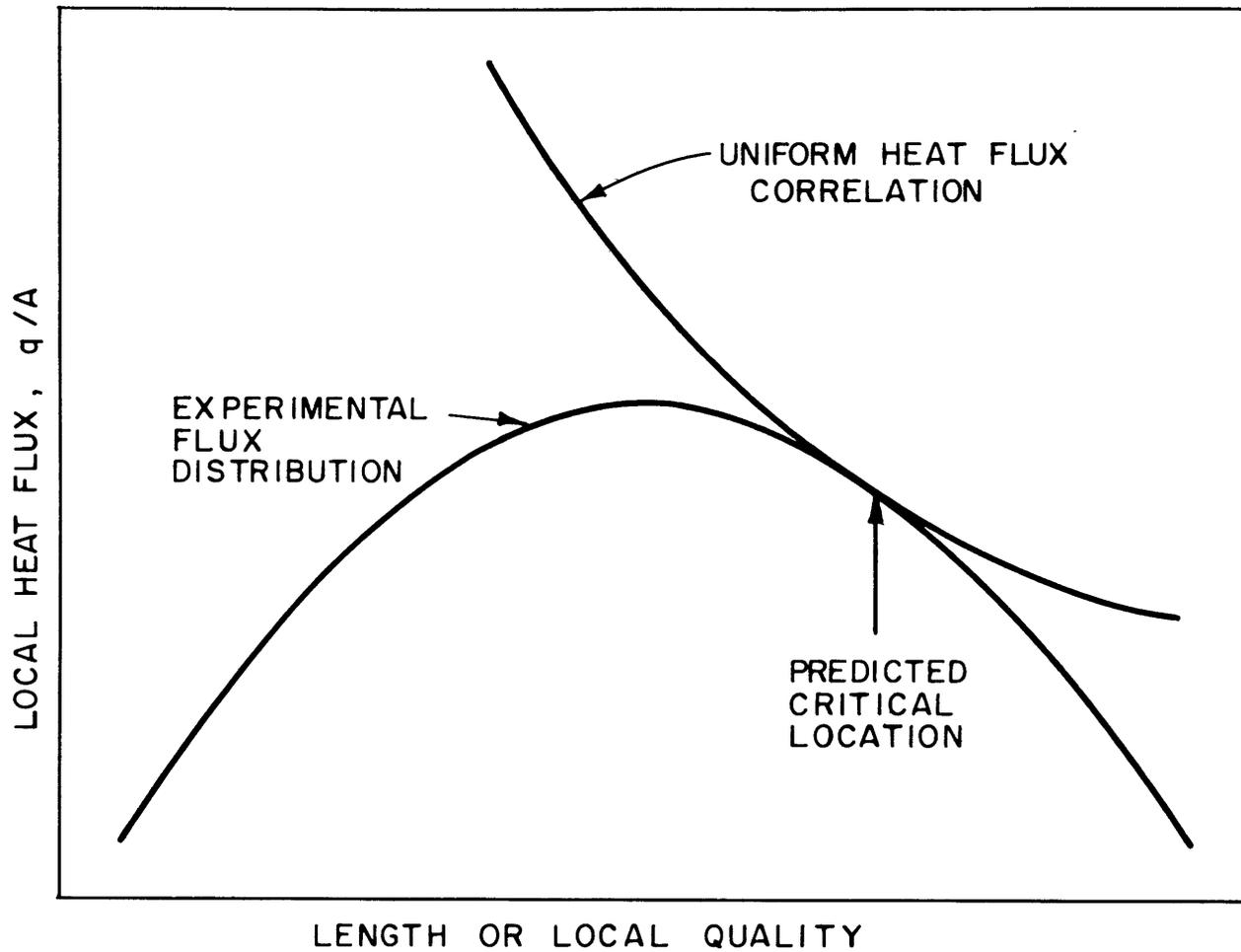
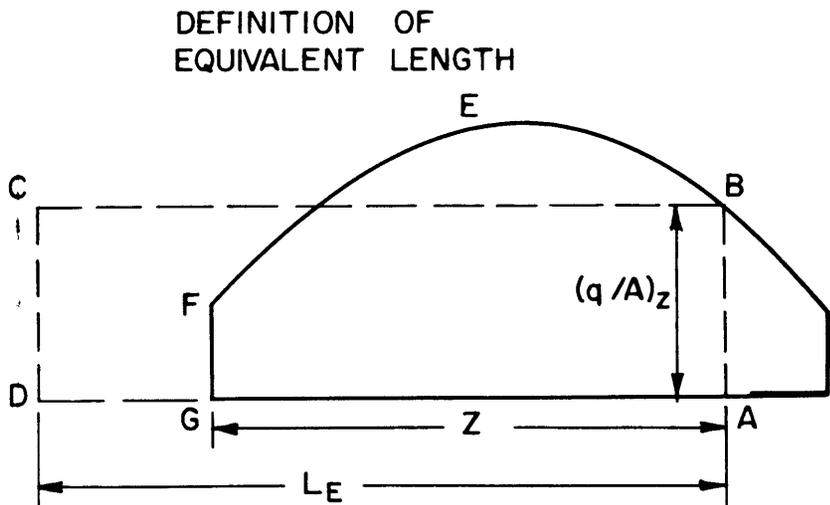


FIGURE 2. PREDICTION OF CRITICAL CONDITION BY LOCAL CONDITION METHOD OF JANSSEN AND KERVINEN (REF. 6)



$$L_e = \frac{1}{(q/A)_z} \int \phi_{MAX} \cos\left(\frac{\pi Z}{L_T}\right) dz$$

ie AREA ABCD = AREA ABEFG

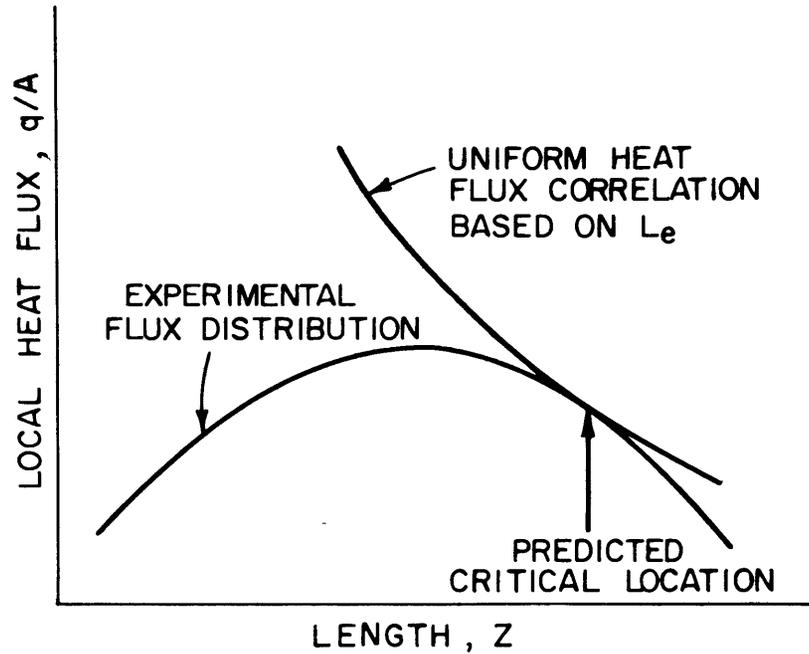


FIGURE 3. PREDICTION OF CRITICAL CONDITION BY EQUIVALENT LENGTH METHOD OF LEE AND OBERTELLI (REF 9)

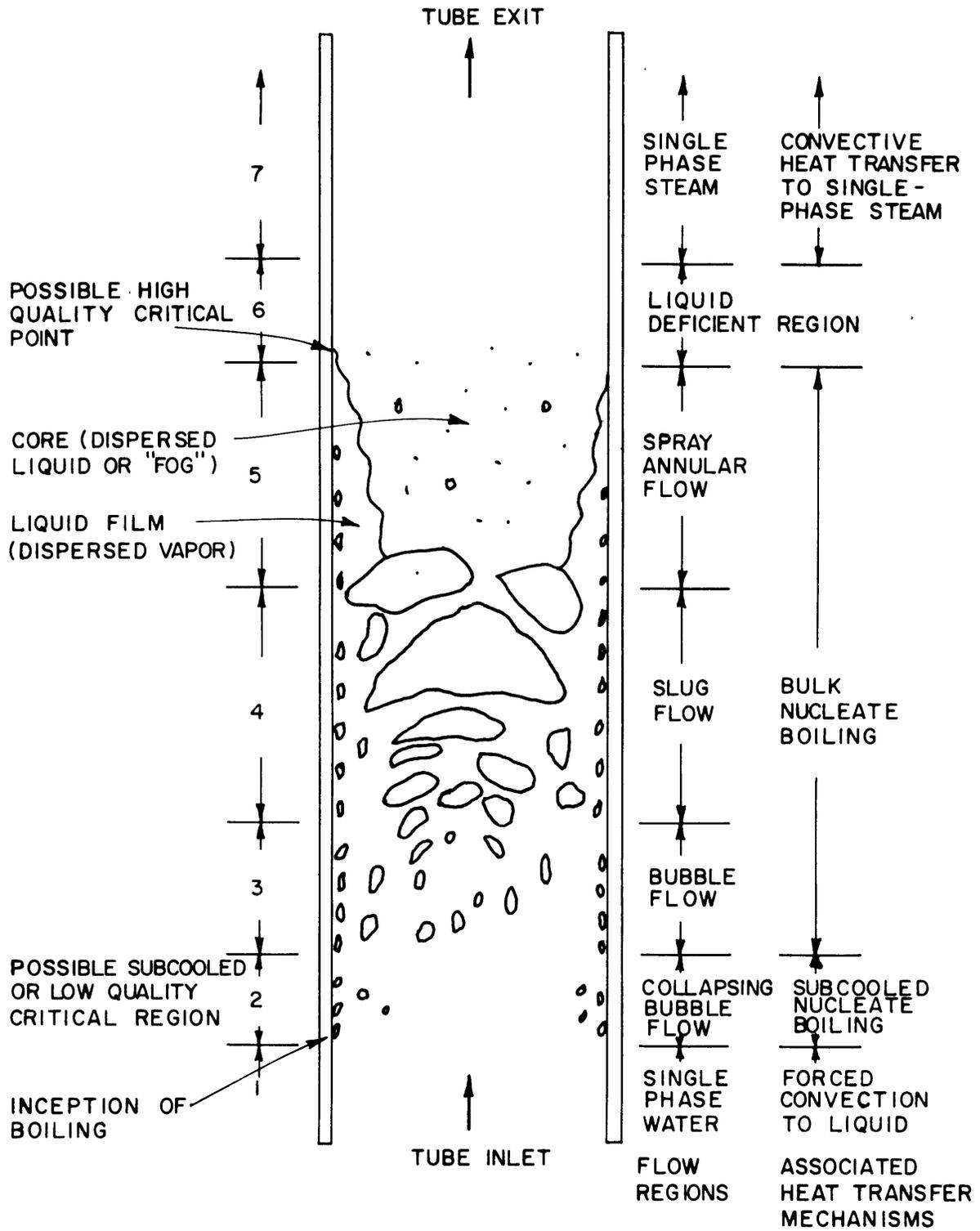


FIGURE 4. REGIMES OF TWO - PHASE FLOW

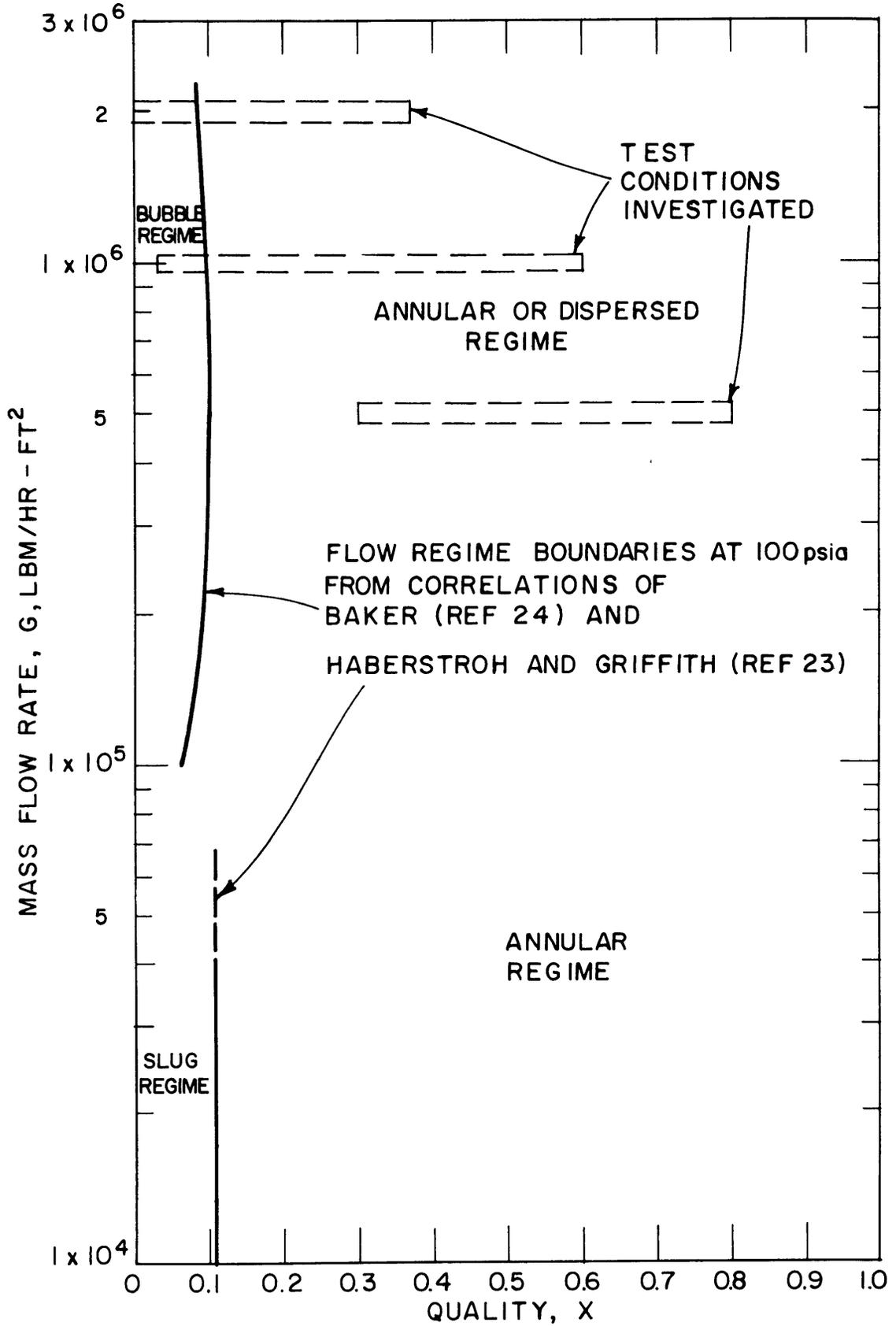


FIGURE 5. FLOW REGIME MAP FOR TEST CONDITIONS

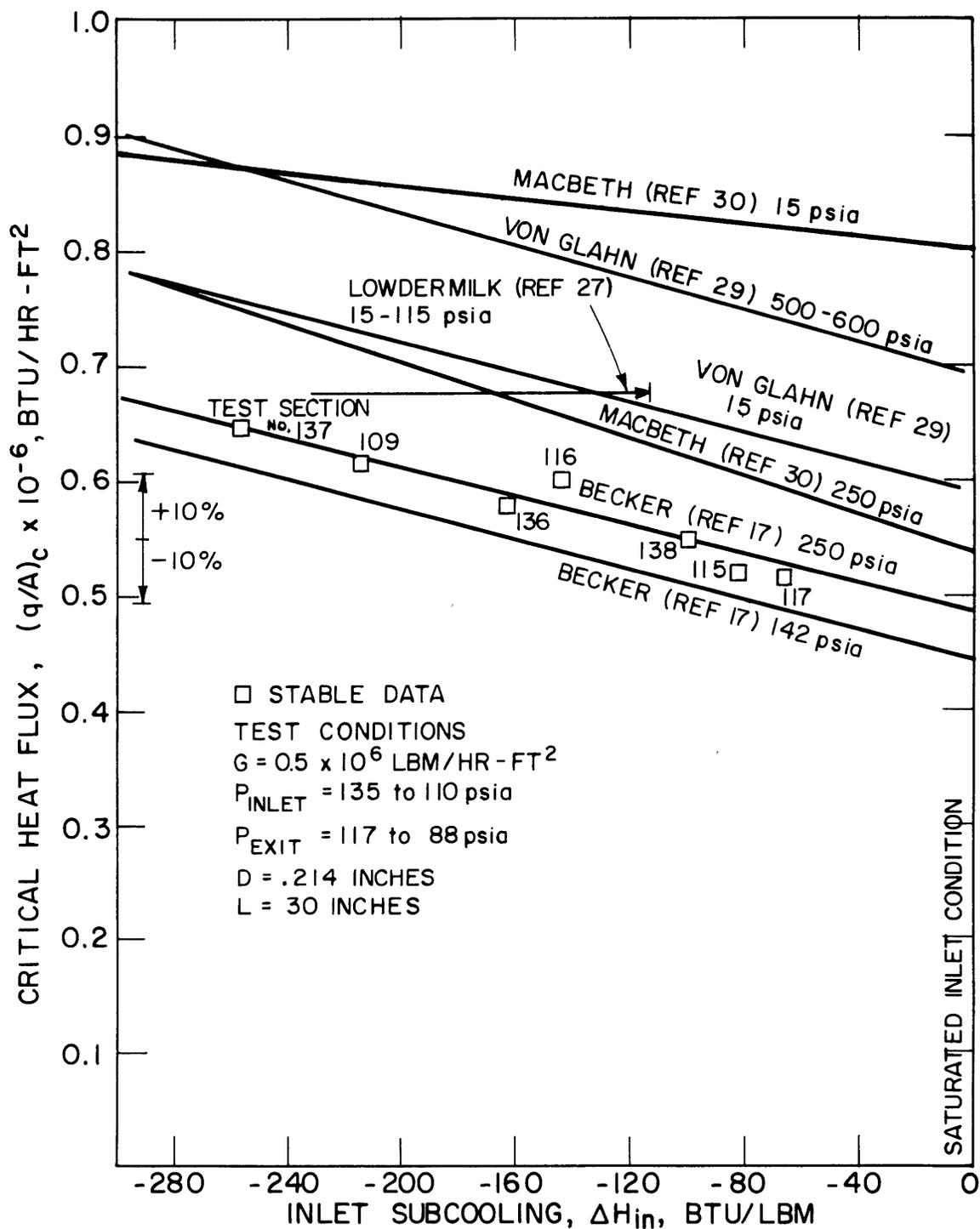


FIGURE 6. COMPARISON OF UNIFORM FLUX DATA WITH EXISTING CORRELATIONS, $G = 0.5 \times 10^6$ LBM/HR-FT²

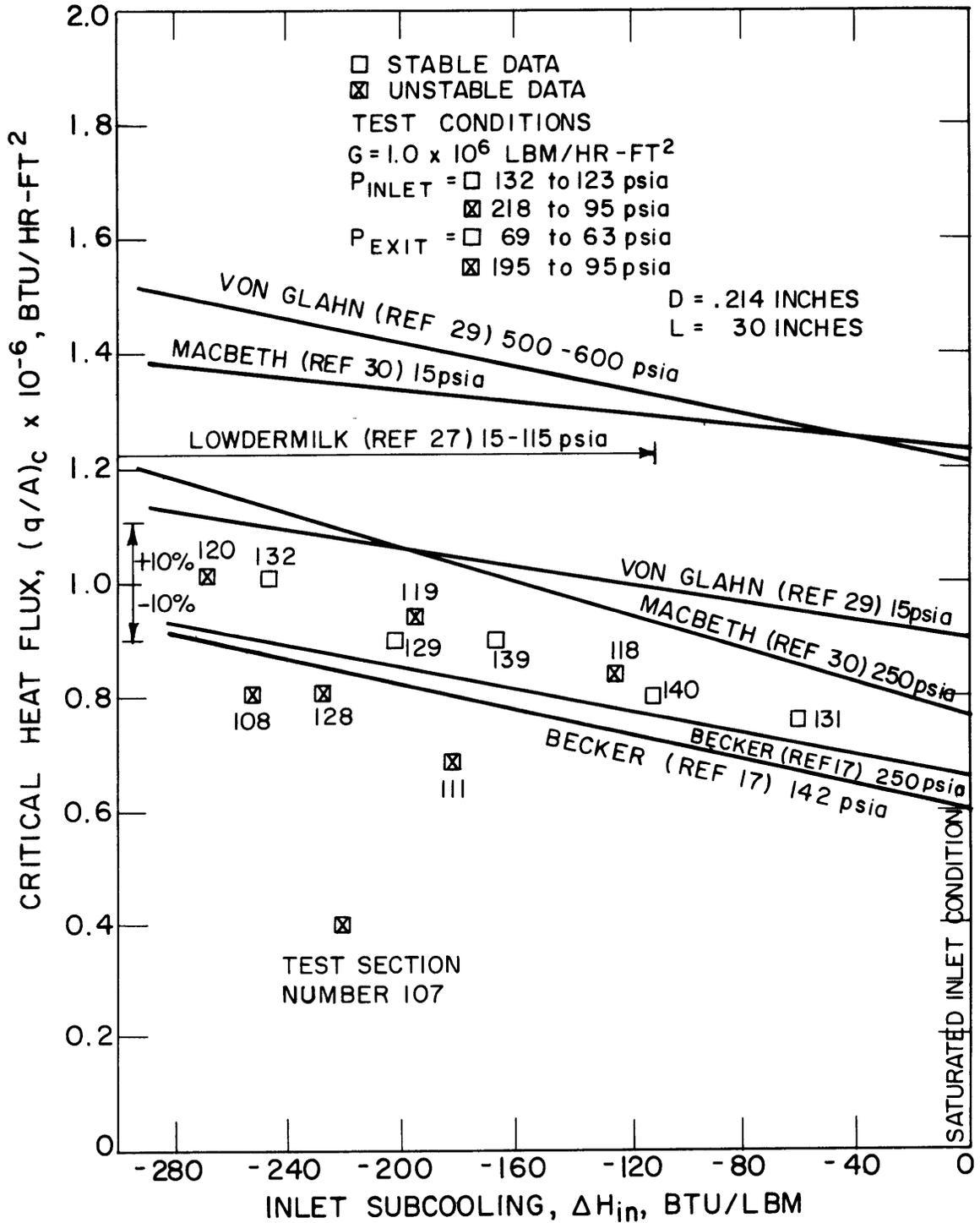


FIGURE 7. COMPARISON OF UNIFORM FLUX DATA WITH EXISTING CORRELATIONS, $G = 1.0 \times 10^6$ LBM/HR-FT²

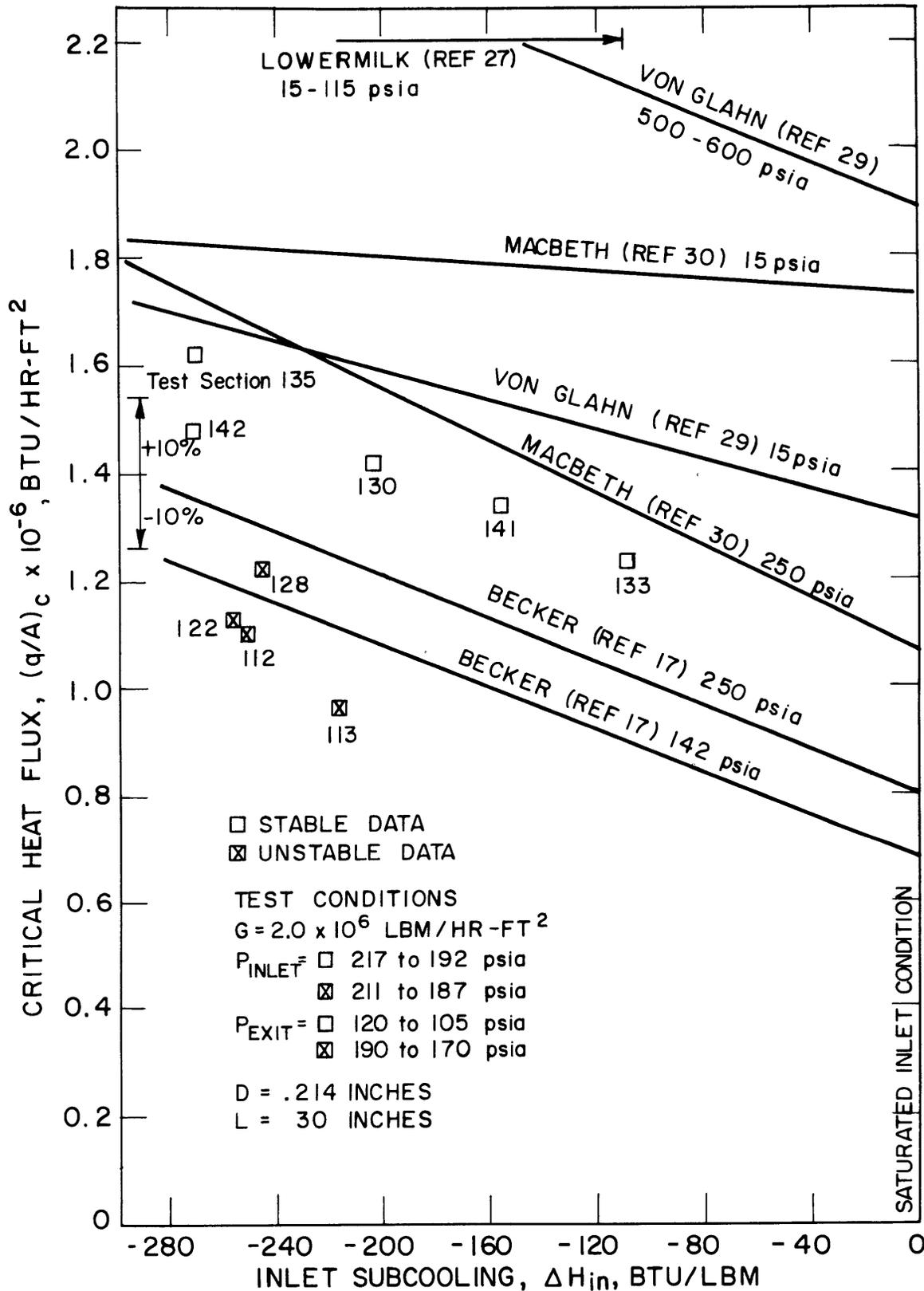


FIGURE 8. COMPARISON OF UNIFORM FLUX DATA WITH EXISTING CORRELATIONS, $G = 2.0 \times 10^6$ LBM/HR-FT²

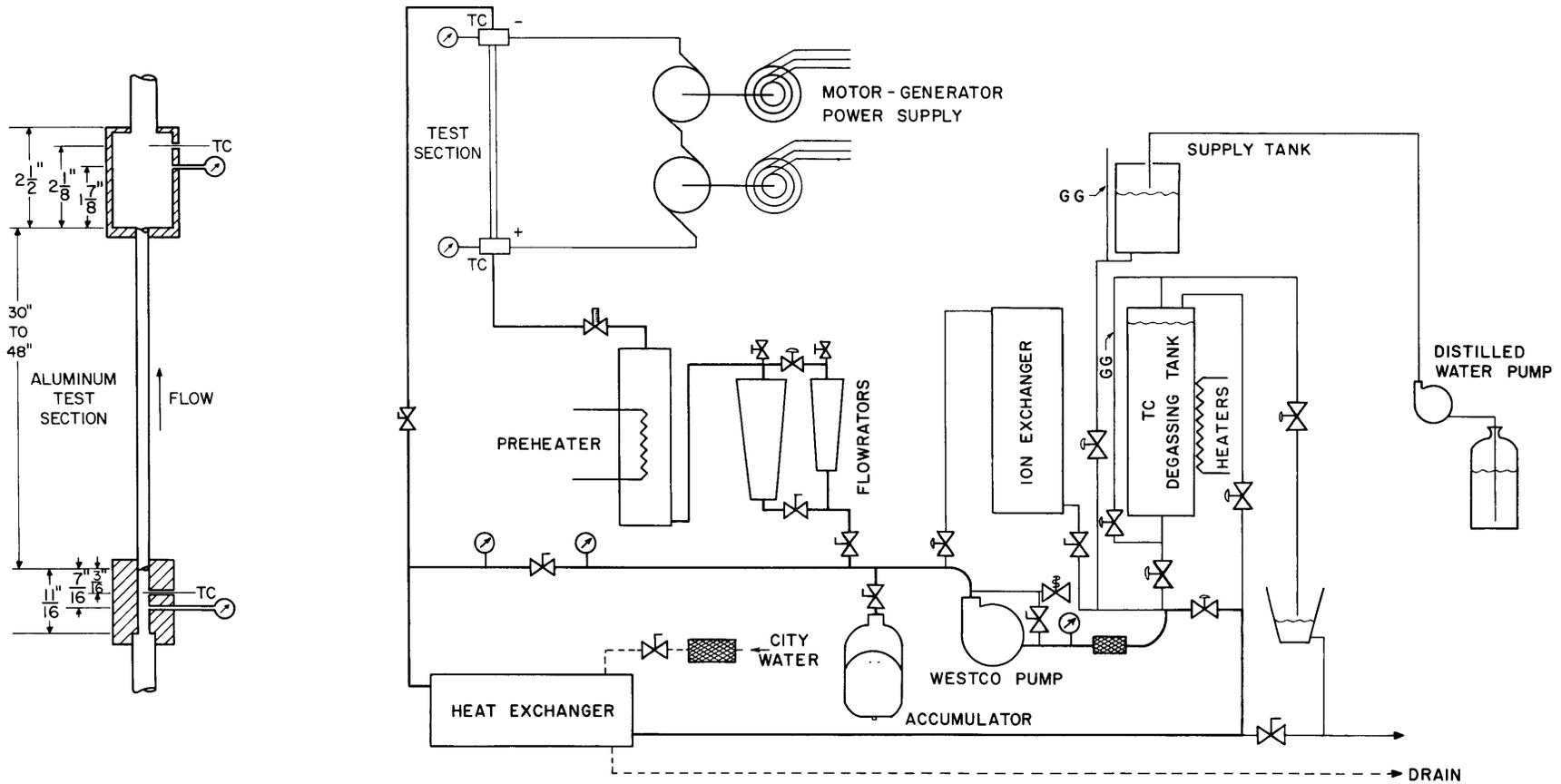


FIGURE 9. SCHEMATIC LAYOUT OF EXPERIMENTAL FACILITY AND TEST SECTION

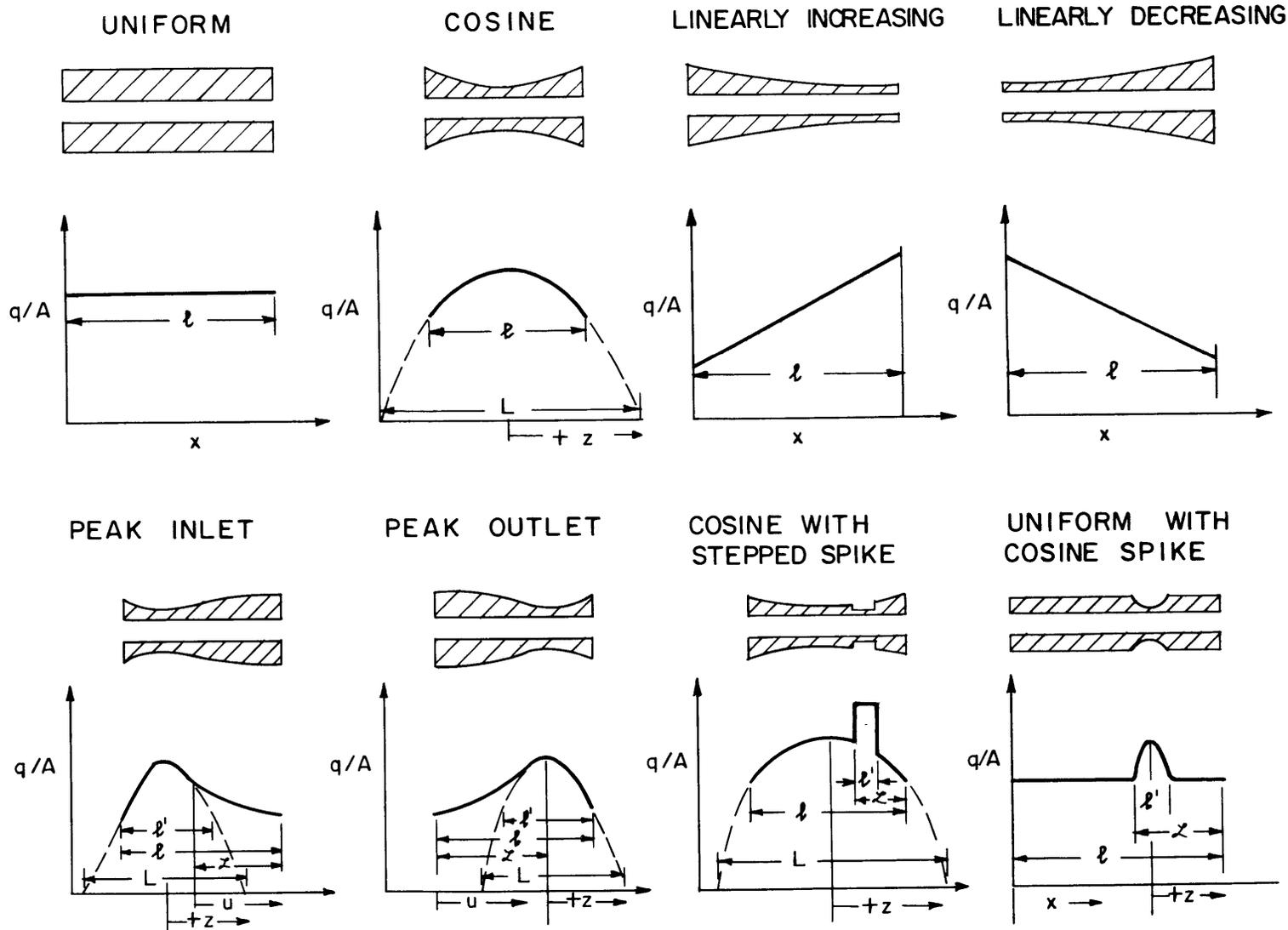


FIGURE 10. AXIAL FLUX DISTRIBUTIONS TESTED

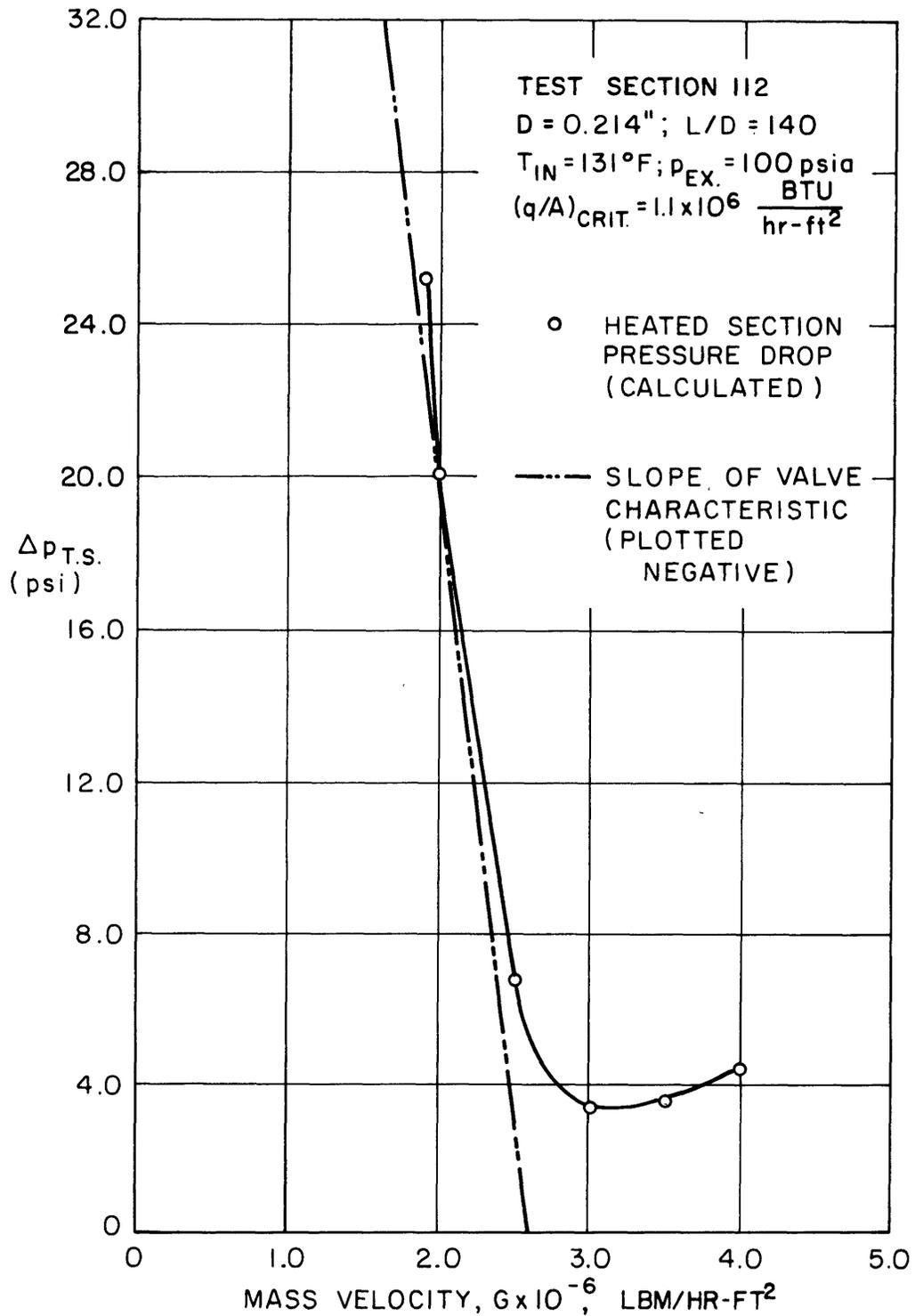


FIGURE 11 : CONFIRMATION FOR TEST SECTION 112 THAT THE OVERALL SLOPE GOES TO ZERO AT THE FLOW RATE (G=2.0X10⁶ LBM/HR-FT²) WHERE OSCILLATION OCCURED

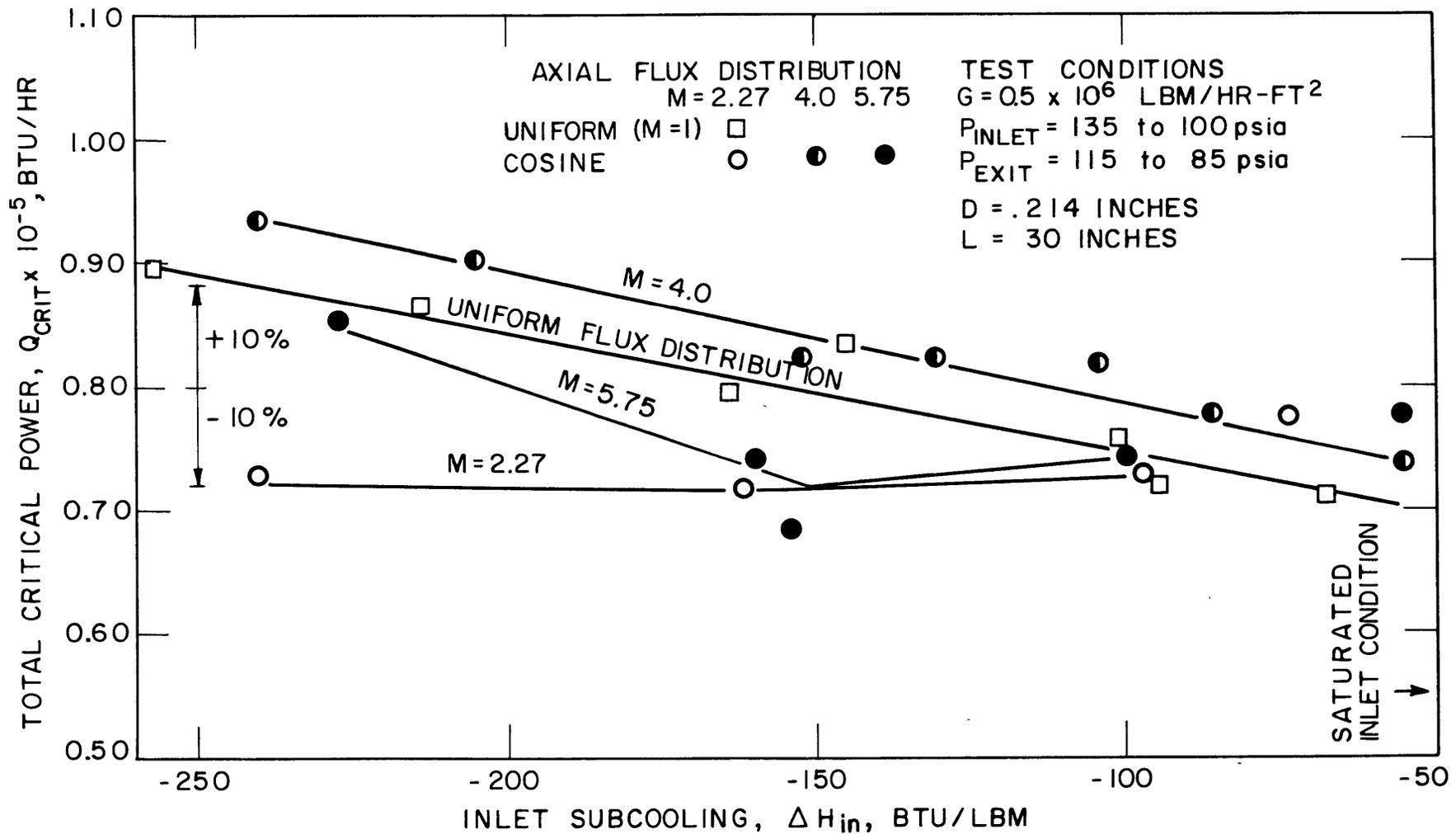


FIGURE 12. TOTAL CRITICAL POWER FOR UNIFORM AND COSINE FLUX DISTRIBUTIONS AT $G = 0.5 \times 10^6$ LBM/HR-FT²

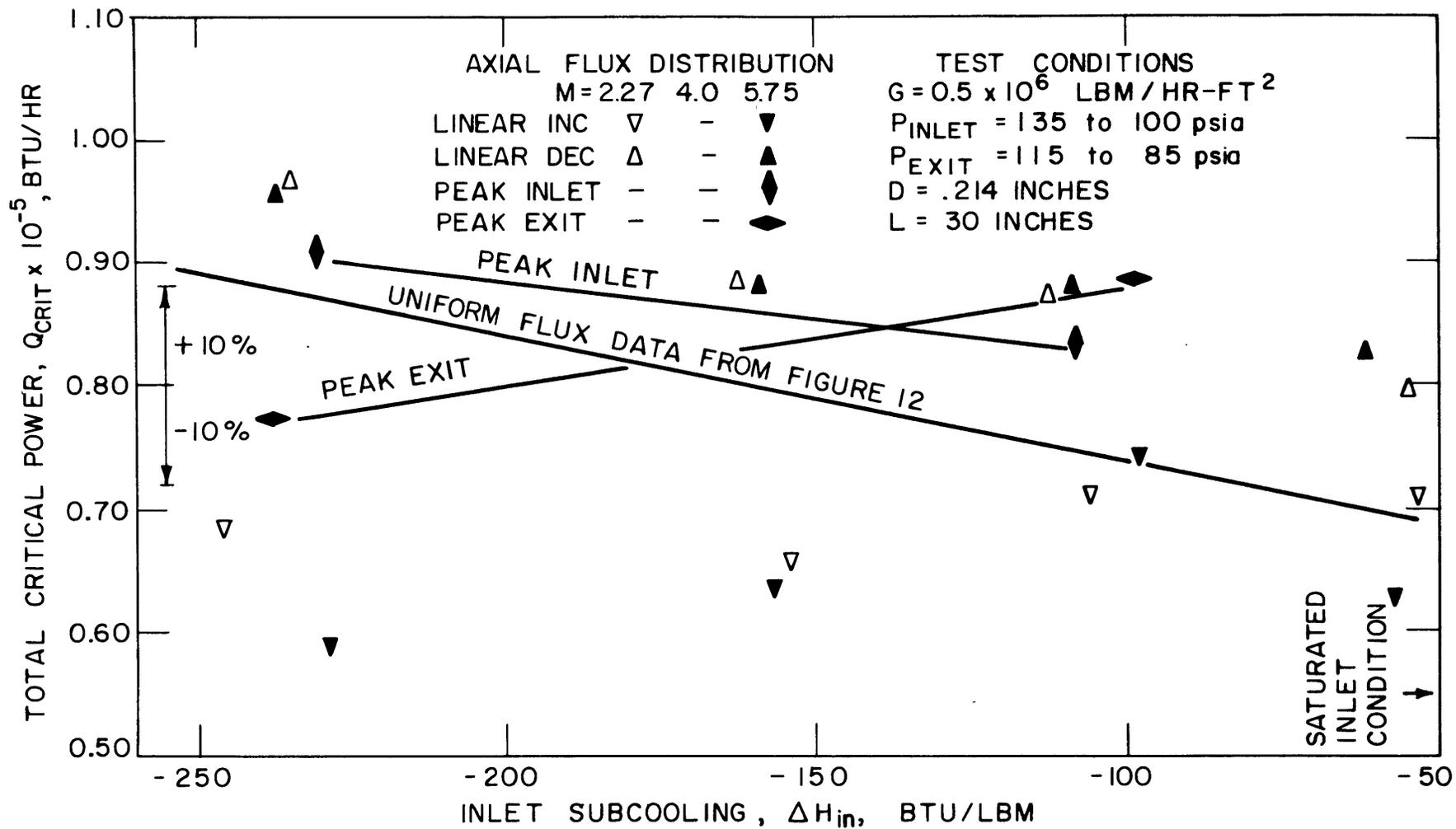


FIGURE 13. TOTAL CRITICAL POWER FOR LINEAR AND PEAKED FLUX DISTRIBUTIONS AT $G = 0.5 \times 10^6$ LBM/HR-FT²

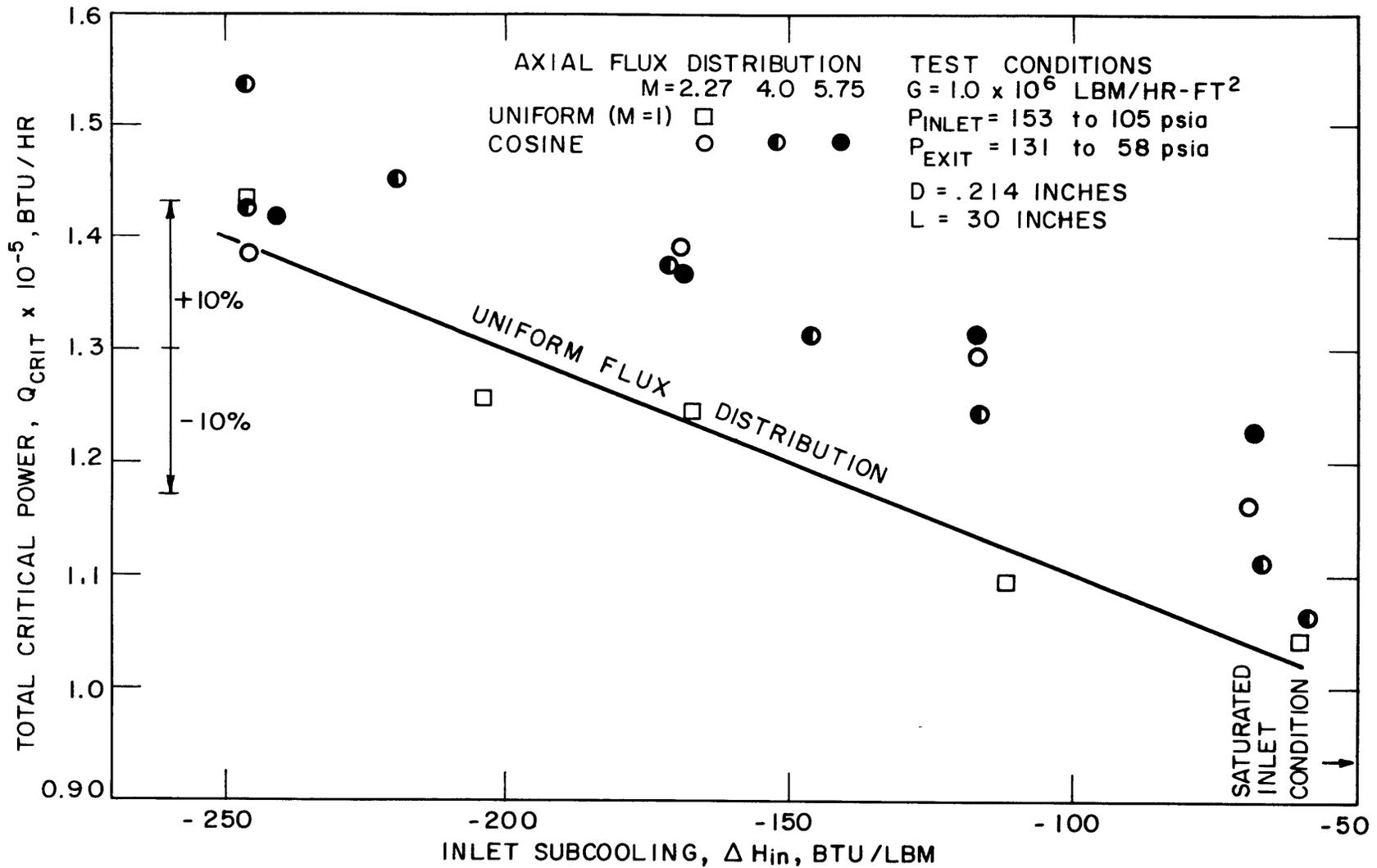


FIGURE 15. TOTAL CRITICAL POWER FOR UNIFORM AND COSINE FLUX DISTRIBUTIONS AT $G = 1.0 \times 10^6$ LBM/HR-FT²

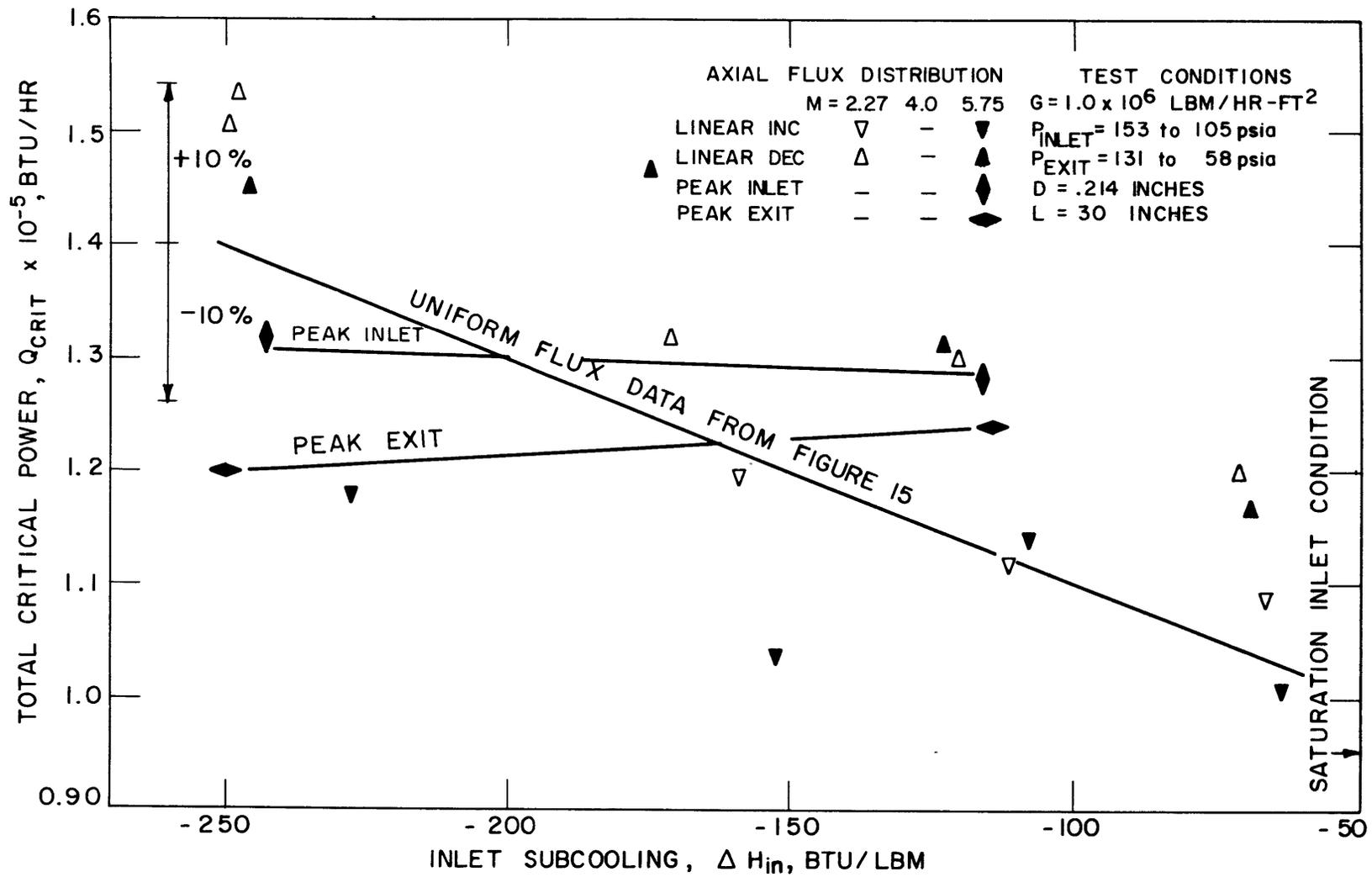


FIGURE 16. TOTAL CRITICAL POWER FOR LINEAR AND PEAKED FLUX DISTRIBUTIONS AT $G = 1.0 \times 10^6$ LBM/HR-FT²

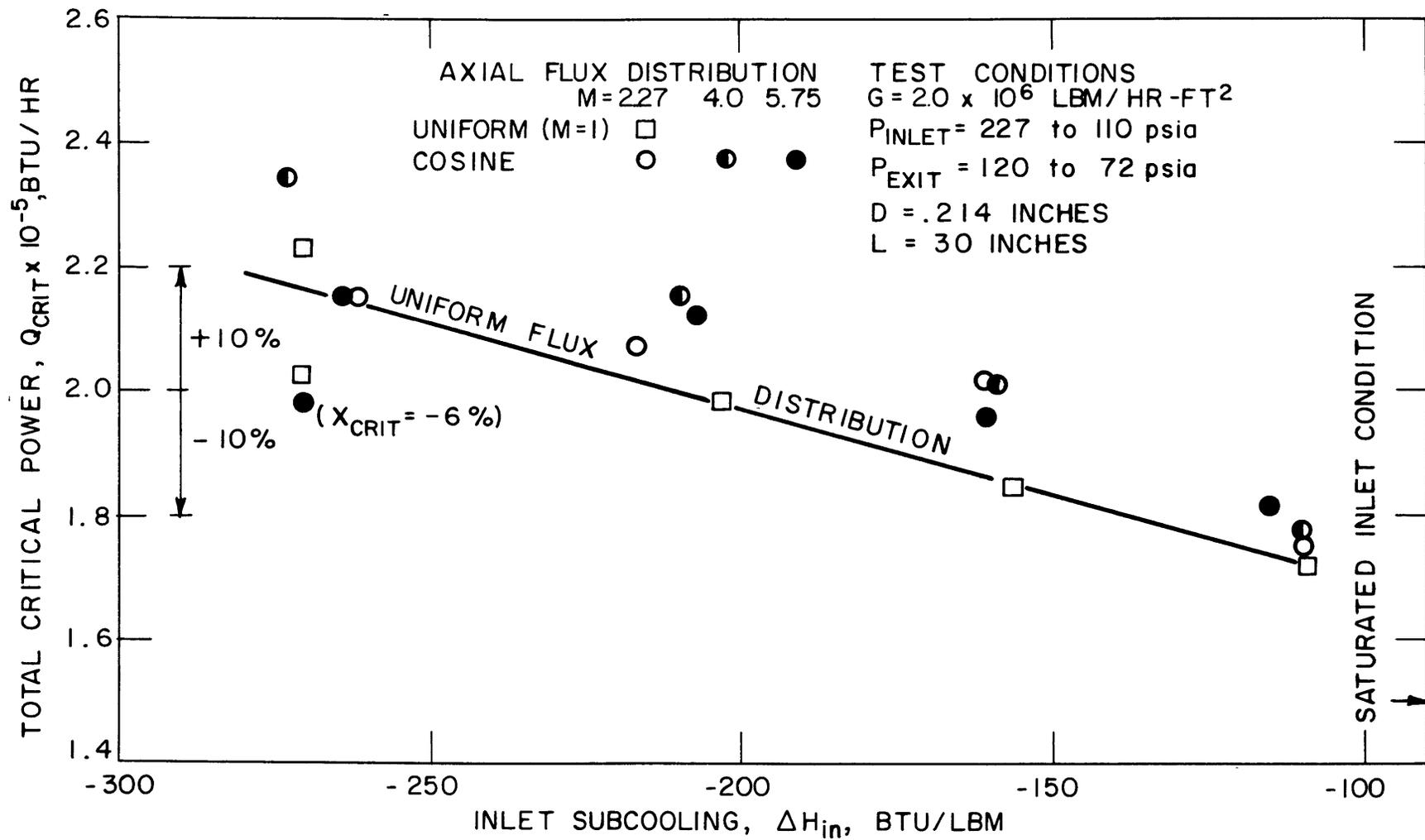


FIGURE 18. TOTAL CRITICAL POWER FOR UNIFORM AND COSINE FLUX DISTRIBUTIONS AT $G = 2.0 \times 10^6$ LBM/HR-FT²

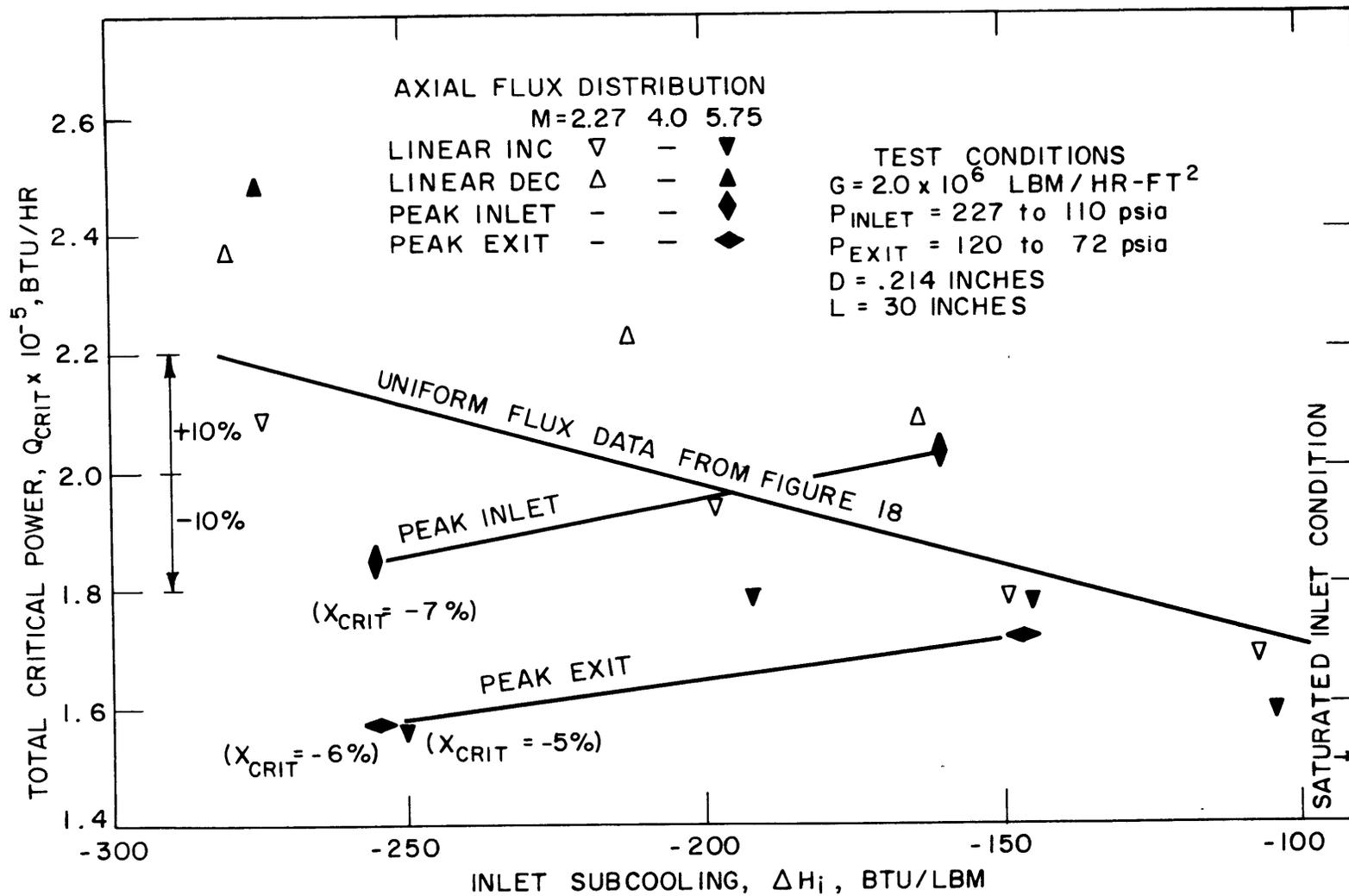


FIGURE 19. TOTAL CRITICAL POWER FOR LINEAR AND PEAKED FLUX DISTRIBUTIONS AT $G = 2.0 \times 10^6$ LBM/HR-FT²

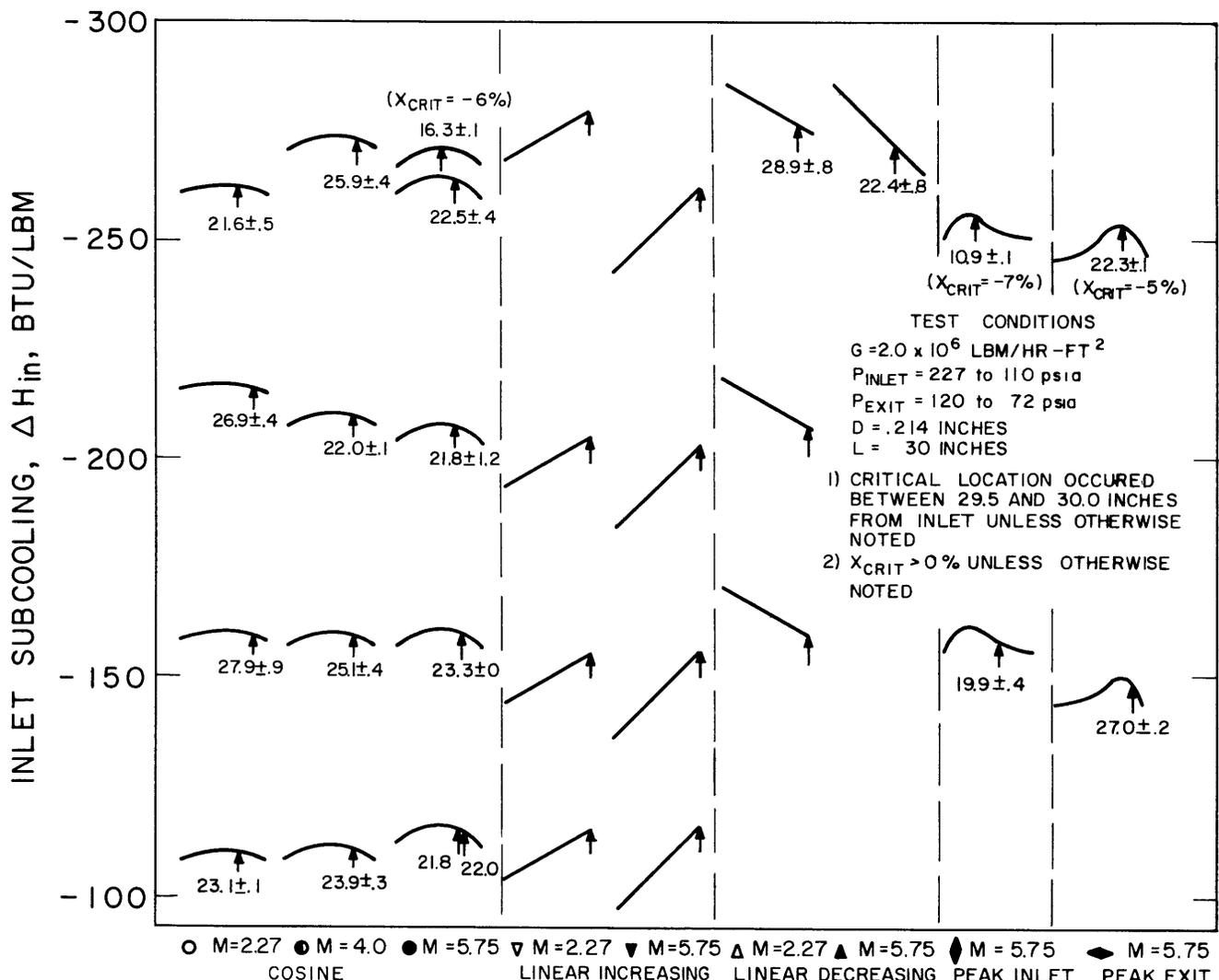


FIGURE 20. CRITICAL LOCATIONS (INCHES FROM INLET) FOR THE NONUNIFORM AXIAL FLUX DISTRIBUTIONS INVESTIGATED AT $G = 2.0 \times 10^6$ LBM/HR-FT²

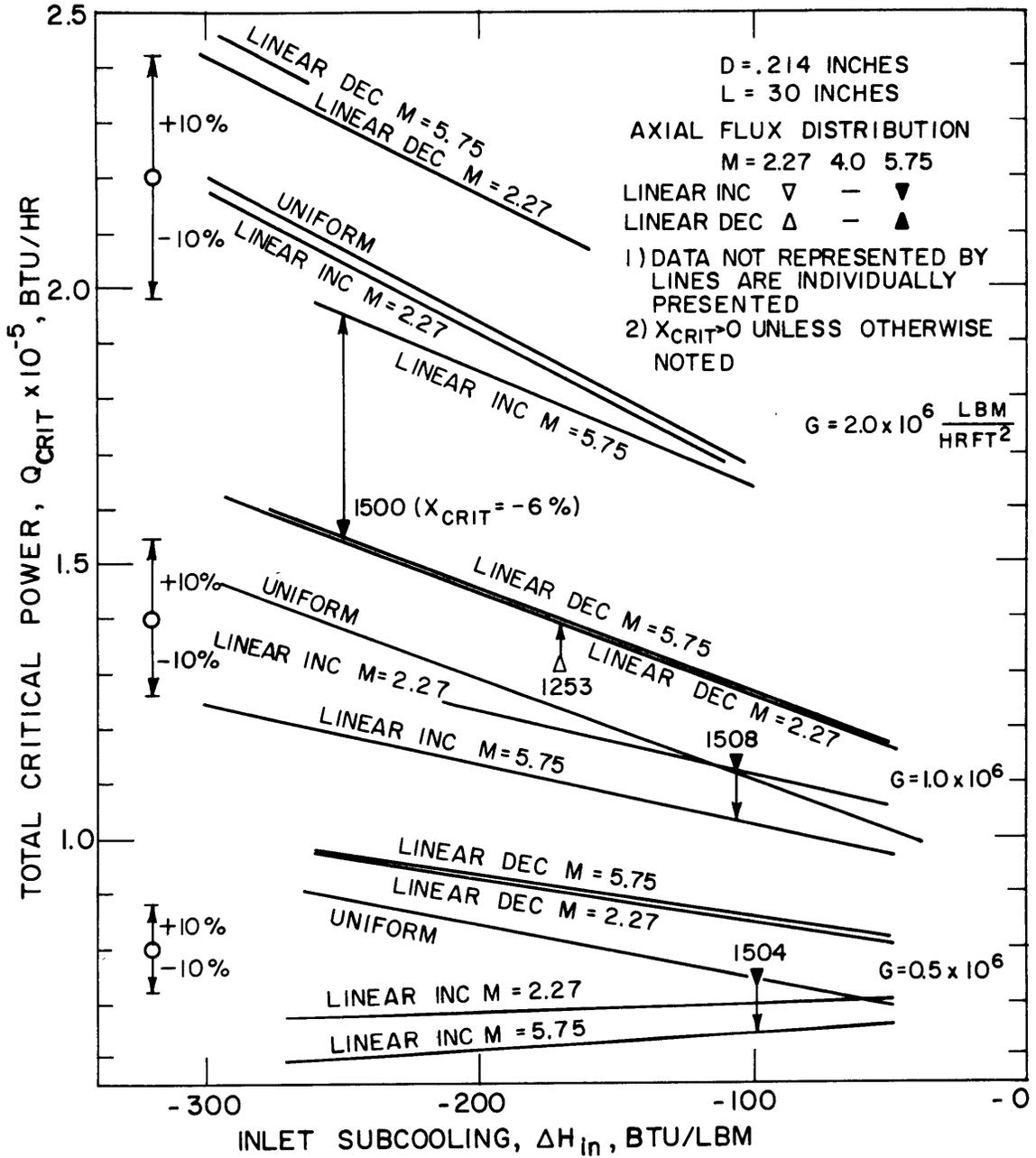


FIGURE 21. SUMMARY OF EFFECT OF LINEAR INCREASING AND DECREASING FLUX DISTRIBUTIONS ON TOTAL CRITICAL POWER

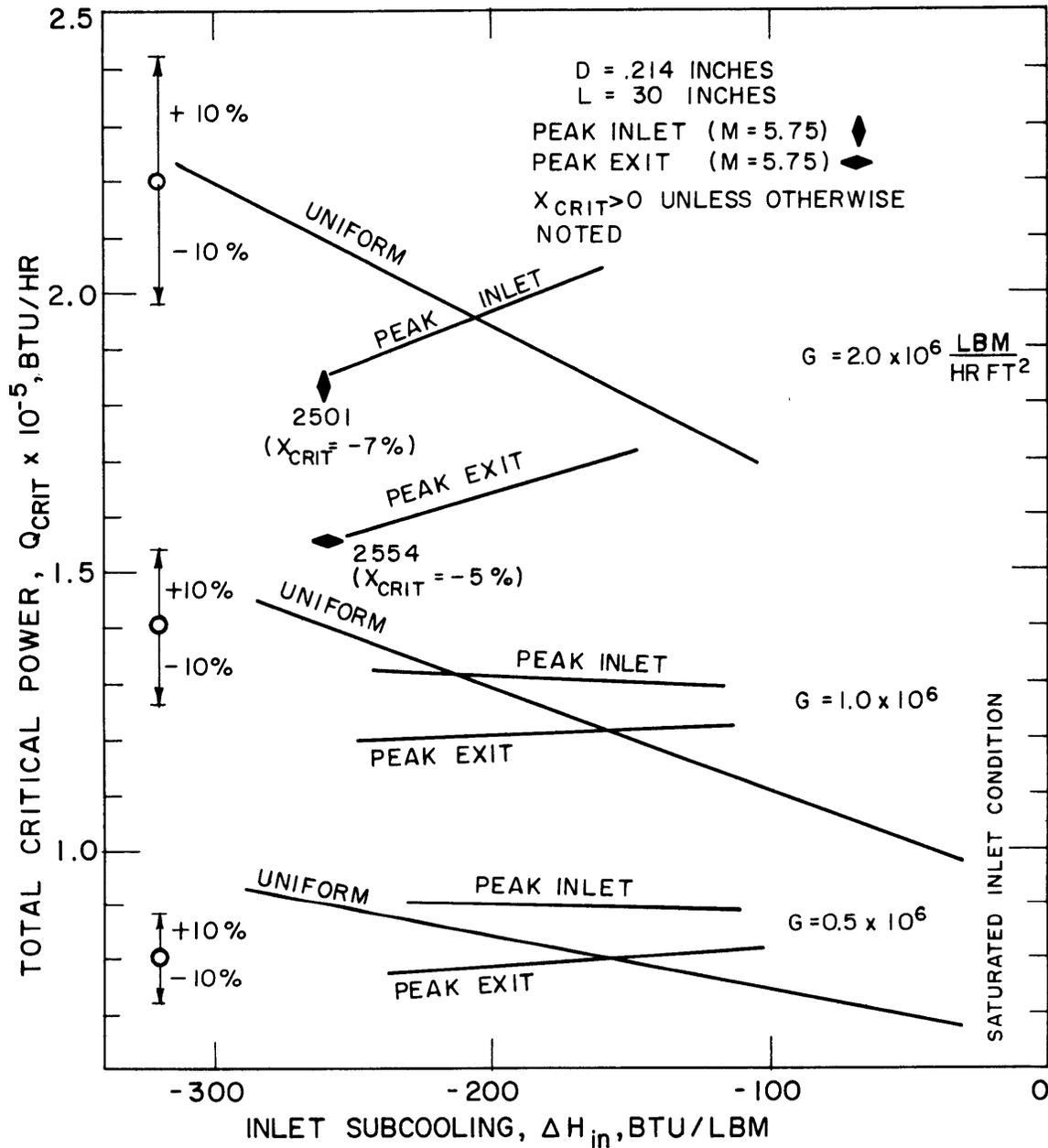


FIGURE 22. SUMMARY OF EFFECT OF PEAK INLET AND EXIT FLUX DISTRIBUTIONS ON TOTAL CRITICAL POWER

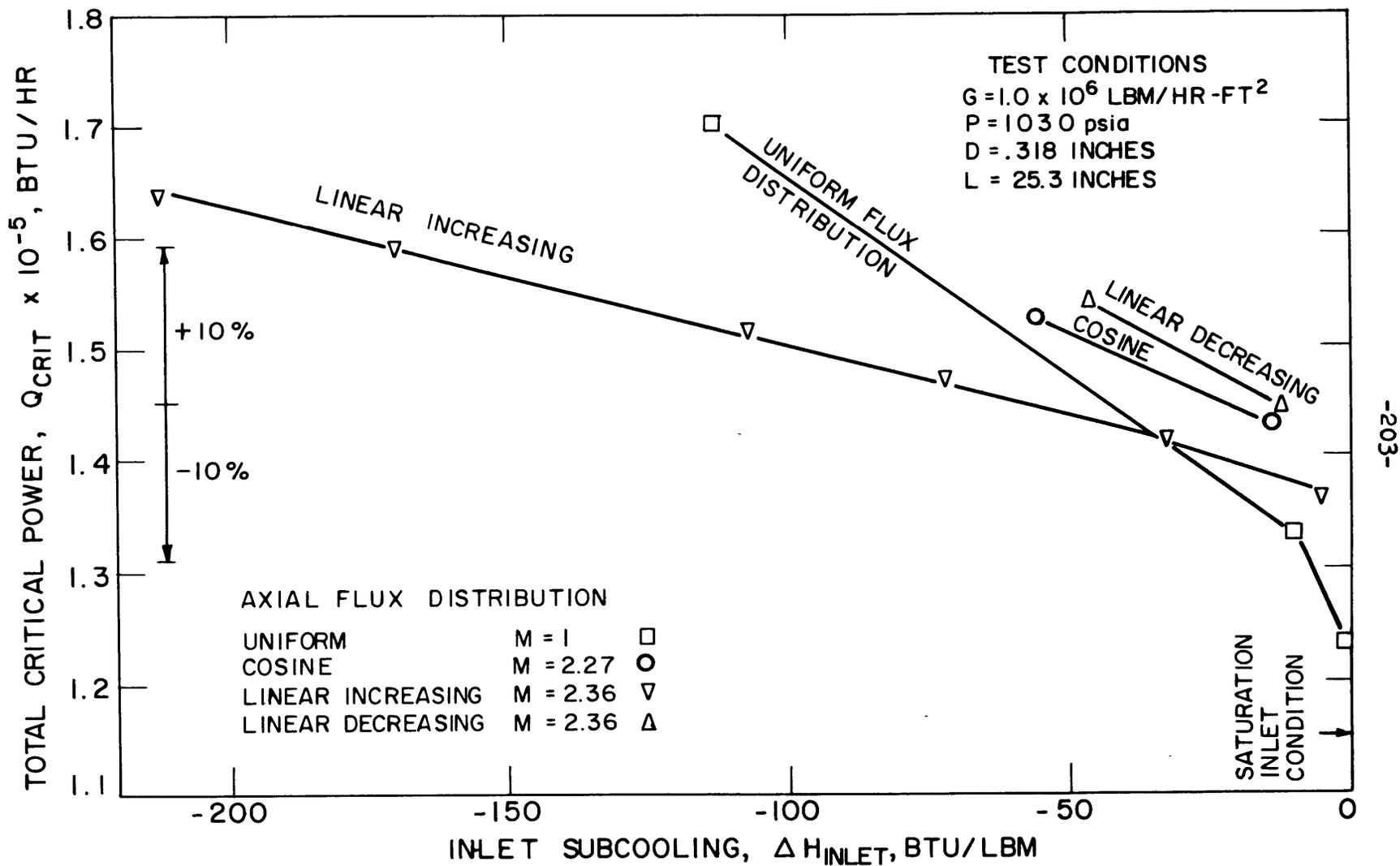


FIGURE 23. TOTAL CRITICAL POWER FOR DATA OF BERTOLETTI ET AL. (REF. II)

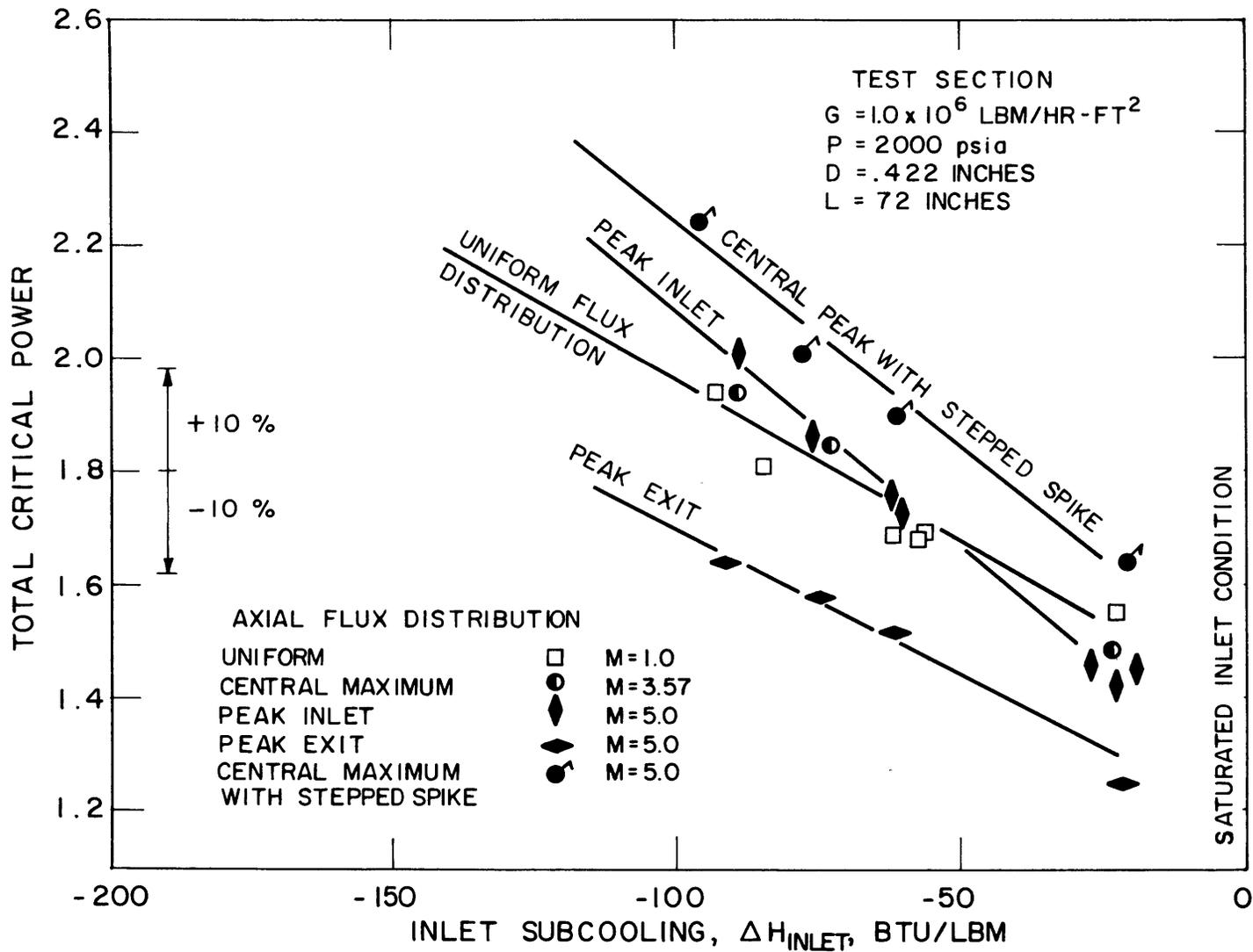


FIGURE 24. TOTAL CRITICAL POWER FOR DATA OF SWENSON (REF. 5)

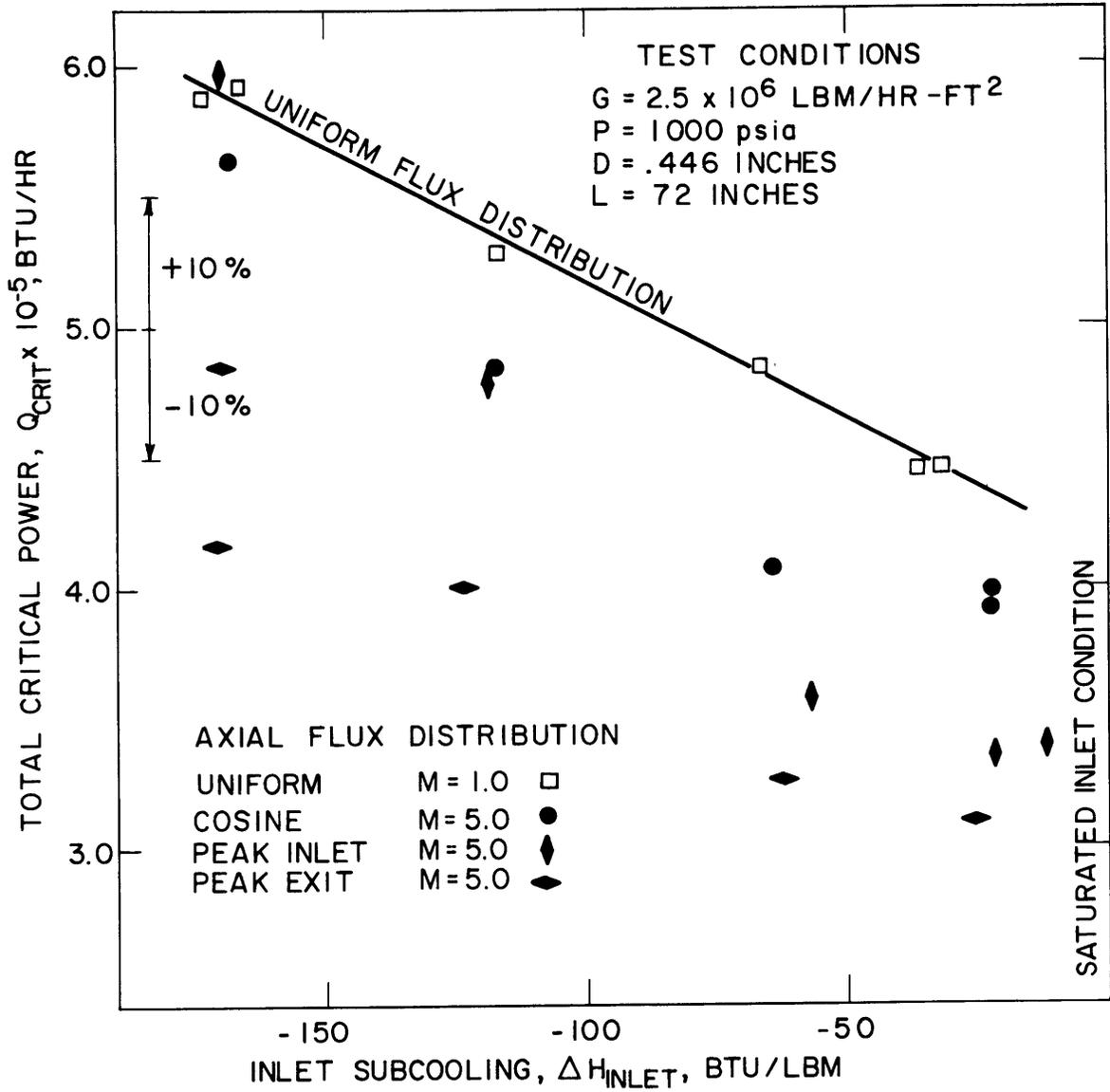


FIGURE 25 TOTAL CRITICAL POWER FOR DATA OF BABCOCK AND WILCOX (REF. 15)

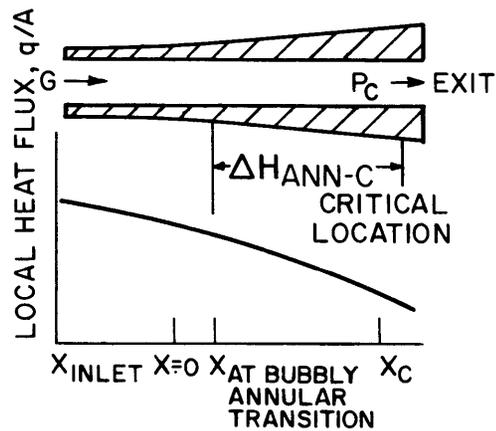


FIGURE 26a. LINEAR DECREASING HEAT FLUX

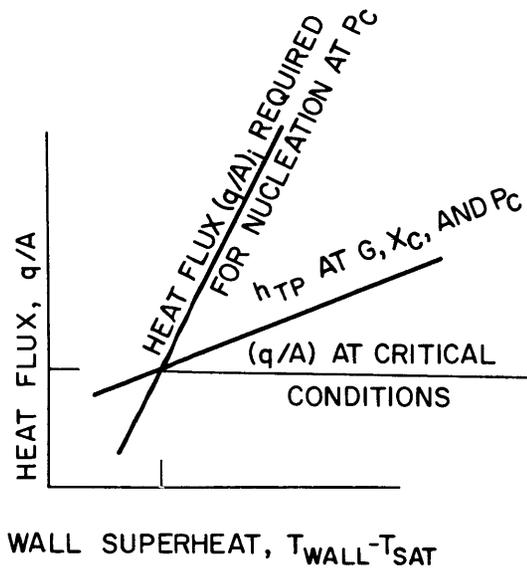


FIGURE 26b. $(q/A)_i$ AT CRITICAL CONDITIONS

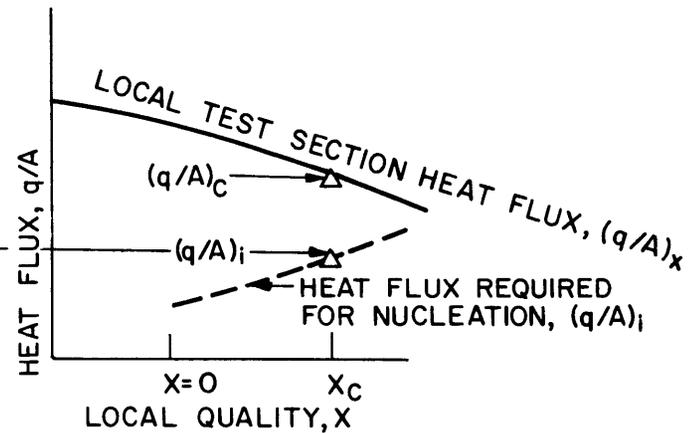


FIGURE 26c. HEAT FLUX CONDITIONS ALONG ENTIRE TEST SECTION

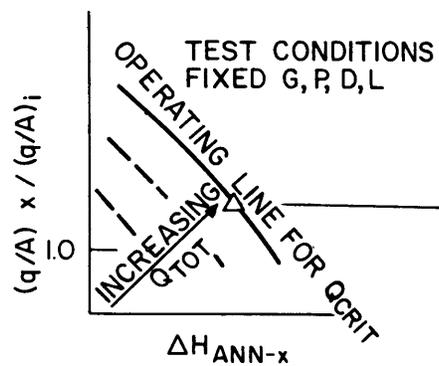


FIGURE 26d. OPERATING LINES FOR TEST SECTION FOR Q_{TOT} EQUAL AND LESS THAN Q_{CRIT}

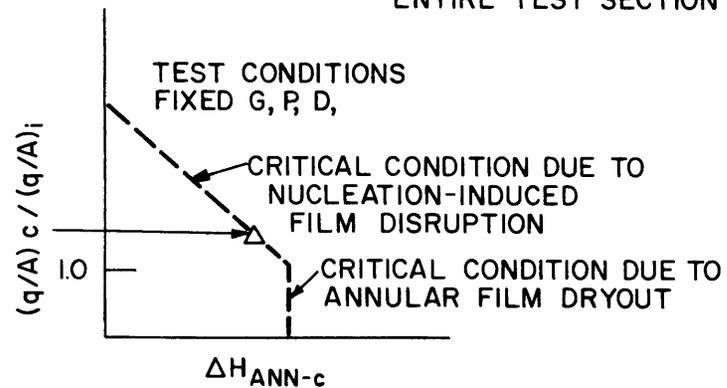


FIGURE 26e. EXPECTED LOCUS OF CRITICAL CONDITIONS

MAXIMUM CAVITY RADIUS (FT) REQUIRED FOR VARIOUS PRESSURES

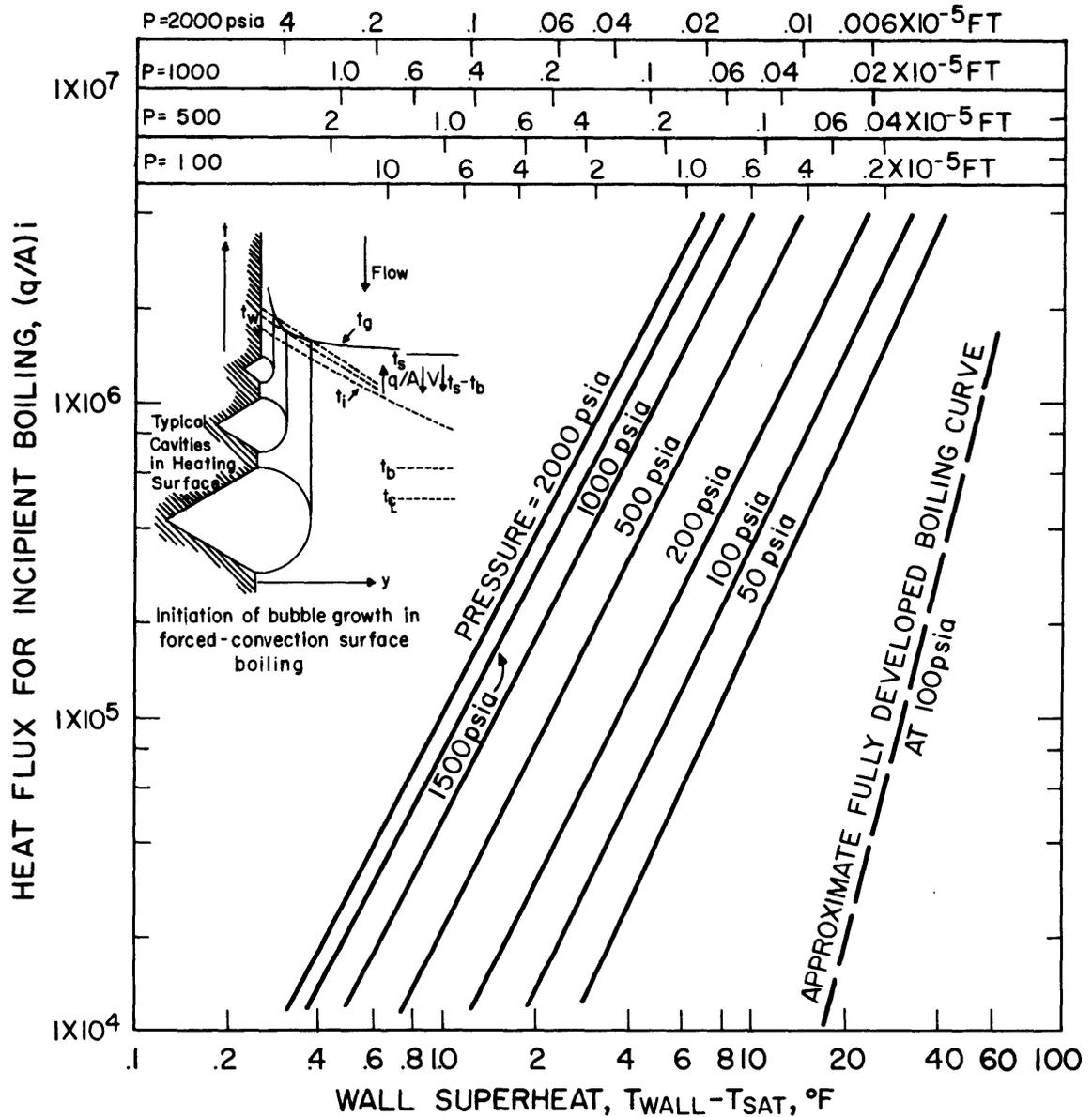


FIGURE 27. BERGLES-ROHSENOW CRITERIA (REF 35) FOR INCIPIENT BOILING $(q/A)_i = 15.60 P^{1.156} (T_{WALL} - T_{SAT})^{2.30} / P^{0.0234}$

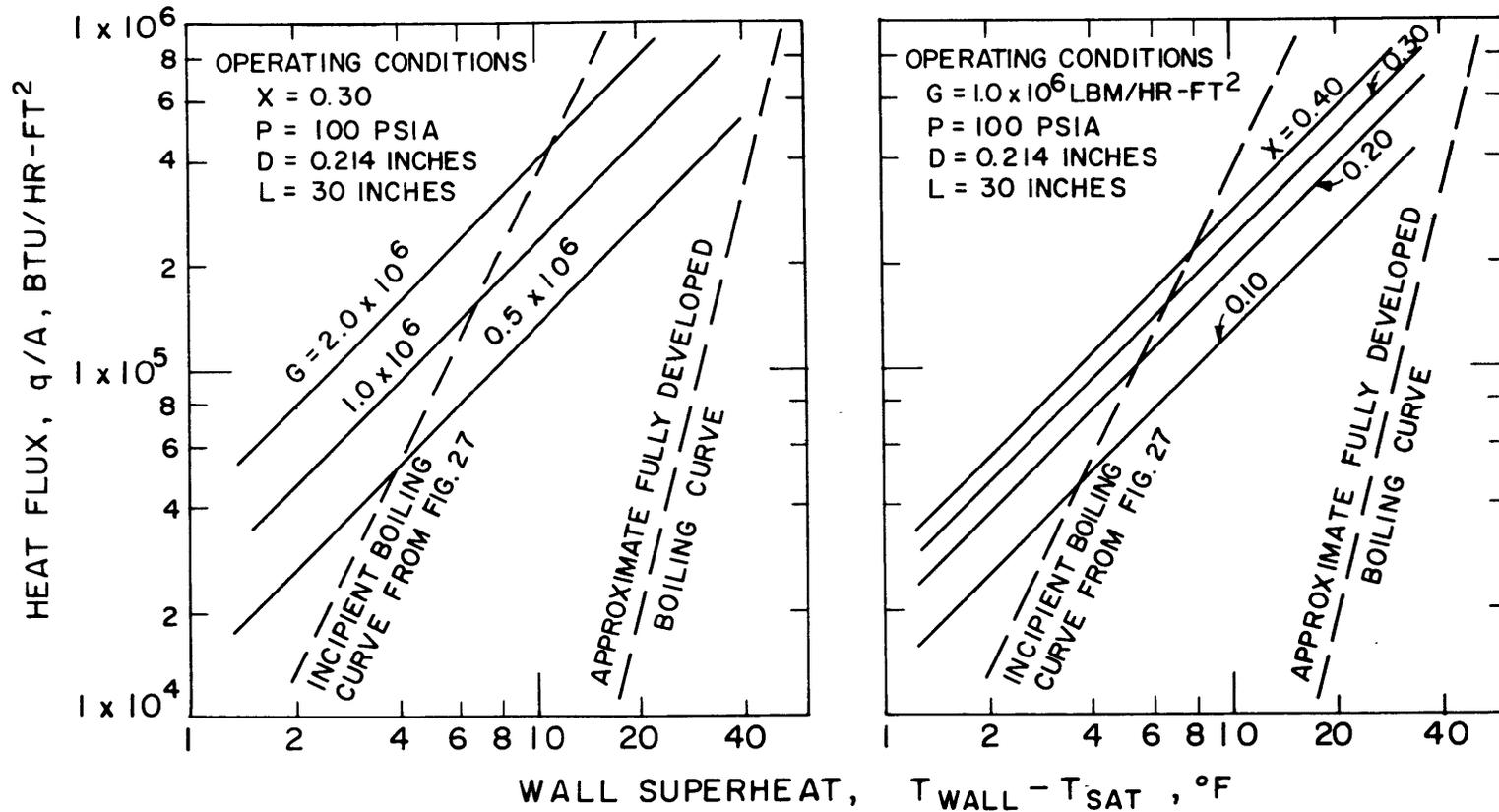


FIGURE 28. VARIATION OF TWO PHASE HEAT TRANSFER COEFFICIENT (h) WITH MASS FLOW RATE (G) AND QUALITY (X)

h_{TP} PER DENGLER-ADDOMS CORRELATION (REF 38)

$$h_{TP} = 3.5h_L (1/X_{tt})^{0.5} \text{ where } h_L = 0.023 \left(\frac{k_L}{D} \right) \left(\frac{GD}{\mu_L} \right)^{0.8} (Pr_L)^{0.4}$$

$$\frac{1}{X_{tt}} = \left(\frac{X}{1-X} \right)^{0.9} \left(\frac{v_v}{v_L} \right)^{0.5} \left(\frac{\mu_v}{\mu_L} \right)^{0.1}$$

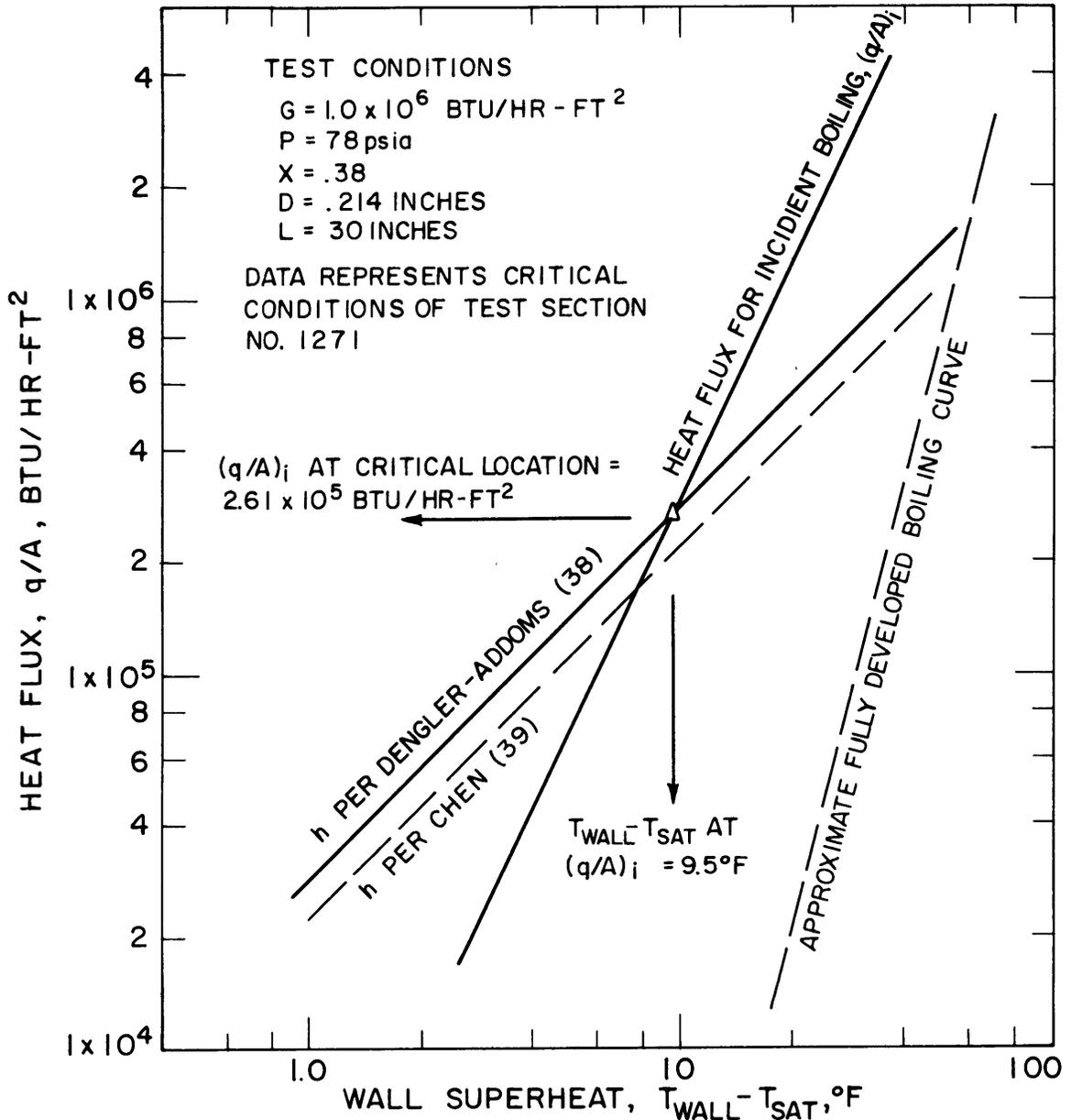


FIGURE 29. TYPICAL DETERMINATION OF HEAT FLUX REQUIRED FOR INCIPIENT BOILING, $(q/A)_i$, AT THE CRITICAL LOCATION

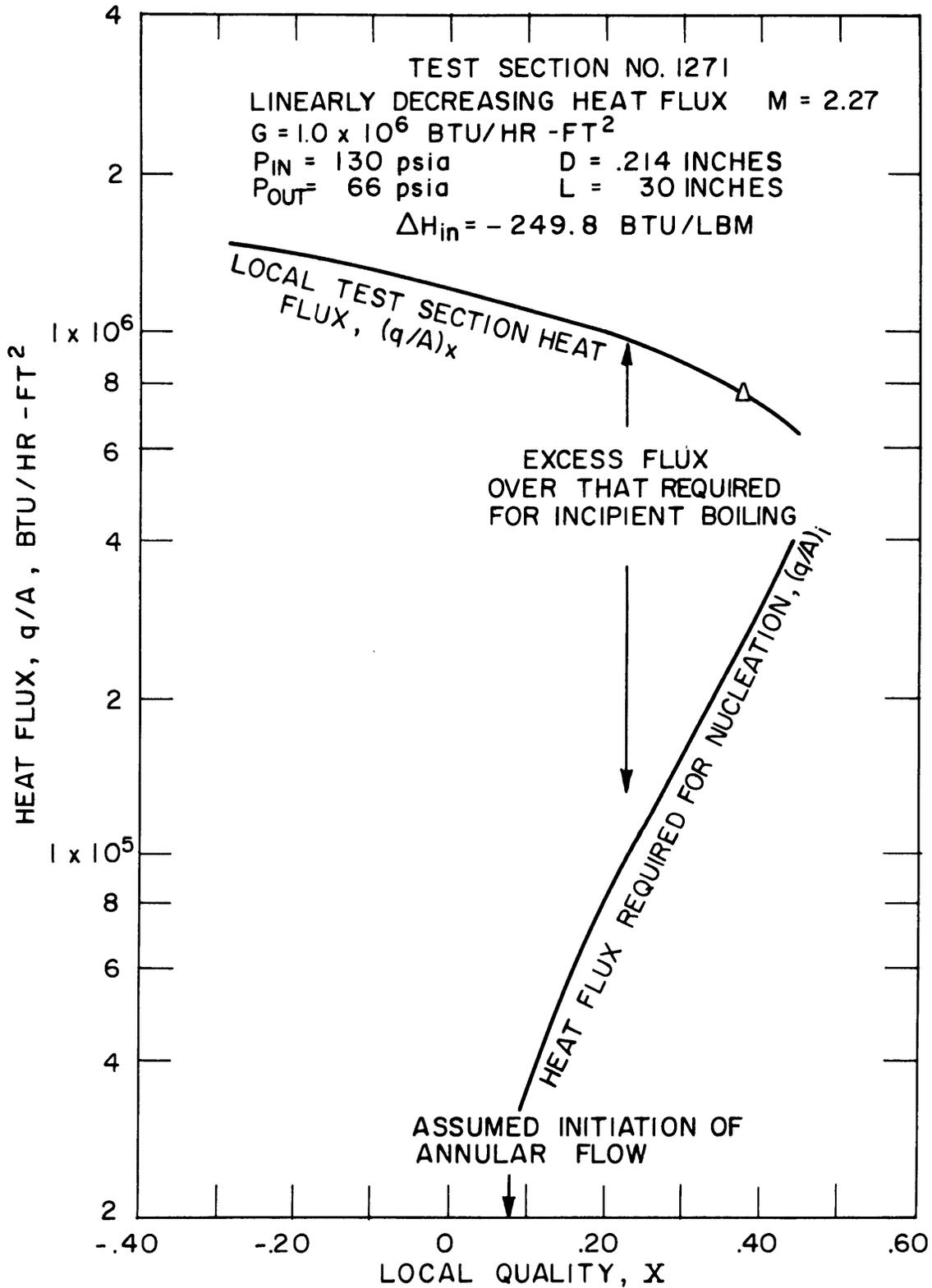


FIGURE 30. HEAT FLUX CONDITIONS ALONG TEST SECTION LENGTH

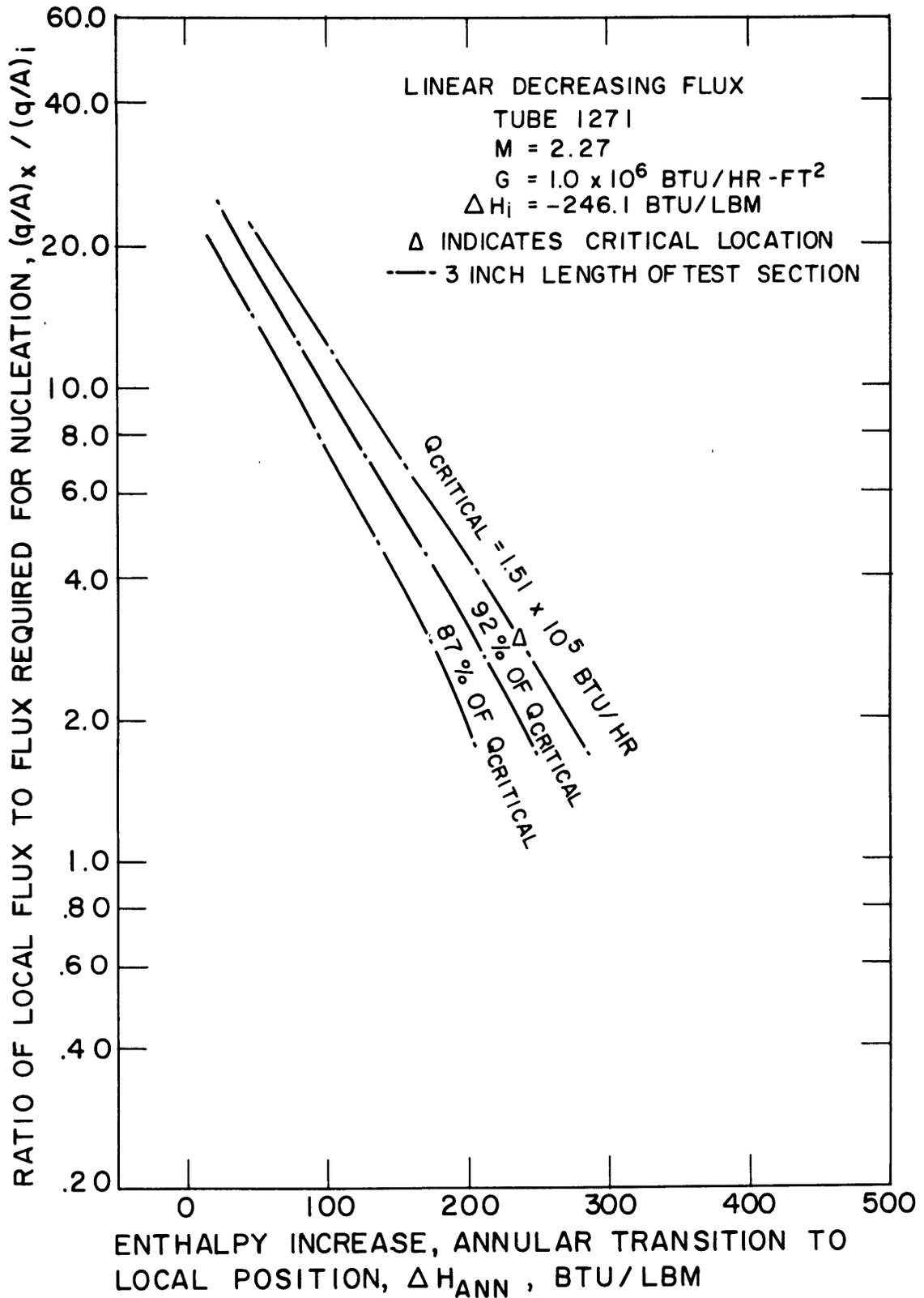


FIGURE 31. OPERATING LINES FOR TEST SECTION 1271 FOR Q_{TOT} EQUAL TO AND LESS THAN Q_{CRIT}

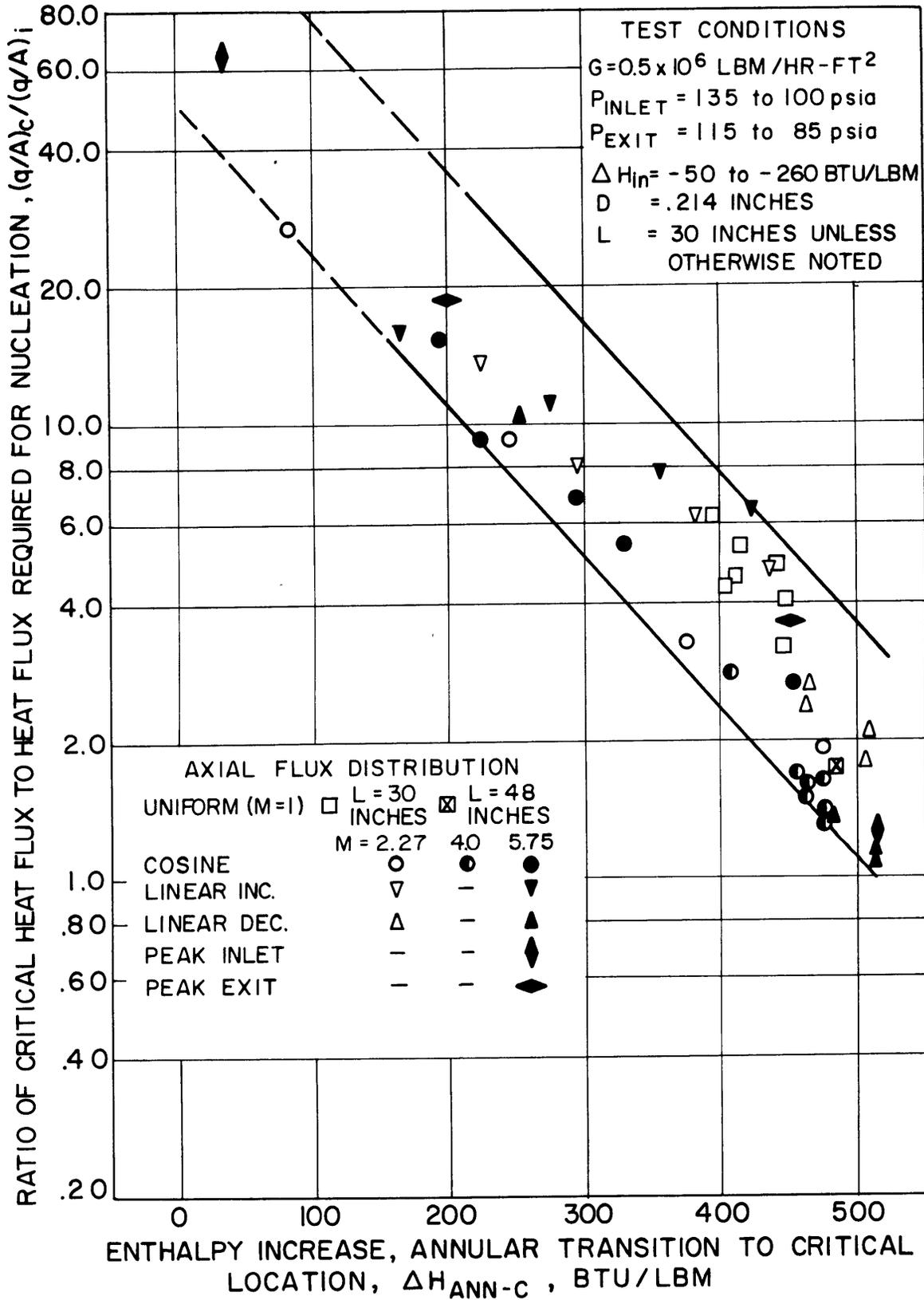


FIGURE 32. CRITICAL FLUX RESULTS AT $G = 0.5 \times 10^6$ LBM/HR-FT²

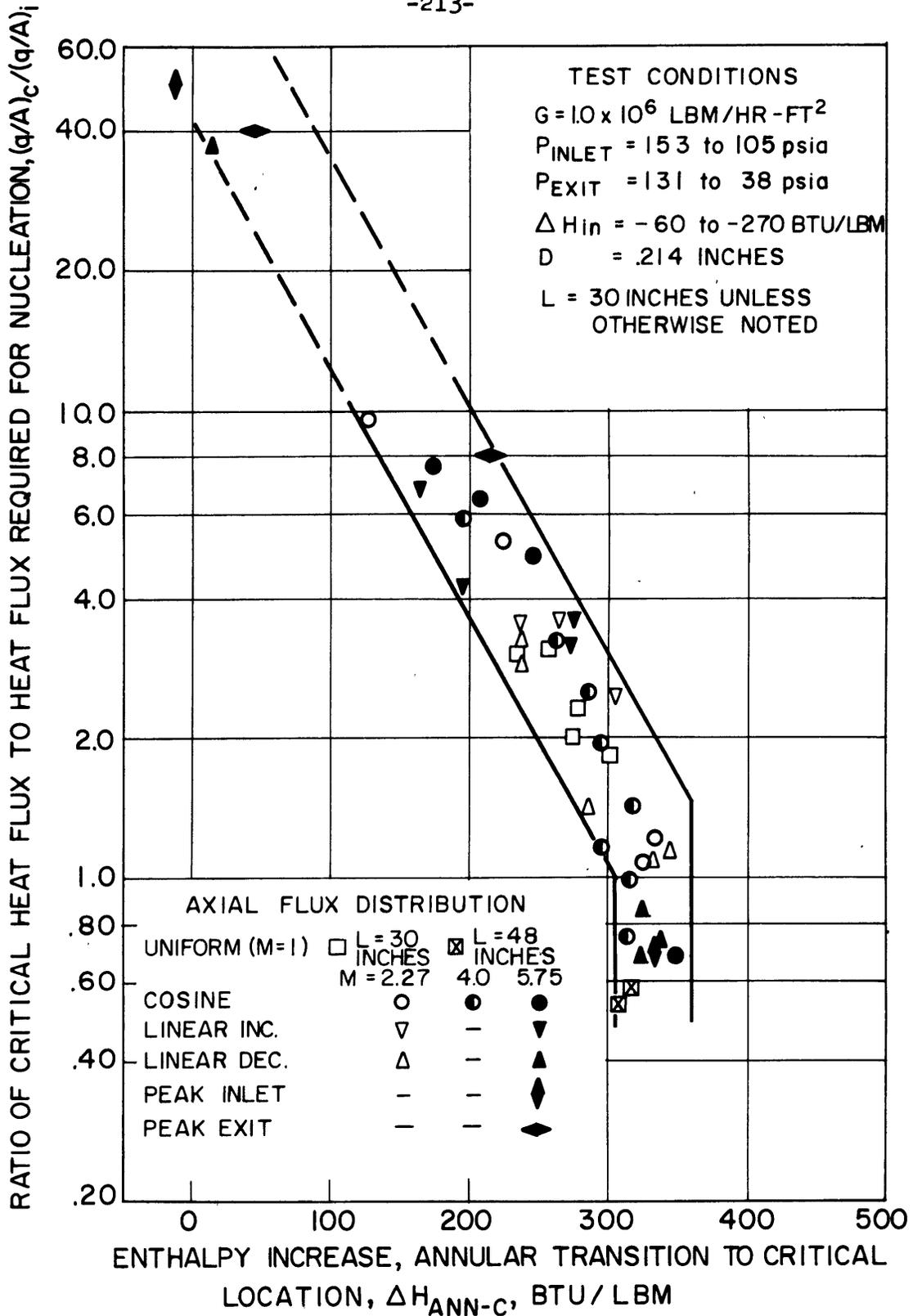


FIGURE 33. CRITICAL FLUX RESULTS AT $G = 1.0 \times 10^6$ LBM/HR-FT²

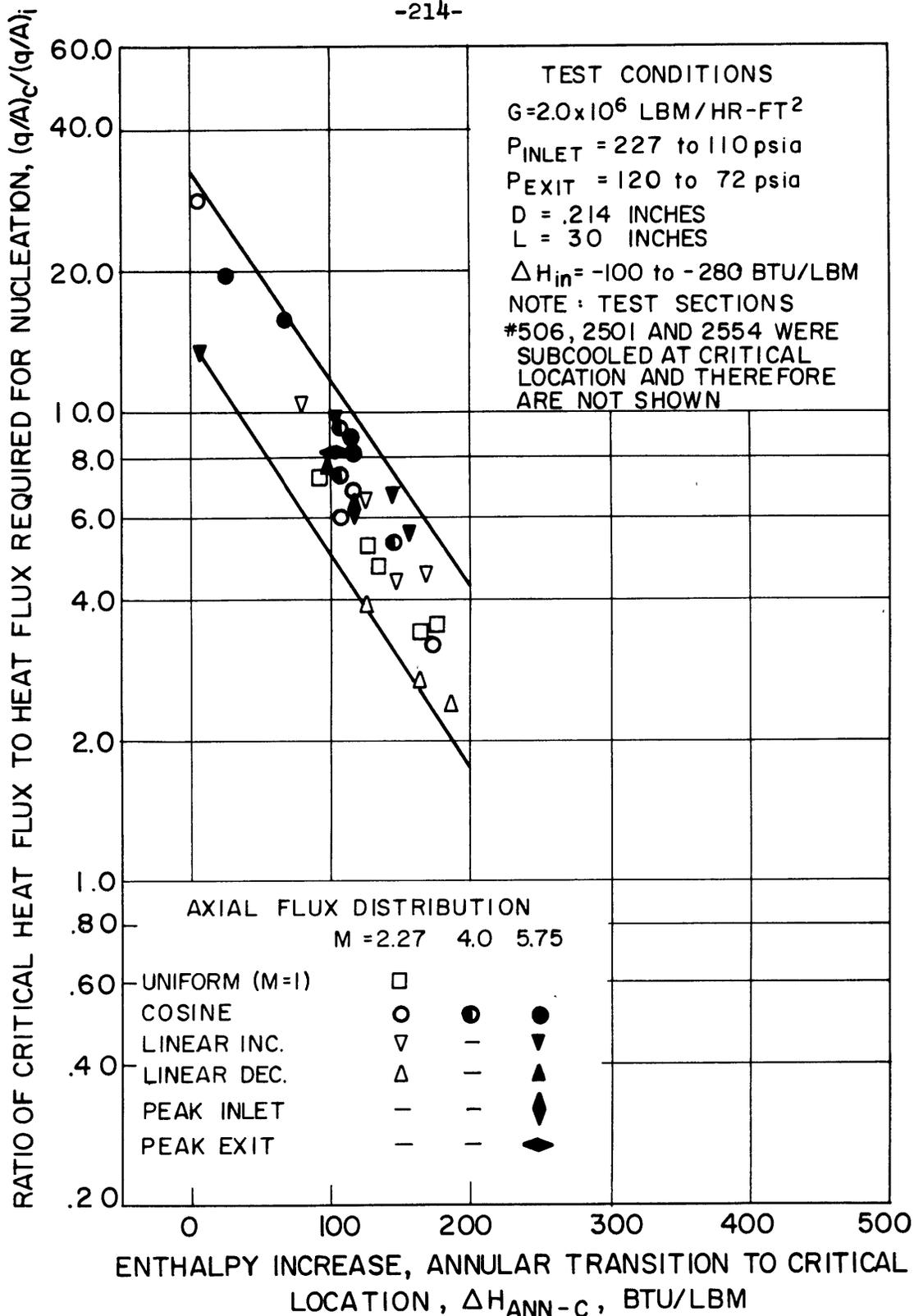


FIGURE 34. CRITICAL FLUX RESULTS AT $G = 2.0 \times 10^6$ LBM/HR-FT²

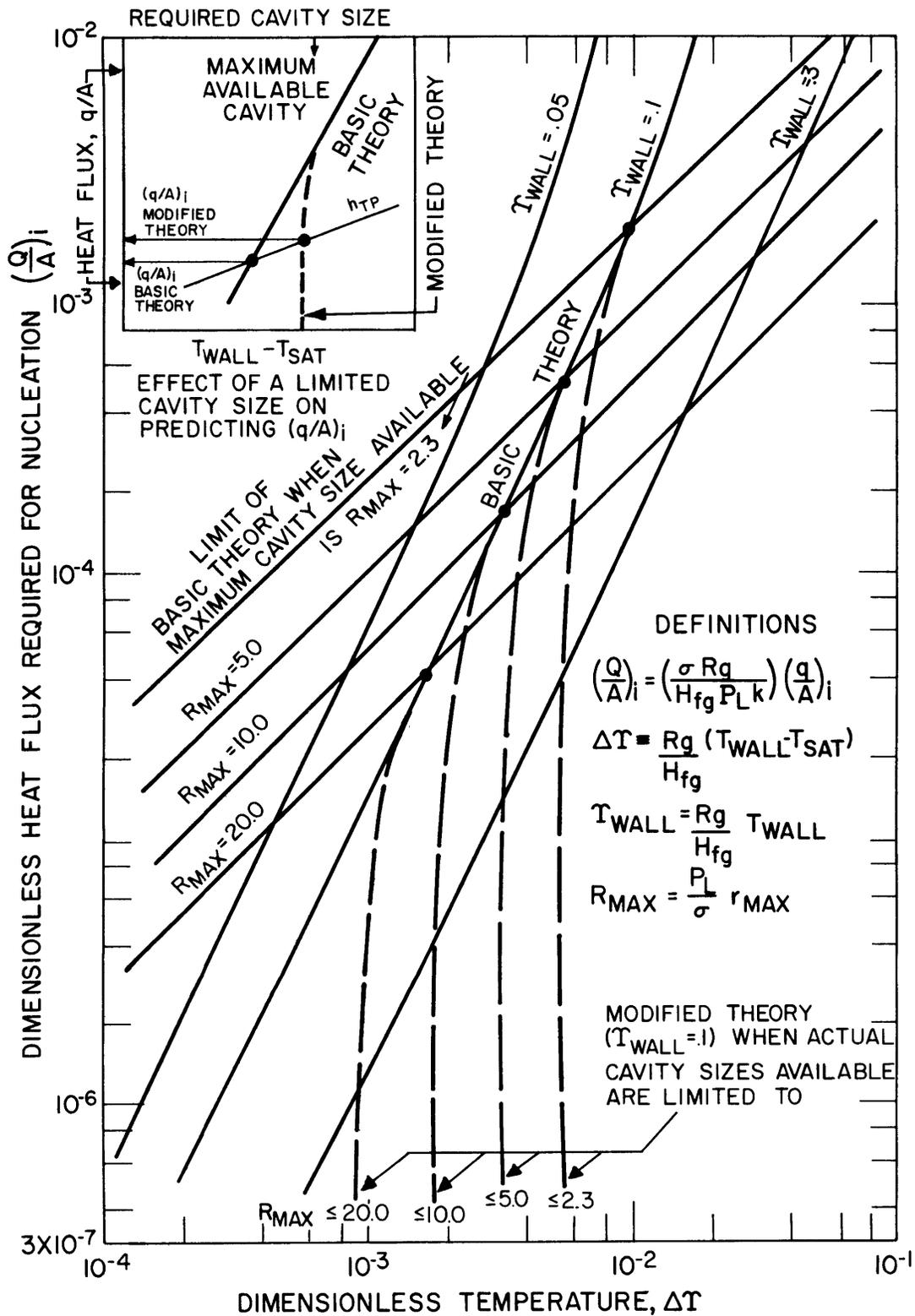


FIGURE 35. DIMENSIONLESS REPRESENTATION OF BERGLES-ROHSENOW NUCLEATION THEORY. THE EFFECT OF LIMITED MAXIMUM CAVITY SIZES IS SHOWN FOR P=100 psia ($T_w \sim .1$) ONLY

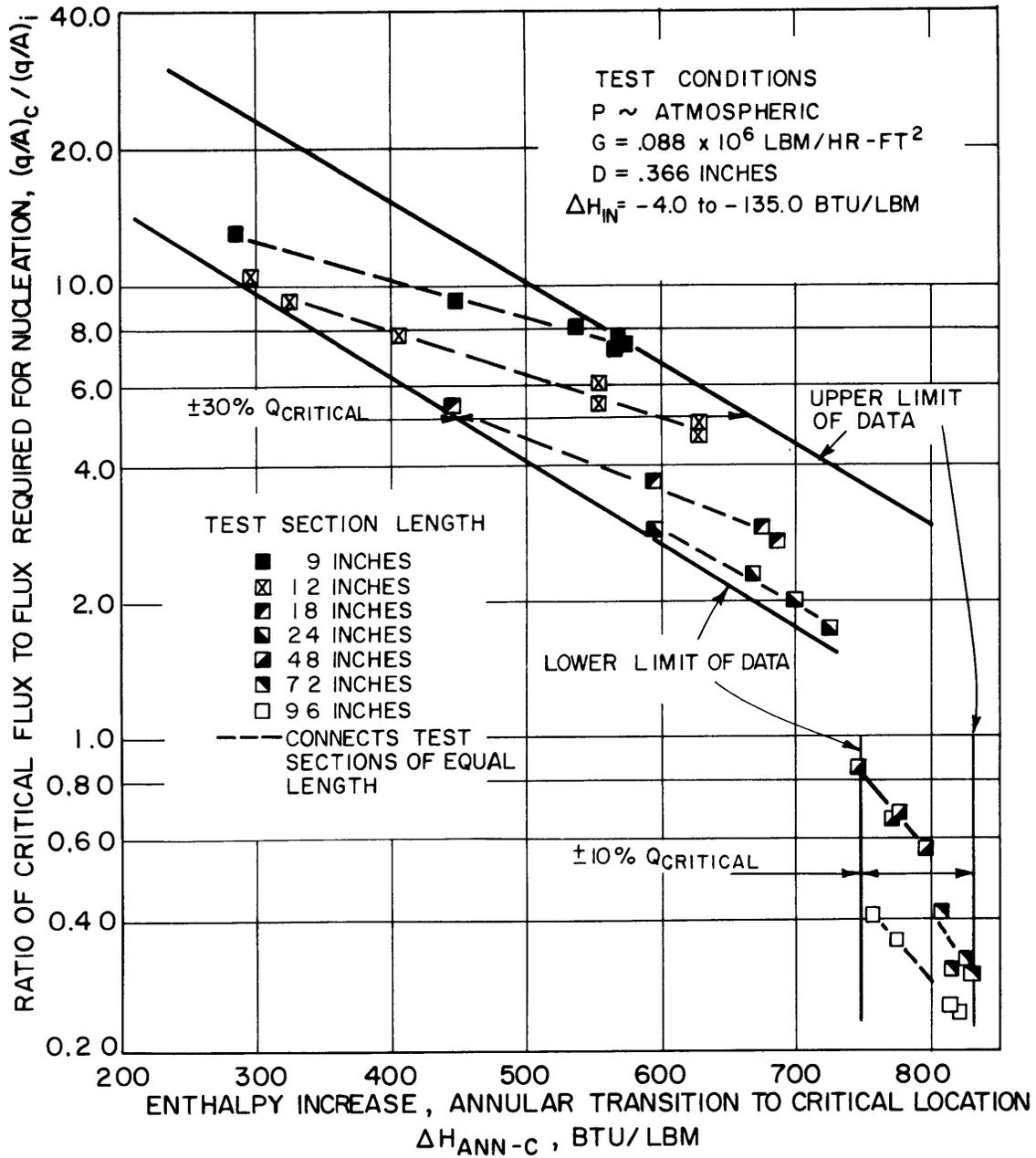


FIGURE 36. UNIFORM FLUX DISTRIBUTION DATA OF HEWITT ET AL. (REF41)

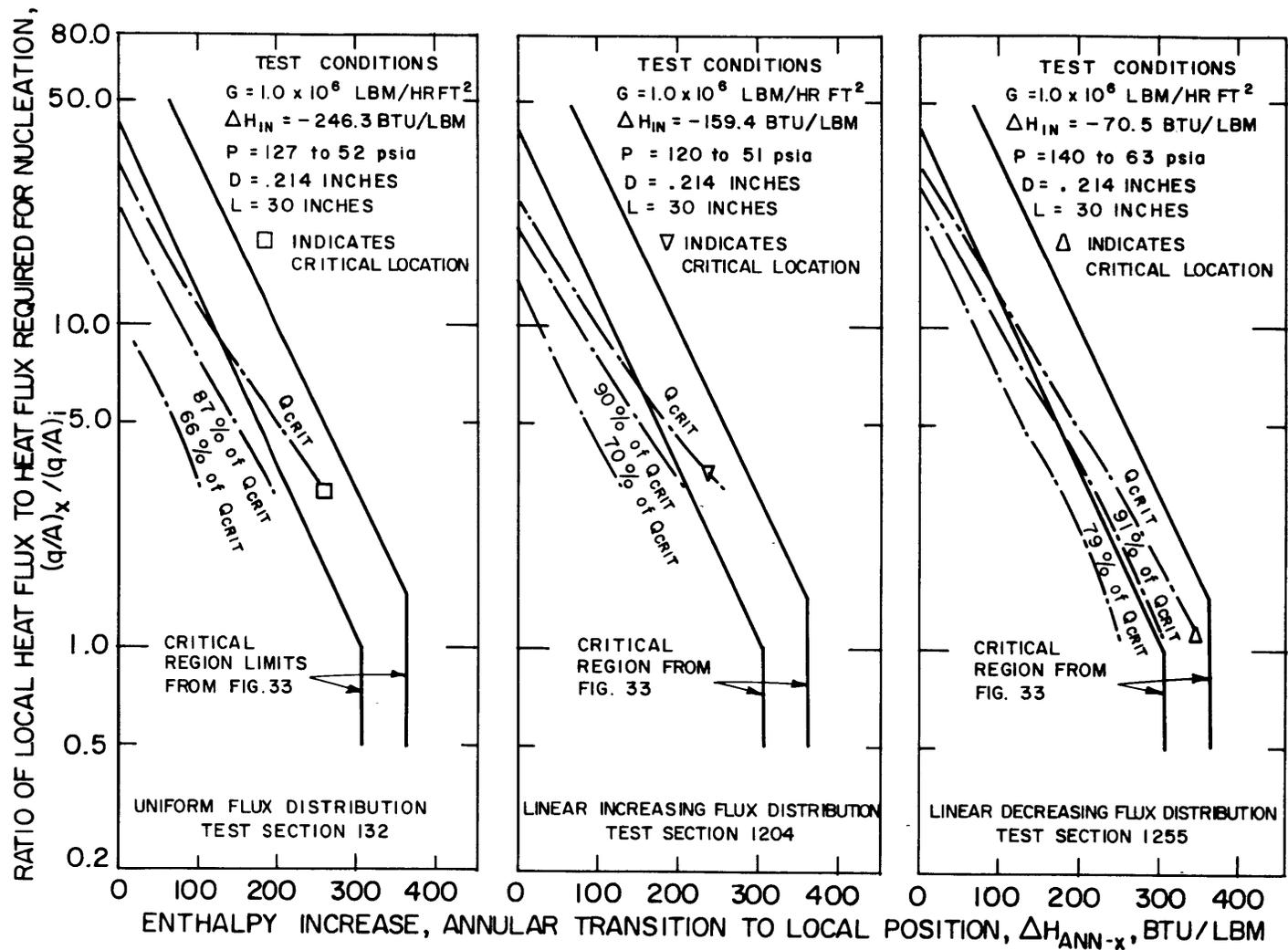


FIGURE 37. OPERATING HISTORIES FOR TOTAL INPUT POWER UP TO THE CRITICAL POWER (UNIFORM AND LINEAR FLUX DISTRIBUTIONS)

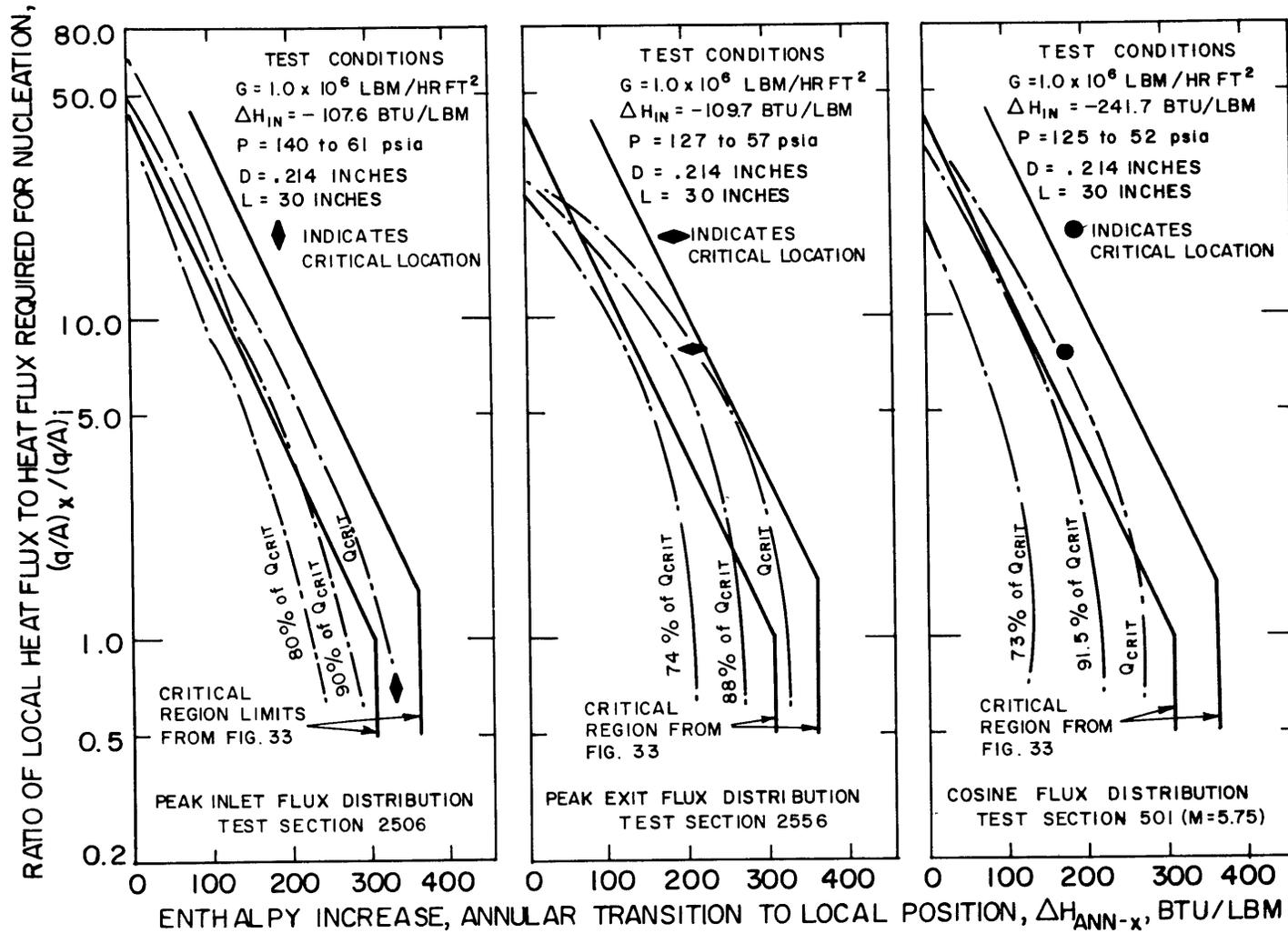


FIGURE 38. OPERATING HISTORIES FOR TOTAL INPUT POWER UP TO THE CRITICAL POWER (COSINE AND PEAKED FLUX DISTRIBUTIONS)

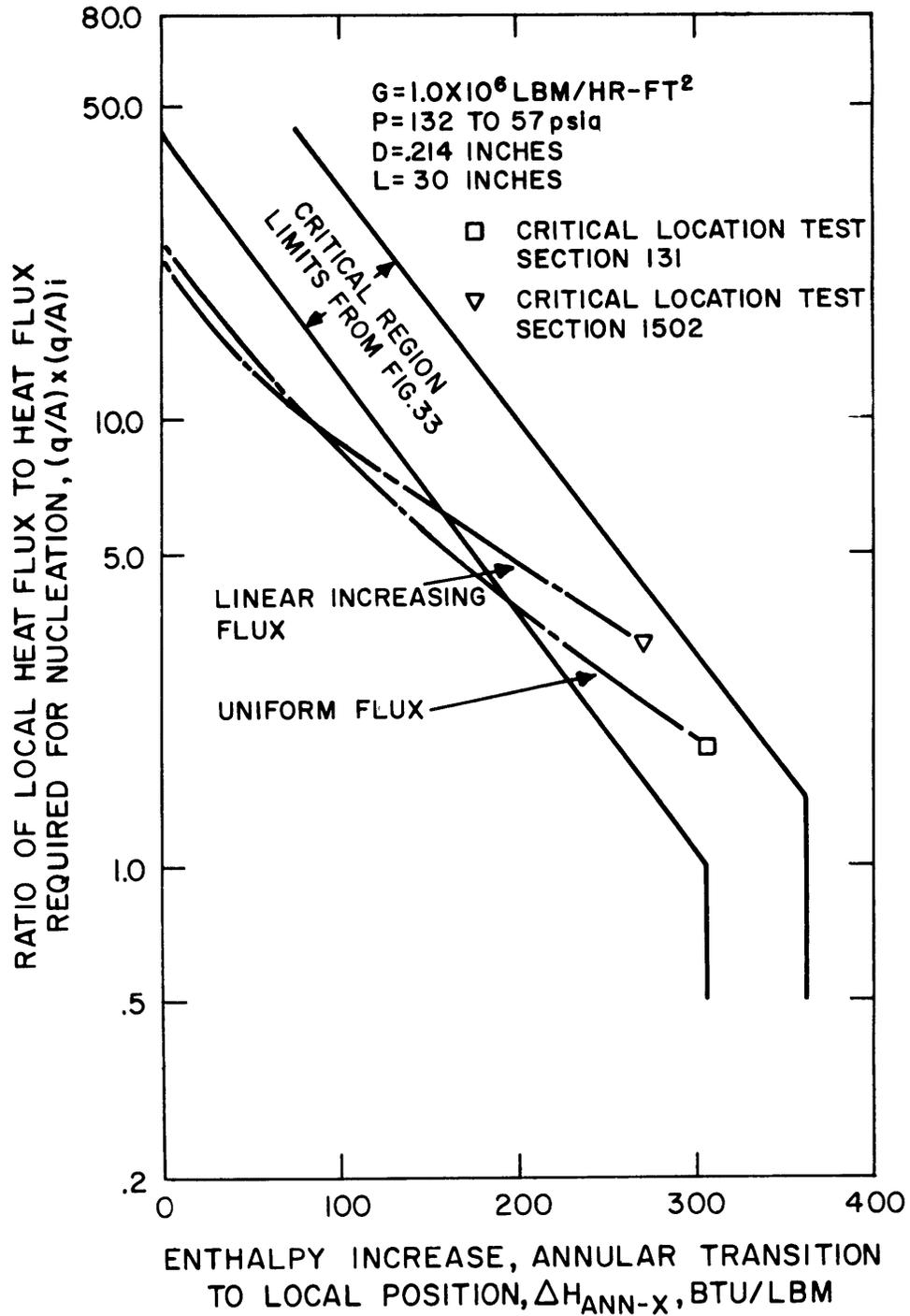


FIGURE 39. EFFECT OF AXIAL FLUX DISTRIBUTION ON THE CRITICAL LOCATION

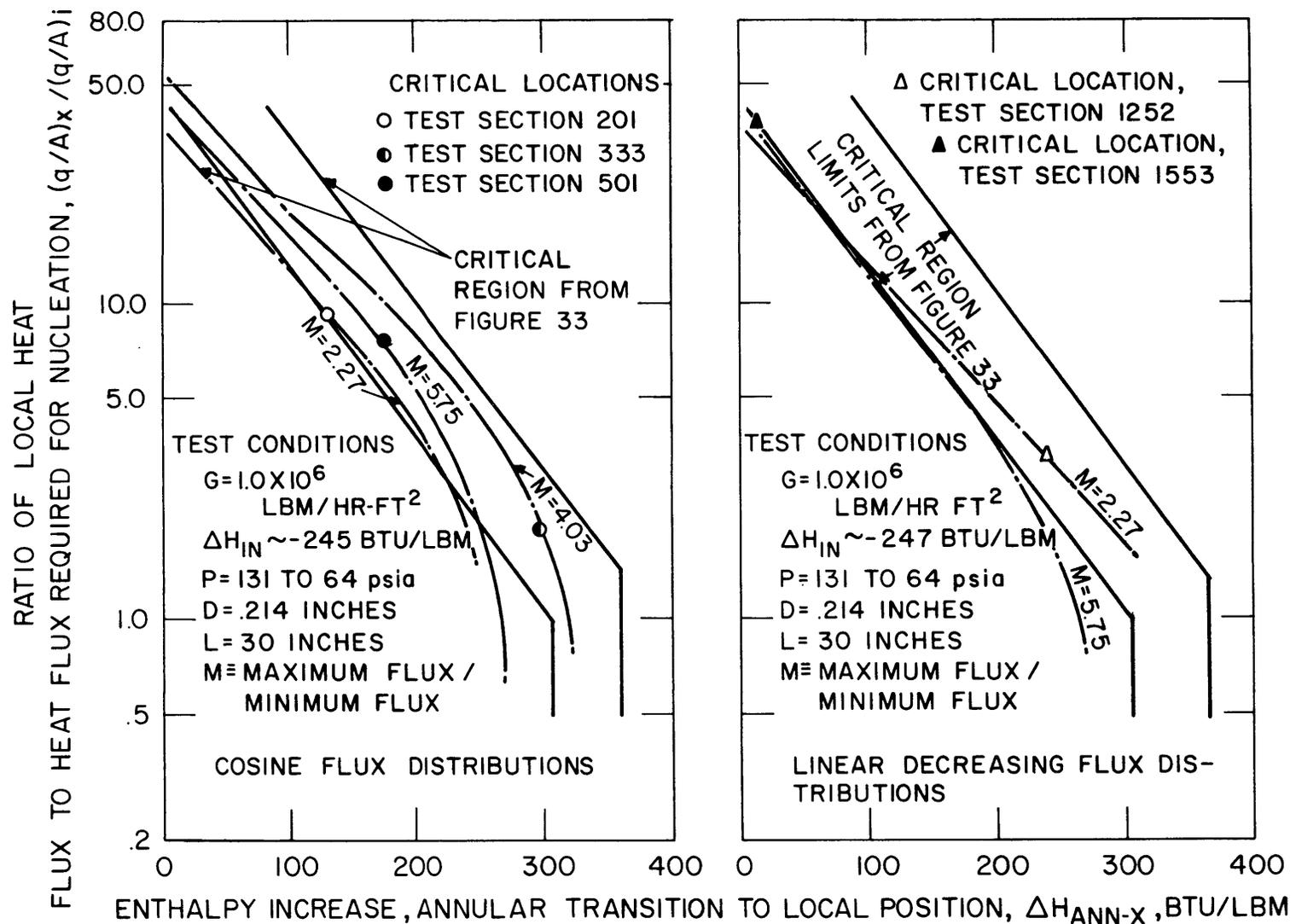


FIGURE 40. THE EFFECT OF M VALUE (RATIO OF MAXIMUM TO MINIMUM FLUX) ON THE CRITICAL LOCATION

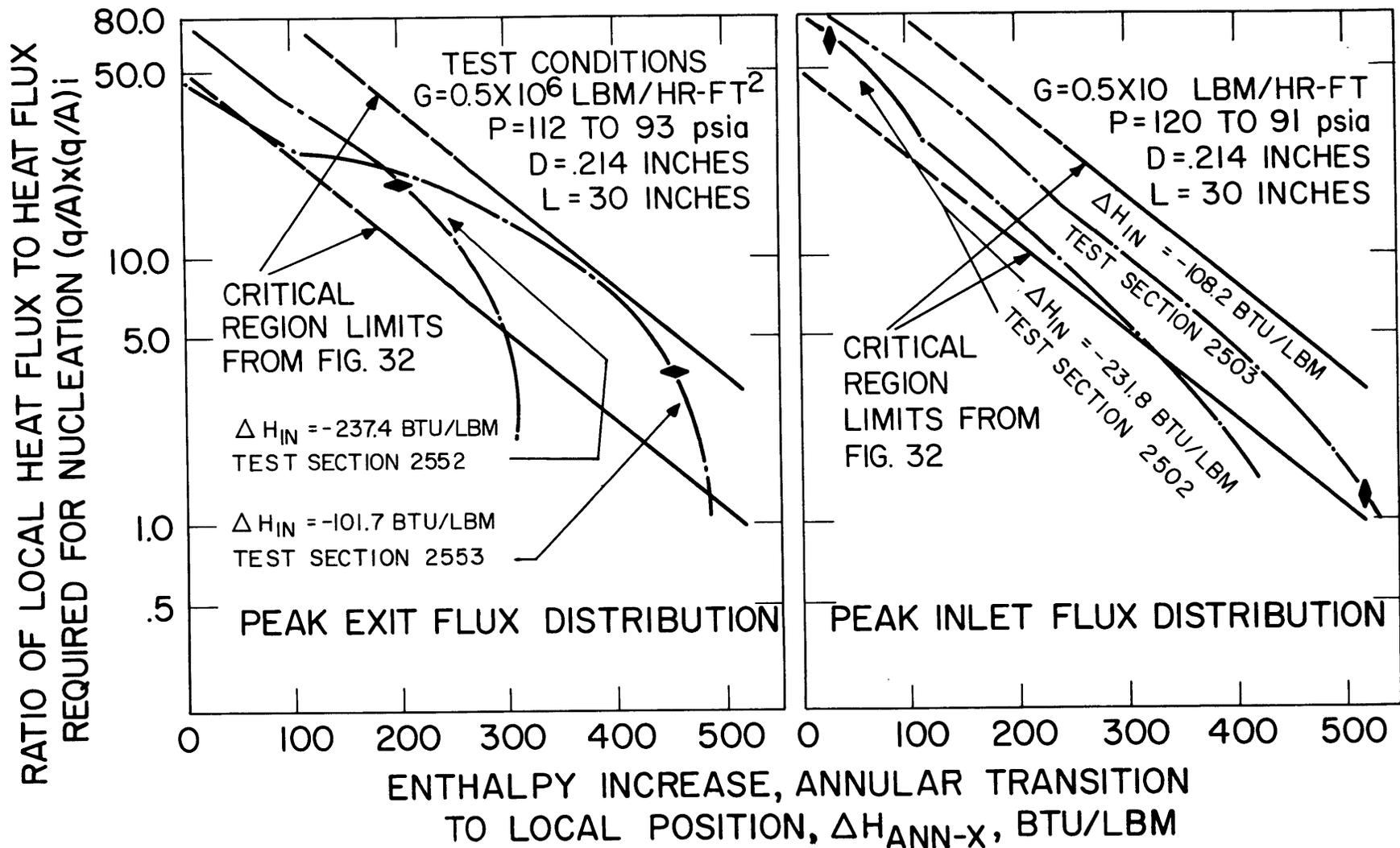


FIGURE 41. THE EFFECT OF INLET SUBCOOLING ON THE CRITICAL LOCATION (PEAK EXIT AND INLET FLUX DISTRIBUTIONS)

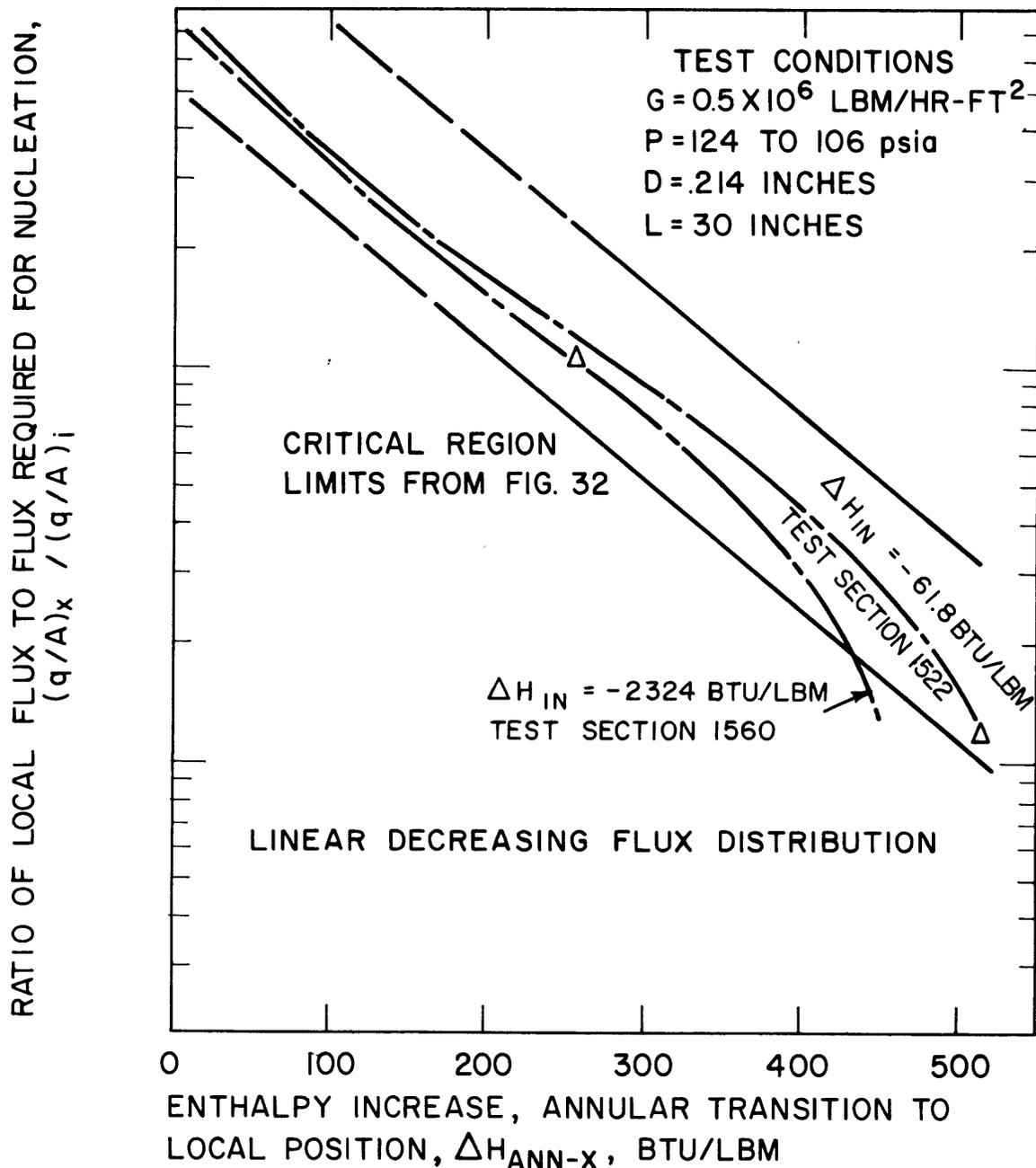


FIGURE 42. THE EFFECT OF INLET SUBCOOLING ON THE CRITICAL LOCATION (LINEAR DECREASING FLUX DISTRIBUTION)

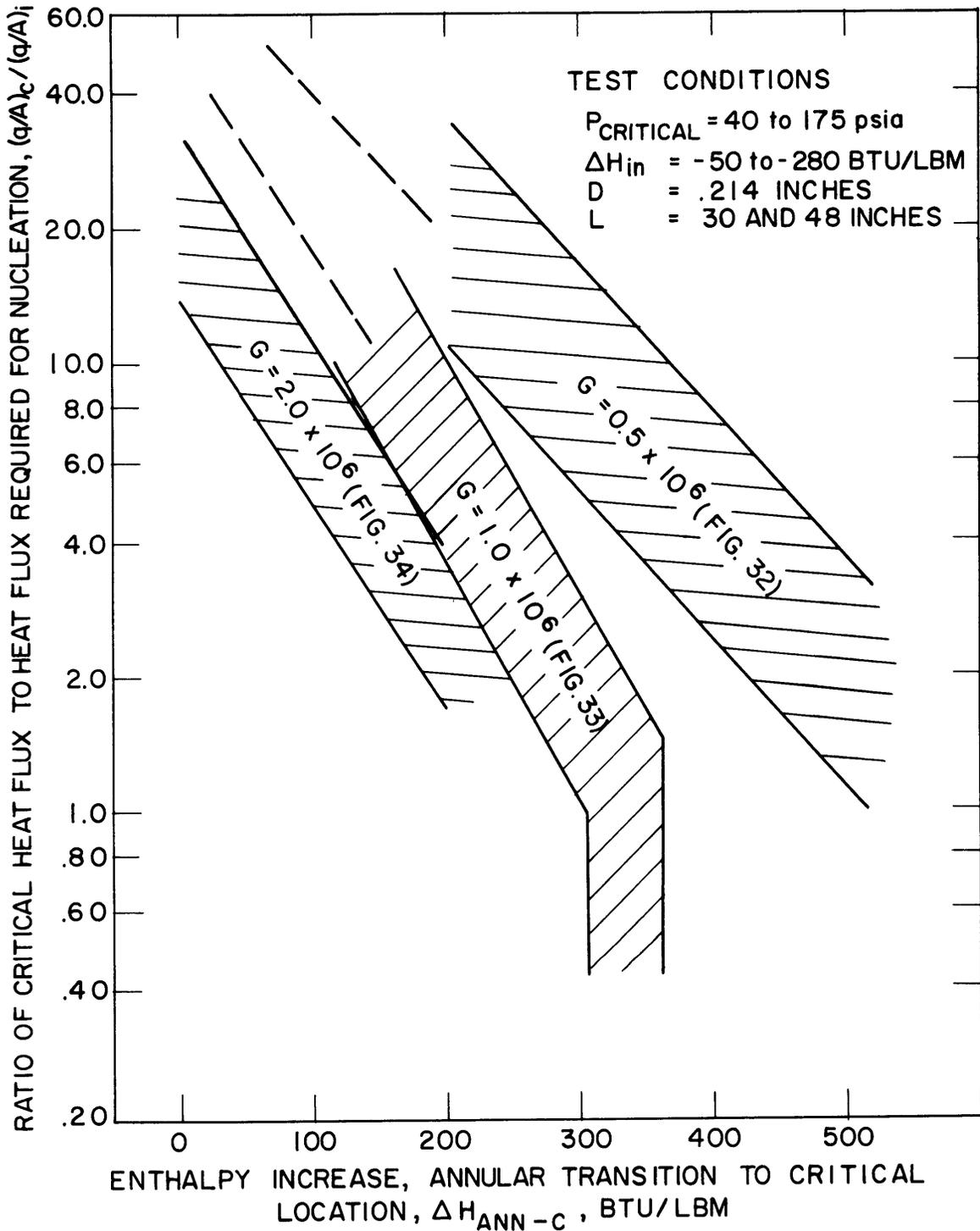


FIGURE 43. COMPARISON OF CRITICAL FLUX RESULTS FOR THE RANGE OF MASS VELOCITIES INVESTIGATED

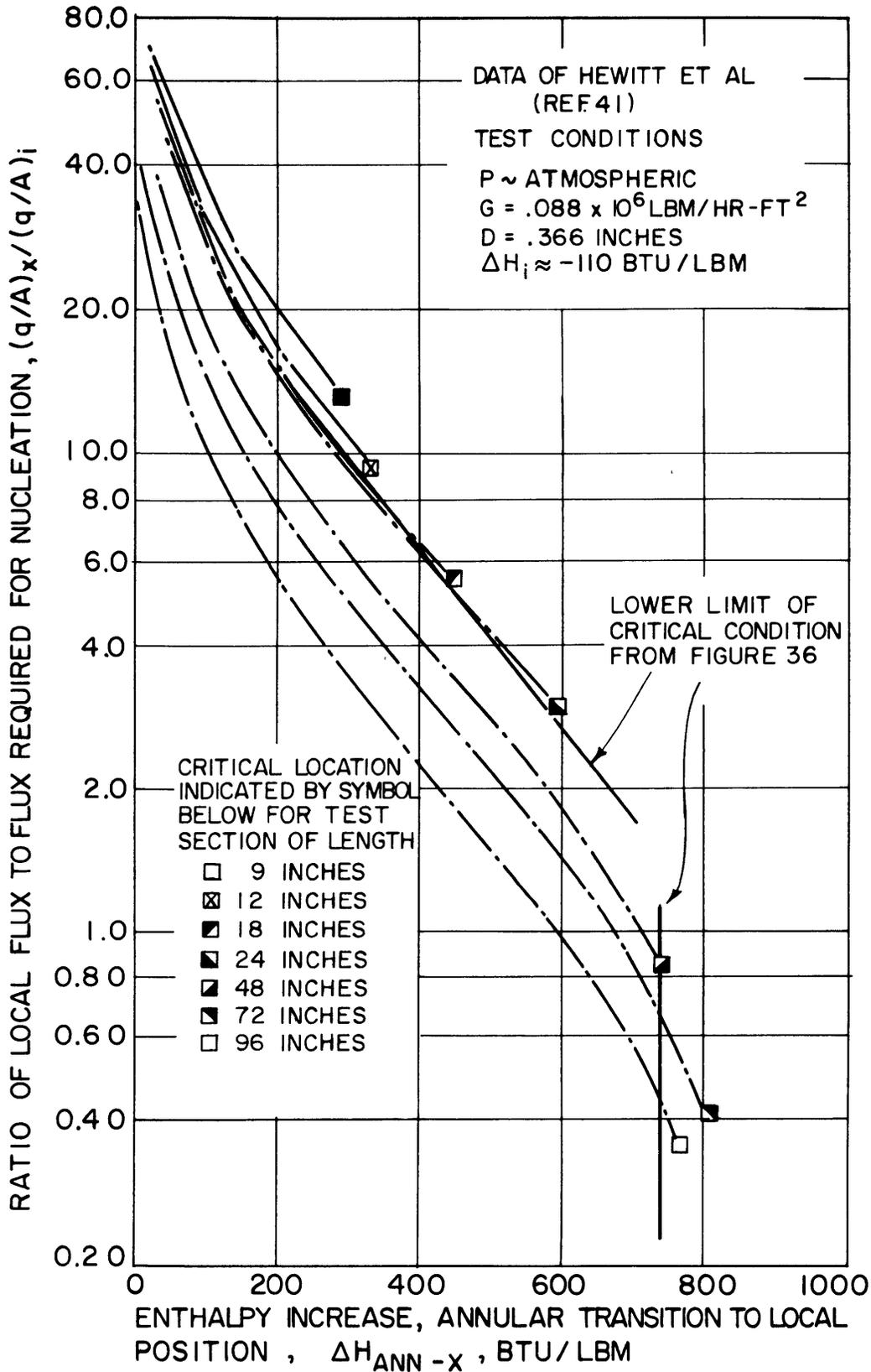


FIGURE 44. EFFECT OF LENGTH ON THE CRITICAL CONDITION

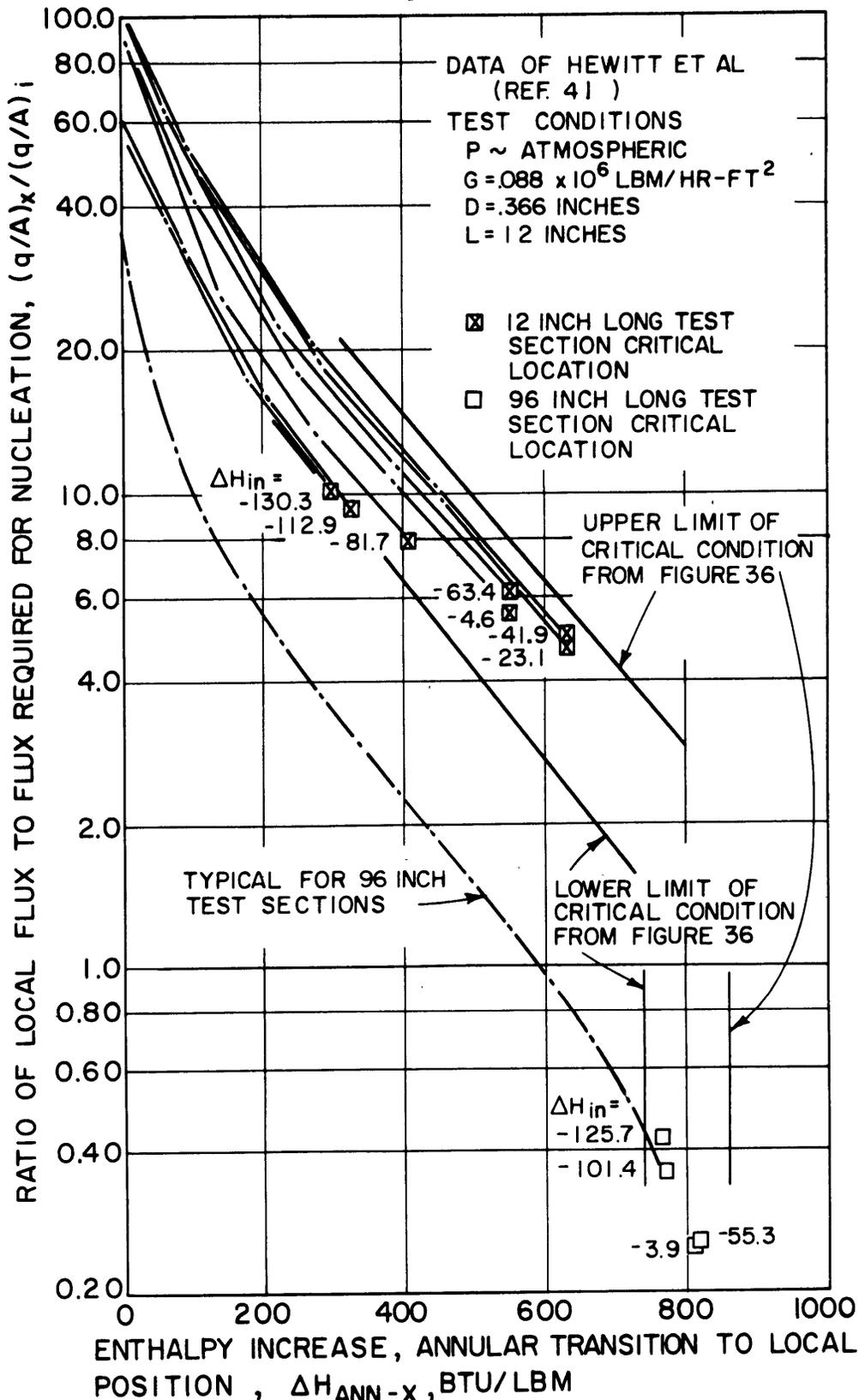


FIGURE 45. EFFECT OF INLET SUBCOOLING ON THE CRITICAL CONDITION

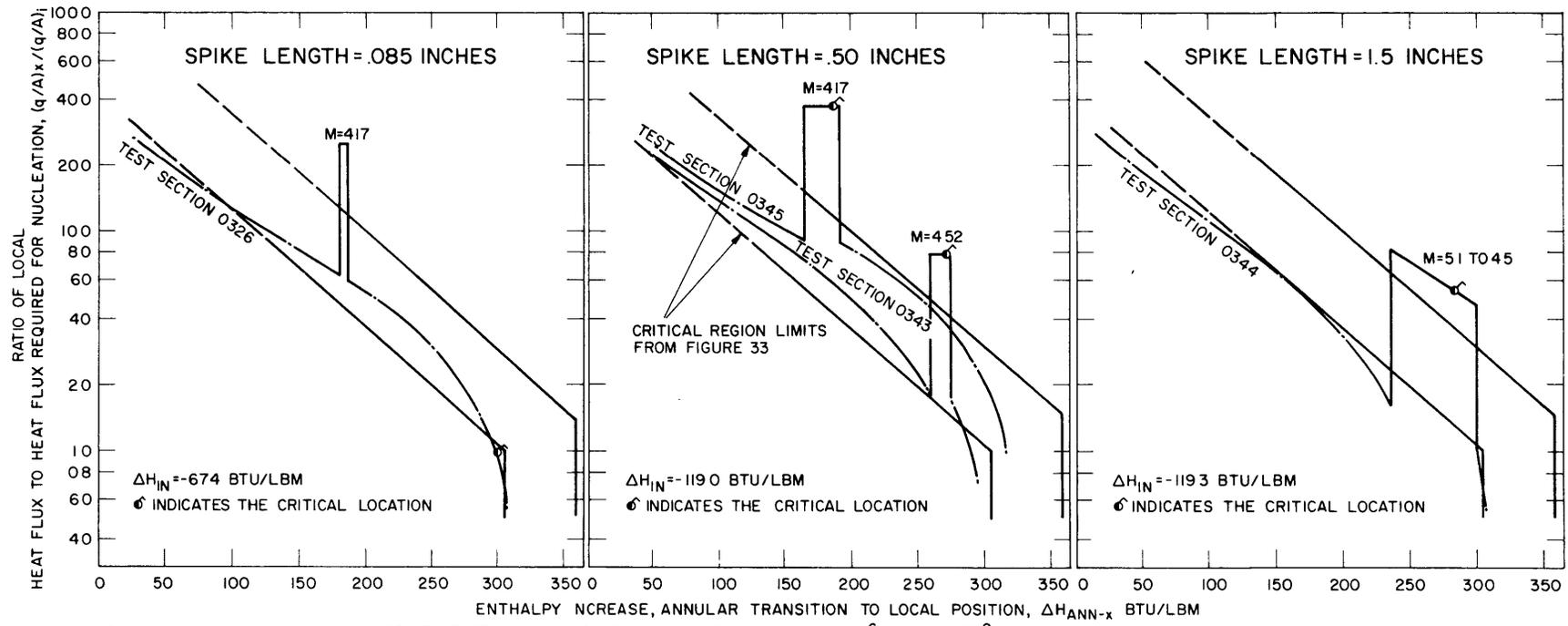


FIGURE 46 THE EFFECT OF FLUX SPIKE LENGTH ON THE CRITICAL CONDITION FOR $G=10 \times 10^6$ LBM/HR-FT²

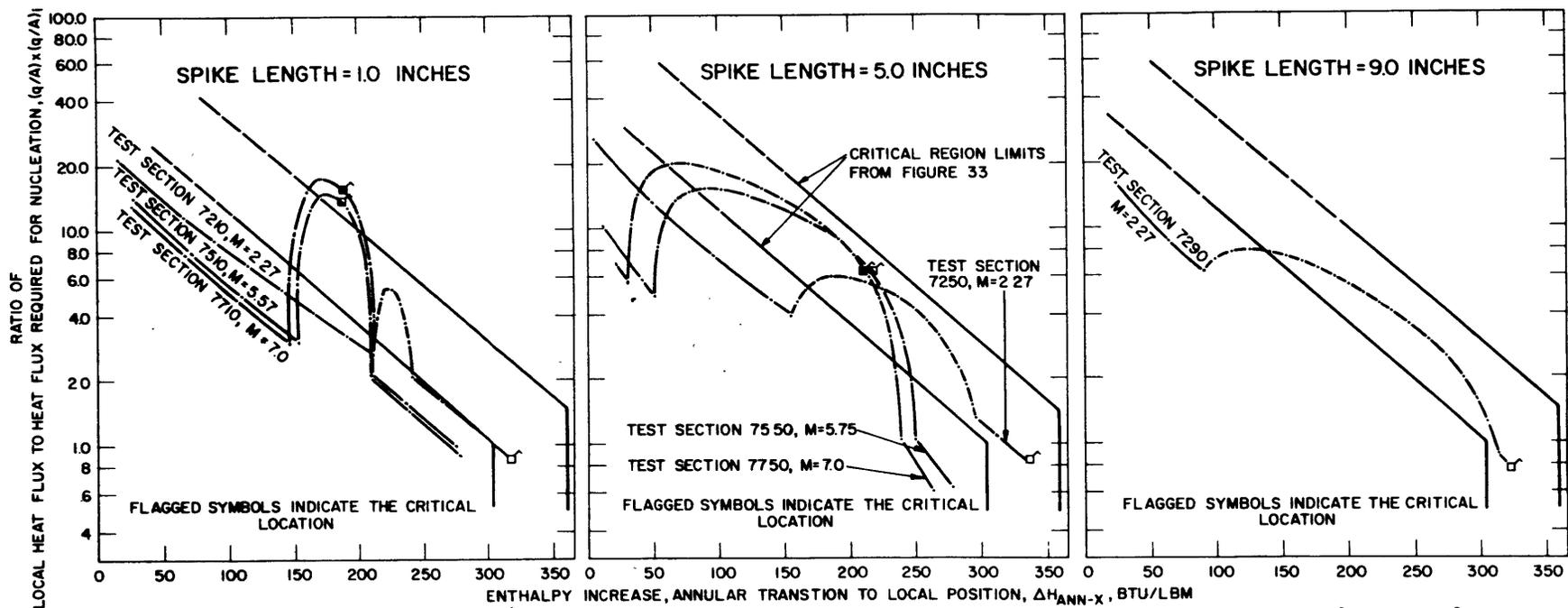


FIGURE 47. THE EFFECT OF FLUX SPIKE LENGTH AND M VALUE (RATIO OF MAXIMUM TO MINIMUM FLUX) ON THE CRITICAL CONDITION FOR $G = 1.0 \times 10^6$ LBM/HR-FT² AND $\Delta H_{IN} \approx -110$ BTU/LBM

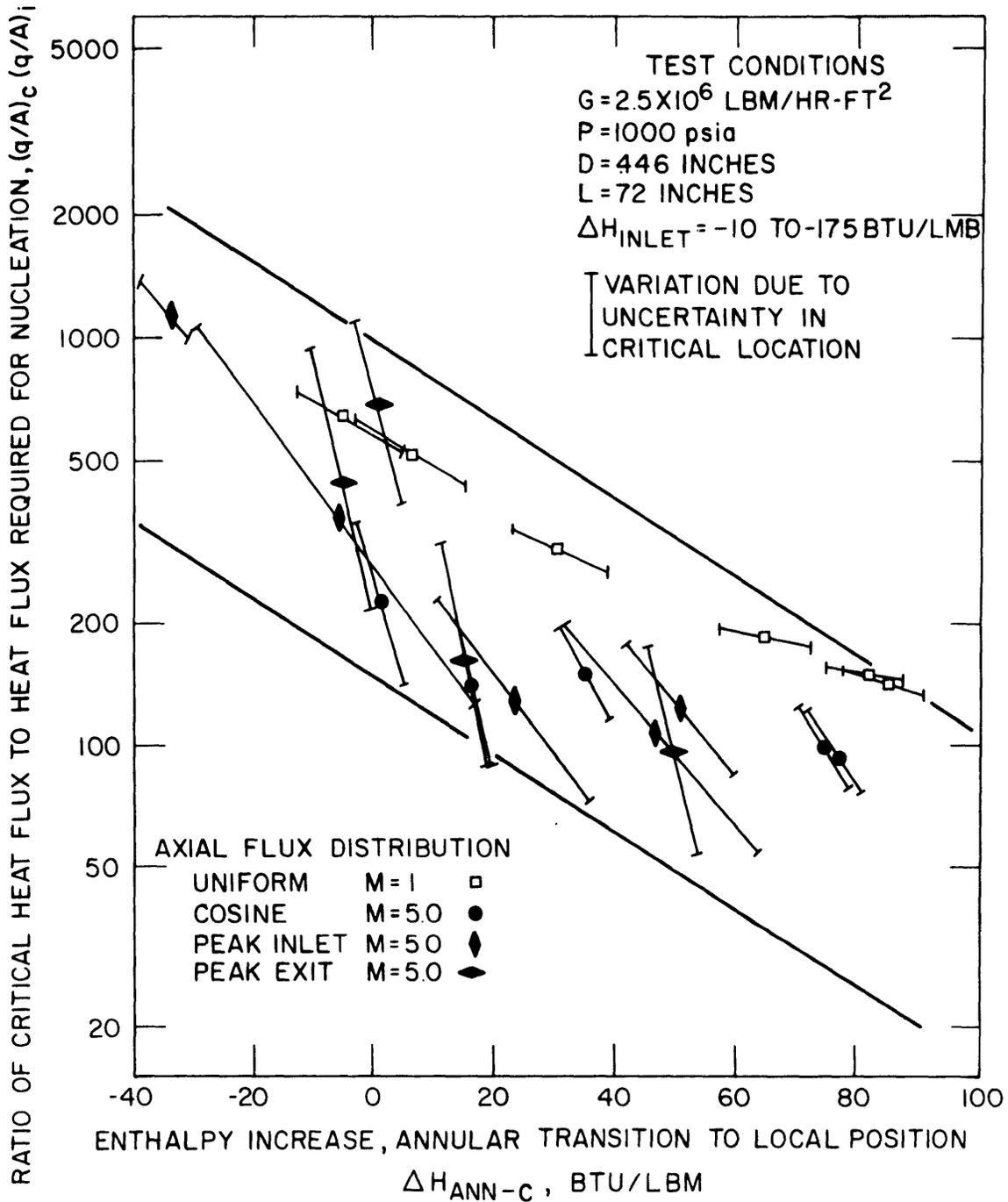


FIGURE 48. CRITICAL FLUX RESULTS AT 1000 PSIA FROM BABCOCK AND WILCOX DATA (REFERENCE 15)

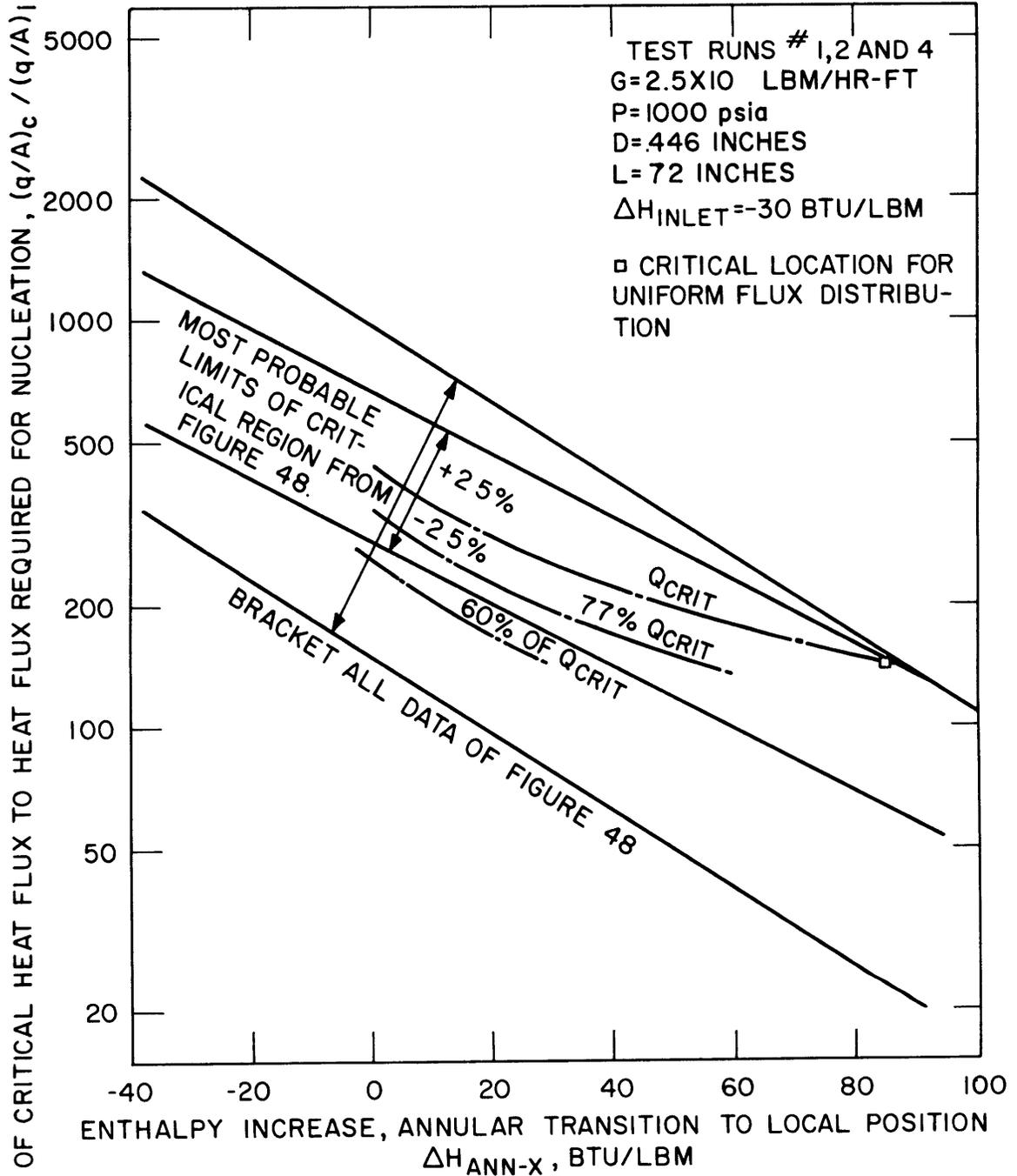


FIGURE 49. ESTIMATION OF THE CRITICAL REGION WIDTH (IN % TOTAL INPUT POWER) OF FIGURE 48 FOR 1000 psia DATA (REFERENCE 15)

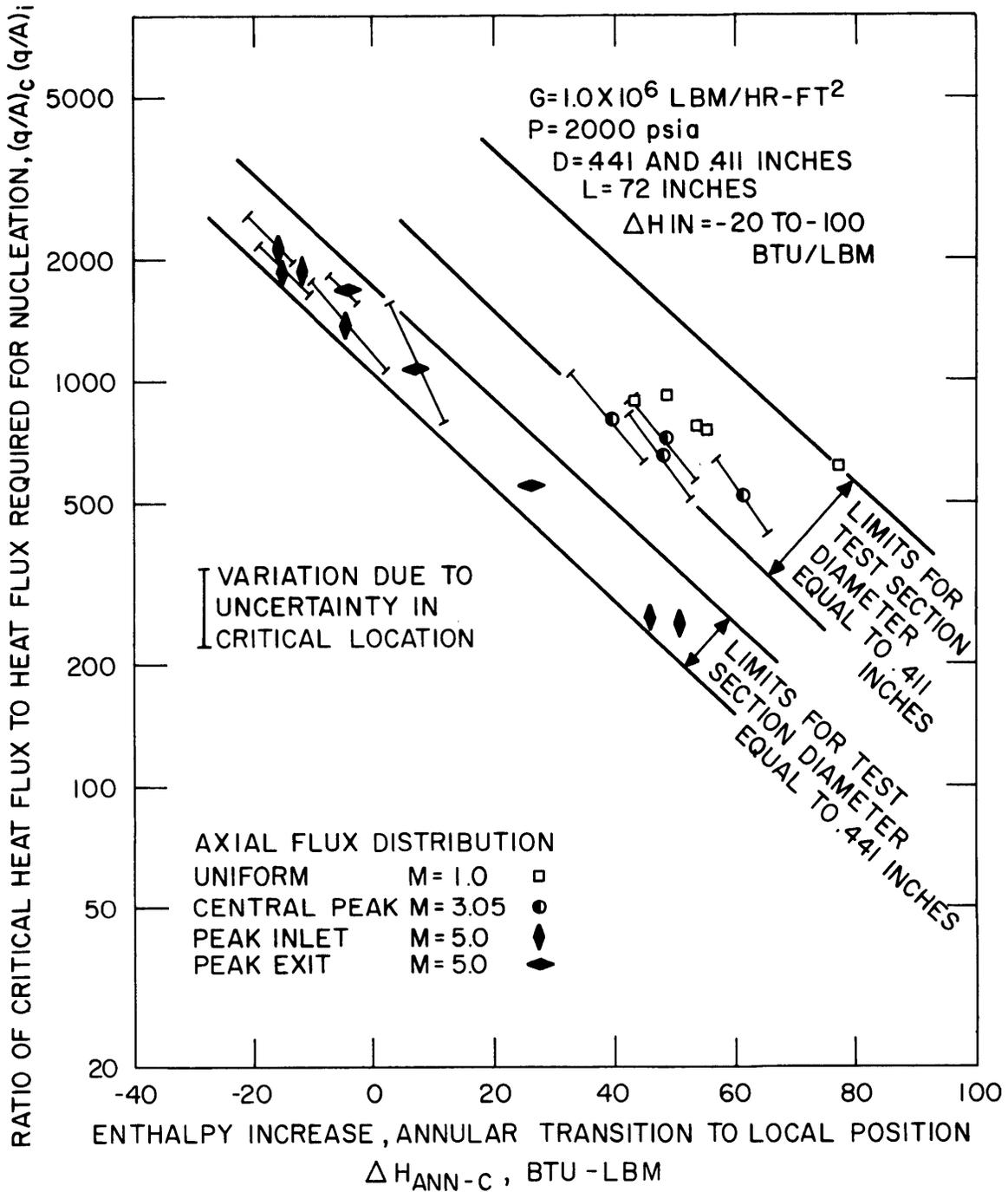


FIGURE 50. CRITICAL FLUX RESULTS AT 2000 PSIA FROM BABCOCK AND WILCOX DATA (REFERENCE 5)

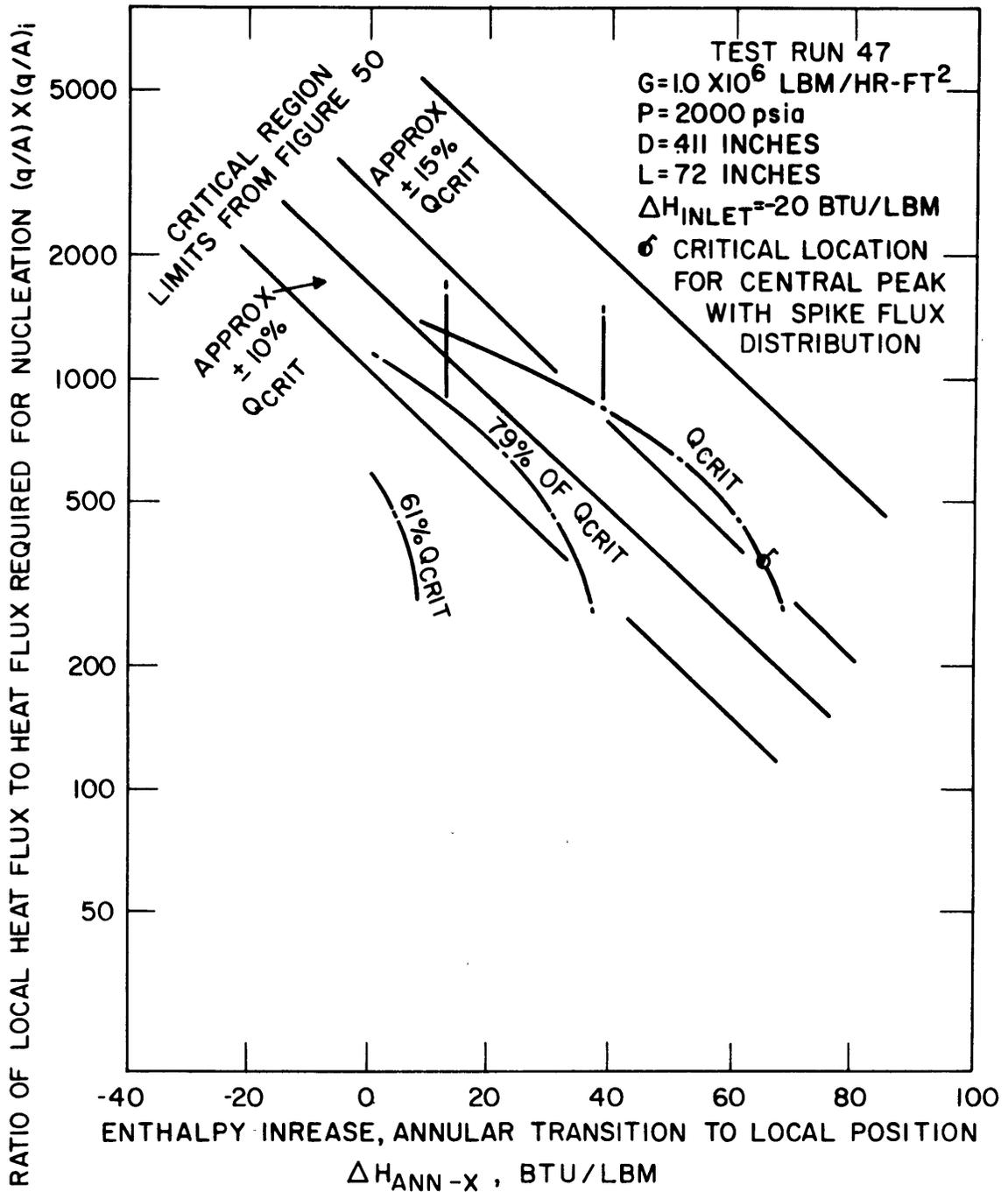


FIGURE 51. ESTIMATION OF THE CRITICAL REGION WIDTH (IN % TOTAL INPUT POWER) OF FIGURE 50 FOR 2000PSIA DATA REFERENCE 5)

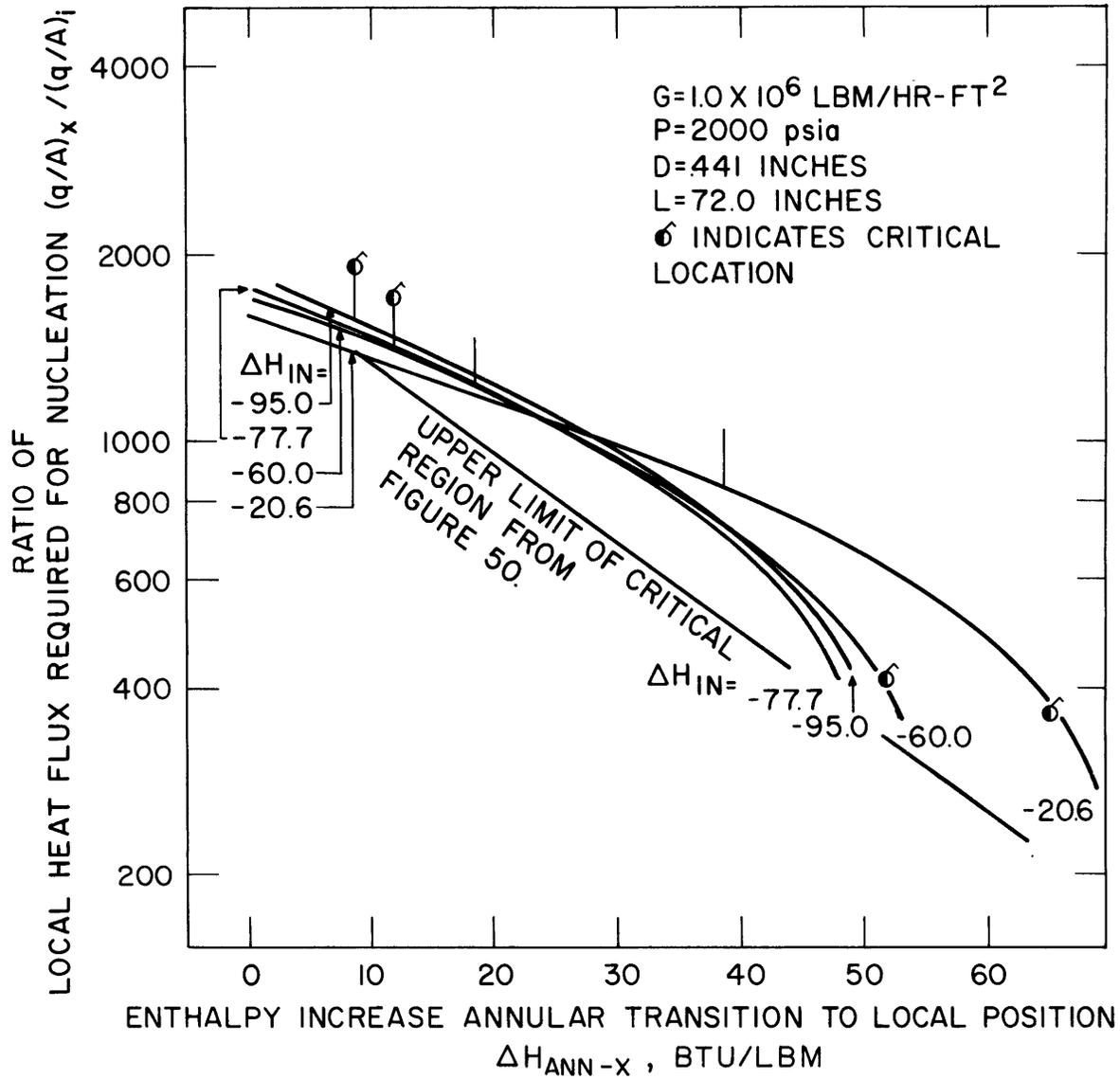


FIGURE 52. THE EFFECT OF INLET SUBCOOLING ON CRITICAL FLUX RESULTS FOR COSINE FLUX DISTRIBUTION WITH FLUX SPIKE (REFERENCE 5)